GEOSCIENCE CANADA

JOURNAL OF THE GEOLOGICAL ASSOCIATION OF CANADA
JOURNAL DE L'ASSOCIATION GÉOLOGIQUE DU CANADA

Respecting Stratigraphy: Documenting geologic rates and processes

Taking the pulse at Repulse Bay: Neoarchean magmatism and cratonization

Klipping the metamorphic rocks at St. Cyr, Yukon

Oceanic Island Basalt: Metals transitioning from the mantle

A Giant of Geology: Celebrating Eduard Suess

2015 VOLUME 42

Publisher/Éditeur
Geological Association of Canada
c/o Department of Earth Sciences
Memorial University of Newfoundland
St. John's NL Canada A1B 3X5
Tel: (709) 864-7660
Fax: (709) 864-2532
gacpub@mun.ca
gac@mun.ca
www.gac.ca

Print Edition: ISSN 0315-0941
Online Edition: ISSN 1911-4850

Volume 42

A journal published quarterly by the Geological Association of Canada, incorporating the Proceedings.
Une revue trimestrielle publiée par l'Association géologique du Canada et qui en diffuse les actes.

Subscriptions: Receiving four issues of Geoscience Canada per year for $45 is one of the benefits of being a GAC member. To obtain institutional subscriptions, please contact Érudit: www.erudit.org

Abonnement: Recevoir quatre numéros par année pour 45,00 $ du magazine Geoscience est l'un des avantages réservés aux membres de l'AGC. Pour les abonnements institutionnels, s'il vous plaît contacter Érudit: www.erudit.org

Those wishing to submit material for publication in Geoscience Canada should refer to the Instructions to Authors on the GAC® Web site, www.gac.ca

AUTHORS PLEASE NOTE:
Please use the web address http://journals.hil.unb.ca/index.php/GC/index for submissions; please do not submit articles directly to the editor.

The Mission of the Geological Association of Canada is to facilitate the scientific well-being and professional development of its members, the learned discussion of geoscience in Canada, and the advancement, dissemination and wise use of geosciences in public, professional and academic life.

Opinions expressed and interpretations presented are those of the authors and do not necessarily reflect those of the editors, publishers and other contributors. Your comments are welcome.

Cover Photo: The photograph, taken in 1981, is in the Cantilever Range of the southeastern Coast Mountains, west of Fraser River, and approximately 15 km SW of Lytton, British Columbia. Boulders in the foreground are of massive, clean granodiorite of latest Cretaceous age (K-Ar ages: Biotite ~64 Ma; Hornblende ~69 Ma). Just south of this locality the granodiorite intrudes highly deformed, greenschist grade rocks of Bridge River terrane and Jurassic–Cretaceous strata of Tyaughton-Methow basin. *Photo credit: Jim Monger.*

GAC MEDALLIST SERIES

Logan Medallist 3. Making Stratigraphy Respectable: From Stamp Collecting to Astronomical Calibration

Andrew D. Miall

Department of Earth Sciences
University of Toronto
Toronto, Ontario, M5S 3B1, Canada
Email: miall@es.utoronto.ca

SUMMARY

The modern science of stratigraphy is founded on a nineteenth-century empirical base – the lithostratigraphy and biostratigraphy of basin-fill successions. This stratigraphic record comprises the most complete data set available for reconstructing the tectonic and climatic history of Earth. However, it has taken two hundred years of evolution of concepts and methods for the science to evolve from what Ernest Rutherford scornfully termed "stamp collecting" to a modern dynamic science characterized by an array of refined methods for documenting geological rates and processes.

Major developments in the evolution of the science of stratigraphy include the growth of an ever-more precise geological time scale, the birth of sedimentology and basin-analysis methods, the influence of plate tectonics and, most importantly, the development, since the late 1970s, of the concepts of sequence stratigraphy. Refinements in these concepts have required the integration of all pre-existing data and methods into a modern, multidisciplinary approach, as exemplified by the current drive to apply the retrodicted history of Earth's orbital behaviour to the construction of a high-precision 'astrochronological' time scale back to at least the Mesozoic record.

At its core, stratigraphy, like much of geology, is a field-based science. The field context of a stratigraphic sample or succession remains the most important starting point for any advanced mapping, analytical or modeling work.

RÉSUMÉ

La science moderne de la stratigraphie repose sur une base empirique du XIXe siècle, soit la lithostratigraphie et la biostratigraphie de successions de remplissage de bassins sédimentaires. Cette archive stratigraphique est constituée de la base de données la plus complète permettant de reconstituer l'histoire tectonique et climatique de la Terre. Cela dit, il aura fallu deux cents ans d'évolution des concepts et des méthodes pour que cette activité passe de l'état de « timbromanie », comme disait dédaigneusement Ernest Rutherford, à l'état de science moderne dynamique caractérisée par sa panoplie de méthodes permettant de documenter les rythmes et processus géologiques.

Les principaux développements de l'évolution de la science de la stratigraphie proviennent de l'élaboration d'une échelle géologique toujours plus précise, l'avènement de la sédimentologie et des méthodes d'analyse des bassins, de l'influence de la tectonique des plaques et, surtout du développement depuis la fin des années 1970, des concepts de stratigraphie séquentielle. Des raffinements dans ces concepts ont nécessité l'intégration de toutes les données et méthodes existantes dans une approche moderne, multidisciplinaire, comme le montre ce mouvement actuel qui entend utiliser la reconstitution de l'histoire du comportement orbital de la Terre pour l'élaboration d'une échelle temporelle « astrochronologique » de haute précision, remontant jusqu'au Mésozoïque au moins.

Comme pour la géologie, la stratigraphie est une science de terrain. Le contexte de terrain d'un échantillon stratigraphique ou d'une succession demeure le point de départ le plus important, pour tout travail sérieux de cartographie, d'analyse ou de modélisation.

Traduit par le Traducteur

STRATIGRAPHY AS A DESCRIPTIVE, EMPIRICAL SCIENCE

Stratigraphy is the study of layered rocks. It has a reputation as a dull, descriptive science. It could well have been one of the disciplines Ernest Rutherford, the eminent geophysicist, was thinking about when he made his famous remark early in the twentieth century: "All science is either physics or stamp collecting." My own introduction to the subject, as a student in the early 1960s, contained lengthy lists of formation names and detailed descriptions of lithologies and fossil content, with little in the way of enlightenment about what it all meant. In

Geoscience Canada, v. 42, http://www.dx.doi.org/10.12789/geocanj.2015.42.072 pages 271-302

truth, then, it did not mean much. However, the stratigraphic record is the major repository of information about Earth history, including paleogeography and climate, and the course of evolution. Modern methods, described here, have evolved into a powerful multidisciplinary science.

Stratigraphy is at its core a descriptive science, like most of the rest of the traditional geological disciplines and, indeed, like most field-based sciences, such as biology and oceanography. All such disciplines have fallen victim to 'physics envy,' which refers to "the envy (perceived or real) of scholars in other disciplines for the mathematical precision of fundamental concepts obtained by physicists" (from Wikipedia). To a degree this is understandable. The rise of geology in the mid- to late nineteenth century following the fundamental contributions of Charles Lyell and his generation, was followed by the rise of physics. Eminent physicists, such as William Thomson (Lord Kelvin), began to make pronouncements about the Earth, and helped to create physics envy by such statements as "what cannot be stated in numbers is not science" (Mackin 1963). It is one of the better known stories about the history of geology that Lord Kelvin's estimate of the age of the Earth (a few tens of millions of years) conflicted with the Hutton–Lyell concepts of deep geologic time, but was mistakenly accorded considerable respect because it was based on calculations by a physicist (Hallam 1989). The conflict was not resolved until the discovery early in the twentieth century of radioactive decay and the realization that this provided a source of internal heat that rendered obsolete the idea of an Earth that had merely cooled from a primary molten state – the hypothesis favoured by Kelvin. Ernest Rutherford was one of the leading figures in developing ideas about radioactive heat that challenged Lord Kelvin, but nonetheless, although his work supported the conclusions that geologists had been arriving at about the length of geologic time, based on their field observations and deductive reasoning, Rutherford contributed to the rise in the authority of physics as the preeminent science.

In a landmark paper on cycles and rhythms in geology, and the measurement of geologic time, written shortly after the discovery of the concept of radioisotopic dating, Barrell (1917, p. 749) complained about physics and physicists thus:

> *Not only did physicists destroy the conclusions previously built by physicists, but, based on radioactivity, methods were found of measuring the life of uranium minerals and consequently of the rocks which envelop them. … Many geologists, adjusted to the previous limitations, shook their heads in sorrow and indignation at the new promulgations of this dictatorial hierarchy of exact scientists. In a way, this skepticism of geologists was a correct mental attitude. The exact formulas of a mathematical science often conceal the uncertain foundation of assumptions on which the reasoning rests and may give a false appearance of precise demonstration to highly erroneous results.*

Barrell's self-confidence seems not to have been typical of the times, however. J. Tuzo Wilson (1985), a leading Canadian geologist who (much) later developed several of the key concepts about plate tectonics, and did much to explain and popularize the subject in the 1970s, captured well the flavour of this period of physics dominance:

> *… on returning to the University of Toronto in 1927 I applied to transfer from a major in physics to one in geology. My professors were appalled. Physics was then in its heydey, but geology was held in very low esteem. Ernest Rutherford had compared it to postage-stamp collecting for it consisted of making maps by identifying and locating rocks and fossils. Instruments and methods were primitive and geology lacked general theories, which were scorned as "armchair geology." This was in striking contrast to the precise theories common in physics, but few considered that Wegener's concept of continents slowly drifting about had any merit, and no one, that I can recall, realized that therein lay the explanation for the lack of theories in geology.*

Hallam (1989, p. 233) has a slightly different view on this subject: "Rutherford may have had his tongue in his cheek when he uttered his notorious dictum, 'All science is either physics or stamp collecting', but Kelvin would doubtless have earnestly approved of this reductionist attitude, for he is on record as saying that data that cannot be quantified are hardly worthy of a scientist's attention."

The problem persisted. Baker (2000) commented thus:

> *In his history of earth science, entitled The Dark Side of the Earth, British geophysicist and science writer Robert Muir Wood argues that geology reached its intellectual peak around 1900. During the twentieth century, according to Wood, geology's intellectual decline coincided with the rise of modern physics, chemistry, and biology. In the 1960s and 1970s, however, a new earth science developed, replacing anachronistic "geological" concerns and methods with the global view and scientific methodologies of geophysics. Geochemist and science minister of France, Claude Allègre offers somewhat similar views on how much modern geochemical science has supplanted the "mapping mentality" of geology. According to these scholars, rigorous, scientific geophysical, geochemical and (presumably) geobiological approaches are now replacing the outmoded geological one.*

Torrens (2002, p. 252) noted that "Robert Muir Wood asserted in 1985 that 'stratigraphy and fossil correlation [were] the backbone of [old] Geology', whereas the new 'Earth Science is revealed by geophysics and geochemistry' (Muir Wood 1985, p. 190). Torrens (2002, p. 252) also cited Robert Dietz, who noted (1994, p. 2) that: "Geology had evolved from an observational and field science into largely a laboratory science with instrumental capabilities that have improved data collection and data processing by orders of magnitude."

As Hallam (1989, p. 221–222) argued, these views display a serious misunderstanding of the nature of Geology, especially the need for the traditional stratigraphic data base from which to build geological histories that could now incorporate the new plate-tectonic principles. And not all have agreed that the move from field to laboratory has been such an advance. Many eminent, field-based geologists have felt the need to downplay the primacy of numerical, experimental data of the type that would be familiar to a physicist or a chemist, and to restate the importance of carefully structured field observations, and the building of temporary, inductive hypotheses, followed by further observation and testing, employing the methods of multiple working hypotheses. Read (1952), a petrologist, is famous for his remark that the "best geologist is the one who has seen the most rocks" (cited by Ager 1970). Francis Pettijohn, one of

the founders of modern sedimentology, issued a warning in his memoirs in 1984, likening the rush into the exotic peripheries around what he saw as the true core of geology – with stratigraphy at its centre – to "a doughnut with nothing in the middle" (Pettijohn 1984, p. 203). Earlier he had said (Pettijohn 1956, p. 1457) "Nothing, my friends, is so sobering as an outcrop. And many a fine theory has been punctured by a drill hole." More recently, Dewey has rightly noted (1999, p. 3), "core, field-based geology is [still] the most important, challenging and demanding part of the science."

As modern laboratory techniques have grown in importance and as the computer has become ever more central to scientific activities this emphasis on the field has become ever more important. Geology deals with a complex Earth; the rock record is the product of numerous interacting processes acting simultaneously over a wide range of time scales; and earth history is explored using a wide array of interrelated techniques, some based on direct field observation, some based on remote sensing, some on sampling followed by laboratory measurement, and with numerical simulation and modeling assuming ever greater usefulness. All these data must be reconciled, and, beyond the kinds of basic stratigraphic prediction that Pettijohn was referring to in his remark about outcrops and drill holes (cited above), few of the conclusions about the geological past are amenable to direct testing, as would be a hypothesis in physics or chemistry. This is what makes geology different, and this is why many of the philosophical and methodological discussions about science are not applicable to geology.

Hallam (1989, p. 221) stated:

> *There has often in the past been some tension between geologists and physicists with a common interest in problems of earth history, which is a natural consequence of their difference in aptitude, training, and outlook. Geologists tend to be staunchly empirical in their approach, to respect careful observation and distrust broad generalization; they are too well aware of nature's complexity. Those with a physics background tend to be impatient of what they see as an overwhelming preoccupation with trivial detail and lack of interest in devising tests for major theories, and with the geologists' traditional failure to think in numerate terms.*

Torrens (2002, p. 252) suggested that "Largely as a result of contemporary changes in attitude toward old and new, the teaching of stratigraphy has declined to a surprising extent. It is a complex and 'difficult' subject, which became no longer seen as central." However, as explained below, stratigraphy is no longer the descriptive 'stamp collecting' enterprise that it might once have been. The meticulousness of modern inductive observational methods is matched by an array of deductive methodologies that have entirely changed the science over the last half-century. I leave it to the likes of Vic Baker, Carol Cleland, Robert Frodeman, and others to explain philosophies of science and to answer the complaint quoted by Baker from former GSA president H. L. Fairchild that "Geologists have been far too generous in allowing other people to make their philosophy for them" (V. Baker, p. v, in Baker 2013).

However, the tension between geology and the more experimental and numerical 'hard' sciences has persisted to the present day. As recently as 2008 an eminent Canadian geophysicist explained to me that he did not like working with geologists or supervising students of geology, because, he said, "Geologists can't count."

THE SIGNIFICANCE OF FIELD CONTEXT

The answer to my rude geophysicist colleague then and now is to explain field context. All the elaborate, refined geochemical probing and geophysical sensing of rocks, and the digital models and computer visualization of them, are of zero value if we don't know where the rocks come from. This is not just a matter of geographic location or of sample position in a stratigraphic section, but relates to the complete geological background of the rocks of interest. Torrens (2002, p. 254) said "The history of stratigraphy … reveals how, now that we can measure many things so precisely, it is important that we understand exactly what our measurements are attempting to reveal." Later in this paper I detail the many vital strands of the stratigraphic science that now enable us to reconstruct, in substantial detail, the geological history and significance of sedimentary sections, which may include, for example, the regional geological history, structural, geochemical, magmatic or metamorphic development, or paleoclimatic or paleoceanographic evolution, of the section under study. Indeed, it is largely from the sedimentary record that our knowledge of the details of earth history comes. Field context means acute observation and recording of many visually observable and measurable details, the requirements and parameters of which are determined by the advanced applications now being applied to the sedimentary record. Field context may include three-dimensional position, vertical and lateral stratigraphic relations, the nature of bedding and bed contacts, the nature of surrounding lithofacies, observable sedimentary structures, fossil content, ichnofacies, and so on, at all scales from that of the largest outcrop to the sub-microscopic. Geology owns field context. At its core, this is what geology is about.

Here are some examples of the importance of field context. Figure 1 illustrates an apparently continuous succession of shallow marine limestone beds characterized by flat to undulating bedding planes, and minor channeling. Close inspection reveals abundant intraclast brecciation. Lithofacies appear similar throughout, and there is nothing about this outcrop to suggest that geochemical or geophysical characteristics would vary significantly from top to bottom. However, the bedding surface at the level of the geologist's shoulder is the boundary between the Sauk and Tippecanoe sequences, a craton-wide unconformity that can be traced for several thousand kilometres, and represents millions of years of missing time. Careful 'old fashioned' mapping, including the collection and analysis of fossil content for the purpose of assigning chronostratigraphic ages, was required in order for this outcrop to be assigned to its correct geological position.

Figure 2 illustrates an example of the modern approach to the documentation of elapsed time in the rock record. The outcrop has been designated a Global Stratigraphic Section and Point for the Cambrian–Ordovician boundary on the basis of its rich fauna. Facies studies demonstrate that the mudstone layers are deep-water deposits, and contain such open marine fossils as graptolites, whereas the interbedded limestone layers originated as shallow water deposits with a rich shelly fauna (trilobites, brachiopods, etc.), and were transported to a deep water setting by sediment gravity flows down the ancient Lau-

Figure 1. An outcrop of the Sauk-Tippecanoe contact, Aguathuna Quarry, near Port au Port, western Newfoundland.

rentian continental margin. Under ideal circumstances, ages of rocks such as these may now be assigned with accuracies in the 10^5 year range, based on quantitative methods of biostratigraphic correlation (Sadler et al. 2009).

Figure 3 illustrates one of the products of highly detailed biostratigraphic study representing more than one hundred years of intense research. These are three of thirteen sections, each about 5 m thick, measured over a distance of about 80 km, representing the Inferior Oolite formation (Aalenian-Bathonian) of southern England. Modern chronostratigraphic calibration has shown that the sections span a total of about 10 million years. There are 56 faunal horizons in these sections, averaging 180,000 years in duration, but none of the sections contain all of these horizons and in none of them is the preserved record the same.

Overall, it is impossible to distinguish any ordered pattern to the record of sedimentation and erosion in these sections. How typical is this of shallow marine sedimentation in general? Does the availability of an unusually detailed ammonite biostratigraphy enable us to develop a much more detailed record of local change than would otherwise be available? And should this section therefore be regarded as a model for the interpretation of other shallow marine carbonate sections? Would it be correct to conclude that many other shallow marine (and nonmarine?) successions should similarly be regarded as containing numerous local diastems? If so, what does this tell us about short- to long-term sedimentary processes? No clear answers are available to any of these questions, but without the detailed biostratigraphic and facies observations none of them could even be asked.

Figure 4 illustrates a succession of thin-bedded turbidites. Calculations of sedimentation rate and of the elapsed time represented by successions of this type are notoriously difficult, but careful examination of the sedimentary facies of each bed can offer guidance. The turbidite sandstone beds each accumulated in the space of a few hours to days, whereas the elapsed time represented by the intervening mudstone is very difficult to estimate, and depends on the depositional process. Finely laminated mudstone beds may represent pelagic deposits accumulated over tens to hundreds of thousands of years, or longer, but it is increasingly being recognized that mud is commonly transported and rapidly deposited within active current regimes. Petrographic studies show that mudstone layers are commonly deposited as silt-sized aggregate

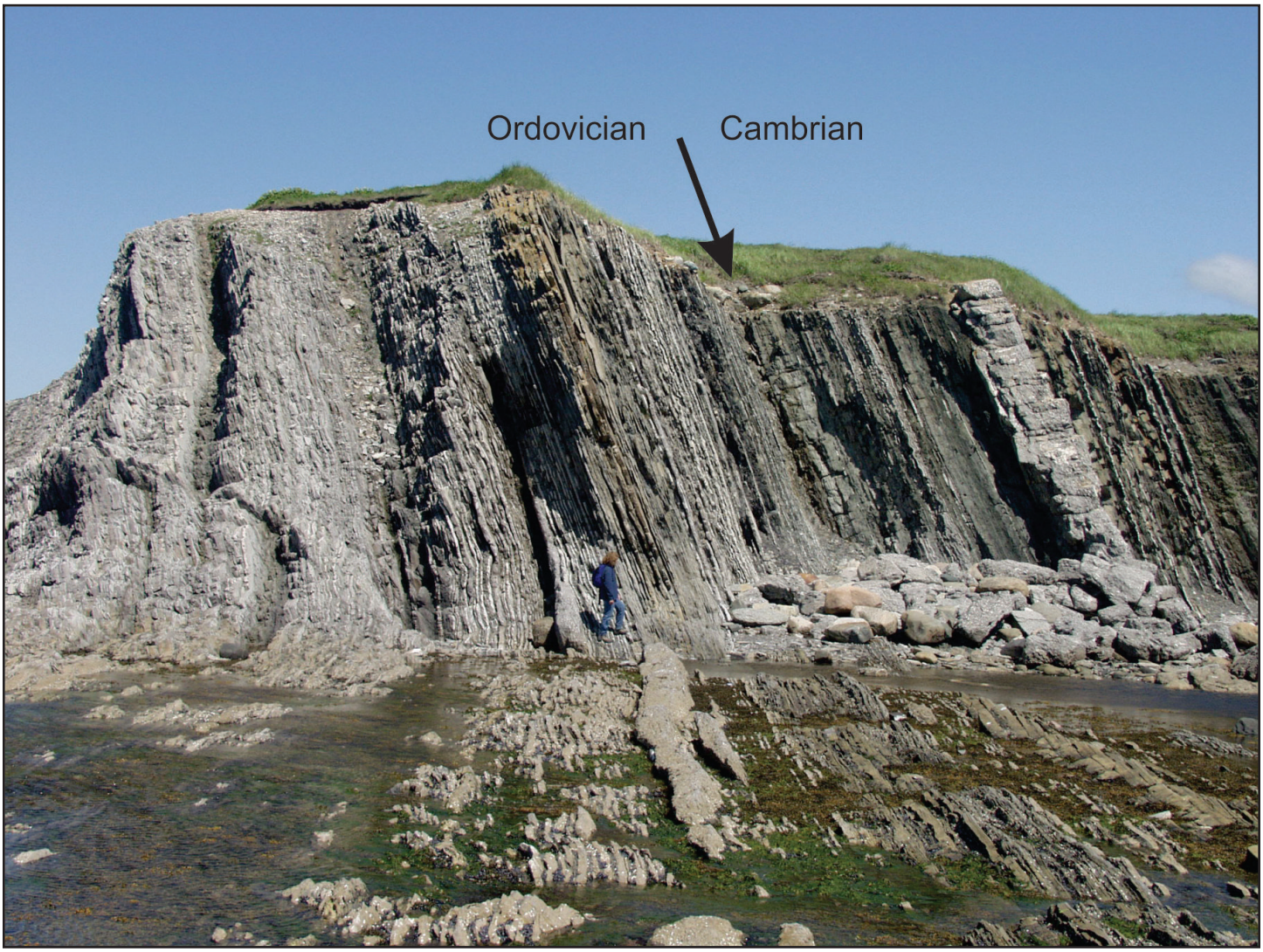

Figure 2. The Global Stratigraphic Section and Point (GSSP) for the Cambrian–Ordovician boundary at Green Point, Gros Morne National Park, Newfoundland.

particles. Careful studies of fine-scale sedimentary structures commonly reveal a complexity of bedforms showing that mud floccules may be moved by tidal and other currents, with some units deposited by wave or storm activity over time periods of hours to days (e.g. Plint et al. 2012; Schieber et al. 2013).

Another example of the importance of modern stratigraphic research is the type of succession illustrated in Figure 5. These interbedded sandstone and shale layers contain clear evidence of shallow marine sedimentation in the form of sedimentary structures, fossil content and trace fossils. We now know that deposits of this type are replete with hiatuses, and that as little as 10% of the elapsed time embodied in this section may be actually represented by sediment. Bedding planes at facies contacts, such as those visible in Figure 5, may represent tens to hundreds of thousands of years of elapsed time (Miall 2015). Detailed stratigraphic reconstructions and subsurface studies using well data and reflection seismic methods demonstrate that many deposits of this type develop by lateral accretion of low-angle clinoform slopes on basin margins (e.g. Johannessen and Steel 2005; Plint et al. 2009). Much of the elapsed time is represented by the lateral growth of the clinoforms. Exposures of the top surface of a clinoform are surfaces of sediment bypass, which explains the lengthy hiatuses at some key bedding contacts. How can we distinguish the bounding surfaces of clinoforms from the bedding planes that result from short-term autogenic changes in shallow marine sedimentary processes?

A brief mention may also be made here of three long-standing controversies in sedimentary geology, solutions to which were arrived at by the application of modern tools of sedimentology and basin analysis.

1) The term 'till' has long been applied to the coarse, poorly-sorted, boulder-rich deposits laid down by continental glaciers. In the ancient record, many deposits of this type have been termed till, the glacial origin of which is apparently supported by the presence of such glacial indicators as striated pavements and dropstones, and this has generated a false impression of the importance of continental glaciation. However, modern facies analysis observations demonstrate that many, if not most such deposits in the ancient record were laid down by sediment gravity flows in subaqueous settings (e.g. McMechan 2000). The detritus may be glacigenic, as indicated by associated dropstone facies, the presence of striated pavements, etc., but the final depositional process was one of sub-

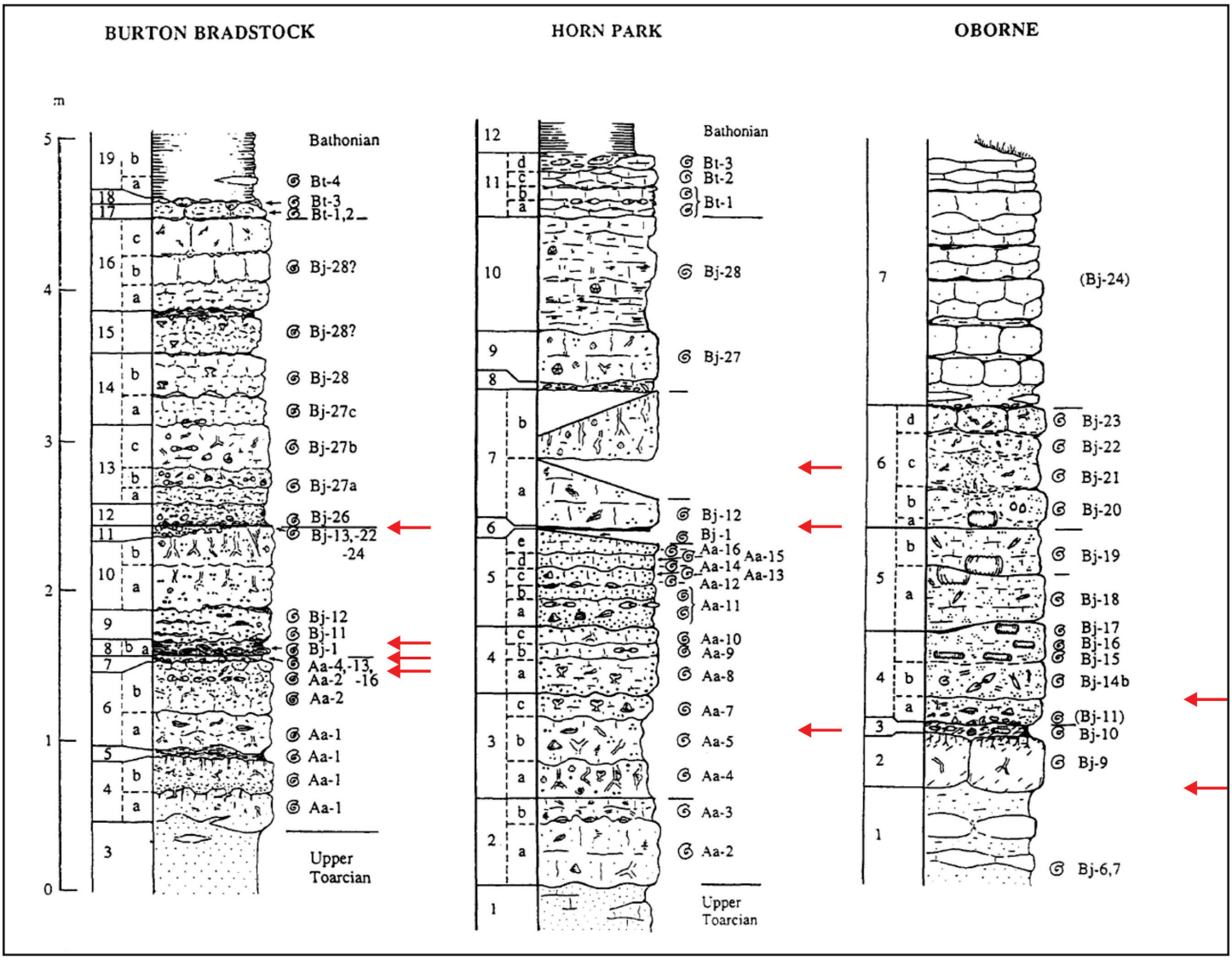

Figure 3. Examples of the sections through the Inferior Oolite (Middle Jurassic) of southern England, showing the numbered ammonite faunas and the bedding surfaces identified as hiatuses (red arrows) (adapted from Callomon 1995).

aqueous reworking. Clast fabrics, the presence of graded bedding, and an association with thick units of marine or lacustrine mudrocks (with or without dropstones) are the key indicators. Till *sensu stricto*, deposited in continental settings, has a low preservation potential and is rare in the rock record. The non-genetic term 'diamict' (termed diamictite when lithified), is preferred. Very similar rocks may occur in non-glacial volcaniclastic settings (Eyles et al. 1983).

2) The Snowball Earth hypothesis holds that during the Neoproterozoic the Earth passed through a period when it became largely or entirely frozen (Hoffman et al. 1998). The evidence consists of widely dispersed suites of coarse conglomeratic deposits interpreted as glacigenic in origin, and the hypothesis is apparently supported by the carbon isotope geochemistry of the successions. All the conglomerate deposits were thought to be of the same age, indicating a simultaneous, Earth-wide freeze-up. However, careful sedimentological and chronostratigraphic analysis of the worldwide occurrences of these rocks indicates that there was more than one Neoproterozoic glacial episode, that many of the deposits are reworked submarine sediment–gravity flow deposits containing ample evidence of active marine currents and of a hydrological cycle inconsistent with a frozen Earth, and that some are entirely volcaniclastic in origin, indicating no relationship whatever to glaciation (Eyles and Januszczak 2004; Allen and Etienne 2008).

3) The important early publications that set out the new techniques of seismic stratigraphy contained the hypothesis that the cycles of change in accommodation that lead to the accumulation of stratigraphic sequences are caused largely or entirely by eustatic changes in sea level on 10^6–10^7 time scale (Vail et al. 1977). However, subsequent re-examination of many sequence assemblages has, in many instances, revealed indisputable evidence of local or regional tectonic control, and it has been argued that for most of the geological record, chronostratigraphic evidence has not been adequate to demonstrate the global synchroneity of the sequences that would be a necessary attribute of sequences that are of eustatic origin (Miall and Miall 2001). Modern studies using the refined methods described in this paper are suggesting a quite

Figure 4. Thin-bedded turbidites, Annot, France.

different idea: the importance of high-frequency orbital climatic and/or glacioeustatic control of parts of the ancient rock record on a 10^4–10^5-year time scale (Hilgen et al. 2015).

As these examples have demonstrated, only the application of all available modern tools of sedimentary geology, including facies analysis, sequence stratigraphy and chronostratigraphy, has yielded the interpretations presented here.

The eminent stratigrapher, P.D. Krynine is reputed to have said, in 1941, "Stratigraphy can be defined as the complete triumph of terminology over facts and common sense." But what has just been described here is not the stratigraphy that Krynine knew.

DEDUCTIVE MODELS AND HYPOTHESES IN STRATIGRAPHY

The modern science of stratigraphy – what I termed 'sophisticated stratigraphy' in a recent review (Miall 2013) – operates by the dynamic interplay between an array of deductive models and hypotheses which express our understanding of the operation of earth system science in the sedimentary realm. Most of these are qualitative, in the sense that they depend on descriptive data, but all are characterized by rigour in the protocols for field data collection, description and processing. Among the more important hypotheses and models are:

- The law of superposition of strata
- The principle of faunal succession
- Walther's Law
- The concept of facies
- Flow regime concept
- Cyclic sedimentation
- Facies models
- Autogenic and allogenic processes and the relationships between them
- The inductive foundation of Global Stratigraphic Sections and Points as the basis of chronostratigraphy
- Concept of accommodation
- Sequence stratigraphy
- Quantitative basin models
- Orbital forcing, cyclostratigraphy and astrochronology

The first eight in this list are amongst the most important components of **sedimentology** a science that did not exist in its modern form until the 1960s. **Chronostratigraphy** is one of the oldest components of stratigraphy, based in the first instance on the discoveries about the successions of rock types and fossil faunas that William Smith used in the construction of the first ever geological map (Smith 1815), discoveries that were studied intensively during the nineteenth century, leading to significant developments in the field of **biostratigraphy**.

Figure 5. Shallow-marine Cretaceous strata at the WAC Bennett dam, near Fort St. John, British Columbia.

Chronostratigraphy has evolved into a highly precise science with the development of an array of dating methods and field procedures. It was the evolution of **sequence stratigraphy** in the 1990s that began to bring all of this together into the modern dynamic science which stratigraphy now represents.

THE EVOLUTION OF MODERN STRATIGRAPHY

Beginnings (Nineteenth Century)

I do not deal here with the work of Steno, Hutton, Lyell and others, from whom came the concepts of uniformitarianism. This history has been amply covered elsewhere.

Middleton (2005) divided the history of sedimentology into six periods or stages. The first stage ended about 1830 with the publication of Lyell's (1830–1833) master work that led to the general acceptance of **uniformitarianism**, or **actualism**, as the basis for geology. What follows in this paper falls into his second period. The subsequent discussion does not adhere to his subdivision into 'periods' because I focus on specific themes which overlapped in time.

Two key early developments were the recognition of the concept of **facies** (Gressly 1838), and the establishment of **Walther's Law** (Walther 1893–1894). Teichert (1958), Middleton (1973) and Woodford (1973) reviewed the history and use of the concepts in light of contemporary ideas. Note the dates of these papers (1958, 1973), in light of the stages of development summarized below, because they help to explain the chronological evolution of modern stratigraphic thought and theory. Walther's Law is discussed further below.

Developments in biostratigraphy were enormously important in establishing some of the basic ideas about stratal succession, relative ages, and correlation. The evolution of the concepts of zone and stage are discussed in detail elsewhere (Hancock 1977; Miall 2004), topics that are not repeated here. Stratigraphic paleontology was a central theme of stratigraphy until relatively recent times. In fact, the first professional society in the field of sedimentary geology, the *Society of Economic Paleontologists and Mineralogists*, founded in Tulsa in 1931, emphasized this fact in the title of the society. Paleontology and mineralogy were important elements of petroleum geology and basin analysis until the seismic revolution of the 1970s, mainly because of their use in the identification and correlation of rock units in petroleum-bearing basins.

Cyclic Sedimentation (1932–1968)

Implicit in the early work on facies and on Walther's Law is the concept of recurrence of certain environments and their deposits. The idea of cyclicity became explicit with the study of the Carboniferous deposits of the US mid-continent in the early 1930s, which consist of repetitions of a coal-bearing, clastic–carbonate succession. These came to be called **cyclothems**. Wanless and Weller (1932, p. 1003) are credited with the original definition of this term:

> *The word "cyclothem" is therefore proposed to designate a series of beds deposited during a single sedimentary cycle of the type that prevailed during the Pennsylvanian period.*

Shepard and Wanless (1935) and Wanless and Shepard (1936) subsequently attributed the cyclicity to cycles of glacioeustatic sea-level change, an explanation that has never been challenged.

The beginnings of an understanding of the significance of the lithofacies signatures of common environmental settings is implicit in the paper by Nanz (1954), where coarsening- and fining-upward trends extracted from some modern sedimentary environments in Texas are presented. There is no discussion of repetitiveness or cyclicity in this paper, but the work was clearly foundational for the very important papers by Nanz's Shell colleagues that followed less than a decade later (see below).

Duff and Walton (1962) demonstrated that the cyclothem concept had become very popular by the early 1960s. For example, J.R.L. Allen, who is credited as one of the two originators of the meandering river point-bar model for fluvial deposits, used the term cyclothem for cycles in the Old Red

Sandstone in his first papers on these deposits (Allen 1962, 1964). Duff and Walton (1962) addressed the widespread use (and misuse) of the term cyclothem, and discussed such related concepts as modal cycle, ideal cycle, idealized cycle, and theoretical cycle, the differences between cyclicity, rhythmicity and repetition, and the possible value of statistical methods for refining cyclic concepts. They speculated about the possibility of repeated delta-lobe migration as a cause of cyclicity, in contrast to the prevailing interpretation of the cycles as the product of sea-level change.

With Carboniferous coal-bearing deposits as the focus, two edited compilations dealing with cyclic sedimentation made essential contributions to the birth of modern sedimentology at about this time. Merriam (1964), based in Kansas, provided a focus on the US mid-continent deposits, while Duff et al. (1967) dealt at length with European examples. The Kansas publication included a study of cyclic mechanisms by Beerbower (1964) that introduced the concepts of **autocyclic** and **allocyclic** processes. Autocyclic processes refer to the processes that lead to the natural redistribution of energy and sediment within a depositional system (e.g. meander migration, shoreline progradation) — the preference is now to use the term **autogenic** because the processes are not always truly cyclic — whereas **allocyclic** (**allogenic**) processes are those generated outside the sedimentary system by changes in discharge, load, and slope. Beerbower (1964) was dealing specifically with alluvial deposits in this paper, but his two terms have subsequently found universal application for other environments and their deposits. The term **allogenic** is now used to refer to processes external to a sedimentary basin, including eustasy, tectonism and climate change.

Another important contribution at this time was that by Visher (1965). The purpose of his paper was to build on the ideas contained in Walther's Law to highlight the importance of the vertical profile in environmental interpretation. He provided detailed descriptions of the profiles for six clastic environments, regressive marine, fluvial (channel or valley-fill), lacustrine, deltaic, transgressive marine, and bathyal-abyssal, drawing on both modern settings and ancient examples. This was, therefore, one of the first comprehensive attempts to apply the principles of actualism (uniformitarianism) to sedimentological interpretations. Interestingly (and this highlights one of the arguments of this paper that some ideas develop as separate lines of research, which take time to come together), Visher's paper makes no reference to what are now the classic papers on Bouma's turbidite model (Bouma 1962), or Allen's (1964, 1965) work on alluvial deposits, which include his block diagram of a fluvial point-bar. However, Beerbower's (1964) description of autocyclicity and Duff and Walton's (1962) speculation about deltaic processes (neither of which are referenced by Visher) indicate the beginnings of what shortly became a flood of new work providing the basis for the facies model revolution. Early applications of these ideas to the interpretation of the subsurface are exemplified by Berg's (1968) study of an interpreted point-bar complex constituting a reservoir unit in Wyoming.

Basin Analysis and the Big Picture (1948–1977)

Driven in large measure by the needs of the petroleum industry to understand subsurface stratigraphic successions, geologists devised a number of ways to explore the broader origins of a basin fill and understand its paleogeographic evolution. Until the plate-tectonics revolution of the 1970s, basins were interpreted in terms of the **geosyncline theory**, which reached its full expression in this period with the definition of a range of classes based on structural and stratigraphic attributes (Kay 1951), many of which, as the plate-tectonics paradigm subsequently revealed, had little to do with the actual dynamics of continental crust.

Whereas the facies model revolution of the 1970s dealt with sedimentology on the relatively small scale of individual depositional systems (rivers, deltas, submarine fans, reefs, etc.), paleogeographic reconstruction for industry meant attempting to understand entire basins. Provenance studies based on detrital petrography were central to this work, hence the title of the first specialized journal in this field, the *Journal of Sedimentary Petrology*, founded in 1931. Isopachs revealed broad subsidence patterns, and (for outcrop work) regional paleocurrent studies confirmed regional transport patterns, even in the absence of the understanding of the hydraulics of sedimentary structures that came later with the development of the flow regime concept. Krumbein (1948) pioneered the generation of lithofacies maps based on such indices as a clastic–carbonate ratio. Dapples et al. (1948) demonstrated how these maps could be used to deduce tectonic controls in a basin. The subject of stratigraphy meant classical lithostratigraphy. The books and reviews by Pettijohn (1949, 1962; Potter and Pettijohn 1963), and Krumbein and Sloss (1951), and Levorsen's (1954) textbook on petroleum geology exemplify this approach.

However, some interesting new ideas that we would now classify under the headings of basin architecture, accommodation and sequence stacking patterns began to emerge, although little of this work was widely used at the time, it being only from the perspective of modern sequence methods that we can look back and see how a few individuals were ahead of their times. Rich (1951) described what we would now term the continental shelf, the continental slope and the deep basin as the **undaform**, **clinoform**, and **fondoform**, respectively, and provided descriptions of the processes and resulting sedimentary facies to be expected in each setting. The only one of his terms to survive is **clinoform**, although now it is used as a general term for deposits exhibiting a significant depositional dip (e.g. prograding continental slopes and deltas), rather than as a term for a depositional environment. Van Siclen (1958) examined the late Paleozoic cyclothems where they tip over the southern continental margin which, at that time, lay within what is now central Texas. His work includes a diagram of the stratigraphic response of a continental margin to sea-level change and variations in sediment supply that is very similar to present-day sequence models. Oliver and Cowper (1963, 1965) may have been the first to specifically identify 'clino' beds in the subsurface using Rich's concepts in a stratigraphic reconstruction based on petrophysical log correlation. Curray (1964) was among the first to recognize the importance of the relationships between sea level and sediment supply. He noted that fluvial and strandplain aggradation and shoreface retreat predominate under conditions of rising sea level and low sediment supply, whereas river entrenchment and deltaic progradation predominate under conditions of falling sea level and high sediment supply. Curtis (1970) carried these ideas further,

illustrating the effects of variations in the balance between subsidence and sediment supply as controls on the stacking patterns of deltas, concepts that are now encapsulated by the terms **progradation**, **aggradation** and **retrogradation**. Frazier (1974) subdivided the Mississippi deltaic successions into **transgressive**, **progradational**, and **aggradational** phases, and discussed autogenic (delta switching) and glacioeustatic sedimentary controls.

Perhaps it is because Texas specializes in bigness; this may be the explanation why some critical concepts concerning large-scale sedimentological environments were first developed there. The location of petroleum research laboratories, such as that of Shell Oil in Texas (referred to below) may also have been very influential. I refer to the concept of the **depositional system**, the concept that takes sedimentological analysis beyond the shoreface or the river meander or the reef talus slope to an analysis that encompasses entire systems. Fisk's (1944) work on the lower Mississippi valley and delta is an early example of this approach, but it was the later work of William L. Fisher that better exemplifies this next step and was more influential. The work he and his colleagues carried out on the deltas and other depositional systems of the Texas coast (Fisher et al. 1969, 1972) established a whole different scale of operation. Application of current subsurface stratigraphic methods to part of the Eocene section of the Gulf Coast (Fisher and McGowen 1967) demonstrated that existing rivers and deltas along a huge swath of the Gulf Coast had occupied essentially the same map locations for about 40 million years. The depositional systems approach provided the foundation for the **systems tracts** that became a critical part of sequence stratigraphy twenty years later. Lastly, in a paper that appears in the famous memoir that introduced seismic stratigraphy to the geological community (Payton 1977), Brown and Fisher (1977) summarized the ideas of this important group of stratigraphers at the Bureau of Economic Geology (at the University of Texas) and helped to bridge the intellectual next step from large-scale sedimentology to sequence stratigraphy.

The Meaning of 'Facies' (1949–1973)

The concept of **facies** and the importance of **Walther's Law** were well understood and used in continental Europe during the nineteenth century, according to Teichert (1958), but did not become widely used in the English-speaking world until the 1930s.

On November 11th 1948 a conference was organized by the Geological Society of America in New York to discuss "Sedimentary facies in geologic history." This was a landmark event, the outcome of which was a Geological Society of America Memoir (Longwell 1949) that marked the beginnings of several important developments. The memoir begins with a lengthy paper by Moore (1949) which set the scene by describing and illustrating, with the use of a block diagram, the various facies present within a modern carbonate reef complex in Java, from which he derived this definition:

> *Sedimentary facies are areally segregated parts of different nature belonging to any genetically related body of sedimentary deposits.*

The paper includes numerous examples of complex stratigraphic relationships from the Phanerozoic record of the United States, illustrating the inter-tonguing of facies of a wide range of environments. Moore's paper also includes an interpretation of the cyclicity exhibited by the cyclothems of the mid-continent, accompanied by a diagram showing how different facies develop as a result of repeated transgression and regression. Other papers by E.D. McKee, E.M. Spieker, and others, provide many other examples of complex stratigraphy, indicating that by this time there was a sophisticated understanding of the diachronous nature of facies in the stratigraphic record, and its control by sea-level change. The concluding contribution in this memoir is a lengthy paper by Sloss et al. (1949) in which the concept of the **sequence** is first described.

A decade later, Teichert (1958, p. 2719), working from Gressly's original discussion, explained the derivation of the term facies:

> *Facies is a Latin word meaning face, figure, appearance, aspect, look, condition. It signifies not so much a concrete thing, as an abstract idea. The word was introduced into geological literature by Nicolaus Steno (1669, p. 68–75) for the entire aspect of a part of the earth's surface during a certain interval of geologic time.*

In his abstract, Teichert (1958, p. 2718) provided this succinct definition:

> [Facies means] *the sum of lithologic and paleontologic characteristics of a sedimentary rock from which its origin and the environment of its formation may be inferred.*

Teichert (1958) asserted that the concept of **facies associations** and the importance of **vertical facies successions** were well understood by nineteenth-century European geologists.

Interest in the work of the founders of modern sedimentology was renewed in the 1960s, with the new developments in the study of modern sediments, structures and environments. Woodford (1973, p. 3737) translated Gressly's (1838) 'second law' as follows:

> *Facies of the same petrographic and geologic nature assume, in different formations, very similar paleontologic characteristics and even succeed each other generally across a more or less numerous series of formations lying one upon the other.*

Middleton (1973, p. 981) provided a translation of Walther's methodology from the original German. Walther referred to it as '**ontology**' (**actualism**, or **uniformitarianism**, in modern usage) as follows:

> *It consists in trying to investigate the events of the past through modern phenomena. From being (existence), we explain becoming (genesis).*

Middleton's (1973, p. 982) translation of Walther's original statement of his Law is as follows:

> *The various deposits of the same facies-area and similarly the sum of the rocks of different facies-areas are formed beside each other in space, though in a cross-section we see them lying on top of each other. … it is a basic statement of far-reaching significance that only those facies and facies-areas can be superimposed primarily which can be observed beside each other at the present time.*

Middleton (1973, p. 980) suggested that "Walther must be named with Sorby, Gilbert, Grabau, and a few others, as one of the founders of the modern sciences of sedimentology and paleoecology," although he pointed out that whereas Walther's

work was cited and acknowledged in much of the pioneer work in the early 20th century, in the first modern treatment of the subject of facies (Longwell 1949) there was no explicit mention of Walther or his Law. He had a much greater influence in Russia, where facies studies were termed '**comparative lithology**.'

Fluid Hydraulics and Sedimentary Structures (1953–1976)

A key step in the development of modern sedimentology was the emergence of the idea that sedimentary structures represent measurable and repeatable physical processes, and that they therefore provide information on depositional environments and processes. Early work on the subject included the observations by Sorby (1859, 1908) and Gilbert (1884, 1899) on sedimentary structures, and Gilbert's experimental work (Gilbert 1914). Sorby (1852) was the first to recognize the utility of crossbedding for determining current directions. However, as Allen (1993) pointed out, it was not until the appearance of the synthesis by Potter and Pettijohn (1963) that the richness and significance of the preserved record caught the general attention of sedimentary geologists.

A necessary first step towards a modern study of sedimentary structures is accurate description and classification. McKee and Weir (1953) made an important contribution in this direction, with their description of the scales of structures, their internal architecture and bounding surfaces. It is in this paper that the familiar terms **planar**- and **trough-cross-stratification** first appear. A decade later, a comprehensive classification by Allen (1963a) introduced a set of Greek letters for different types of crossbedding, a system that was widely used for some time. Several illustrated atlases of sedimentary structures also appeared during this period (Pettijohn and Potter 1964; Conybeare and Crook 1968), indicating that sedimentary geologists were coming to grips with the full range of preserved and observable structures.

By the 1950s, sedimentary geologists had become more widely aware of the directional information contained in sedimentary structures, and some pioneering studies of what came to be known as **paleocurrent analysis** were being performed. For example, Reiche (1938) analyzed eolian crossbedding, Stokes (1945) studied primary current lineation in fluvial sandstone, and several authors were dealing with grain and clast orientation (e.g. Krumbein 1939). Pettijohn (1962) provided an overview of the subject, with many examples of the different techniques for analysis and data display that were then in use. Curray (1956) published what became the standard work on the statistical treatment of paleocurrent data.

Meanwhile, several pioneers were attempting to make sedimentary structures in the laboratory, in part as a means to understand the sedimentary record. There was also an interest in understanding fluid hydraulics from an engineering perspective, to aid in the construction of marine facilities, such as bridges and breakwaters. Kuenen and Migliorini (1950), in a classic paper, brought together flume experiments and observations of the ancient record to demonstrate that graded bedding could be generated by turbidity currents. As with many such contributions, it had been preceded by observations and suggestions by many other authors, but this was the paper that brought these observations together into the comprehensive synthesis that made it the benchmark contribution that it became. The term **turbidite** was subsequently coined by Kuenen (1957). McKee (1957), following his many years observing cross-stratification in outcrop, particularly in fluvial and eolian deposits in the Colorado Plateau area, experimented with the formation of cross-stratification by traction currents in a flume.

The critical theoretical breakthrough at this time was the series of flume experiments carried out by the US Geological Survey to study sediment transport and the generation of bedforms. This resulted in the definition of the **flow regime concept**, and the recognition of **lower** and **upper flow regimes** based on flow characteristics (particularly the structure of turbulence), sediment load and resulting bedforms (Simons and Richardson 1961). At this time, Allen (1963b) reviewed the observational work of Sorby and made one of the first attempts to interpret sedimentary structures in terms of flow regimes. However, the most important next step was a symposium organized by Middleton (1965), which brought together current field and experimental studies in a set of papers that firmly established flow regime concepts as a basic tool for understanding the formation of hydraulic sedimentary structures formed by traction currents as preserved in the rock record.

Middleton (1966a, b, 1967) extended the work of Kuenen with further experiments on turbidity currents and the origins of graded bedding, work that was ultimately to lead to a significant new classification of sediment gravity flows, of which it was now apparent that turbidity currents were only one type (Middleton and Hampton 1976). Reference is made in the first of these papers to field observations of turbidites by Roger G. Walker (1965), a reference which marks the beginning of a significant professional collaboration, to which I return later.

Walker's (1967, 1973) field experience with turbidites led to a proposal for the calculation of an index of the proximal-to-distal changes that occur down-flow within a turbidite. This marked an attempt at an increasingly quantitative approach to the study of sedimentary structures, although this index was not to survive an increasing knowledge of the complexities of the submarine fan environment within which most turbidites are deposited.

The important new developments in this field were well summarized in a short course, organized by the Society for Sedimentary Geologists, the manual for which provides an excellent review of the state of knowledge at this time (Harms et al. 1975). This review contains the first description and definition of hummocky cross-stratification (HCS), and the recognition of this structure as a key indicator of combined-flow (unimodal and oscillatory) storm sedimentation.

Early Studies of Modern Environments (1954–1972)

As noted above, references to modern depositional settings appear in much of the early stratigraphic literature, but in the 1950s studies of 'the modern' became more focused. Much of this was due to the recognition by some oil companies of the value of understanding the primary origins of petroleum-bearing rocks. A leader in this field was the research team at Shell Development Company.

Some of the earliest of these studies of modern environments were carried out in carbonate environments, including

the work of Illing (1954), and Newell and Rigby (1957) on the Great Bahamas Bank, and Ginsburg and Lowenstam (1958) on the Florida platform. This, and other work on ancient carbonate deposits (referred to below), led to two approaches to the classification of carbonate rocks (Folk 1962; Dunham 1962) that are still used today. In fact, these two papers (which appeared in the same SEPM Special Publication) are among the most important of the 'classic' papers mentioned in this paper, because of their long survival. Later studies of the Bahamas and Florida by Purdy (1963a, b) and Ball (1967) contributed much to the subsequent growth of facies models for carbonate platforms and reefs.

The other outstanding set of classic works consists of the research on the Texas coastal plain by Bernard, Leblanc and their colleagues at Shell, building on the preliminary work of Nanz (1954). The first facies model for barrier islands emerged from the work of these individuals on Galveston Island (Bernard et al. 1959, 1962). The point-bar model for meandering rivers is also attributed to this group, based on their studies of the Brazos River (Bernard et al. 1962; Bernard and Major 1963).

The Mississippi River and Delta is one of the largest of modern fluvial–delta systems, and its location in the centre of one of the most important, well-populated, industrial and tourist regions of the United States, in a petroleum province that generates a quarter of the US domestic supply, has led to intensive environmental and geological studies. The stratigraphic significance and complexity of the deposits of this system were first brought to geologists' attention by the detailed work of Fisk (1944). From the point of view of the growth of sedimentology the studies of Frazier (1967) were more significant, providing architectural block diagrams that illustrated the growth of distributaries in a river-dominated delta. Later studies by Fisher et al. (1969, 1972) broadened the scope of delta studies to other regions of the Texas coast and to other deltas worldwide, providing an essential basis for the subsequent development of formal delta facies models. Shepard et al. (1960) edited a collection of broader studies of the Gulf Coast.

Exploration methods for the continental shelf and deep oceans were primitive, until the introduction of side-scan sonar methods and improvements in navigation. The GLORIA sonar system was developed in 1970, but did not receive widespread use for geological purposes until it was adopted by the US Geological Survey in 1984 at the commencement of a program to map the newly established US Exclusive Economic Zone. The Deep Sea Drilling Project (DSDP) began in 1968. Extensive use of seismic stratigraphic techniques had to await the developments taking place in Shell, Exxon and BP, as noted below (in particular, the work of Vail et al. 1977). Sedimentological studies of the continental shelves and slopes, and the deep basin were being carried out at this time, but the main breakthroughs in sedimentological analysis came from studies of the ancient sedimentary record, and are referred to below.

Facies Model Concept (1959–2010)

By the late 1950s a key idea was emerging that environments could be categorized into a limited number of depositional configurations, which are amenable to basic descriptive summaries. The first explicit use of the term '**facies model**' was in a conference report by Potter (1959, p. 1292). He opened the report with the following words:

> *A discussion concerning sedimentary rocks was held at the Illinois State Geological Survey on 4-5 Nov. 1958, for the purpose of pooling the knowledge and experience of the group concerning three topics: the existence and number of sedimentary associations; the possibility of establishing a model for each association that would emphasize the areal distribution of lithologic units within it; and the exploration of the spatial and sequential relations between the associations.*

Later, on the same page, this definition is provided:

> *A facies model was defined as the distribution pattern or arrangement of lithologic units within any given association. In the early stages of geological exploration, the function of the model is to improve prediction of the distribution of lithologic types.*

Note that the essential basis for a facies model is the recognition of a distinctive **facies association**. Much work to identify these associations now ensued.

A mention should be made here of the term **process-response model**. This term has sometimes been used with essentially the same meaning as facies model. Whitten's (1964, p. 455) discussion of this term quoted from Krumbein and Sloss (1963, p. 501), who:

> *suggested that in the search for "... generalizing principles it is a useful philosophical device to recognize models – actual or conceptual frameworks to which observations are referred as an aid in identification and as a basis for prediction."*

The journal *Sedimentology* was founded by the International Association of Sedimentologists (IAS) in 1962. The editor was Aart Brouwer from the University of Leyden in the Netherlands, representing what had become a strong Dutch school of sedimentological studies. All the early work on tidal flat sedimentation emerged from this school (e.g. Van Straaten 1954). The then President of the IAS, the American marine geologist Francis Shepard said this, in the preface on p. 1 of v. 1 of the new journal:

> *As this is written, there appear to be several primary purposes in sedimentological studies. One is to relate more completely the present day sediments to ancient sedimentary rocks. Although much has been done in this field recently, there are numerous types of sedimentary rocks for which no equivalent has yet been found in the sediments of today and some correlations need careful reexamination to see if they are correctly interpreted. Another need is for more careful study of sedimentary structures that are often obscured both in old and recent sediments. These structures can be very useful in interpreting paleoclimates and conditions of deposition of ancient sediments. A third important field to investigate is the geochemistry of sediments. Some of the early indications from the chemical nature of sediments have proven misleading and are in need of further study to explain apparent anomalies. Fourth, the rates of sedimentation can be given much more study with all of the new radioactive counting methods.*

In an introductory assessment of sedimentary studies immediately following the preface, editor Brouwer (1962, p. 2–3) reviewed the early history and origins of the separate discipline now called **Sedimentology**:

> *Essential parts are derived from sedimentary petrography,*

> *others from stratigraphy and still others have a purely palaeontological source. Perhaps stratigraphy takes a more or less central position, and many definitions recently given of stratigraphy (Hedberg 1948; Weller 1960; and others) seem to include nearly all of sedimentology, at least of ancient rocks. This is quite understandable, as sedimentary rocks are the stratigrapher's natural environment. Three modem textbooks, whose scope is mainly sedimentological, have "stratigraphy" in their title (Krumbein and Sloss 1951; Dunbar and Rodgers 1957; Weller 1960).*

The reference to sedimentary petrography should be noted here. The first journal to deal specifically with sedimentological topics, the *Journal of Sedimentary Petrology*, was founded in 1931, and initially dealt exclusively with petrographic studies, including studies of detrital composition and provenance, and diagenesis. The scope of the journal gradually widened, and the name was changed to the *Journal of Sedimentary Research* in 1994. According to Gerard V. Middleton (2005) the term **Sedimentology** was coined by A.C. Trowbridge in 1925 and first used in print by Waddell in (1933), but did not come into common usage until the 1950s.

Now began a focused program to identify specific lithofacies and lithofacies associations by direct comparison between modern sediments and the preserved record. The comparison went both ways, determined in large measure by the initial interests of the researcher. One of the first of these studies was that by Beales (1958, p. 1846) who proposed the term **bahamite** for "the granular limestone that closely resembles the present deposits of the interior of the Bahamas Banks described by Illing (1954)." Although this new term did not become part of the sedimentological lexicon, the methods pioneered by Beales and his colleagues were about to become part of the mainstream.

Two classic studies appeared in the early 1960s, Bouma's (1962) turbidite model and Allen's (1964) point-bar model for meandering river deposits. Both are concerned primarily with interpretation of the rock record, but make extensive reference to deposits and structures forming at the present day.

There appeared a flood of new work during the 1960s and 1970s making use of the new facies model concepts. Potter (1967) reviewed sandstone environments. He stated (Potter 1967, p. 360):

> *The facies-model concept with its emphasis on the existence of relatively few recurring models represents cause-and-effect "deterministic geology"– an approach that attempts to relate distribution and orientation of sand bodies in a basin to measurable, causal factors.*

However, much of Potter's discussion dealt with grain size and other petrographic issues, and discussions about the shape and orientation of sand bodies (of importance for stratigraphic trap prospecting) rather than facies modeling, as this term has come to be understood.

An edited compilation that appeared in the middle of this period (Rigby and Hamblin 1972) provides another good snapshot of the state of sedimentology at this time. It opens with a brief review of the topic of 'environmental indicators' by H.R. Gould and this is followed by a classification of sedimentary environments by E.J. Crosby, and by eleven chapters providing details of seven depositional environments (three chapters on alluvial sediments and one discussing the use of trace fossils). There were also several important new textbooks published during this period (e.g. Blatt et al. 1972; Reineck and Singh 1973; Wilson 1975; Friedman and Sanders 1978; Reading 1978). That by Blatt et al (1972) contains the first summary of depositional environments specifically focused on the concept of the facies model (and using that term in the chapter heading).

The critical contribution at this time was the development by Walker (1976) of a formal, theoretical description of the concept of the facies model and its value as a summary and a predictor. Central to this work was a new concept that environments could be characterized by a discrete and limited number of specific facies states. Drawing on Middleton's (1973) restatement of Walther's Law, Walker emphasized the importance of the vertical succession of facies, and introduced the **facies relationship diagram**, a semi-quantitative expression of the range of vertical transitions revealed by careful vertical measurement of a stratigraphic succession. Reference was made to a detailed study of de Raaf et al. (1965), which was the first to employ the concept of facies states and the use of a facies relationship diagram. Another study of vertical facies relationships at this time was that by Miall (1973) using the basic concepts of Markov chain analysis.

Walker's (1976, figure 4) diagram summarizing the construction of a facies model as a process of 'distilling away the local variability' to arrive at the 'pure essence of environmental summary' has been much reproduced.

Walker's (1976) paper appeared first in this journal, *Geoscience Canada* (founded and edited by his colleague at McMaster University, Gerard Middleton), and was intended as the introductory paper in a series of invited articles written mainly by Canadian sedimentologists dealing with specific environments and facies models. The series was later published as a stand-alone volume (Walker 1979) which became a best-seller and subsequently, under changing editorships, went into four editions (Walker 1984, Walker and James 1992; James and Dalrymple 2010). Its success was due in large measure to the concise nature of the descriptions, the elegant diagrams, and the emphasis on the nature of the vertical profile, making this a very practical approach for undergraduate teaching and for work with well logs and cores. A close competitor was the edited volume compiled by Reading (1978), a book written at a more advanced, graduate to professional level by him and some of his graduate students at the University of Oxford. This book went into two later editions (1986, 1996).

Among the other widely used facies models that appeared in the *Geoscience Canada* series (and subsequently in Walker 1979) was a treatment of continental shelf sedimentation highlighting the rock record of hummocky cross-stratification, and a simple and elegant model for submarine fans based almost entirely on ancient fan deposits in California and Italy. In this book, carbonate facies models were compiled and co-authored by Noel P. James, who became a co-editor of later editions. **Ichnology**, the study of trace fossils, evolved into an enormously valuable subsurface facies analysis tool, allowing detailed analysis of sedimentary environments in drill core, as well as throwing much useful light on the significance of stratal surfaces, with the preservation of evidence of non-deposition and early lithification (Frey and Pemberton 1984; McEachern et al. 2010).

By the mid-1970s the stage was set for Sedimentology to flourish. The Walker (1979) *Facies Models* volume, and Reading's (1978) textbook were enormously influential. However, through the 1980s sedimentology remained largely isolated from the 'big-picture' concepts that were emerging from the plate-tectonics revolution, and developments in seismic stratigraphy. These I discuss below. Textbooks that appeared during this period (e.g. Miall 1984; Matthews 1984; Boggs 1987) deal with all these topics essentially in isolation, as separate chapters with little cross-referencing. As I argue below, it took the maturing of sequence stratigraphy to bring these topics together into what we may now term sophisticated stratigraphy.

The Impact of the Plate-Tectonics Revolution on Basin Studies (1959–1988)

The plate-tectonics revolution explained where and why basins form, provided a quantitative basis for their subsidence and uplift behaviour, and elucidated the relationships between sedimentation and tectonics. As far as sedimentary geology is concerned, the revolution was not complete until the mid-1970s, when the re-classification of basins in terms of their plate tectonic setting reached maturity. However, some important preliminary studies pointed the way.

Bally (1989, p. 397–398) noted the work of Drake et al. (1959) "who first tried to reconcile modern geophysical–oceanographic observations with the geosynclinal concept" and that of Dietz (1963) and Dietz and Holden (1974) who were the first to equate Kay's 'miogeosyncline' with the plate tectonic concept of an Atlantic-type passive continental margin. Mitchell and Reading (1969) made one of the first attempts to reinterpret the old tectono-stratigraphic concepts of **flysch** and **molasse** in terms of the new plate tectonics.

But it was John Bird and John Dewey, in two papers published in 1970, who completely revolutionized our understanding of the origins of sedimentary basins (and much of the rest of geology) with reference to the geology of the Appalachian orogen, in particular, that portion of it exposed throughout the island of Newfoundland (Bird and Dewey 1970; Dewey and Bird 1970). Dickinson (1971) made reference to all of this work in his own first pass at relating sedimentary basins to plate tectonics.

These breakthroughs of the 1970s initiated a worldwide explosion of studies of basins and tectonic belts exploring the new plate tectonic concepts. Through the 1970s, a series of books and papers was published containing the results (Dickinson 1974; Dott and Shaver 1974; Burk and Drake 1974; Strangway 1980; Miall 1980, 1984). One of the more important of these contributions was a paper by Dickinson (1974) which constituted the first comprehensive attempt to classify sedimentary basins of all types in terms of their plate tectonic settings. This paper was particularly notable for the extensive treatment of arc-related basins, and was followed up by a more detailed paper on this subject (Dickinson and Seely 1979) that remained the standard work on the subject for many years. This latter work was based in part on the recognition of a series of arc-related sedimentary basins within the Cordillera (Dickinson 1976), especially the Great Valley basin of California, which has long served as a type example of a forearc basin (e.g. Ingersoll 1978a, b, 1979).

Miall (1984, p. 367) argued that, by the application of judicious simplification and by skillful synthesis we can systematize the descriptions of depositional systems (their facies assemblages and architecture), structural geology, petrology, and plate tectonic setting into a series of **basin models**, for the purpose of interpreting modern and ancient sedimentary basins. Dickinson (1980, 1981) used the term **petrotectonic assemblages** with the same meaning. These basin models are then a powerful tool for interpreting regional plate tectonic history.

Another important era in the field of basin analysis was initiated by the development of quantitative, geophysically based models of crustal subsidence, commencing in the late 1970s. The importance of these models to the development of stratigraphy was that they provided the basis for the development of quantitative models of subsidence and accommodation generation that greatly improved our understanding of large-scale basin architectures. The main breakthrough in the development of a modern extensional margin basin model was made by McKenzie (1978), based in part on his studies of the subsidence of the Aegean Sea. This classic paper introduced the concept of crustal stretching and thinning during the initial sea-floor spreading event, and showed quantitatively how this could account for the subsidence history of Atlantic-type margins. Many of the important early tests of this model were carried out on the Atlantic margin of the United States. Stratigraphic data were obtained from ten Continental Offshore Stratigraphic Test (COST) wells drilled on the continental shelf off New England between 1976 and 1982, and led to the development of formal backstripping procedures (Watts and Ryan 1976; Steckler and Watts 1978; Watts 1989) and to simple computer graphic models of subsiding margins (Watts 1981) that were very useful in illustrating the development of the basic architecture of Atlantic-type margins. Dewey (1982) emphasized their simple two-stage development: the early phase of rifting, typically capped by a regional unconformity, followed by a thermal relaxation phase which generates a distinctive pattern of long-term onlap of the basement.

An important modification of the McKenzie model was to recognize the importance of simple shear during continental extension, as expressed by through-going extensional crustal detachment faults (Wernicke 1985). This style of crustal extension was first recognized in the Basin and Range Province of Nevada, and was suggested by preliminary seismic data from the facing continental margins of Iberia and the Grand Banks of Newfoundland (Tankard and Welsink 1987). The North Sea basin is the best studied rift basin, and has provided many insights regarding subsidence styles and structural geology (White and McKenzie 1988).

Turning to the other major class of sedimentary basins, those formed by flexural loading of the crust, it was Barrell (1917, p. 787) who was the first to realize that "the thick nonmarine strata of the Gangetic plains accumulated in space made available by subsidence of the Indian crust beneath the mass of thrust plates of the Himalayan Range" (Jordan 1995, p. 334). Price (1973) revived the concept of regional isostatic subsidence beneath the supracrustal load of a fold–thrust belt that generates the marginal moat we now term a foreland basin (a term introduced by Dickinson 1974), based on his work in the southern Canadian Cordillera. Beaumont (1981) and Jor-

dan (1981) were the first to propose quantitative flexural models for foreland basins, constraining the models with detailed knowledge of the structure and stratigraphy of the studied basins. It is clear that the crust must have mechanical strength for a wide foredeep, such as the Alberta Basin or the Himalayan foreland basin, to be created. The classic architecture of a foreland basin is defined by the isopachs of the sediment fill, which is that of an asymmetric lozenge, with a depocentre adjacent to the location of the crustal load, tapering along strike and also thinning gradually away from the orogen towards the craton.

Two major developments contributed to our current understanding of these basins. Firstly, exploration drilling and reflection seismic data led to an understanding of the structure and dynamics of the fold–thrust belts that border foreland basins and, during uplift, provide much of their sediment. Secondly, a growing knowledge of crustal properties permitted the development of quantitative models relating crustal loading, subsidence, and sedimentation. A significant development during the 1960s and 1970s was the elucidation of the structure of the fold–thrust belts that flank many orogenic uplifts and clearly served as the source for the clastic wedges referred to above. McConnell (1887) was one of the first to emphasize the importance of thrust faulting and crustal shortening in the formation of fold–thrust belts, based on his work in the Rocky Mountains of Alberta. As noted by Berg (1962), the mapping of faults in the Rocky Mountains of the United States and their interpretation in terms of overthrusting became routine in the 1930s. However, as his paper demonstrates, seismic and drilling data available in the early 1960s provided only very limited information about the deep structure of thrust belts. The release of seismic exploration data from the southern Rocky Mountains of Canada by Shell Canada led to a landmark study by Bally et al. (1966) and set the stage for modern structural analyses of fold–thrust belts. A series of papers by Chevron geologist Clinton Dahlstrom, concluding with a major work in 1970, laid out the major theoretical principles for the understanding of the thrust faulting mechanism (Dahlstrom 1970).

The final piece of the puzzle was to explain accommodation generation and the occurrence or regional tilts and gentle angular unconformities on cratons hundreds of kilometres from plate margins — the phenomenon termed **epeirogeny**. Modeling of mantle processes indicated the presence of convection currents that caused heating and uplift or cooling and subsidence of the crust. Gurnis (1988, 1990, 1992) termed this **dynamic topography**. Cloetingh (1988) described the process of **intraplate stress** (also termed **in-plane stress**) whereby horizontal stresses exerted on plates, such as the outward-directed compressive stress from sea-floor spreading centres ('ridge push'), may be expressed as intraplate earthquakes that cumulatively develop faults and long-wavelength folds.

Unconformities and the Issue of Time in Stratigraphy (1909–1970)

Although some of the ideas discussed in this section have been around for many years, the issue of time in stratigraphy did not begin to have a major influence on the science until Ager's work in the 1970s, and it was not until the full flowering of sequence stratigraphy in the 1990s that such contributions as Barrell's accommodation diagram and Wheeler's chronostratigraphic charts (both discussed below) were fully integrated into the science of stratigraphy.

The science of geology began with James Hutton's observations in and around Scotland in the late eighteenth century. His discovery of the angular Silurian–Devonian unconformity at Siccar Point on the coast of southeast Scotland gave rise to Playfair's (1802) famous remark about the "abyss of time."

A predominant strand in geological work during the nineteenth and early twentieth centuries was the gradual documentation of the lithostratigraphy and biostratigraphy of sedimentary basins worldwide. As documented elsewhere (Berry 1968, 1987; Hancock 1977; Conkin and Conkin 1984; Miall 2004), some remarkably refined zonation schemes resulted from this work, and stratigraphic terminology and methods gradually evolved to facilitate description and classification, but until the development of radioisotopic dating by Ernest Rutherford and Arthur Holmes (Holmes' first book on the geological time scale was published in 1913) the development of a quantitative understanding of earth processes was limited (I do not discuss the early evolution of biostratigraphic concepts here. See the references cited above).

Geological mapping and research in North America during the 'frontier' period is usefully summarized by Blackwelder (1909), who discussed the various types of sedimentary break (angular versus structurally conformable) and the duration of the missing time that they represented. His paper contained what is probably the first chronostratigraphic chart for the interior (cratonic) stratigraphy of North America, showing what was then known about the extent of the major Phanerozoic stratigraphic units on this continent and the unconformities that separate them.

In a paper that was remarkably ahead of its time, Barrell (1917, p. 747–748) set out what we now refer to as the concept of **accommodation**:

> *In all stratigraphic measures of time, so far as the writer is aware, the rate of deposition of a sedimentary series has been previously regarded as dependent on the type of sediment, whether sandstone, shale, or limestone, combined with the present rate of supply of such sediment to regions of deposition. Here is developed an opposite view: that the deposition of nearly all sediments occurs just below the local baselevel, represented by wave base or river flood level, and is dependent on upward oscillations of baselevel or downward oscillations of the bottom, either of which makes room for sediments below baselevel. According to this control, the rate of vertical thickening is something less than the rate of supply, and the balance is carried farther by the agents of transportation.*

Barrell (1917) was probably the first to understand the relationships among sedimentation, preservation, and accommodation. He constructed a diagram showing the "Sedimentary Record made by Harmonic Oscillation in Baselevel" (Barrell 1917, p. 796) that is remarkably similar to diagrams that have appeared in some of the Exxon sequence model publications since the 1980s (e.g. Van Wagoner et al. 1990, figure 39). It shows that when long-term and short-term curves of sea-level change are combined, the oscillations of base level provide only limited time periods when base-level is rising and sediments can accumulate. In his diagram "Only one-sixth of time is recorded" by sediments (Barrell 1917, p. 797). This remarkable diagram 1) anticipated Jervey's (1988) ideas about sedi-

mentary accommodation that became fundamental to models of sequence stratigraphy, 2) also anticipated Ager's (1981, 1993) point that the sedimentary record is "more gap than record," and 3) constitutes the first systematic exploration of the problem of preservation potential.

During the early part of the twentieth century there was much theorizing about the forces at work within the Earth to form mountain ranges and sedimentary basins. This is summarized elsewhere (e.g. Miall 2004) and not dealt with here, because ultimately it did not contribute much to the development of modern stratigraphy. However, the practical work of petroleum exploration did make a difference. The distinguished petroleum geologist A.I. Levorsen was one of the first to describe in detail some examples of the 'natural groupings of strata on the North American craton:'

> *A second principle of geology which has a wide application to petroleum geology is the concept of successive layers of geology in the earth, each separated by an unconformity. They are present in most of the sedimentary regions of the United States and will probably be found to prevail the world over (Levorsen 1943, p. 907).*

This principle appears to have been arrived at on the basis of practical experience in the field rather than on the basis of theoretical model building. These unconformity-bounded successions, which are now commonly called '**Sloss sequences**,' for reasons which we mention below, are tens to hundreds of metres thick and, we now know, represent tens to hundreds of millions of years of geologic time. They are therefore of a larger order of magnitude than the cyclothems. Levorsen did not directly credit Grabau, Ulrich, or any of the other contemporary theorists who were at work during this period (see Miall 2004), nor did he cite the description of unconformity-bounded 'rock systems' by Blackwelder (1909). Knowledge of these seems to have been simply taken for granted.

The symposium on "Sedimentary facies in geologic history" referred to above contained a lengthy treatment of facies variability in the Paleozoic rocks of the cratonic interior of the United States by Sloss et al. (1949). In this paper much use is made of isopachs and lithofacies maps using Krumbein's (1948) concepts of clastic ratios and sand-shale ratios. The work revealed to the authors the contradictions inherent in current classifications of rock units in North America according to standard geologic time units. The use of the standard time scale (Cambrian, Ordovician, etc.) as a basis for mapping, obscured the fact that the major sedimentary breaks within the succession commonly did not occur at the divisions provided by the time scale, and so they set out to establish 'operational units' for mapping purposes. Thus were born the first **sequences** for the North American interior: the Sauk, Tippecanoe, Kaskaskia and Absaroka.

The Sloss et al. (1949) paper in the symposium volume (Longwell 1949) is followed by nearly 50 pages of published discussion by many of the leading American geologists of the day, in which the issues raised by detailed mapping and the concepts and classifications available at the time for their systematization were fully discussed. This broader discussion is dealt with at length elsewhere (Miall 2004; Miall 2010, Chap. 1). For the purpose of this review, the importance of the Sloss et al. (1949) paper and the wider discussion of sedimentary facies contained in the other papers is that it clearly confirmed, at the time of publication, the need for a systematic differentiation of descriptive terminologies for 'time' and for the 'rocks.' This had been provided by Schenk and Muller (1941), who proposed the following codification of stratigraphic terminology:

Time division (for abstract concept of time)	Time-stratigraphic division (for rock classification)
Era	-
Period	System
Epoch	Series
Age	Stage
Phase	Zone

Harry E. Wheeler (Wheeler 1958, p. 1050) argued that a time-rock (chronostratigraphic) unit could not be both a 'material rock unit' and one whose boundaries could be extended from the type section as isochronous surfaces, because such isochronous surfaces would in many localities be represented by an unconformity. Wheeler developed the concept of the chronostratigraphic cross-section, in which the vertical dimension in a stratigraphic cross-section is drawn with a time scale instead of a thickness scale. In this way, time gaps (unconformities) become readily apparent, and the nature of time correlation may be accurately indicated. Such diagrams have come to be termed '**Wheeler plots**.' Wheeler cited with approval the early work of Sloss and his colleagues, referred to in more detail below:

> As a tangible framework on which to hang pertinent faunal and lithic data, the *sequence* of Sloss, Krumbein and Dapples (1949, pp. 110-11) generally fulfills these requirements. Paraphrasing these authors' discussion, a *sequence comprises an assemblage of strata exhibiting similar responses to similar tectonic environments over wide areas, separated by objective horizons without specific time significance* (Wheeler 1958, p. 1050; italics as in original).

Sequences came later to be called simply '**unconformity-bounded units**.'

Wheeler's (1958) methods are now universally accepted, although in practice they are still rarely applied. Ager (1973) is famous for his remark that "the sedimentary record is more gap than record." In a later book he expanded on the theme of gaps. Following a description of the major unconformities in the record at the Grand Canyon, he said, (Ager 1993, p. 14):

> *We talk about such obvious breaks, but there are also gaps on a much smaller scale, which may add up to vastly more unrecorded time. Every bedding plane is, in effect, an unconformity. It may seem paradoxical, but to me the gaps probably cover most of earth history, not the dirt that happened to accumulate in the moments between. It was during the breaks that most events probably occurred.*

Dott (1983, 1996) similarly warned about the episodic nature of sedimentation. However, as discussed elsewhere (Miall 2015), stratigraphers are still not dealing fully with the issue of time and its representation in the rock record.

The evolution of chronostratigraphic methods and the increasing accuracy and precision with which sedimentary rocks can be dated is discussed in detail elsewhere (Miall 2004; Miall 2010, Chap. 14). A landmark in the development of modern stratigraphy was the adoption in the 1970s of the GSSP principle for the fixing of major chronostratigraphic boundaries. GSSP stands for **Global Stratigraphic Sections**

and Points, and is a system for identifying outcrop sections that are accepted by the international community as marking the boundaries of stages and series (McLaren 1970).

Sequences and Seismic Stratigraphy (1963–1977)

Building on his earlier work (Sloss et al. 1949), further analysis by Sloss (1963) added two more sequences of Mesozoic–Cenozoic age to the North American suite (Zuni, Tejas) and firmly established the concept of the large-scale control of cratonic stratigraphy by cycles of sea-level change lasting tens of millions of years. In later work, Sloss (1972) demonstrated a crude correlation of these sequences with a similar stratigraphy on the Russian Platform, thereby confirming that global sea-level cycles constituted a major sedimentary control. However, Sloss, unlike his student Peter Vail, was never convinced that global eustasy told the entire story (Sloss 1988, 1991). In his 1963 paper Sloss included a pair of diagrammatic cross-sections of the Sauk and Tippecanoe sequence across the cratonic interior of North America that clearly indicated an angular unconformity between the two sequences, a relationship that could only have been developed as a result of broad warping of the craton before deposition of the Tippecanoe sediments.

Ross (1991) pointed out that all the essential ideas that form the basis for modern sequence stratigraphy were in place by the 1960s. The concept of repetitive episodes of deposition separated by regional unconformities was developed by Wheeler and Sloss in the 1940s and 1950s. The concept of the 'ideal' or 'model' sequence had been developed for the mid-continent cyclothems in the 1930s. The hypothesis of glacioeustasy was also widely discussed at that time. Van Siclen (1958) provided a diagram of the stratigraphic response of a continental margin to sea-level change and variations in sediment supply that is very similar to present-day sequence models. An important symposium on cyclic sedimentation convened by the Kansas Geological Survey marks a major milestone in the progress of research in this area (Merriam 1964); yet the subject did not 'catch on.' There are probably two main reasons for this. Firstly, during the 1960s and 1970s sedimentologists were preoccupied mainly by autogenic processes and the process-response model, and by the implications of plate tectonics for large-scale basin architecture. Secondly, geologists lacked the right kind of data. It was not until the advent of high-quality seismic reflection data in the 1970s, and the development of the interpretive skills required to exploit these data, that the value and importance of sequence concepts became widely appreciated. Shell, British Petroleum, and Exxon were all actively developing these skills in their research and development laboratories in the 1970s. The first published use of the term '**seismic stratigraphy**' was in a paper by Fisher et al. (1973) describing a subsurface succession in Brazil (the term appeared in the Portuguese language as 'estratigrafia sismica'). Peter Vail, working with Exxon, was the first to present his ideas in the English-speaking world, at the 1974 annual meeting of the Geological Society of America, but it was his presentation the following year at the American Association of Petroleum Geologists (Vail 1975) that caught the attention of the petroleum geology community. This was the beginning of the modern revolution in the science of stratigraphy.

The key idea that Vail and his colleagues proposed was that large-scale stratigraphic architecture could be reconstructed from reflection seismic records. Their publication of Memoir 26 of the American Association of Petroleum Geologists (Vail et al. 1977) was one of the major landmark events in the development of modern stratigraphy. Vail had learned about sequences from his graduate supervisor, Larry Sloss, and added to these his own ideas about global sea-level change (eustasy) as the major allogenic control of sequence development. The debate about global eustasy was long and controversial, and has been amply aired elsewhere (see Miall 2010). However, what emerged from the debate was the critical importance of the 'big-picture' in stratigraphic reconstruction, and the predictive value of sequence models. Having once seen a seismic record interpreted in terms of seismic stratigraphy, with its emphasis on seismic terminations and regional unconformities, and the common occurrence of clinoform architectures, old concepts of 'layer-cake' stratigraphy were dead forever.

It also seems likely that, working in the Gulf Coast, Vail learned from the 'big-picture' stratigraphers at the Bureau of Economic Geology. The regional view exemplified by work such as the Texas atlas (Fisher et al. 1972) and the seismic interpretation that these individuals were already working on, and which eventually appeared in the same AAPG Memoir (Brown and Fisher 1977) were very influential in helping sedimentary geologists understand the large-scale setting and tectonic influences on sedimentary basins at the very time that geophysical basin models were providing the quantitative basis for the plate tectonic interpretations of these basins.

Peter Vail has come to be called the 'Father' of sequence stratigraphy, while his graduate supervisor, Larry Sloss, has posthumously earned the title of the 'Grandfather' of sequence stratigraphy.

Architectural Elements: Sedimentology in Two and Three Dimensions (1983–1990)

Lithofacies maps and isopachs, and the reconstruction of regional paleocurrent patterns had become standard tools of the sedimentary geologist (or basin analyst) by the 1970s (the second edition of the Potter and Pettijohn book *Paleocurrents and basin analysis* was published in 1977), but they often failed to capture the fine detail of sedimentary processes that were by now emerging from facies studies. As Miall (1984, Sect. 5.3) pointed out, these mapping methods tended to produce generalizations that did not always reflect the rapidly shifting patterns of depositional systems that could now be reconstructed from detailed sedimentological study of outcrops, well records and cores.

There was a scale mismatch. Lithofacies maps typically dealt with large map areas (tens to hundreds of kilometres across) and sections tens of metres thick, grouping together depositional systems that may have undergone rapid paleogeographic change, thus obscuring local detail. Facies studies at this time (the 1970s to early 1980s) were one-dimensional, focusing on the vertical profile in drill records or outcrops (typically a few metres to tens of metres high). What was clearly needed were the tools to put the observations together. Three-dimensional sedimentological studies provided part of the answer, particularly for outcrop analysis, and sequence studies focused on the larger picture.

Work on fluvial systems by Allen (1983) and by Ramos and his colleagues (Ramos and Sopeña 1983; Ramos et al. 1986) led the way. These papers focused on large two-dimensional outcrops of complex fluvial deposits and offered classifications of the lithofacies units that described them in two or three dimensions. Picking up on this early work, Miall (1985, 1988a, b) offered a systematized approach that re-stated the lithofacies classification idea in terms of a limited suite of **architectural elements** that, it was proposed, constitute the basic building blocks of fluvial assemblages. One of the strengths of the approach is the ability to relate paleocurrent observations to the fine detail of the channel and bar complexes, revealing whole new insights into the bar construction and preservation processes. Comparable approaches have subsequently been adopted for other depositional environments. The use of photomosaics as base maps for analysing large outcrops has become standard, and there have been technological developments, such as the use of LIDAR methods for outcrop documentation, facilitating the digitization of observations, corrections for scale problems and perspective effects in ground observations, and so on.

Sequence Stratigraphy (1986–1990)

In the decade following the publication of AAPG Memoir 26 (Payton 1977) a wholesale re-evaluation of regional stratigraphy was under way. The significance of this revolution can be exemplified by the first publication that applied the new sequence concepts to an important swath of regional geology, the Cardium Sandstone of Alberta. This loosely defined unit is host to the largest oil field hosted in a clastic reservoir in Canada, the Pembina field, and stratigraphic and sedimentological studies of the unit had been under way since it was discovered in 1953. The Pembina reservoir was difficult to understand. It consists of locally as much as 9 m of wave- and tide-deposited conglomerate accumulated some 200 km from the assumed contemporary shoreline. How did it get there? The new interpretation by Plint et al. (1986) reconstructed from well-logs a set of seven basin-wide surfaces of erosion and transgression, implying cycles of base-level change lasting about 125 ka. The interpretation was controversial, and was subject to intense discussion at the time (Rine et al. 1987), but the interpretation has stood the test of time, and has led to a complete remapping of Alberta basin stratigraphy using the new sequence concepts (Mossop and Shetsen 1994).

Meanwhile, researchers working with seismic data, particularly in the research laboratories of Shell, BP and Exxon, were applying sequence concepts to basins around the world, yielding many insights into stratigraphic architecture and regional basin controls, particularly the importance of tectonism, even though the global-eustasy paradigm remained dominant throughout the 1980s and early 1990s. Several atlases were published at this time, taking advantage of the large atlas format to display reflection seismic cross-sections at large scales (Bally 1987). Even more importantly, in 1988 a second major production by the team at Exxon was published (Wilgus et al. 1988), showing in detail how sequence concepts could incorporate facies analysis and could be applied to outcrop studies. The **systems tract** concept reached a full expression in several key papers in this book (Posamentier and Vail 1988; Posamentier et al. 1988), building on experimental models of Jervey (1988) that essentially reinvented Barrell's (1917) ideas about accommodation and its control on sedimentation, and developed them further in the light of modern facies concepts.

Another important publication from the Exxon team was that by Van Wagoner et al. (1990) which presented the results of several detailed field mapping projects and extended the reach of sequence concepts further, to regional outcrop and subsurface studies. Largely on the basis of these two publications by the Exxon team, the term seismic stratigraphy began to be replaced in common use by the more general term **sequence stratigraphy.**

Reconciling Facies Models with Sequence Stratigraphy (1990)

By the year 1990 a moment of tension had arrived in the evolution of sophisticated stratigraphy. The enormously successful facies model approach, focusing on very detailed local studies, including meticulous analysis of drill cores, had resulted in a proliferation of sedimentological studies and numerous refinements of ideas about how to classify and subdivide sedimentary environments in an ever expanding range of tectonic and climatic settings. Most interpretations dwelt at length on autogenic sedimentary processes. Meanwhile, sequence stratigraphy had introduced an entirely different scale of research, encompassing whole basins, and focusing on allogenic controls, particularly sea-level change. In addition, the architectural element approach to facies studies departed from the clean simplicity of the vertical profile by suggesting multi-dimensional assemblages of sedimentary building blocks in patterns difficult to pin down and classify.

The problems may be exemplified by an examination of a paper by Walker (1990), who was attempting to reconcile his facies model approach to the new concepts and methods. He (Walker 1990, p. 779) complained that the architectural element approach, which treated elements as building blocks that could be assembled in multiple ways (Miall 1985), constituted 'sedimentological anarchy.' Walker (1990) conceded that the proliferation of information about environments and facies associations that had resulted from the explosion of facies studies rendered the simple facies model approach for complex depositional systems (such as submarine fans) inadequate. He referred approvingly to the depositional systems approach exemplified by Fisher and McGowen (1967).

> *Future facies modeling must emphasize these contemporaneous, linked depositional environments, and their response to tectonics and changes of relative sea level. This will combine the strengths of classical facies modeling with the recognition that widely spaced and "distinct" geographic environments (summarized as models) can be rapidly superimposed as part of one transgressive or regressive system (Walker 1990, p. 780).*

Walker (1990, p. 781) also expressed concern regarding the new concepts of sequence stratigraphy, which were becoming popular at this time. He pointed out the ambiguity in some of the definitions (e.g. that of the **parasequence**), the uncertainty with regard to scale, and the lack of clarity in such expressions as 'relatively conformable.' The issue of scale arises with reference to such expressions as 'genetically related' strata. In facies model studies, genetically related implies gradational contacts between lithofacies that are related to each other in

the sense implied by Walther's Law. In sequence stratigraphy, genetically related means the deposits formed during a full cycle of base-level change, although, as Walker (1990, p. 784) pointed out, using Galloway's (1989) **genetic stratigraphic sequence model** implies that strata above and below a subaerial erosion surface (the E/T surfaces of Plint et al. 1986), are genetically related, which they are certainly not.

While reluctant to fully embrace the new methods and terminology of sequence stratigraphy, Walker (1990) conceded that the regional patterns and the emphasis on large-scale sedimentary controls that were being revealed by sequence studies were valuable. As a compromise he proposed the adoption of the new system of **allostratigraphy** that had been proposed in 1983 by the North American Commission on Stratigraphic Nomenclature. Allostratigraphy is based on the recognition, mapping and subdivision of unconformity-bounded units. For example, a typical sequence, in the sense implied by Vail et al. (1977) constitutes an alloformation.

The Full Flowering of Modern Sequence-Stratigraphic Methods

When sequence stratigraphy was introduced to the geological community through the landmark publications of the Exxon Group (Payton 1977; Wilgus et al. 1988; Van Wagoner et al. 1990) it came with an overriding hypothesis that eustatic sea-level change was the main driver of changes in accommodation, and hence of sequence architecture. Doubts about the universal applicability of this hypothesis began to emerge in the 1980s, and by the mid-1990s most earth scientists had accepted that other factors, including climate change and regional tectonism may play a key role (Miall 1995). The controversy is described in detail in Miall (2010, Chap. 12).

The realization that many allogenic processes are at work during the accumulation of a basin fill gave renewed impetus to stratigraphic studies, because it became clear that sequence methods, combining the large scale of reflection seismic surveying with the facies scale of the outcrop or drill core, could be very powerful tools for the reconstruction of geologic history, as well as provide much more useful predictive stratigraphic models for petroleum exploration and development. The increasing use of horizontal 'seiscrop' sections (horizontal sections extracted from three-dimensional data volumes) has led to the development of an entirely new discipline, **seismic geomorphology**, which deals with the analysis of ancient depositional systems based on their preserved landscape architecture and three-dimensional construction (Davies et al. 2007; Hart 2013). Furthermore, the debate about global eustasy placed renewed emphasis on the need for accurate global chronostratigraphic correlations in order to test regional and global correlations, and this also encouraged new work in this field.

The flourishing of sequence stratigraphy as a research topic inevitably led to differences of interpretation and even to differences in the methods for defining sequences. For example, Hunt and Tucker (1992) showed how the Exxon sequence model was quite inadequate in dealing with the falling stage of a base-level cycle. Galloway (1989) proposed defining sequence boundaries at the maximum flooding surface rather than the subaerial erosion surface and its basinward correlative conformity. This and other controversies hindered the development of a uniform methodology and common language for dealing with sequences on a formal basis.

Catuneanu (2006), in what has become the standard textbook on sequence stratigraphy addressed these topics and showed how different approaches could be reconciled if care is taken with descriptions and definitions. In a series of papers culminating in a review for *Newsletters on Stratigraphy* he and selected colleagues have been leading the way in the work to gain acceptance for sequence stratigraphy as the appropriate formal basis for modern stratigraphic work (Catuneanu et al. 2009, 2010, 2011). More recently, Steel and Milliken (2013) have provided a very useful documentation of the many incremental additions to our knowledge of siliciclastic facies associations and models and their incorporation into sequence-stratigraphic interpretations.

Modern theoretical and experimental work is making substantial contributions to our understanding of processes of sedimentation and sequence generation. The specially designed experimental facility (eXperimental EarthScape Facility, or XES) described by Paola (2000) and Paola et al. (2001, 2009) is particularly well equipped to explore what Sheets et al. (2002) termed the stratigraphic 'mesoscale,' the time scale of years to thousands of years. Within this time frame, "the depositional pattern shifts from reflecting the short-term flow pattern to reflecting long-term basinal accommodation. Individual events are averaged to produce large-scale stratal patterns" (Sheets et al. 2002, p. 288). At this scale, autogenic processes grade into, or are affected by and modified by allogenic forcing. Muto and Steel (2004) demonstrated that, given steady conditions of discharge and sediment supply, prograding deltas will eventually start to 'autoincise' over the mesoscale time scale. Strong and Paola (2008) explored the evolving nature of valley incision, terrace formation and valley fill, and demonstrated that the valley-floor surface that ultimately is preserved in the geological record during a cycle of base-level change is an erosion surface that never actually existed in its entirety as a topographic surface in its preserved form, because it undergoes continuous modification by erosion or sedimentation until final burial. Kim and Paola (2007) demonstrated that the autogenic process of delta and channel switching may, under the influence of fault movement, develop cyclothem-like cycles over time periods of 10^5 years.

Meanwhile, the research theme centred on facies analysis is by no means complete. Advances in the understanding of processes and environments continue, aided by the experimental work touched on above and by improved observational methods. Three topics merit note: 1) the increasing recognition of the importance of cool water environments for carbonate sedimentation (James and Lukasik 2010), 2) an improved understanding of the development of deep-water turbidite deposits relative to the cycle of sea-level change and sediment delivery patterns, together with a much expanded understanding of the variability and complexity of turbidite systems, due in large measure to developments in marine geology, three-dimensional seismic surveying and large-scale outcrop work (Bouma et al. 1985; Arnott 2010), and 3) the increasing realization that in natural systems mud forms silt- and sand-sized floccules, and most mud is transported and deposited by currents of all kinds. Pelagic settling may be of minor importance as a source of mud deposits (Schieber et al. 2013).

Stratigraphy: The Modern Synthesis

The full flowering of modern stratigraphy represents the amalgamation of the concepts and methods encompassed in all of the separate developments described in the preceding sections. The power of the modern science could not possibly have evolved without the contributions from all of these strands of development. However, for the purpose of education and training, the basic components of modern stratigraphy can be broken down into the following list of seven broad topics. Key references are provided here to some of the main recent reviews and textbooks:

1. Facies analysis methods and facies models (James and Dalrymple 2010).
2. Sequence stratigraphy, concepts, definitions and methods (Catuneanu 2006).
3. Interpretations of the origins of sequences in terms of basin processes (tectonism, eustasy, climate change, etc.) (Miall 2010; Allen and Allen 2013).
4. Basin geodynamics: the origins of basins in terms of plate tectonics and crustal behaviour (Busby and Ingersoll 1995; Miall 1999; Allen and Allen 2013).
5. Modern seismic methods, including seismic geomorphology (Veeken 2007; Davies et al. 2007; Hart 2013).
6. Chronostratigraphy and the Geologic Time Scale (Gradstein et al. 2004, 2012; see also www.stratigraphy.org).
7. Modern formal stratigraphic methods (Salvador 1994). Updated methods at www.stratigraphy.org.

A specialized branch of stratigraphy deals with the Quaternary record. Specialists include archaeologists and anthropologists. Age dating reaches levels of accuracy and precision in the 10^3–10^4-year range, based on dating methods designed specifically for the Recent, including ^{14}C and U–Th radiometric methods, optically stimulated luminescence, cosmogenic radionuclides, and amino-acid geochronometry (http://www.inquasaccom.org/stratigraphic-guide/geochronometry/).

THE ACHIEVEMENTS OF MODERN STRATIGRAPHY

Two hundred years ago, William Smith gave us the first complete geological map (Smith 1815), and started us on the road to an understanding of Earth's geologic history. Lyell (1830–1833) provided the foundation for the future development of sedimentology, based on the principle of uniformitarianism, and Holmes, beginning a little more than one hundred years ago, began the development of the modern geological time scale (culminating in his first book: Holmes 1913). Barrell (1917) was the first to attempt to synthesize these critical developments, but most of his ideas were forgotten or ignored for decades. The development of the formal principles of stratigraphy, the evolution of sedimentology as a mature discipline, the stimulus provided by seismic stratigraphy, all have been necessary developments in the evolution of the modern synthesis that constitutes the science described in this review. So where have we arrived at today, and what may we predict as possible future developments and outcomes from the application of this science?

High-Resolution Stratigraphy

The current 'best practices' for chronostratigraphic analysis make use of the techniques of High-Resolution Event Stratigraphy, or HiRES. "The cornerstone of HiRES is the integration of every available piece of stratigraphic information into a single set of data that can be cross-correlated and internally calibrated" (Cramer et al. 2015, p. 138). Originally conceived by Kauffman (1986, 1988), the guiding principle is that there are many features of a sedimentary section, beyond biostratigraphy, that may be used to develop tools for correlation and dating. Stratigraphic events, such as storm beds, tephras, and flooding events, may have limited regional extents, but when used in combination across multiple stratigraphic sections and integrated with chemostratigraphic, magnetostratigraphic and other indicators, they may permit highly detailed stratigraphic syntheses to be developed. Figure 6 illustrates the principles involved in the development of an 'integrated event stratigraphy.' The application of this methodology is not necessarily straightforward. Individual events may be diachronous to a greater or lesser degree, particularly first and last occurrence taxon data, reflecting environmental control and migration patterns. For example, for HiRES work in the Paleozoic record, it remains a question whether conodonts or graptolites provide the most chronostratigraphically reliable information (Cramer et al. 2015). Other events, such as storm beds may be very confined in their distribution, and hiatuses of varying duration and extent complicate the record. Chemostratigraphic signatures vary in their diachroneity. Cramer et al. (2015, p. 148–149) suggested that given the long residence time of strontium and the magnitude of the Sr reservoir in the marine environment, the $^{87}Sr/^{86}Sr$ composition of ocean waters should be quite stable over long time scales, whereas the shorter residence time of ^{13}C makes $\delta^{13}C$ a higher-precision chronostratigraphic tool, but one with an imprecision in the 10^{3-4}-year range reflecting a mixing time of a few thousand years. For many parts of the Phanerozoic time scale the dates of chronostratigraphic boundaries can now be provided with precision in a range of 10^5 years (e.g. Sadler et al. 2009).

The Modern Geologic Time Scale

A quantum leap forward was achieved by the *International Commission on Stratigraphy* with the publication in 2004 of its updated Geologic Time Scale (GTS2004: Gradstein et al. 2004). Gradstein et al. (2012) subsequently published their own updated version (although this is not an official product of the International Stratigraphic Commission). The 2004 version incorporates numerous new data points, documented with the use of quantitative biostratigraphy, much-improved radiometric dating methods, chemostratigraphy and (for the Neogene) cyclostratigraphy. The new scale (Fig. 7) presents us with unprecedented opportunities for the comparison and calibration of detailed local and regional studies of rates and processes. Paleogene, Mesozoic and most Paleozoic ages are given to the nearest 100,000 years, although for parts of the scale, potential errors of >1 m.y. remain. This scale, like all before it, incorporates numerous revisions of assigned ages. Almost all major chronostratigraphic boundaries in the Mesozoic and Paleozoic have been revised by several million years relative to earlier scales, such as that of Berggren et al. (1995), reflecting new data or changing interpretations of earlier data. There is no sign, yet, that the time scale has finally stabilized, although the incremental changes from one scale to the next do appear to be getting smaller.

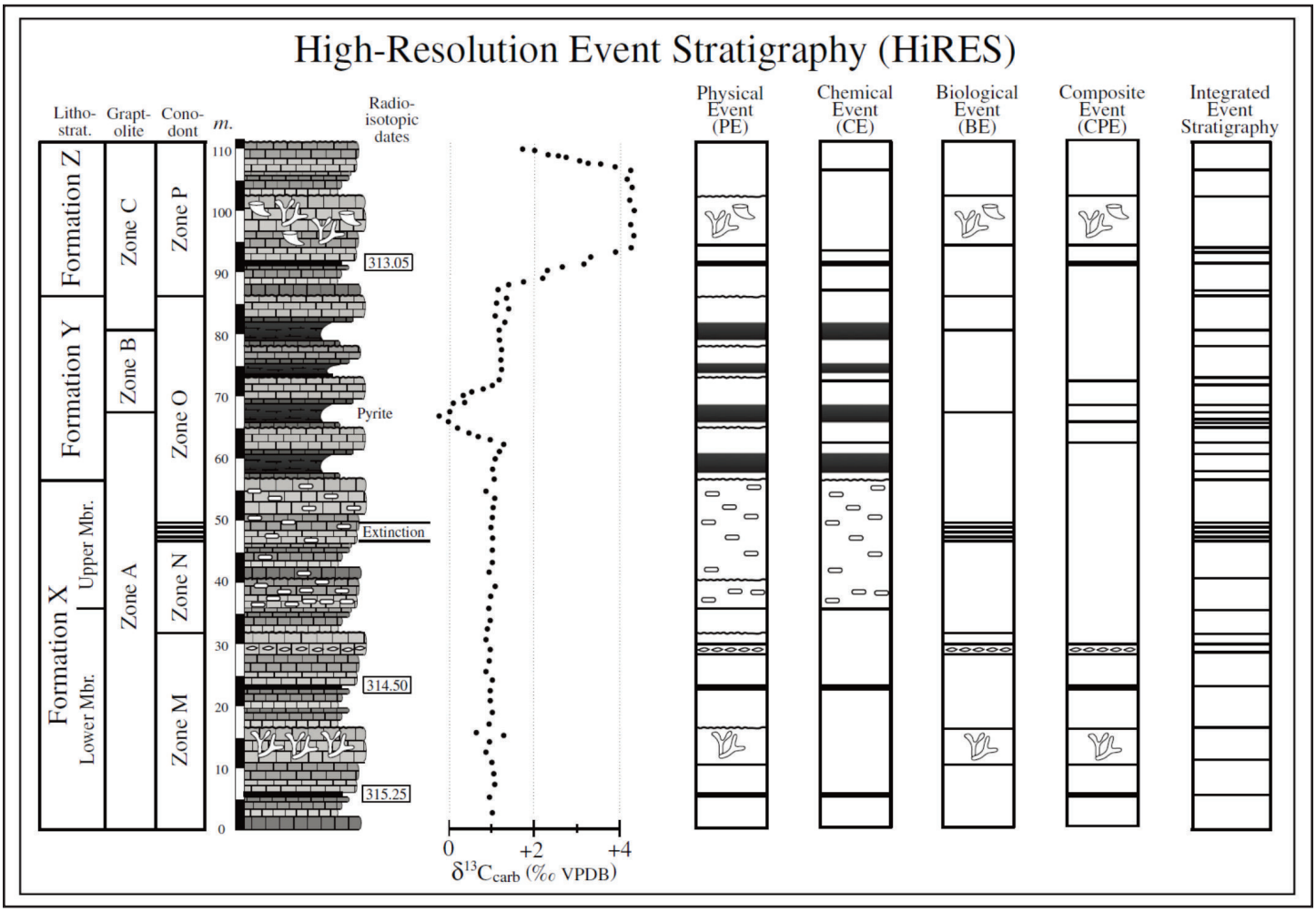

Figure 6. Demonstration of High-Resolution Event Stratigraphy (HiRES) concepts and methods by using a hypothetical stratigraphic section and data (modified from Kauffman 1988). Lithostratigraphic nomenclature, biostratigraphy, lithostratigraphy, biotic events, radioisotopic age determinations, and stable carbon isotope stratigraphy are shown at the left. The five columns shown on the right illustrate the principles of HiRES in which all stratigraphic information is included and a series of 'events' is delimited within the section. All of the chronostratigraphically useful horizons are combined into the integrated event stratigraphy at the far right. In principle, the lithostratigraphic names and biozones at the far left provide a total of 12 discrete horizons for correlation, whereas the integrated event stratigraphy at the far right provides many more potential discrete horizons for correlation and an improved chronostratigraphic resolution (Cramer et al. 2015, their figure 2, p. 139).

Currently finalized global stratotypes for systems, series and stages were identified by Gradstein et al. (2004, 2012) and are posted on the website (www.stratigraphy.org), with references to published documentation, most of which consists of reports in the journal *Episodes* by representatives from boundary working groups. Realistic error estimates are provided for Phanerozoic stages, and range from very small values (10^4-year range) for most of the Cenozoic, the time scale for which is increasingly linked to an astrochronological record, to as much as ± 4 m.y. for several stages between the Middle Jurassic and Early Cretaceous. Figure 8 illustrates the expected error in age estimation through the Phanerozoic, based on information available in 2007. The refinement of the scale expected to accrue from the integration of astrochronology (see next section) into the data base (Fig. 8E) may be regarded as optimistic, but the key workers in this field make a good case for such a development.

Many questions in the earth sciences have at their centre the questions "When did this happen?" and "What were the rates of these processes?" An accurate and high-precision time scale is an essential underpinning to much geological research.

Cyclostratigraphy and Astrochronology

Cyclostratigraphy: The subdiscipline of stratigraphy that deals with the identification, characterization, correlation, and interpretation of cyclic variations in the stratigraphic record.

Astrochronology: The dating of sedimentary units by calibration of the cyclostratigraphic record with astronomically tuned time scales. Accuracy and precision in the 10^4–10^5-year time range may be achievable.

Tuning: Adjusting the frequencies, including harmonics, of a complex record preserved in a natural succession to best-fit a predicted astronomical signal.

Croll (1864) and Gilbert (1895) were the first to realize that variations in the Earth's orbital behaviour may affect the amount and distribution of solar radiation received at the Earth's surface, by latitude and by season, and could be the cause of major climate variations. Several classic studies were undertaken to search for orbital frequencies in the rock record, and theoretical work on the distribution of insolation was carried out by the Serbian mathematician Milankovitch (1930, 1941), who showed how orbital oscillations could affect the distribution of solar radiation over the earth's surface. Howev-

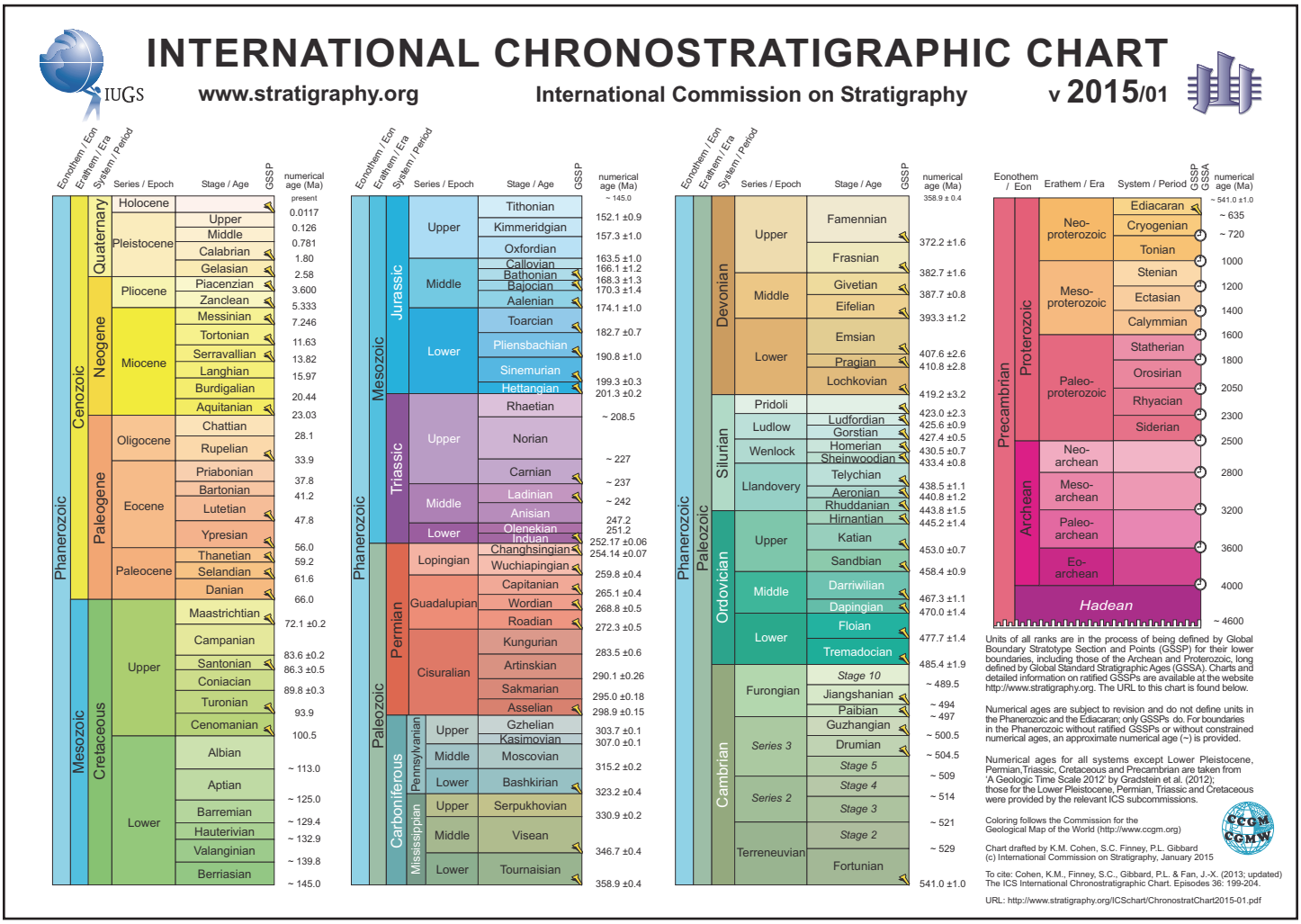

Figure 7. The Geological Time Scale (www.stratigraphy.org). Reproduced by permission © ICS International Commission on Stratigraphy [2015].

er, it was not for some years that the necessary data from the sedimentary record was obtained to support his model. Emiliani (1955) was the first to discover periodicities in the Pleistocene marine isotopic record, and the work by Hays et al. (1976) is regarded by many (e.g. de Boer and Smith 1994) as the definitive study that marked the beginning of a more widespread acceptance of orbital forcing, the so-called **Milankovitch processes**, as a major cause of stratigraphic cyclicity on a 10^4–10^5-year frequency – what is now termed the **Milankovitch band**. The model is now firmly established, particularly since accurate chronostratigraphic dating of marine sediments has led to the documentation of the record of faunal variations and temperature changes in numerous upper Cenozoic sections (Gradstein et al. 2004; Hilgen et al. 2015; see summary in Miall 2010, Sects. 7.2, 11.3). These show remarkably close agreement with the predictions made from astronomical observations. Many high-frequency sequence records are now interpreted in terms of the orbital-forcing model (summaries and reviews in Miall 2010, Chap. 11; Hilgen et al. 2015).

The idea that the preserved orbital record could be used as a kind of 'pacemaker' of Earth history and form the basis for a high-precision time scale has been around for some time (e.g. House 1985). Pioneering studies to establish the astrochronological time scale were led by Fritz Hilgen. A reliable scale was first established for the youngest Cenozoic strata, back to about 5 Ma (Hilgen 1991; Berggren et al. 1995; Hilgen et al. 2006). Over the succeeding decade, astronomically calibrated sections were used to extend the astrochronological time scale back to 14.84 Ma, the base of the Serravallian stage, in the mid-Miocene (www.stratigraphy.org), and research is proceeding to extend the time scale not only to the base of the Cenozoic, but through at least the Mesozoic (Hilgen et al. 2006, 2015; Hinnov and Ogg 2007).

For the older part of the geological record (particularly the Mesozoic and Paleozoic), several studies have now established convincing 'floating' scales for specific stratigraphic intervals; that is, scales that exhibit reliable orbital frequencies, once tuned, but that cannot yet necessarily be precisely correlated to the numerical time scale because of residual imprecisions in numerical dating methods (Hilgen et al. 2015). This project is generating an intense focus on the accuracy and precision of radioisotopic dating methods and the practices of high-resolution stratigraphy, with resulting incremental improvements in the accuracy and precision of the geological time scale (e.g. Sageman et al. 2014).

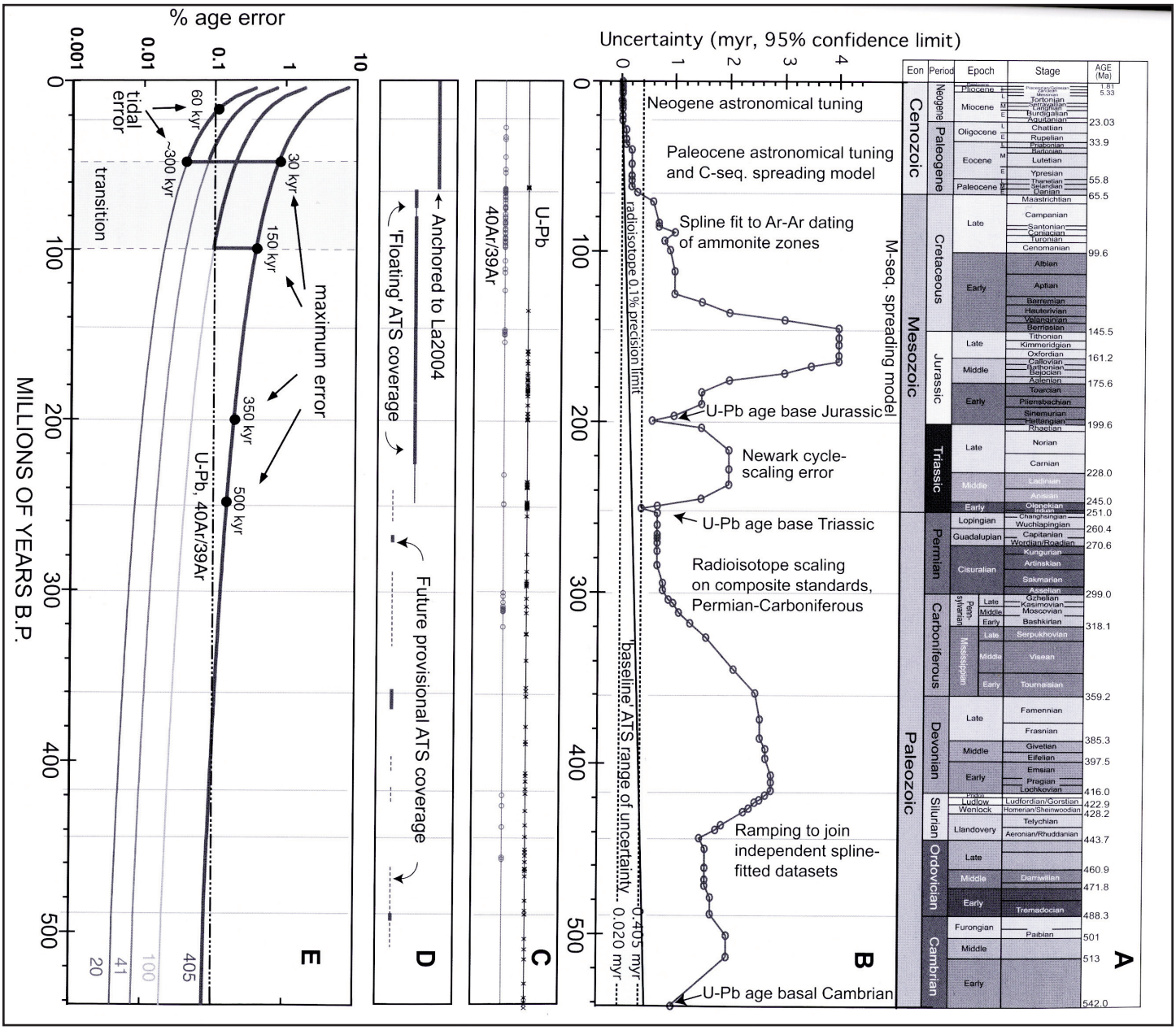

Figure 8. A. The standard divisions of the Phanerozoic International Geologic Time Scale (Gradstein et al. 2004). **B.** Estimated uncertainty (95% confidence level) in the ages of stage boundaries. **C.** Distribution of radiometric ages used in the construction of the time scale. **D.** Documented and potential astrochronological time series. **E.** Estimated error to be expected when the astrochronological time scale through the Phanerozoic is completed and integrated into the International Geologic Time Scale. The curves are labeled according to present-day Milankovitch frequencies. The 405-kyr frequency is the one which cyclostratigraphers are currently retrodicting back into the distant geological past with the greatest confidence (Hilgen et al. 2015; diagram from Hinnov and Ogg 2007).

Sedimentation Rates and Missing Time

Uniformitarianism is still the fundamental principle on which geology is built, but stratigraphers and sedimentologists have long had difficulty reconciling the concept of the uniformity of process over time with the wide range of time scales and rates of processes over which sedimentation takes place. Since the work of Barrell (1917) it has been understood that the sedimentary record is highly fragmentary. In many sedimentary basins as little as 10% of elapsed time may be represented by preserved sediment, when modern measurement of sedimentation rates in present-day environments are taken into account. However, many key concepts in sedimentary geology carry an implication of continuity in the sedimentary record: the practices of stratigraphic classification and correlation, Walther's Law, cyclic sedimentation, facies models, sequence stratigraphy – all are based on the fundamental principle that "the present is the key to the past" and its reverse. In practice, also, we assume that ancient sedimentary records representing much longer intervals than the human time scale ($\geq 10^4$ a) may be reliably compared with observations made over the much shorter time scales accessible to human observation. Questions persist concerning the relevance and significance of transient processes and ephemeral modern deposits to the interpretation of the rock record, given questions about the highly variable preservability of different sedimentary facies. Ager's (1973) remark that the stratigraphic record is "more gap than

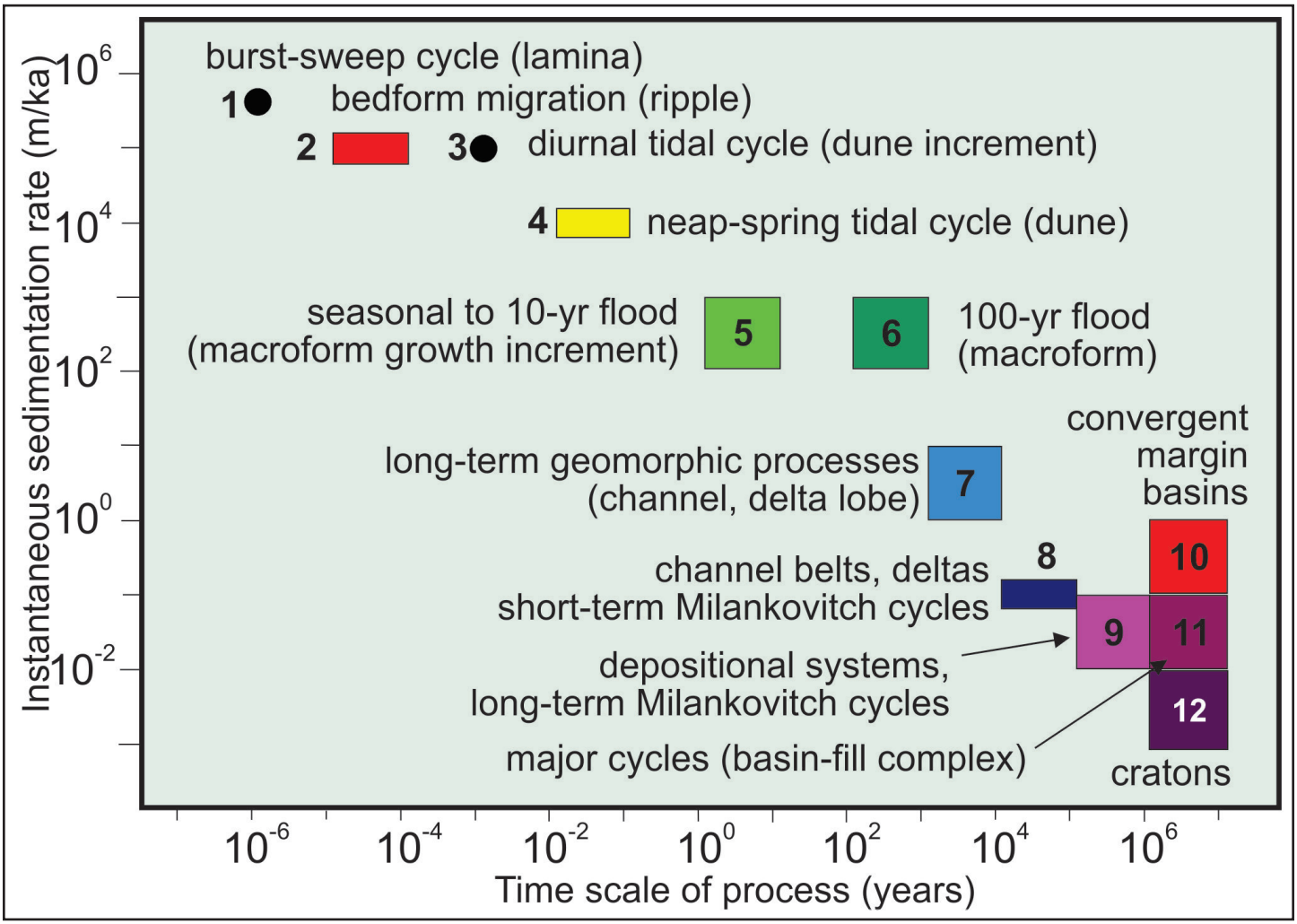

Figure 9. Sedimentation rates and sedimentary processes over time scales spanning 14 orders of magnitude. The numbers associated with each box refer to a Sedimentation Rate Scale described by Miall (2015).

record" is widely cited, but hides a complexity that has yet to be satisfactorily resolved.

It has long been realized that rates of sedimentation measured in modern depositional environments or the ancient record vary in inverse proportion to the time scale over which they are measured. Sadler (1981, 1999) documented this in detail, using 25,000 records of accumulation rates. His synthesis showed that measured sedimentation rates vary by twelve orders of magnitude, from 10^{-4} to 10^{7} m/ka. This huge range of values reflects the range of sedimentation rates at different scales (Fig. 9) and the increasing number and duration of intervals of non-deposition or erosion factored into the measurements as the length of the measured stratigraphic record increases.

Analysis of depositional and erosional processes over the full range of time scales provides insights into long-term geological preservation. At time scales of seconds to months (10^{-1}–10^{-6} years), preservation of individual lithofacies units is essentially random, reflecting autogenic processes, such as diurnal changes in current speed and tidal activity (although topographically lower deposits, such as dune troughs, channel bases, have somewhat higher preservation potential). Packages of strata that survive long enough are subject to the next cycle of preservational processes, such as autogenic channel switching, the '100-year flood,' or storm activity at the 10^{0}–10^{3}-yr time scale. At the 10^{4}–10^{5}-yr time scale, so-called 'high-frequency' geological processes come into play, including orbital forcing of climate and sea level, and local tectonic episodicity. Ultimately, all remaining stratigraphic accumulations are subject to the long-term (10^{6}–10^{7} yr) geological (largely tectonic) controls on basin accommodation (Miall 2015).

An important insight emerging from this analysis has critical implications for the application of uniformitarianist principles. Geological processes interpreted from successions accumulated over the post-glacial period, such as those of the Mississippi and Rhine-Meuse deltas (descriptions and analyses of which comprise substantial contributions to sedimentological literature on fluvial and deltaic systems) can only be used as analogs for interpretations of geological processes up to the 10^{4}-year time scale. The geological record contains many examples of coastal fluvial-deltaic successions spanning millions of years, but a 10^{6}–10^{7}-year record cannot be interpreted simply by 'scaling-up' an analysis carried out on a 10^{4}–10^{5}-year time scale. Firstly, coastal successions, such as those on present day continental margins could be largely eliminated by subaerial erosion during the next glacial cycle of lowered sea level as

the geological preservation machine begins to operate over the next longer time scale. Secondly, the time scales implied for sedimentary processes would be wrong. For example, sequence models for fluvial systems, which relate channel stacking behaviour to rates of sedimentary accommodation, are largely based on measurements of rates of sedimentation and channel switching in modern rivers and in post-glacial alluvial valley fills, at time scales no greater than 10^3 years. Applications of these models to the ancient record deal mostly with so-called third-order sequences (durations in the 10^6 yr range) for which calculated accumulation rates are one to three orders of magnitude slower than those on which the sequence models are based (Miall 2014). Colombera et al. (2015) confirmed, by a detailed study of twenty ancient fluvial systems, that there is no relationship between channel-stacking pattern and aggradation rate. It is suggested that the observed changes in channel-stacking patterns that have been observed in the rock record are the product of longer term processes, such as tectonically controlled changes in paleoslope or sediment supply (Miall 2014).

Sequence Stratigraphy as a Key to Earth Processes

The range of sedimentation rates and the durations of hiatuses are fractal-like. They comprise a range of discrete geological processes that control sedimentation, erosion, and long-term preservation. The fractal model provides an elegant basis for integrating our knowledge of sedimentary processes with modern data on varying sedimentation rates and varying scales of hiatuses (Miall 2015). Sequence stratigraphy is essentially a study of the repetitive cycle of accumulation followed by the next gap, at various time scales. The larger, more obvious gaps define for us the major sequences, over a range of time scales. The prominence of particular ranges of accumulation-plus-gap length in the first data sets compiled by Vail et al. (1977) was what led to their establishment of the sequence hierarchy of first-order, second-order, and so on. That this has now been shown to be an incomplete representation of nature (Schlager 2005; Miall 2010) does not alter the fact that there is a limited range of processes that control accumulation. These have fairly well defined rates which, nevertheless, overlap in time to some extent. A review of these sequence-generating mechanisms was compiled by Miall (1995) during a lengthy controversy regarding the importance or otherwise of eustatic sea-level changes as the major controlling mechanism (Dewey and Pitman 1998; Miall and Miall 2001).

Much research into basinal processes has been stimulated directly or indirectly by developments in sequence stratigraphy, and significant advances have been made in the understanding of sedimentary cyclic processes, particularly the geological record of orbital forcing (e.g. de Boer and Smith 1994; Hilgen et al. 2015), and the nature of high-frequency tectonism (e.g. Macdonald 1991; Williams and Dobb 1993).

The Search for Fossil Fuels

The concept of the **petroleum system** has evolved as the essential key to the understanding of how and why fossil fuels accumulate in sedimentary basins. Stratigraphy is at the centre of this enterprise, as noted here:

1. **Source:** The accumulation of plant and animal remains constitute the source of oil, gas and coal. Stratigraphy and sedimentology explain how, where and why.
2. **Maturation:** The generation of fluid oil and gas and the maturation of plant matter into coal are depth- and temperature-dependent, studies of which are the domain of basin analysis.
3. **Migration:** Of oil and gas requires a porosity–permeability plumbing system, which is largely a question of the primary depositional control on lithofacies distribution, with possible subsequent modification by diagenesis and structural deformation.
4. **Reservoir:** The accumulation of oil and gas in discrete pools requires the combination of the three remaining elements of the system. Porous and permeable reservoirs are the product of a range of specific sedimentary processes, such as organic reef growth, the accumulation of clean sands on a beach or in submarine fan complexes at the base of a continental slope (albeit with subsequent diagenetic modification). Much sedimentological research owes its primary motivation to a desire to understand the processes that lead to such accumulations.
5. **Seal:** The converse of a reservoir: a unit that is not porous or permeable.
6. **Trap:** Many petroleum traps are of a type termed **stratigraphic traps**, in which it is the limited extent and configuration of the porous reservoir unit that defines the trap and therefore the pool itself.

Unconventional resources, including shale gas, tight oil and oil sands operate under modified petroleum systems. For shale gas and tight oil migration is of negligible significance. These are commonly described as self-sourced resources. The petroleum matures in place and remains there because of very limited porosity and permeability. Stratigraphic methods are no less important in the development of these resources – not all shale units are equally productive, and much may be learned from petrographic and fracture studies.

The techniques that have evolved to maximize discovery success and development efficiency are among the most technically advanced in the geological sciences and have contributed significantly to the evolution of stratigraphy and sedimentology. Three-dimensional reflection seismic methods reach their maximum effectiveness when the user turns to sedimentology, in particular the new field of seismic geomorphology, to interpret reflection patterns. Directional drilling has become a vital engineering tool for the exploitation of many oil and gas reserves, and its greatest efficiency in practice comes when the tool is directed in real time by the application of **geosteering** methods, which employ down-hole geophysics and well-sample data to direct the drill bit through the desired stratigraphic unit.

In all of these cases, describing the configuration of the reservoir, determining its situation within the regional sequence stratigraphy and defining its basinal setting, constitute important elements in the development of a petroleum play. Numerical modeling and graphic visualization of these

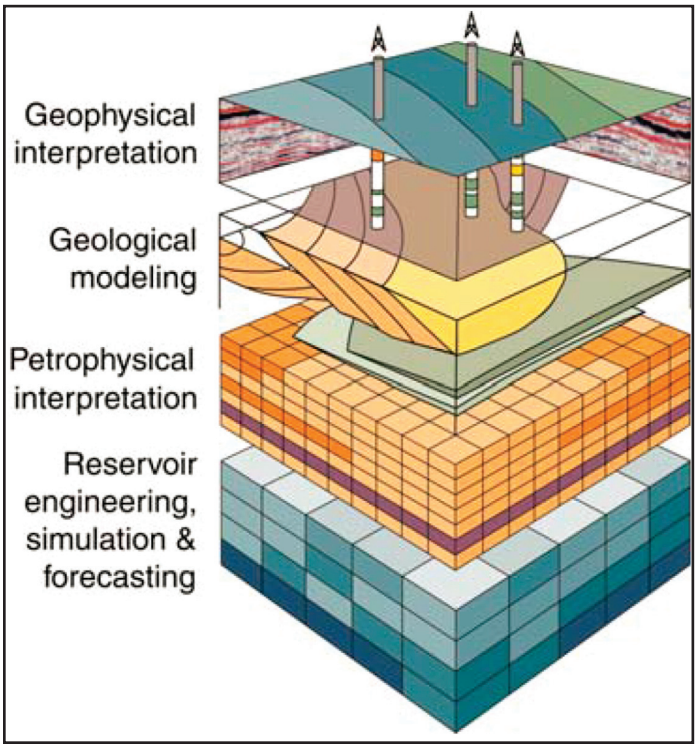

Figure 10. The 3-D modeling process as used in hydrocarbon development. Stratigraphy, as defined in its broadest sense, is essential to the geophysical interpretation and to the geological input into the model (the top two layers). Petrophysical and reservoir engineering interpretations are carried out by statistical sampling and numerical modeling of the stratigraphy, using three-dimensional grid blocks, and it is on the quantitative basis provided by these steps that production programs are designed by the engineers (Bentley and Smith 2008).

elements are essential components of the development process, and require a meticulous attention to the input data from the geological team managing the project (Fig. 10).

CONCLUSIONS

Doyle and Bennett (1998, p. 1) stated that "Stratigraphy is the key to understand the Earth, its materials, structure and past life. It encompasses everything that has happened in the history of the planet." In this statement is the recognition that the stratigraphic history of layered sedimentary rocks preserved on the continents and on the ocean floors constitutes the documented record of Earth history. No other branch of geology can provide this information. Historical geology depends largely on the study of the stratigraphic record. It is from the rocks that we know about the evolution of life, the plate-tectonic development of the earth's crust, and ancient climate changes.

If earth scientists are ever to contribute significantly to the current debate about climate change, their contribution will be to offer a precise record of natural paleoclimatic variability, including the nature of greenhouse and icehouse climates, and such climatic events as the Paleocene–Eocene Thermal Maximum. This natural history should provide a base-line against which to evaluate anthropogenic influences. It is stratigraphy, in its modern complexity, that will provide this base line. Our layers have meaning. These are the files wherein our answers lie.

ACKNOWLEDGEMENTS

Thanks are due to my wife, Charlene, for her more than 46 years of support and encouragement. I thank her, in particular, for her companionship in the field, and for contributing her sociological wisdom to the collaborative work we have done to explore the elements of social construction in the development of the science of Stratigraphy. Thanks are due to Bill Fisher for reviewing the historical sections of this paper. Ron Steel, Martin Gibling and Bob Dalrymple read earlier versions of the paper and provided many useful suggestions.

REFERENCES

Ager, D.V., 1970, On seeing the most rocks: Proceedings of the Geologists' Association, v. 81, p. 421–427, http://dx.doi.org/ 10.1016/s0016-7878(70)80004-9.

Ager, D.V., 1973, The nature of the stratigraphical record: John Wiley, New York, NY, 114 p.

Ager, D.V., 1981, The nature of the stratigraphical record (Second Edition): John Wiley, New York, NY, 122 p.

Ager, D.V., 1993, The new catastrophism: The importance of the rare event in geological history: Cambridge University Press, 231 p.

Allen, J.R.L., 1962, Petrology, origin and deposition of the highest Lower Old Red Sandstone of Shropshire, England: Journal of Sedimentary Petrology (Research), v. 32, p. 657–697, http://dx.doi.org/10.1306/74D70D49-2B21-11D7-8648000102C1865D.

Allen, J.R.L., 1963a, The classification of cross-stratified units. With notes on their origin: Sedimentology, v. 2, p. 93–114, http://dx.doi.org/10.1111/j.1365-3091.1963.tb01204.x.

Allen, J.R.L., 1963b, Henry Clifton Sorby and the sedimentary structures of sands and sandstones in relation to flow conditions: Geologie en Mijnbouw, v. 42, p. 223–228.

Allen, J.R.L., 1964, Studies in fluviatile sedimentation: six cyclothems from the Lower Old Red Sandstone, Anglo-Welsh basin: Sedimentology, v. 3, p. 163–198, http://dx.doi.org/10.1111/j.1365-3091.1964.tb00459.x.

Allen, J.R.L., 1965, A review of the origin and characteristics of recent alluvial sediments: Sedimentology, v. 5, p. 89–191, http://dx.doi.org/10.1111/j.1365-3091.1965.tb01561.x.

Allen, J.R.L., 1983, Studies in fluviatile sedimentation: Bars, bar-complexes and sandstone sheets (low-sinuosity braided streams) in the Brownstones (L. Devonian), Welsh Borders: Sedimentary Geology, v. 33, p. 237–293, http://dx.doi.org/10.1016/0037-0738(83)90076-3.

Allen, J.R.L., 1993, Sedimentary structures: Sorby and the last decade: Journal of the Geological Society, v. 150, p. 417–425, http://dx.doi.org/10.1144/gsjgs.150.3.0417.

Allen, P.A., and Allen, J.R., 2013, Basin analysis: Principles and application to petroleum play assessment: Wiley-Blackwell, Chichester, 619 p.

Allen, P.A., and Etienne, J.L., 2008, Sedimentary challenge to Snowball Earth: Nature Geoscience, v. 1, p. 817–825, http://dx.doi.org/10.1038/ngeo355.

Arnott, R.W.C., 2010, Deep-marine sediments and sedimentary systems, *in* James, N.P., and Dalrymple, R.W., *eds.*, Facies Models 4: GEOtext 6, Geological Association of Canada, St. John's, NL, p. 295–322.

Baker, V.R., 2000, Let Earth Speak, *in* Schneiderman, J., *ed.*, The earth around us: maintaining a livable planet: Freeman, New York, p. 358–367.

Baker, V.R., *ed.*, 2013, Rethinking the fabric of geology: Geological Society of America, Special Papers, v. 502, 185 p., http://dx.doi.org/10.1130/9780813725024.

Ball, M.M., 1967, Carbonate sand bodies of Florida and the Bahamas: Journal of Sedimentary Petrology (Research), v. 37, p. 556–591, http://dx.doi.org/10.1306/74D7171C-2B21-11D7-8648000102C1865D.

Bally, A.W., *ed.*, 1987, Atlas of seismic stratigraphy: American Association of Petroleum Geologists Studies in Geology 27, in 3 volumes.

Bally, A.W., 1989, Phanerozoic basins of North America, *in* Bally, A.W., and Palmer, A.R., *eds.*, The geology of North America—an overview: The geology of North America, Geological Society of America, v. A, p. 397–446, http://dx.doi.org/10.1130/DNAG-GNA-A.397.

Bally, A.W., Gordy, P.L., and Stewart, G.A., 1966, Structure, seismic data and orogenic evolution of southern Canadian Rockies: Bulletin of Canadian Petroleum Geology, v. 14, p. 337–381.

Barrell, Joseph, 1917, Rhythms and the measurements of geologic time: Geological Society of America Bulletin, v. 28, p. 745–904, http://dx.doi.org/10.1130/GSAB-28-745.

Beales, F.W., 1958, Ancient sediments of Bahaman type: American Association of Petroleum Geologists, v. 42, p. 1845–1880.

Beaumont, C., 1981, Foreland basins: Geophysical Journal International, v. 65, p. 291–329, http://dx.doi.org/10.1111/j.1365-246X.1981.tb02715.x.

Beerbower, J.R., 1964, Cyclothems and cyclic depositional mechanisms in alluvial

plain sedimentation: Geological Survey of Kansas Bulletin 169, v. 1, p. 31–42.
Bentley, M., and Smith, S., 2008, Scenario-based reservoir modelling: the need for more determinism and less anchoring, *in* Robinson, A., Griffiths, P., Price, S., Hegre, J., and Muggeridge, A., *eds.*, The Future of Geological Modelling in Hydrocarbon Development: Geological Society, London, Special Publications, v. 309, p. 145–159, http://dx.doi.org/10.1144/sp309.11.
Berg, R.R., 1962, Mountain flank thrusting in Rocky Mountain foreland, Wyoming and Colorado: American Association of Petroleum Geologists Bulletin, v. 46, p. 2019–2032.
Berg, R.R., 1968, Point-bar origin of Fall River Sandstone reservoirs, northeastern Wyoming: American Association of Petroleum Geologists Bulletin, v. 52, p. 2116–2122.
Berggren, W.A., Kent, D.V., Aubry, M.-P., and Hardenbol, J., *eds.,* 1995, Geochronology, time scales and global stratigraphic correlation: Society for Sedimentary Geology Special Publication 54, 386 p.
Bernard, H.A., and Major, C.J., 1963, Recent meander belt deposits of the Brazos River: an alluvial "sand" model (Abstract): American Association of Petroleum Geologists Bulletin, v. 47, p. 350.
Bernard, H.A., Major, C.F., Jr., and Parrott, B.S., 1959, The Galveston Barrier Island and environs – a model for predicting reservoir occurrence and trend: Transactions of the Gulf Coast Association of Geological Societies, v. 9, p. 221–224.
Bernard, H.A., Leblanc, R.J., and Major, C.J., 1962, Recent and Pleistocene geology of southeast Texas, *in* Rainwater, E.H., and Zingula, R.P., *eds.*, Geology of the Gulf Coast and central Texas: Geological Society of America, Guidebook for 1962 Annual Meeting, p. 175–224.
Berry, W.B.N., 1968, Growth of prehistoric time scale, based on organic evolution: W.H. Freeman and Co., San Francisco, 158 p.
Berry, W.B.N., 1987, Growth of prehistoric time scale based on organic evolution (Revised Edition): Blackwell Science, Oxford, 202 p.
Bird, J.M., and Dewey, J.F., 1970, Lithosphere plate-continental margin tectonics and the evolution of the Appalachian Orogen: Geological Society of America Bulletin, v. 81, p. 1031–1060, http://dx.doi.org/10.1130/0016-7606(1970)81[1031:LPMTAT]2.0.CO;2.
Blackwelder, E., 1909, The valuation of unconformities: The Journal of Geology, v. 17, p. 289–299, http://dx.doi.org/10.1086/621610.
Blatt, H., Middleton, G.V., and Murray, R.C., 1972, Origin of sedimentary rocks: Prentice-Hall, Englewood Cliffs, NJ, 634 p.
Boggs, S., Jr., 1987, Principles of sedimentology and stratigraphy: Prentice Hall, Englewood Cliffs, NJ, 784 p.
Bouma, A.H., 1962, Sedimentology of some flysch deposits: Elsevier, Amsterdam, 168 p.
Bouma, A.H., Normark, W.R., and Barnes, N.E., *eds.*, 1985, Submarine fans and related turbidite systems: Springer-Verlag Inc., Berlin and New York, 351 p., http://dx.doi.org/10.1007/978-1-4612-5114-9.
Brouwer, A., 1962, Past and present in Sedimentology: Sedimentology, v. 1, p. 2–6, http://dx.doi.org/10.1111/j.1365-3091.1962.tb01143.x.
Brown, L.F., Jr., and Fisher, W.L., 1977, Seismic-stratigraphic interpretation of depositional systems: examples from Brazilian rift and pull-apart basins, *in* Payton, C.E., *ed.*, Seismic stratigraphy — applications to hydrocarbon exploration: American Association of Petroleum Geologists Memoir 26, p. 213–248.
Burk, C.A., and Drake, C.L., *eds.*, 1974, The geology of continental margins: Springer-Verlag, New York, 1009 p., http://dx.doi.org/10.1007/978-3-662-01141-6.
Busby, C.J., and Ingersoll, R.V., *eds.*, 1995, Tectonics of sedimentary basins: Blackwell Science, Oxford, 579 p.
Callomon, J.H., 1995, Time from fossils: S.S. Buckman and Jurassic high-resolution geochronology, *in* Le Bas, M.J., *ed.*, Milestones in Geology: Geological Society, London, Memoirs, v. 16, p. 127–150, http://dx.doi.org/10.1144/gsl.mem.1995.016.01.14.
Catuneanu, O., 2006, Principles of sequence stratigraphy: Elsevier, Amsterdam, 375 p.
Catuneanu, O., Abreu, V., Bhattacharya, J.P., Blum, M.D., Dalrymple, R.W., Eriksson, P.G., Fielding, C.R., Fisher, W.L., Galloway, W.E., Gibling, M.R., Giles, K.A., Holbrook, J.M., Jordan, R., Kendall, C.G.St.C., Macurda, B., Martinsen, O.J., Miall, A.D., Neal, J.E., Nummedal, D., Pomar, L., Posamentier, H.W., Pratt, B.R., Sarg, J.F., Shanley, K.W., Steel, R.J., Strasser, A., Tucker, M.E., and Winker, C., 2009, Toward the standardization of sequence stratigraphy: Earth-Science Reviews, v. 92, p. 1–33, http://dx.doi.org/10.1016/j.earscirev.2008.10.003.
Catuneanu, O., Bhattacharya, J.P., Blum, M.D., Dalrymple, R.W., Eriksson, P.G., Fielding, C.R., Fisher, W.L., Galloway, W.E., Gianolla, P., Gibling, M.R., Giles, K.A., Holbrook, J.M., Jordan, R., Kendall, C.G.St.C., Macurda, B., Martinsen, O.J., Miall, A.D., Nummedal, D., Posamentier, H.W., Pratt, B.R,. Shanley, K.W., Steel, R.J., Strasser, A., and Tucker, M.E., 2010, Sequence stratigraphy: common ground after three decades of development: First Break, v. 28, p. 41–54, http://dx.doi.org/10.3997/1365-2397.2010002.
Catuneanu, O., Galloway, W.E., Kendall, C.G.St.C., Miall, A.D., Posamentier, H.W., Strasser A., and Tucker, M.E., 2011, Sequence Stratigraphy: Methodology and Nomenclature: Report to ISSC: Newsletters on Stratigraphy, v. 44, p. 173–245, http://dx.doi.org/10.1127/0078-0421/2011/0011.
Cloetingh, S., 1988, Intraplate stresses: A new element in basin analysis, *in* Kleinspehn, K.L., and Paola, C., *eds.*, New Perspectives in basin analysis: Springer-Verlag, New York, p. 205–230, http://dx.doi.org/10.1007/978-1-4612-3788-4_10.
Colombera, L., Mountney, N.P., and McCaffrey, W.D., 2015, A meta-study of relationships between fluvial channel-body stacking pattern and aggradation rate: Implications for sequence stratigraphy: Geology, v. 43, p. 283–286, http://dx.doi.org/10.1130/G36385.1.
Conkin, B.M., and Conkin, J.E., *eds.*, 1984, Stratigraphy: foundations and concepts: Benchmark Papers in Geology, Van Nostrand Reinhold, New York, 363 p.
Conybeare, C.E.B., and Crook, K.A.W., 1968, Manual of sedimentary structures: Australian Bureau of Mineral Resources, Geology and Geophysics, Bulletin 102, 327 p.
Cramer, B.D., Vandenbroucke, T.R.A., and Ludvigson, G.A., 2015, High-resolution event stratigraphy (HiRES) and the quantification of stratigraphic uncertainty: Silurian examples of the quest for precision in stratigraphy: Earth-Science Reviews, v. 141, p. 136–153, http://dx.doi.org/10.1016/j.earscirev.2014.11.011.
Croll, J., 1864, On the physical cause of the change of climate during geological epochs: Philosophical Magazine, v. 28, p. 435–436.
Curray, J.R., 1956, The analysis of two-dimensional orientation data: The Journal of Geology, v. 64, p. 117–131, http://dx.doi.org/10.1086/626329.
Curray, J.R., 1964, Transgressions and regressions, *in* Miller, R.L., *ed.*, Papers in marine geology, Shepard Commemorative volume: MacMillan Press, New York, p. 175–203.
Curtis, D.M., 1970, Miocene deltaic sedimentation, Louisiana Gulf Coast, *in* Morgan, J.P., *ed.*, Deltaic sedimentation modern and ancient: Society of Economic Paleontologists and Mineralogists (SEPM) Special Publications, v. 15, p. 293–308.
Dahlstrom, C.D.A., 1970, Structural geology in the eastern margin of the Canadian Rocky Mountains: Bulletin of Canadian Petroleum Geology, v. 18, p. 332–406.
Dapples, E.C., Krumbein, W.C., and Sloss, L.L., 1948, Tectonic control of lithologic associations: American Association of Petroleum Geologists Bulletin, v. 32, p. 1924–1947.
Davies, R.J., Posamentier, H.W., Wood, L.J., and Cartwright, J.A., *eds.*, 2007, Seismic geomorphology: applications to hydrocarbon exploration and production: Geological Society, London, Special Publications, v. 277, 274 p., http://dx.doi.org/10.1144/GSL.SP.2007.277.01.16.
de Boer, P.L., and Smith, D.G., *eds.*, 1994, Orbital forcing and cyclic sequences: International Association of Sedimentologists Special Publication 19, 559 p.
De Raaf, J.F.M., Reading, H.G., and Walker, R.G., 1965, Cyclic sedimentation in the Lower Westphalian of North Devon, England: Sedimentology, v. 4, p. 1–52, http://dx.doi.org/10.1111/j.1365-3091.1965.tb01282.x.
Dewey, J.F., 1982, Plate tectonics and the evolution of the British Isles: Journal of the Geological Society, v. 139, p. 371–412, http://dx.doi.org/10.1144/gsjgs.139.4.0371.
Dewey, J.F., 1999, Reply when awarded the Wollaston medal: Geological Society, London, 1999 Awards.
Dewey, J.F., and Bird, J.M., 1970, Plate tectonics and geosynclines: Tectonophysics, v. 10, p. 625–638, http://dx.doi.org/10.1016/0040-1951(70)90050-8.
Dewey, J.F., and Pitman, W.C., 1998, Sea-level changes: mechanisms, magnitudes and rates, *in* Pindell, J.L., and Drake, C.L., *eds.*, Paleogeographic evolution and nonglacial eustacy, northern South America: Society of Economic Paleontologists and Mineralogists (SEPM) Special Publications, v. 58, p. 1–16, http://dx.doi.org/10.2110/pec.98.58.0001.
Dickinson, W.R., 1971, Plate tectonic models of geosynclines: Earth and Planetary Science Letters, v. 10, p. 165–174, http://dx.doi.org/10.1016/0012-821X(71)90002-1.
Dickinson, W.R., 1974, Plate tectonics and sedimentation, *in* Dickinson, W.R., *ed.*, Tectonics and sedimentation: Society of Economic Paleontologists and Mineralogists (SEPM) Special Publications, v. 22, p. 1–27, http://dx.doi.org/10.2110/pec.74.22.0001.
Dickinson, W.R., 1976, Sedimentary basins developed during evolution of Mesozoic–Cenozoic arc-trench system in western North America: Canadian Journal of Earth Sciences, v. 13, p. 1268–1287, http://dx.doi.org/10.1139/e76-129.
Dickinson, W.R., 1980, Plate tectonics and key petrologic associations, *in* Strangway, D.W., *ed.*, The continental crust and its mineral deposits: Geological Association of Canada Special Paper 20, p. 341–360.
Dickinson, W.R., 1981, Plate tectonics and the continental margin of California, *in* Ernst, W.G., *ed.*, The geotectonic development of California: Prentice-Hall Inc., Englewood Cliffs, NJ, p. 1–28.
Dickinson, W.R., and Seely, D.R., 1979, Structure and stratigraphy of forearc

regions: American Association of Petroleum Geologists Bulletin, v. 63, p. 2–31.
Dietz, R.S., 1963, Collapsing continental rises: An actualistic concept of geosynclines and mountain building: The Journal of Geology, v. 71, p. 314–333, http://dx.doi.org/10.1086/626904.
Dietz, R.S., 1994, Earth, sea and sky: Life and times of a journeyman geologist: Annual Review of Earth and Planetary Sciences, v. 22, p. 1–33, http://dx.doi.org/10.1146/annurev.ea.22.050194.000245.
Dietz, R.S., and Holden, J.C., 1974, Collapsing continental rises: actualistic concept of geosynclines—a review, *in* Dott, R.H., Jr., and Shaver, R.H., *eds.*, Modern and ancient geosynclinal sedimentation: Society of Economic Paleontologists and Mineralogists (SEPM) Special Publications, v. 19, p. 14–25, http://dx.doi.org/10.2110/pec.74.19.0014.
Dott, R.H., Jr., 1983, 1982 SEPM Presidential Address: Episodic sedimentation—how normal is average? How rare is rare? Does it matter?: Journal of Sedimentary Petrology (Research), v. 53, p. 5–23, http://dx.doi.org/10.1306/212F8148-2B24-11D7-8648000102C1865D.
Dott, R.H., Jr., 1996, Episodic event deposits versus stratigraphic sequences—shall the twain never meet?: Sedimentary Geology, v. 104, p. 243–247, http://dx.doi.org/10.1016/0037-0738(95)00131-X.
Dott, R.H., Jr., and Shaver, R.H., *eds.*, 1974, Modern and ancient geosynclinal sedimentation: Society of Economic Paleontologists and Mineralogists (SEPM) Special Publications, v. 19, 380 p., http://dx.doi.org/10.2110/pec.74.19.0014.
Doyle, P., and Bennett, M.R., *eds.*, 1998, Unlocking the stratigraphical record: John Wiley and Sons, Chichester, 532 p.
Drake, C.L., Ewing, M., and Sutton, G.H., 1959, Continental margins and geosynclines—the east coast of North America north of Cape Hatteras: Physics and Chemistry of the Earth, v. 3, p. 110–198, http://dx.doi.org/10.1016/0079-1946(59)90005-9.
Duff, P.McL.D., and Walton, E.K., 1962, Statistical basis for cyclothems: a quantitative study of the sedimentary succession in the east Pennine Coalfield: Sedimentology, v. 1, p. 235–255, http://dx.doi.org/10.1111/j.1365-3091.1962.tb01149.x.
Duff, P.McL.D., Hallam, A., and Walton, E.K., *eds.,* 1967, Cyclic sedimentation: Developments in Sedimentology, v. 10, Elsevier, Amsterdam, 280 p., http://dx.doi.org/10.1016/S0070-4571(08)70120-1.
Dunbar, C.O., and Rodgers, J., 1957, Principles of Stratigraphy: Wiley, New York, 356 p.
Dunham, R.J., 1962, Classification of carbonate rocks according to depositional texture, *in* Ham, W.E., *ed.*, Classification of carbonate rocks: American Association of Petroleum Geologists Memoir 1, p. 108–121.
Emiliani, C., 1955, Pleistocene temperatures: The Journal of Geology, v. 63, p. 538–578, http://dx.doi.org/10.1086/626295.
Eyles, N., and Januszczak, N., 2004, 'Zipper-rift': a tectonic model for Neoproterozoic glaciations during the breakup of Rodinia after 750 Ma: Earth-Science Reviews, v. 65, p. 1–73, http://dx.doi.org/10.1016/S0012-8252(03)00080-1.
Eyles, N., Eyles, C.H., and Miall, A.D., 1983, Lithofacies types and vertical profile models; an alternative approach to the description and environmental interpretation of glacial diamict and diamictite sequences: Sedimentology, v. 30, p. 393–410, http://dx.doi.org/10.1111/j.1365-3091.1983.tb00679.x.
Fisher, W.L., and McGowen, J.H., 1967, Depositional systems in the Wilcox Group of Texas and their relationship to occurrence of oil and gas: Transactions of the Gulf Coast Association of Geological Societies, v. 17, p. 105–125.
Fisher, W.L., Brown, L.F., Scott, A.J., and McGowen, J.H., 1969, Delta systems in the exploration for oil and gas: Bureau of Economic Geology, University of Texas, 78 p.
Fisher, W.L., McGowen, J.H., Brown, L.F., Jr., and Groat, C.G., 1972, Environmental geologic atlas of the Texas coastal zone — Galveston-Houston area: Bureau of Economic Geology, University of Texas.
Fisher, W.L., Gama, E., and Ojeda, H.A., 1973, Estratigrafia sismica e sistemas deposicionais da Formação Piaçabuçu: Sociedade Brasileira de Geologia, Anai do XXVII Congresso, v. 3, p. 123–133.
Fisk, H.N., 1944, Geological investigations of the alluvial valley of the lower Mississippi River: U.S. Army Corps of Engineers, Mississippi River Commission, Vicksburg, MS, 78 p.
Folk, R.L., 1962, Spectral subdivision of limestone types, *in* Ham, W.E., *ed.*, Classification of carbonate rocks: American Association of Petroleum Geologists Memoir 1, p. 62–84.
Frazier, D.E., 1967, Recent deltaic deposits of the Mississippi River—their development and chronology: Transactions of the Gulf Coast Association of Geological Societies, v. 17, p. 287–315.
Frazier, D.E., 1974, Depositional episodes: their relationship to the Quaternary stratigraphic framework in the northwestern portion of the Gulf Basin: Bureau of Economic Geology, University of Texas at Austin, Geological Circular 74-1, 26 p.
Frey, R.W., and Pemberton, S.G., 1984, Trace fossil facies models, *in* Walker, R.G., *ed.*, Facies models (Second Edition): Geoscience Canada Reprint Series 1, p. 189–207.
Friedman, G.M., and Sanders, J.E., 1978, Principles of Sedimentology: John Wiley and Sons, New York, 791 p.
Galloway, W.E., 1989, Genetic stratigraphic sequences in basin analysis I: Architecture and genesis of flooding-surface bounded depositional units: American Association of Petroleum Geologists Bulletin, v. 73, p. 125–142.
Gilbert, G.K., 1884, Ripple-marks: Science, v. 3, p. 375–376, http://dx.doi.org/10.1126/science.ns-3.60.375-c.
Gilbert, G.K., 1895, Sedimentary measurement of Cretaceous time: The Journal of Geology, v. 3, p. 121–127, http://dx.doi.org/10.1086/607150.
Gilbert, G.K., 1899, Ripple-marks and cross-bedding: Geological Society of America Bulletin, v. 10, p. 135–140, http://dx.doi.org/10.1130/GSAB-10-135.
Gilbert, G.K., 1914, The transportation of debris by running water: U.S. Geological Survey Professional Paper 86, 263 p.
Ginsburg, R.N., and Lowenstam, H.A., 1958, The influence of marine bottom communities on the depositional environment of sediments: The Journal of Geology, v. 66, p. 310–318, http://dx.doi.org/10.1086/626507.
Gradstein, F.M., Ogg, J.G., and Smith, A.G., *eds.*, 2004, A geologic time scale: Cambridge University Press, Cambridge, 610 p.
Gradstein, F.M., Ogg, J.G., Schmitz, M.D., and Ogg, G.M., 2012, The Geologic time scale 2012: Elsevier, Amsterdam, 2 volumes, 1176 p.
Gressly, A., 1838, Observations géologiques sur le Jura Soleurois: Nouveaux Memoires de la Société Helvétique des Sciences. Naturelles, v. 2, p. 1–112.
Gurnis, M., 1988, Large-scale mantle convection and the aggregation and dispersal of supercontinents: Nature, v. 332, p. 695–699, http://dx.doi.org/10.1038/332695a0.
Gurnis, M., 1990, Bounds on global dynamic topography from Phanerozoic flooding of continental platforms: Nature, v. 344, p. 754–756, http://dx.doi.org/10.1038/344754a0.
Gurnis, M., 1992, Long-term controls on eustatic and epeirogenic motions by mantle convection: GSA Today, v. 2, p. 141–157.
Hallam, A., 1989, Great geological controversies (Second Edition): Oxford University Press, Oxford, 244 p.
Hancock, J.M., 1977, The historic development of biostratigraphic correlation, *in* Kauffman, E.G., and Hazel, J.E., *eds.*, Concepts and methods of biostratigraphy: Dowden, Hutchinson and Ross Inc., Stroudsburg, PA, p. 3–22.
Harms, J.C., Southard, J.B., Spearing, D.R., and Walker, R.G., 1975, Depositional environments as interpreted from primary sedimentary structures and stratification sequences: Society of Economic Paleontologists and Mineralogists Short Course 2, 161 p.
Hart, B.S., 2013, Whither seismic stratigraphy: Interpretation, v. 1, p. SA3–SA20, http://dx.doi.org/10.1190/int-2013-0049.1.
Hays, J.D., Imbrie, J., and Shackleton, N.J., 1976, Variations in the earth's orbit: Pacemaker of the Ice Ages: Science, v. 194, p. 1121–1132, http://dx.doi.org/10.1126/science.194.4270.1121.
Hedberg, H.D., 1948, Time stratigraphic classification of sedimentary rocks: Geological Society of America Bulletin, v. 59, p. 447–462, http://dx.doi.org/10.1130/0016-7606(1948)59[447:TCOSR]2.0.CO;2.
Hilgen, F.J., 1991, Extension of the astronomically calibrated (polarity) time scale to the Miocene/Pliocene boundary: Earth and Planetary Science Letters, v. 107, p. 349–368, http://dx.doi.org/10.1016/0012-821X(91)90082-S.
Hilgen, F.J., Brinkhuis, H., and Zachariasse, W.J., 2006, Unit stratotypes for global stages. The Neogene perspective: Earth-Science Reviews, v. 74, p. 113–125, http://dx.doi.org/10.1016/j.earscirev.2005.09.003.
Hilgen, F.J., Hinnov, L.A., Aziz, H.A., Abels, H.A., Batenburg, S., Bosmans, J.H.C., de Boer, B., Hüsings, S.K., Kuiper, K.F., Lourens, L.J., Rivera, T., Tuenter, E., Van de Wal, R.S.W., Wotzlaw, J.-F., and Zeeden, C., 2015, Stratigraphic continuity and fragmentary sedimentation: the success of cyclostratigraphy as part of integrated stratigraphy, *in* Smith, D.G., Bailey, R.J., Burgess, P.M., and Fraser, A.J., *eds.,* Strata and time: Probing the Gaps in Our Understanding; Geological Society, London, Special Publications, v. 404, p. 157–197, http://dx.doi.org/10.1144/SP404.12.
Hinnov, L.A., and Ogg, J.G., 2007, Cyclostratigraphy and the astronomical time scale: Stratigraphy, v. 4, p. 239–251.
Hoffman, P.F., Kaufman, A.J., Halverson, G.P., and Schrag, D.P., 1998, A Neoproterozoic snowball Earth: Science, v. 281, p. 1342–1346, http://dx.doi.org/10.1126/science.281.5381.1342.
Holmes, A., 1913, The age of the Earth: Harper, London.
House, M.R., 1985, A new approach to an absolute timescale from measurements of orbital cycles and sedimentary microrhythms: Nature, v. 315, p. 721–725, http://dx.doi.org/10.1038/315721a0.
Hunt, D., and Tucker, M.E., 1992, Stranded parasequences and the forced regressive wedge systems tract: deposition during base-level fall: Sedimentary Geology, v. 81, p. 1–9, http://dx.doi.org/10.1016/0037-0738(92)90052-S.

Illing, L.V., 1954, Bahaman calcareous sands: American Association of Petroleum Geologists, v. 38, p. 1–95.

Ingersoll, R.V., 1978a, Submarine fan facies of the Upper Cretaceous Great Valley Sequence, northern and central California: Sedimentary Geology, v. 21, p. 205–230, http://dx.doi.org/10.1016/0037-0738(78)90009-X.

Ingersoll, R.V., 1978b, Petrofacies and petrologic evolution of the Late Cretaceous fore-arc basin, northern and central California: The Journal of Geology, v. 86, p. 335–352, http://dx.doi.org/10.1086/649695.

Ingersoll, R.V., 1979, Evolution of the Late Cretaceous forearc basin, northern and central California: Geological Society of America Bulletin, v. 90, p. 813–826, http://dx.doi.org/10.1130/0016-7606(1979)90<813:EOTLCF>2.0.CO;2.

James, N.P., and Dalrymple, R.W., *eds.*, 2010, Facies Models 4: GEOtext 6: Geological Association of Canada, St. John's, NL, 586 p.

James, N.P., and Lukasik, J., 2010, Cool- and cold-water neritic carbonates, *in* James, N.P., and Dalrymple, R.W., *eds.*, Facies Models 4: GEOtext 6: Geological Association of Canada, St. John's, NL, p. 371–420.

Jervey, M.T., 1988, Quantitative geological modeling of siliciclastic rock sequences and their seismic expression, *in* Wilgus, C.K., Hastings, B.S., Posamentier, H.W., Van Wagoner, J.C., Ross, C.A., and Kendall, C.G.St.C., *eds.*, Sea-level Changes - an integrated approach: Society of Economic Paleontologists and Mineralogists (SEPM) Special Publications, v. 42, p. 47–69, http://dx.doi.org/10.2110/pec.88.01.0047.

Johannessen, E.P., and Steel, R.J., 2005, Shelf-margin clinoforms and prediction of deepwater sands: Basin Research, v. 17, p. 521–550, http://dx.doi.org/10.1111/j.1365-2117.2005.00278.x.

Jordan, T.E., 1981, Thrust loads and foreland basin evolution, Cretaceous, western United States: American Association of Petroleum Geologists Bulletin, v. 65, p. 2506–2520.

Jordan, T.E., 1995, Retroarc foreland and related basins*, in* Busby, C.J., and Ingersoll, R.V., *eds.*, Tectonics of sedimentary basins: Blackwell Science, Oxford, p. 331–362.

Kauffman, E.G., 1986, High-resolution event stratigraphy: regional and global Cretaceous bio-events, *in* Walliser, O.H., *ed.,* Global Bio-events: Lecture Notes on Earth History, v. 8: Springer-Verlag, Berlin, p. 277–335, http://dx.doi.org/10.1007/bfb0010215.

Kauffman, E.G., 1988, Concepts and methods of high-resolution event stratigraphy: Annual Review of Earth and Planetary Sciences, v. 16, p. 605–654, http://dx.doi.org/10.1146/annurev.ea.16.050188.003133.

Kay, M., 1951, North American geosynclines: Geological Society of America Memoirs, v. 48, p. 1–132, http://dx.doi.org/10.1130/mem48-p1.

Kim, W., and Paola, C., 2007, Long-period cyclic sedimentation with constant tectonic forcing in an experimental relay ramp: Geology, v. 35, p. 331–334, http://dx.doi.org/10.1130/G23194A.1.

Krumbein, W.C., 1939, Preferred orientation of pebbles in sedimentary deposits: The Journal of Geology, v. 47, p. 673–706, http://dx.doi.org/10.1086/624827.

Krumbein, W.C., 1948, Lithofacies maps and regional sedimentary-stratigraphic analysis: American Association of Petroleum Geologists, v. 32, p. 1909–1923.

Krumbein, W.C., and Sloss, L.L., 1951, Stratigraphy and Sedimentation: Freeman, San Francisco, 497 p.

Krumbein, W.C., and Sloss, L.L., 1963, Stratigraphy and sedimentation (Second Edition): W.H. Freeman and Co., San Francisco, 660 p.

Kuenen, Ph.H., 1957, Review of Marine Sand-Transporting Mechanisms: Journal of the Alberta Society of Petroleum Geologists, v. 5, No. 4, p. 59–62

Kuenen, Ph.H., and Migliorini, C.I., 1950, Turbidity currents as a cause of graded bedding: The Journal of Geology, v. 58, p. 91–127, http://dx.doi.org/10.1086/625710.

Levorsen, A.I., 1943, Discovery thinking: American Association of Petroleum Geologists Bulletin, v. 27, p. 887–928.

Levorsen, A.I., 1954, Geology of petroleum: W.H. Freeman, San Francisco, 703 p.

Longwell, C.R., *ed.*, 1949, Sedimentary facies in geologic history: Geological Society of America Memoirs, v. 39, 172 p., http://dx.doi.org/10.1130/MEM39-pv.

Lyell, C., 1830–1833, Principles of Geology, 3 volumes: John Murray, London (reprinted by Johnson Reprint Corp., New York, 1969).

Macdonald, D.I.M., *ed.*, 1991, Sedimentation, tectonics and eustasy: sea-level changes at active margins: International Association of Sedimentologists Special Publication 12, 518 p.

Mackin, J. H., 1963, Rational and empirical methods of investigation in geology, *in* Albritton, C.C., *ed.*, The fabric of geology: Freeman, Cooper and Company, San Francisco, p. 135–163.

Matthews, R.K., 1984, Dynamic Stratigraphy (Second Edition): Prentice-Hall, Englewood Cliffs, NJ, 489 p.

McConnell, R.G., 1887, Report of the geological structure of a portion of the Rocky Mountains, accompanied by a section measured near the 51st parallel: Geological Survey of Canada, Annual Report 1886, p. 1D–41D.

McEachern, J.A., Pemberton, S.G., Gingras, M.K., and Bann, K.L., 2010, Ichnology and facies models, *in* James, N.P., and Dalrymple, R.W., *eds.*, Facies Models 4: Geotext 6: Geological Association of Canada, St John's, NL, p. 19–58.

McKee, E.D., 1957, Flume experiments on the production of stratification and cross-stratification: Journal of Sedimentary Petrology (Research), v. 27, p. 129–134, http://dx.doi.org/10.1306/74D70678-2B21-11D7-8648000102C1865D.

McKee, E.D., and Weir, G.W., 1953, Terminology for stratification and cross-stratification in sedimentary rocks: Geological Society of America Bulletin, v. 64, p. 381–390, http://dx.doi.org/10.1130/0016-7606(1953)64[381:TFSACI]2.0.CO;2.

McKenzie, D., 1978, Some remarks on the development of sedimentary basins: Earth and Planetary Science Letters, v. 40, p. 25–32, http://dx.doi.org/10.1016/0012-821X(78)90071-7.

McLaren, D.J., 1970, Presidential address: time, life and boundaries: Journal of Paleontology, v. 44, p. 801–813.

McMechan, M.E., 2000, Vreeland diamictites – Neoproterozoic glaciogenic slope deposits, Rocky Mountains, northeast British Columbia: Bulletin of Canadian Petroleum Geology, v. 48, p. 246–261, http://dx.doi.org/10.2113/48.3.246.

Merriam, D.F., *ed.*, 1964, Symposium on cyclic sedimentation: Kansas Geological Survey Bulletin 169, 636 p.

Miall, A.D., 1973, Markov chain analysis applied to an ancient alluvial plain succession: Sedimentology, v. 20, p. 347–364, http://dx.doi.org/10.1111/j.1365-3091.1973.tb01615.x.

Miall, A.D., *ed.*, 1980, Facts and Principles of World Petroleum Occurrence: Canadian Society of Petroleum Geologists Memoir 6, 1003 p.

Miall, A.D., 1984, Principles of sedimentary basin analysis: Springer-Verlag, Berlin, 490 p., http://dx.doi.org/10.1007/978-1-4757-4232-9.

Miall, A.D., 1985, Architectural-element analysis: A new method of facies analysis applied to fluvial deposits: Earth-Science Reviews, v. 22, p. 261–308, http://dx.doi.org/10.1016/0012-8252(85)90001-7.

Miall, A.D., 1988a, Reservoir heterogeneities in fluvial sandstones: lessons from outcrop studies: American Association of Petroleum Geologists Bulletin, v. 72, p. 682–697.

Miall, A.D., 1988b, Facies architecture in clastic sedimentary basins, *in* Kleinspehn, K., and Paola, C., *eds.*, New perspectives in basin analysis: Springer-Verlag Inc., New York, p. 67–81, http://dx.doi.org/10.1007/978-1-4612-3788-4_4.

Miall, A.D., 1995, Whither stratigraphy?: Sedimentary Geology, v. 100, p. 5–20, http://dx.doi.org/10.1016/0037-0738(95)00100-X.

Miall, A.D., 1999, Principles of sedimentary basin analysis (Third Edition): Springer-Verlag Inc., New York, 616 p.

Miall, A.D., 2004, Empiricism and model building in stratigraphy: the historical roots of present-day practices. Stratigraphy: American Museum of Natural History, v. 1, p. 3–25.

Miall, A.D., 2010, The geology of stratigraphic sequences (Second Edition): Springer-Verlag, Berlin, 522 p., http://dx.doi.org/10.1007/978-3-642-05027-5.

Miall, A.D., 2013, Sophisticated stratigraphy, *in* Bickford, M.E., *ed.*, The web of geological sciences: Advances, impacts and interactions: Geological Society of America Special Papers, v. 500, p. 169–190, http://dx.doi.org/10.1130/2013.2500(05).

Miall, A.D., 2014, Fluvial depositional systems: Springer-Verlag, Berlin 316 p., http://dx.doi.org/10.1007/978-3-319-00666-6.

Miall, A.D., 2015, Updating uniformitarianism: stratigraphy as just a set of 'frozen accidents,' *in* Smith, D.G., Bailey, R.J., Burgess, P.M., and Fraser, A.J., *eds.*, Strata and time: Geological Society, London, Special Publications, v. 404, p. 11–36, http://dx.doi.org/10.1144/SP404.4.

Miall, A.D., and Miall, C.E., 2001, Sequence stratigraphy as a scientific enterprise: the evolution and persistence of conflicting paradigms: Earth-Science Reviews, v. 54, p. 321–348, http://dx.doi.org/10.1016/S0012-8252(00)00041-6.

Middleton, G.V., *ed.*, 1965, Primary sedimentary structures and their hydrodynamic interpretation: Society of Economic Paleontologists and Mineralogists (SEPM) Special Publications, v. 12, 265 p.

Middleton, G.V., 1966a, Experiments on density and turbidity currents: I. Motion of the head: Canadian Journal of Earth Sciences, v. 3, p. 523–546, http://dx.doi.org/10.1139/e66-038.

Middleton, G.V., 1966b, Experiments on density and turbidity currents: II. Uniform flow of density currents: Canadian Journal of Earth Sciences, v. 3, p. 627–637, http://dx.doi.org/10.1139/e66-044.

Middleton, G.V., 1967, Experiments on density and turbidity currents: III. Deposition of sediment: Canadian Journal of Earth Sciences, v. 4, p. 475–505, http://dx.doi.org/10.1139/e67-025.

Middleton, G.V., 1973, "Johannes Walther's law of the correlation of facies:" Geological Society of America Bulletin, v. 84, p. 979–988, http://dx.doi.org/10.1130/0016-7606(1973)84<979:JWLOTC>2.0.CO;2.

Middleton, G.V., 2005, Sedimentology, History, *in* Middleton, G.V., *ed.*, Encyclopedia of sediments and sedimentary rocks: Springer-Verlag, Berlin, p. 628–635.

Middleton, G.V., and Hampton, M.A., 1976, Subaqueous sediment transport and deposition by sediment gravity flows, *in* Stanley, D.J., and Swift, D.J.P., *eds.*, Marine sediment transport and environmental management: Wiley, New York, p. 197–218.

Milankovitch, M., 1930, Mathematische klimalehre und astronomische theorie der klimaschwankungen, *in* Koppen, W., and Geiger, R., *eds.*, Handbuch der klimatologie, I (A): Gebruder Borntraeger, Berlin, p. 1–176.

Milankovitch, M., 1941, Kanon der Erdbestrahlung und seine Anwendung auf das Eiszeitenproblem: Akad. Royale Serbe, v. 133, 633 p.

Mitchell, A.H., and Reading, H.G., 1969, Continental margins, geosynclines and ocean floor spreading: The Journal of Geology, v. 77, p. 629–646, http://dx.doi.org/10.1086/627462.

Moore, R.C., 1949, Meaning of facies, *in* Longwell, C., *ed.*, Sedimentary facies in geologic history: Geological Society of America Memoirs, v. 39, p. 1–34, http://dx.doi.org/10.1130/MEM39-p1.

Mossop, G.D., and Shetsen, I*., compilers,* 1994, Geological Atlas of the Western Canada Sedimentary Basin: Canadian Society of Petroleum Geologists, 510 p.

Muir Wood, R., 1985, The dark side of the Earth: George Allen and Unwin, 246 p.

Muto, T., and Steel, R.J., 2004, Autogenic response of fluvial deltas to steady sea-level fall: Implications from flume-tank experiments: Geology, v. 32, p. 401–404, http://dx.doi.org/10.1130/G20269.1.

Nanz, R.H., Jr., 1954, Genesis of Oligocene sandstone reservoir, Seeligson field, Jim Wells and Kleberg Counties, Texas: American Association of Petroleum Geologists Bulletin, v. 38, p. 96–117.

Newell, N.D., and Rigby, J.K., 1957, Geological studies on the Great Bahama Bank: Society of Economic Paleontologists and Mineralogists (SEPM) Special Publications, v. 5, p. 15–72, http://dx.doi.org/10.2110/pec.57.01.0015.

Oliver, T.A., and Cowper, N.W., 1963, Depositional environments of the Ireton Formation, central Alberta: Bulletin of Canadian Petroleum Geology, v. 11, p. 183–202.

Oliver, T.A., and Cowper, N.W., 1965, Depositional environments of Ireton Formation, central Alberta: Bulletin of the American Association of Petroleum Geologists, v. 49, p. 1410–1425.

Paola, C., 2000, Quantitative models of sedimentary basin filling: Sedimentology, v. 47 (S1), p. 121–178, http://dx.doi.org/10.1046/j.1365-3091.2000.00006.x.

Paola, C., Mullin, J., Ellis, C., Mohrig, D.C., Swenson, J.B., Parker, G., Hickson, T., Heller, P.L., Pratson, L., Syvitski, J., Sheets, B., and Strong, N., 2001, Experimental stratigraphy: GSA Today, v. 11, p. 4–9, http://dx.doi.org/10.1130/1052-5173(2001)011<0004:ES>2.0.CO;2.

Paola, C., Straub, K., Mohrig, D., and Reinhardt, L., 2009, The "unreasonable effectiveness" of stratigraphic and geomorphic experiments: Earth-Science Reviews, v. 97, p. 1–43, http://dx.doi.org/10.1016/j.earscirev.2009.05.003.

Payton, C.E., *ed.*, 1977, Seismic stratigraphy—applications to hydrocarbon exploration: American Association of Petroleum Geologists Memoir 26, 516 p.

Pettijohn, F.J., 1949, Sedimentary rocks: Harper and Bros, New York, 513 p.

Pettijohn, F.J., 1956, In defence of outdoor geology: American Association of Petroleum Geologists Bulletin, v. 40, p. 1455–1461.

Pettijohn, F.J., 1962, Paleocurrents and paleogeography: American Association of Petroleum Geologists Bulletin, v. 46, p. 1468–1493.

Pettijohn, F.J., 1984, Memoirs of an unrepentant field geologist: A candid profile of some geologists and their science, 1921–1981: University of Chicago Press, Chicago, 260 p.

Pettijohn, F.J., and Potter, P.E., 1964, Atlas and glossary of primary sedimentary structures: Springer-Verlag, New York, 370 p., http://dx.doi.org/10.1007/978-3-642-94899-2.

Playfair, J., 1802, Illustrations of the Huttonian theory of the Earth: Dover Publications, (White, G.W., *ed*., 1956)*,* New York, 528 p.

Plint, A.G., Walker, R.G., and Bergman, K.M., 1986, Cardium Formation 6. Stratigraphic framework of the Cardium in subsurface: Bulletin of Canadian Petroleum Geology, v. 34, p. 213–225.

Plint, A.G., Tyagi, A., Hay, M.J., Varban, B.L., Zhang, H., and Roca, X., 2009, Clinoforms, paleobathymetry, and mud dispersal across the Western Canada Cretaceous Foreland Basin: Evidence from the Cenomanian Dunvegan Formation and contiguous strata: Journal of Sedimentary Research, v. 79, p. 144–161, http://dx.doi.org/10.2110/jsr.2009.020.

Plint, A.G., Macquaker, J.H.S., and Varban, B.L., 2012, Bedload transport of mud across a wide, storm-influenced ramp: Cenomanian–Turonian Kaskapau Formation, Western Canada Foreland Basin: Journal of Sedimentary Research , v. 82, p. 801–822, http://dx.doi.org/10.2110/jsr.2012.64.

Posamentier, H.W., and Vail, P.R., 1988, Eustatic controls on clastic deposition II—Sequence and systems tract models, *in* Wilgus, C.K., Hastings, B.S., Posamentier, H.W., Van Wagoner, J.C., Ross, C.A., and Kendall, C.G.St.C., *eds.*, Sea-level Changes: an integrated approach: Society of Economic Paleontologists and Mineralogists (SEPM) Special Publications, v. 42, p. 125–154, http://dx.doi.org/10.2110/pec.88.01.0125.

Posamentier, H.W., Jervey, M.T., and Vail, P.R., 1988, Eustatic controls on clastic deposition I—Conceptual framework, *in* Wilgus, C.K., Hastings, B.S., Posamentier, H.W., Van Wagoner, J.C., Ross, C.A., and Kendall, C.G.St.C., *eds.,* Sea-level Changes: an integrated approach: Society of Economic Paleontologists and Mineralogists (SEPM) Special Publications, v. 42, p. 109–124, http://dx.doi.org/10.2110/pec.88.01.0109.

Potter, P.E., 1959, Facies models conference: Science, (Meetings), v. 129, p. 1292–1294, http:/dx.doi.org/10.1126/science.129.3358.1292.

Potter, P.E., 1967, Sand bodies and sedimentary environments: A review: American Association of Petroleum Geologists Bulletin, v. 51, p. 337–365.

Potter, P.E., and Pettijohn, F.J., 1963, Paleocurrents and basin analysis: Springer-Verlag, Berlin, 296 p., http://dx.doi.org/10.1007/978-3-662-01020-4.

Potter, P.E., and Pettijohn, F.J., 1977, Paleocurrents and basin analysis (Second Edition): Academic Press, San Diego, CA, 296 p., http://dx.doi.org/10.1007/978-3-642-61887-1.

Price, R.A., 1973, Large-scale gravitational flow of supracrustal rocks, southern Canadian Rockies, *in* DeJong, K.A., and Scholten, R.A., *eds.*, Gravity and tectonics: John Wiley, New York, p. 491–502.

Purdy, E.G., 1963a, Recent calcium carbonate facies of the Great Bahama Bank. 1. Petrography and Reaction Groups: The Journal of Geology, v. 71, p. 334–355.

Purdy, E.G., 1963b, Recent calcium carbonate facies of the Great Bahama Bank. 2. Sedimentary Facies: The Journal of Geology, v. 71, p. 472–497.

Ramos, A., and Sopeña, A., 1983, Gravel bars in low-sinuosity streams (Permian and Triassic, central Spain), *in* Collinson, J.D., and Lewin, J., *eds.*, Modern and ancient fluvial systems: Blackwell Publishing Ltd., Oxford, UK, p. 301–312, http://dx.doi.org/10.1002/9781444303773.ch24.

Ramos, A., Sopeña, A., and Perez-Arlucea, M., 1986, Evolution of Buntsandstein fluvial sedimentation in the northwest Iberian Ranges (central Spain): Journal of Sedimentary Petrology (Research), v. 56, p. 862–875, http://dx.doi.org/10.1306/212F8A6C-2B24-11D7-8648000102C1865D.

Read, H.H., 1952, The geologist as historian, *in* Scientific Objectives: Butterworths, p. 52–67, (reprinted in Proceedings of the Geologists' Association, v. 81, p. 409–420).

Reading, H.G., *ed.*, 1978, Sedimentary environments and facies: Blackwell, Oxford, 557 p.

Reading, H.G., *ed.*, 1986, Sedimentary environments and facies (Second Edition): Blackwell, Oxford, 615 p.

Reading, H.G., *ed.*, 1996, Sedimentary environments: processes, facies and stratigraphy (Third Edition): Blackwell Science, Oxford, 688 p.

Reiche, P., 1938, An analysis of cross-lamination: The Coconino Sandstone: The Journal of Geology, v. 46, p. 905–932, http://dx.doi.org/10.1086/624709.

Reineck, H.E., and Singh, I.B., 1973, Depositional sedimentary environments—with reference to terrigenous clastics: Springer-Verlag, Berlin, 439 p.

Rich, J.L., 1951, Three critical environments of deposition and criteria for recognition of rocks deposited in each of them: Geological Society of America Bulletin, v. 62, p. 1–20, http://dx.doi.org/10.1130/0016-7606(1951)62[1:TCEODA]2.0.CO;2.

Rigby, J.K., and Hamblin, W.K., *eds.*, 1972, Recognition of ancient sedimentary environments: Society of Economic Paleontologists and Mineralogists (SEPM) Special Publications, v. 16, 340 p.

Rine, J.M., Helmold, K.P., Bartlett, G.A., Hayes, B.J.R., Smith, D.G., Plint, A.G., Walker, R.G., and Bergman, K.M., 1987, Cardium Formation 6. Stratigraphic framework of the Cardium in subsurface: Discussions and reply: Bulletin of Canadian Petroleum Geology, v. 35, p. 362–374.

Ross, W.C., 1991, Cyclic stratigraphy, sequence stratigraphy, and stratigraphic modeling from 1964 to 1989: twenty-five years of progress?, *in* Franseen, E.K., Watney, W.L., and Kendall, C.G.St.C., *eds.*, Sedimentary modeling: computer simulations and methods for improved parameter definition: Kansas Geological Survey Bulletin 233, p. 3–8.

Sadler, P.M., 1981, Sediment accumulation rates and the completeness of stratigraphic sections: The Journal of Geology, v. 89, p. 569–584, http://dx.doi.org/10.1086/628623.

Sadler, P.M., 1999, The influence of hiatuses on sediment accumulation rates: GeoResearch Forum, v. 5, p. 15–40.

Sadler, P.M., Cooper, R.A., and Melchin, M., 2009, High-resolution, early Paleozoic (Ordovician–Silurian) time scales: Geological Society of America Bulletin, v. 121, p. 887–906, http://dx.doi.org/10.1130/B26357.1.

Sageman, B.B., Singer, B.S., Meyers, S.R., Siewert, S.E., Walaszczyk, I., Condon, D.J., Jicha, B.R., Obradovich, J.D., and Sawyer, D.A., 2014, Integrating $^{40}Ar/^{39}Ar$, U–Pb and astronomical clocks in the Cretaceous Niobrara Formation, Western Interior Basin, USA: Geological Society of America Bulletin, v. 126, p. 956–973, http://dx.doi.org/10.1130/B30929.1.

Salvador, A., *ed.*, 1994, International Stratigraphic Guide (Second Edition): International Union of Geological Sciences, Trondheim, Norway, and Geological Society of America, Boulder, Colorado, 214 p.

Schenk, H.G., and Muller, S.W.M., 1941, Stratigraphic terminology: Geological Society of America Bulletin, v. 52, p. 1419–1426, http://dx.doi.org/10.1130/GSAB-52-1419.

Schieber, J., Southard, J.B., Kissling, P., Rossman, B., and Ginsburg, R., 2013, Experimental deposition of carbonate mud from moving suspensions: Importance of flocculation and implications for modern and ancient carbonate mud deposition: Journal of Sedimentary Research, v. 83, p. 1026–1032, http://dx.doi.org/10.2110/jsr.2013.77.

Schlager, W., 2005, Carbonate sedimentology and sequence stratigraphy: SEPM Concepts in Sedimentology and Paleontology, # 8, 200 p.

Sheets, B.A., Hickson, T.A., and Paola, C., 2002, Assembling the stratigraphic record: depositional patterns and time-scales in an experimental alluvial basin: Basin Research, v. 14, p. 287–301, http://dx.doi.org/10.1046/j.1365-2117.2002.00185.x.

Shepard, F.P., and Wanless, H.R., 1935, Permo–Carboniferous coal series related to southern hemisphere glaciation: Science, v. 81, p. 521–522, http://dx.doi.org/10.1126/science.81.2108.521.

Shepard, F.P., Phleger, F.B., and van Andel, T.H., *eds.*, 1960, Recent sediments, northwest Gulf of Mexico: American Association of Petroleum Geologists, 394 p.

Simons, D.B., and Richardson, E.V., 1961, Forms of bed roughness in alluvial channels: American Society of Civil Engineers Proceedings, v. 87, No. HY3, p. 87–105.

Sloss, L.L., 1963, Sequences in the cratonic interior of North America: Geological Society of America Bulletin, v. 74, p. 93–114, http://dx.doi.org/10.1130/0016-7606(1963)74[93:SITCIO]2.0.CO;2.

Sloss, L.L., 1972, Synchrony of Phanerozoic sedimentary-tectonic events of the North American craton and the Russian platform: 24th International Geological Congress, Montreal, Section 6, p. 24–32.

Sloss, L.L., 1988, Tectonic evolution of the craton in Phanerozoic time, *in* Sloss, L.L., *ed.*, Sedimentary cover—North American Craton: U.S.: The Geology of North America, Geological Society of America, v. D-2, Boulder, CO, p. 25–51.

Sloss, L.L., 1991, The tectonic factor in sea level change: a countervailing view: Journal of Geophysical Research, v. 96, p. 6609–6617, http://dx.doi.org/10.1029/90JB00840.

Sloss, L.L., Krumbein, W.C., and Dapples, E.C., 1949, Integrated facies analysis; *in* Longwell, C.R., *ed.*, Sedimentary facies in geologic history: Geological Society of America Memoirs, v. 39, p. 91–124, http://dx.doi.org/10.1130/MEM39-p91.

Smith, W., 1815, A memoir to the map and delineation of the strata of England and Wales, with part of Scotland: John Carey, London, 51 p.

Sorby, H.C., 1852, On the oscillation of the currents drifting the sandstone beds of the southeast of Northumberland, and on their general direction in the coal field in the neighbourhood of Edinburgh: Proceedings of the West Yorkshire Geological Society, v. 3, p. 232–240, http://dx.doi.org/10.1144/pygs.3.232.

Sorby, H.C., 1859, On the structures produced by the currents present during the deposition of stratified rocks: The Geologist, v. II, p. 137–147.

Sorby, H.C., 1908, On the application of quantitative methods to the study of the structure and history of rocks: Quarterly Journal of the Geological Society, v. 64, p. 171–233, http://dx.doi.org/10.1144/GSL.JGS.1908.064.01-04.12.

Steckler, M.S., and Watts, A.B., 1978, Subsidence of the Atlantic-type continental margin off New York: Earth and Planetary Science Letters, v. 41, p. 1–13, http://dx.doi.org/10.1016/0012-821X(78)90036-5.

Steel, R.J., and Milliken, K.L., 2013, Major advances in siliciclastic sedimentary geology, 1960–2012, *in* Bickford, M.E., *ed.*, The web of geological sciences: Advances, impacts and interactions: Geological Society of America Special Papers, v. 500, p. 121–167, http://dx.doi.org/10.1130/2013.2500(04).

Steno, Nicolaus, 1669, De Solido intra Solidum naturaliter contento dissertationis prodromus: Florence, 78 p.

Stokes, W.L., 1945, Primary lineation in fluvial sandstones: a criterion of current direction: The Journal of Geology, v. 45, p. 52–54.

Strangway, D.W., *ed.*, 1980, The continental crust and its mineral deposits: Geological Association of Canada Special Paper 20, 804 p.

Strong, N., and Paola, C., 2008, Valleys that never were: Time surfaces versus stratigraphic surfaces: Journal of Sedimentary Research, v. 78, p. 579–593, http://dx.doi.org/10.2110/jsr.2008.059.

Tankard, A.J., and Welsink, H.J., 1987, Extensional tectonics and stratigraphy of Hibernia oil field, Grand Banks, Newfoundland: American Association of Petroleum Geologists Bulletin, v. 71, p. 1210–1232.

Teichert, C., 1958, Concepts of facies: American Association of Petroleum Geologists Bulletin, v. 42, p. 2718–2744.

Torrens, H.S., 2002, Some personal thoughts on stratigraphic precision in the twentieth century, *in* Oldroyd, D.R., *ed.*, The Earth inside and out: Some major contributions to geology in the twentieth century: Geological Society, London, Special Publications, v. 192, p. 251–272, http://dx.doi.org/10.1144/gsl.sp.2002.192.01.14.

Vail, P.R., 1975, Eustatic cycles from seismic data for global stratigraphic analysis (Abstract): American Association of Petroleum Geologists Bulletin, v. 59, p. 2198–2199.

Vail, P.R., Mitchum, R.M., Jr., Todd, R.G., Widmier, J.M., Thompson, S., III, Sangree, J.B., Bubb, J.N., and Hatlelid, W.G., 1977, Seismic stratigraphy and global changes of sea-level, *in* Payton, C.E., *ed.*, Seismic stratigraphy - applications to hydrocarbon exploration: American Association of Petroleum Geologists Memoir 26, p. 49–212.

Van Siclen, D.C., 1958, Depositional topography—examples and theory: American Association of Petroleum Geologists Bulletin, v. 42, p. 1897–1913.

Van Straaten, L.M.J.U., 1954, Composition and structure of recent marine sediments in the Netherlands: Leidse Geol. Mededel., v. 19, p. 1–110.

Van Wagoner, J.C., Mitchum, R.M., Campion, K.M., and Rahmanian, V.D., 1990, Siliciclastic sequence stratigraphy in well logs, cores, and outcrops: American Association of Petroleum Geologists, Methods in Exploration Series 7, 55 p.

Veeken, P.C.H., 2007, Seismic stratigraphy, basin analysis and reservoir characterisation. Handbook of Geophysical Exploration, Volume 37: Elsevier, Amsterdam, 509 p.

Visher, G.S., 1965, Use of vertical profile in environmental reconstruction: American Association of Petroleum Geologists Bulletin, v. 49, p. 41–61.

Waddell, H., 1933, Sedimentation and sedimentology: Science, v. 77, p. 536–537, http://dx.doi.org/10.1126/science.77.2005.536.

Walker, R.G., 1965, The origin and significance of the internal sedimentary structures of turbidites: Proceedings of the Yorkshire Geological Society, v. 35, p. 1–32, http://dx.doi.org/10.1144/pygs.35.1.1.

Walker, R.G., 1967, Turbidite sedimentary structures and their relationship to proximal and distal depositional environments: Journal of Sedimentary Petrology (Research), v. 37, p. 25–43, http://dx.doi.org/10.1306/74D71645-2B21-11D7-8648000102C1865D.

Walker, R.G., 1973, Mopping up the turbidite mess, *in* Ginsburg, R.N., *ed.*, Evolving concepts in sedimentology: Johns Hopkins University Press, Baltimore, p. 1–37.

Walker, R.G., 1976, Facies models 1. General Introduction: Geoscience Canada, v. 3, p. 21–24.

Walker, R.G., *ed.*, 1979, Facies models: Geoscience Canada Reprint Series 1, 211 p.

Walker, R.G., *ed.*, 1984, Facies Models (Second Edition): Geoscience Canada Reprint Series 1, 317 p.

Walker, R.G., 1990, Facies modeling and sequence stratigraphy: Journal of Sedimentary Petrology (Research), v. 60, p. 777–786, http://dx.doi.org/10.1306/212F926E-2B24-11D7-8648000102C1865D.

Walker, R.G., and James, N.P., 1992, Facies models: response to sea-level change: Geological Association of Canada, St. John's, NL, 409 p.

Walther, Johannes, 1893–1894, Einleisung in die Geologie alshistorische Wissemchaft: Jena, Verlag von Gustav Fischer, 3 volumes, 1055 p.

Wanless, H.R., and Shepard, F.P., 1936, Sea level and climatic changes related to Late Paleozoic cycles: Geological Society of America Bulletin, v. 47, p. 1177–1206, http://dx.doi.org/10.1130/GSAB-47-1177.

Wanless, H.R., and Weller, J.M., 1932, Correlation and extent of Pennsylvanian cyclothems: Geological Society of America Bulletin, v. 43, p. 1003–1016, http://dx.doi.org/10.1130/GSAB-43-1003.

Watts, A.B., 1981, The U.S. Atlantic margin: subsidence history, crustal structure and thermal evolution: American Association of Petroleum Geologists, Education Course Notes Series #19, Chapter 2, 75 p.

Watts, A.B., 1989, Lithospheric flexure due to prograding sediment loads: implications for the origin of offlap/onlap patterns in sedimentary basins: Basin Research, v. 2, p. 133–144, http://dx.doi.org/10.1111/j.1365-2117.1989.tb00031.x.

Watts, A.B., and Ryan, W.B.F., 1976, Flexure of the lithosphere and continental margin basins: Tectonophysics, v. 36, p. 25–44, http://dx.doi.org/10.1016/0040-1951(76)90004-4.

Weller, J.M., 1960, Stratigraphic Principles and Practice: Harper, New York, 725 p.

Wernicke, B., 1985, Uniform-sense normal simple shear of the continental lithosphere: Canadian Journal of Earth Sciences, v. 22, p. 108–125, http://dx.doi.org/10.1139/e85-009.

Wheeler, H.E., 1958, Time-stratigraphy: American Association of Petroleum Geologists Bulletin, v. 42, p. 1047–1063.

White, N., and McKenzie, D., 1988, Formation of the "steer's head" geometry of sedimentary basins by differential stretching of the crust and mantle: Geology, v. 16, p. 250–253, http://dx.doi.org/10.1130/0091-7613(1988)016<0250:FOTSSH>2.3.CO;2.

Whitten, E.H.T., 1964, Process-response models in geology: Geological Society of America Bulletin, v. 75, p. 455–464, http://dx.doi.org/10.1130/0016-7606(1964)75[455:PMIG]2.0.CO;2.

Wilgus, C.K., Hastings, B.S., Posamentier, H.W., Van Wagoner, J.C., Ross, C.A., and Kendall, C.G.St.C., *eds.*, 1988, Sea-level changes: an integrated approach: Society of Economic Paleontologists and Mineralogists (SEPM) Special Publications, v. 42, 407 p., http://dx.doi.org/10.2110/pec.88.42.

Williams, G.D., and Dobb, A., *eds.*, 1993, Tectonics and seismic sequence stratigraphy: Geological Society, London, Special Publications, v. 71, 226 p.

Wilson, J.L., 1975, Carbonate facies in geologic history: Springer-Verlag, New York, 471 p., http://dx.doi.org/10.1007/978-1-4612-6383-8.

Wilson, J.T., 1985, Development of ideas about the Canadian Shield: A personal account, *in* Drake, E.T., and Jordan, W.M., *eds.*, Geologists and ideas: A History of North American Geology, Geological Society of America Centennial Special Volume 1, p. 143–150, http://dx.doi.org/10.1130/DNAG-CENT-v1.143.

Woodford, A.O., 1973, Johannes Walther's Law of the Correlation of Facies: Discussion: Geological Society of America Bulletin, v. 84, p. 3737–3740, http://dx.doi.org/10.1130/0016-7606(1973)84<3737:JWLOTC>2.0.CO;2.

Received March 2015
Accepted as revised June 2015

NEW SERIES

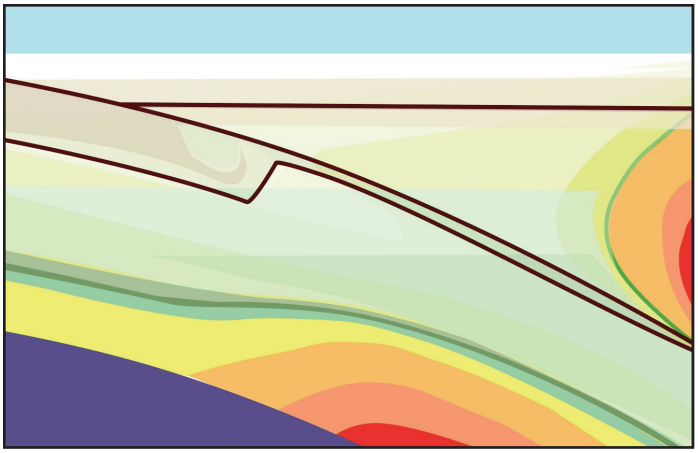

PROLOGUE:
ANDREW HYNES SERIES: TECTONIC PROCESSES

For nearly 40 years, Andrew Hynes of McGill University has contributed to our understanding of fundamental concepts in geosciences, ranging through time from the Archean to the present, and across disciplines from mineralogy and petrology, to structural geology, tectonics, geodynamics and geophysics. Andrew's research deals with fundamental processes that penetrate to the core of our science. In addition to providing comprehensive interpretations, Andrew has been careful to devise critical tests of his models, producing novel and plausible insights. He quantifies the quantifiable without embellishment, clearly states his assumptions and inferences, and provides testable models.

Born in Liverpool, U.K., Andrew emigrated as a teenager to Canada, completing his undergraduate degree at the University of Toronto and a PhD at Cambridge University in 1972. In 1975, he joined McGill as a (very) young professor. He officially retired in 2014, but remains an active researcher. His research was funded by a variety of sources, including continuous funding from N.S.E.R.C. for nearly 40 years. He has had a profound impact on the careers of generations of graduate and undergraduate students, not only at McGill but also in the broader geoscience community, a commitment that earned him the 2013 Canadian Federation of Earth Sciences Mentorship Medal in 2013. Andrew also has contributed to the wider community, including serving two terms as department chair at McGill, as Technical Program Chairman (twice) for annual GAC–MAC meetings, as a member of the editorial boards of several prestigious journals and as a member and Chair of the NSERC Grants Committee for the Solid Earth Sciences.

His publications have a remarkable shelf-life. His PhD research in Greece was one of the first to apply plate tectonic principles to complexly deformed ophiolitic terrains and he discussed the importance of micro-continents in the tectonic evolution of the Mediterranean before they became fashionable in the Cordillera. In the late 1970's, he documented and modeled the mobility of 'immobile' elements in metabasaltic rocks. In the 1980's, his work with Don Francis and students in the Cape Smith Fold Belt contributed to the understanding of komatiitic magmatism, thereby providing major new insights into Early Proterozoic tectonics. He studied amphibole and garnet–muscovite assemblages as indicators of metamorphic grade and style of orogeny, and at the same time pro-

Andrew receiving the 2013 Canadian Federation Earth Sciences Mentorship Medal, at the GAC–MAC annual meeting in Winnipeg, May 2013.

posed provocative models for the stability of the Proterozoic tectosphere, for the initiation of subduction and back-arc spreading in both the modern and Proterozoic worlds, and for the fragmentation of Pangea.

In the 1990's Andrew produced several papers linking geology and geophysics in a seamless fashion. He launched and supervised several student research projects in the Labrador Trough, thereby providing insights into the expression of the Trans-Hudson orogen in that region. He was a driving force behind the Abitibi-Grenville LITHOPROBE Project, and showed that arcuate structures along the Grenville Front are related to flexing of the lithosphere due to loading of pre-existing, Trans-Hudson thrust sheets. About the same time, he demonstrated that basalt geochemistry could be used as a probe for crustal thickness in the Hudson Bay arc, and provided theoretical constraints on the onset of hydrothermal cooling of Earth and the origin of its first continental lithosphere some 4.0 Ga. In a paper (co-authored with David Eaton) that won the 1999 Dave Elliott award for best paper in Canadian Structure and Tectonics, Andrew proposed that lateral ramps to orogenic wedges facilitate rapid unroofing of deep crustal rocks.

Andrew's ongoing interest in geodynamic processes led him to publish papers on the extrusion of deep-crustal rocks in collisional zones, and the relationship between continental growth, crustal thickness change and Earth's thermal efficiency. More recently, Andrew tackled the fundamental problem of subduction initiation and the role of negative buoyancy of oceanic lithosphere, providing evidence that initiation occurs along leaky fracture zones, where flooding of oceanic plates by magma is most likely. And by modeling the effect of extension on an Archean mantle, Andrew provided an explanation for the scarcity of Archean passive margin sediments, and showed that subduction is geodynamically permissible in the Late Archean.

By conducting independent, process-oriented, rigorous research on first-order issues, Andrew has been an outstanding mentor and role model for generations of students. Through his own research and his mentorship of students, his contributions to the geosciences have been immense. We are honoured to dedicate this series of papers on Tectonic Processes to him.

Brendan Murphy, Stephen Johnston, and Boswell (Boz) Wing,
Guest Editors

ANDREW HYNES SERIES: TECTONIC PROCESSES

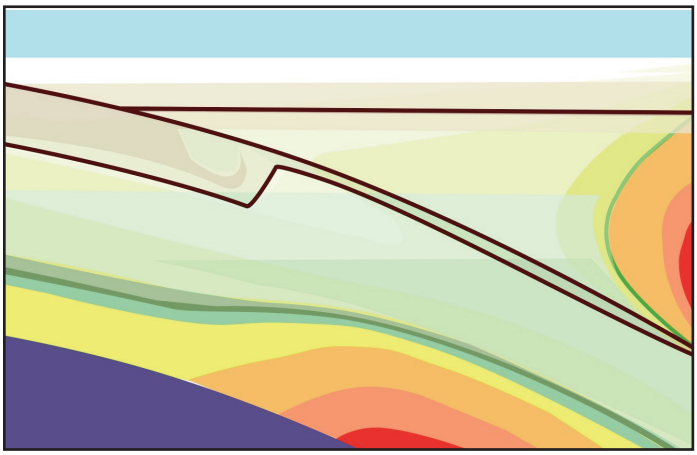

Neoarchean Mantle-derived Magmatism within the Repulse Bay Block, Melville Peninsula, Nunavut: Implications for Archean Crustal Extraction and Cratonization

Crystal LaFlamme[1*], Christopher R.M. McFarlane[1], David Corrigan[2]

[1]Department of Earth Sciences,
University of New Brunswick,
2 Bailey Drive, Fredericton, NB, E3B 5A, Canada

[*]Centre for Exploration Targeting
University of Western Australia
35 Stirling Hwy, Crawley, WA 6009, Australia
Email: crystal.laflamme@uwa.edu.au

[2]Geological Survey of Canada,
601 Booth Street,
Ottawa, Ontario, K1A 0E8, Canada

SUMMARY

The Repulse Bay block (RBb) of the southern Melville Peninsula, Nunavut, lies within the Rae craton and exposes a large (50,000 km^2) area of middle to lower crust. The block is composed of ca. 2.86 Ga and 2.73–2.71 Ga tonalite-trondhjemite-granodiorite (TTG) and granitic gneiss that was derived from an older 3.25 and 3.10 Ga crustal substrate. This period of crustal generation was followed by the emplacement of ca. 2.69–2.66 Ga enderbite, charnockite, and granitoid intrusions with entrained websterite xenoliths. These voluminous batholith-scale bodies (dehydrated and hydrated intrusions), and the associated websterite xenoliths, have similar whole rock geochemical properties, including fractionated light rare earth element (LREE)–heavy (H)REE whole rock patterns and negative Nb, Ti, and Ta anomalies. Dehydrated intrusions and websterite xenoliths also contain similar mineralogy (two pyroxene, biotite, interstitial amphibole) and similar pyroxene trace element compositions. Based on geochemical and mineralogical properties, the two lithologies are interpreted to be related by fractional crystallization, and to be the product of a magmatic cumulate processes. Reworking of the crust in a ca. 2.72 Ga subduction zone setting was followed by ca. 2.69 Ga upwelling of the asthenospheric mantle and the intrusion of massif-type granitoid plutons. Based on a dramatic increase in FeO, Zr, Hf, and LREE content of the most evolved granitoid components from the 2.69–2.66 Ga cumulate intrusion, we propose that those granitoid plutons were in part derived from a metasomatized mantle source enriched by fluids from the subducting oceanic slab that underwent further hybridization (via assimilation) with the crust. Large-scale, mantle-derived Neoarchean sanukitoid-type magmatism played a role in the development of a depleted lower crust and residual sub-continental lithospheric mantle, a crucial element in the preservation of the RBb.

RÉSUMÉ

Le bloc de Repulse Bay (RBb) dans le sud de la péninsule de Melville, au Nunavut, est situé dans le craton de Rae et expose une large zone (50 000 km^2) de croûte moyenne à inférieur. Ce bloc est composé de tonalite-trondhjémite-granodiorite (TTG) daté à ca. 2,86 Ga et 2,73–2,71 Ga, et de gneiss granitique dérivé d'un substrat crustal plus ancien daté à 3,25 Ga et 3,10 Ga. Cette période de croissance crustale a été suivie par la mise en place entre ca. 2,69 et 2,66 Ga d'intrusions d'enderbite, charnockite et de granitoïde incluant des xénolites d'entraînement de websterite. Ces intrusions de taille batholitique (intrusions déshydratées et hydratées) ainsi que les xénolites d'entraînement de websterite associés, ont des propriétés géochimiques sur roche totale semblables notamment leurs profils de fractionnement des terres rares légers (*LREE*) et des terres

rares lourds (*HREE)* ainsi que leurs anomalies négatives en Nb, Ti et Ta. Les intrusions déshydratées et les xénolites de websterite ont aussi des minéralogies similaires (deux pyroxènes, biotite, amphibole interstitielle) ainsi que des compositions semblables en éléments traces de leurs pyroxènes. Étant donné leurs propriétés géochimiques et minéralogiques, ces deux lithologies sont interprétées comme provenant d'une cristallisation fractionnée, et comme étant le produit de processus d'accumulations magmatiques. Le remaniement de la croûte dans un contexte de subduction vers ca. 2,72 Ga, a été suivi vers ca. 2,69 Ga d'une remontée du manteau asthénosphérique et de l'intrusion de granitoïdes de type massif. D'après l'importante augmentation en FeO, Zr, Hf et *LREE* dans les granitoïdes les plus évolués du magmatisme ayant pris place entre ca. 2,69 Ga et 2,66 Ga, nous proposons que ces plutons aient été en partie dérivés d'une source mantélique métasomatisée enrichies par des fluides d'une plaque océanique en subduction et qui a subi une hybridation supplémentaire (par assimilation) avec la croûte. Le magmatisme néoarchéen de type sanukitoïde, dérivé du manteau et de grande échelle, a joué un rôle dans le développement d'une croûte inférieure et d'un manteau lithosphérique continental résiduel appauvri, un élément déterminant pour la préservation du RBb.

Traduit par le Traducteur

INTRODUCTION

The Neoarchean is a discernible era in the formation, evolution and stabilization of large volumes of continental crust (Moyen et al. 2001; Martin and Moyen 2002; Halla et al. 2009; Hawkesworth et al. 2010; Rapp et al. 2010; Laurent et al. 2011; Heilimo et al. 2013). This time period represents a transition to the generation of moderate to high pressure tonalite-trondhjemite-granodiorite (TTG), sanukitoid rocks, and high-K granite (e.g. Shirey and Hanson 1984; Smithies and Champion 2000; Martin et al. 2005; Halla et al. 2009; Rapp et al. 2010; Laurent et al. 2014) and the final stability of Archean cratons that had previously undergone rapid recycling (Hawkesworth et al. 2010). The sanukitoid suite is composed of Neoarchean granitoid lithologies that contain both an 'arc-like' and 'mantle-like' signatures that reflect their generation from a mantle peridotite source, rich in incompatible elements (Stern et al. 1989; Laurent et al. 2014 and references therein). Numerous studies have highlighted the similarities in geochemical characteristics of Neoarchean TTG-type gneiss, sanukitoid rocks and high-K granite (e.g. Smithies and Champion 2000; Martin et al. 2005, 2010; Halla et al. 2009; Rapp et al. 2010) that preserve a mantle affinity (high MgO, Mg #, Ni, Cr, Co, V, etc.) and 'arc-like' signatures (Nb, Ta and Ti troughs, enrichment in LILE and LREE) generally derived from slab melts (Martin and Moyen 2002; Halla 2005; Halla et al. 2009).

High grade, Neoarchean granulite terranes have been observed worldwide and are locally exposed in the northern Superior craton (e.g. Davis et al. 2005; Boily et al. 2009; Heaman et al. 2011). Granulite terranes can preserve regional scale, pyroxene-bearing, massif-type calc-alkalic intrusions (Fyfe 1973; Rudnick and Fountain 1995). Similar to sanukitoid intrusions, these charnockitic intrusions preserve geochemical trace element patterns typical of Neoarchean TTGs and modern day arc environments (Percival and Mortensen 2002). The generation of Neoarchean charnockite intrusions occurred in a period that recorded a fundamental break in Archean crustal evolution worldwide: the cessation of greenstone belt and TTG formation (e.g. Heaman et al. 2011). These hot, CO_2-laden charnockite intrusions (containing igneous ortho- and clinopyroxene) have been described as the driving force for the formation of granulite terranes during their emplacement (Frost and Frost 2008) and may be critical in Neoarchean crust stabilization.

North of the aforementioned northern Superior craton lies the Repulse Bay block (RBb), interpreted to represent (in part) a lower crustal (granulitic) section of the Rae craton that was exhumed during the Paleoproterozoic Trans-Hudson orogeny (LaFlamme et al. 2014b). The Archean crust of the RBb records a number of crustal formation and reworking events including the generation of ca. 2.86 Ga and ca. 2.73–2.71 Ga biotite ± hornblende TTG-type gneiss and sheets of diorite, and ca. 2.69–2.66 Ga biotite–hornblende ± clinopyroxene granitoid rocks and orthopyroxene–clinopyroxene–biotite–hornblende charnockite and enderbite intrusions containing ultramafic xenoliths (LaFlamme et al. 2014a, b). The goal of this paper is to investigate the petrogenesis of these Neoarchean high grade rocks. By investigating the geochemical signature and pressure (*P*)–temperature (*T*) conditions of their formation, we can determine the geodynamic setting in which a regional scale massif-type charnockite suite was generated and speculate on the role anhydrous plutonism had in the stabilization of the continental crust and subsequent preservation of the RBb. Because the RBb is interpreted to be a slice of deeply exhumed Rae craton (LaFlamme et al. 2014b), it serves as a window into the mid-crustal processes presumed to have occurred regionally during cratonization of the Rae Province. This paper seeks to utilize new whole rock and mineral chemical data presented here, in addition to the geological, geochronological, and isotopic framework presented by LaFlamme et al. (2014a) and LaFlamme et al. (2014b), to specifically characterize Neoarchean crustal formation.

REGIONAL GEOLOGY

The Western Churchill Province (WCP) is composed of the Archean granite–greenstone belts and high grade equivalents, and Paleoproterozoic supracrustal sequences and intrusions that underwent numerous tectonothermal episodes (Fig. 1; Berman 2010 and references therein). The north–central segment of the Western Churchill Province is divided into two main crustal divisions, the Rae and Hearne cratons (Hoffman 1988). The Rae craton is made up of Mesoarchean to Neoarchean north-northwesterly trending granite–greenstone belts composed of komatiite, mafic and felsic volcanic rocks, conglomerate, quartzite, pelite, and iron formations (Frisch 2000; Zaleski et al. 2001; Bethune and Scammell 2003; Skulski et al. 2003; Corrigan et al. 2013). Rare Mesoarchean to Neoarchean calc-alkalic gneiss complexes are sandwiched between the low grade belts (Zaleski et al. 2001; Hartlaub et al. 2005; Rayner et al. 2013). Intruded into the granite–greenstone belts and their high-grade equivalent gneiss complexes are ca. 2.73–2.67 Ga calc-alkaline, felsic to intermediate plutonic suites and gneiss (Bethune and Scammell 2003; van Breemen et al. 2007; Rayner et al. 2011; Hinchey et al. 2011).

Based on evidence for a polycyclic tectonic history, exten-

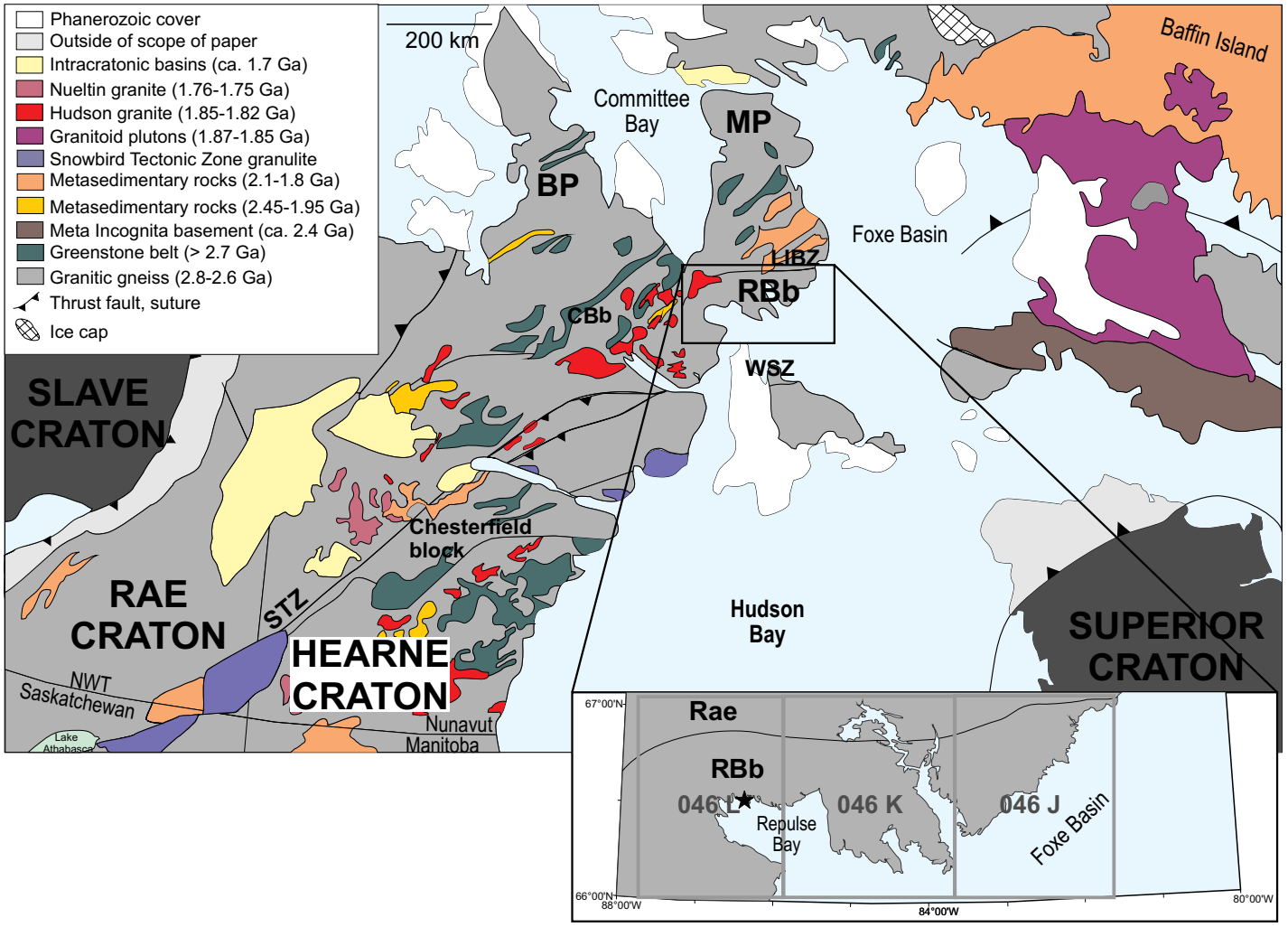

Figure 1. General geology of the western Churchill Province and surrounding area showing the location of the studied area of the Repulse Bay block, Melville Peninsula, Nunavut. Regional scale geology modified from Berman et al. (2005) and references therein. Abbreviations: BP, Boothia Peninsula; CBb, Chesterfield block; LIBZ, Lyon Inlet Boundary Zone; MP, Melville Peninsula; RBb, Repulse Bay block; STZ, Snowbird Tectonic Zone. The study area of the RBb is enclosed by the black box. 1:250,000-scale NTS map sheet 046J, 046K, 046L are overlain on the map as grey boxes. Black star denotes the hamlet of Repulse Bay.

sive plutonism, and distinct mafic dyke swarms, Davis et al. (2006) demonstrated that the Chesterfield block (previously the northwest Hearne subdomain) was accreted to the Rae craton at 2.64–2.61 Ga. The collision between the two cratons resulted in Archean tectonometamorphism at ca. 2.66 Ga and ca. 2.55 Ga (Davis et al. 2006). Collision was followed by 2.62–2.58 Ga 'I-type' dominantly monzogranitic plutonism (Skulski et al. 2003; Davis et al. 2006; van Breemen et al. 2007; Rayner et al. 2011) that has been described in areas as 'high-K' (Hinchey et al. 2011).

LOCAL GEOLOGY

The RBb high grade gneiss complex lies within the Rae craton and occurs at the southern end of the Melville Peninsula, Nunavut. The block is bounded to the north by the Lyon Inlet boundary zone and is interpreted to extend southwards to the Wager shear zone and westwards towards the Committee Bay belt (Fig. 1; see LaFlamme et al. 2014b). The lithologies comprising the block include: 1) ca. 2.86 Ga and 2.73–2.71 Ga granitoid gneiss and metadiorite sheets, 2) ca. 2.69–2.66 Ga charnockite to enderbite and dominantly monzogranitic plutons, and 3) < 1.89 Ga pelite–marble sequences occurring as slivers between tectonized granitoid sheets (LaFlamme et al. 2014b). Lithologies of the RBb are uniformly subhorizontal and undulating. The strike of the units is dominantly east–west and curves to the northeast–southwest in the extreme western portion of the mapped area. The RBb is separated into two segments by the Qaggitalik shear zone; the eastern–central portion of the RBb preserves a deeper (granulite facies) segment of crust than the shallower (upper amphibolite to lower granulite facies) western portion (LaFlamme et al. 2014b). A geological map initially prepared at 1:2,000,000 scale of the study area of the RBb with sample locations is presented in Figure 2.

Archean TTG Protoliths

Granitoid gneiss of the RBb are composed of ca. 2.86 and 2.73 Ga biotite–hornblende tonalite, granodiorite, monzodiorite, monzogranite, and minor trondhjemite gneiss. This unit is heterogeneous and medium- to coarse-grained, and occurs as a moderate to low (green) signal in the combined aeromagnetic and total eU radiometric map (Fig. 3). The gneissic fabric is

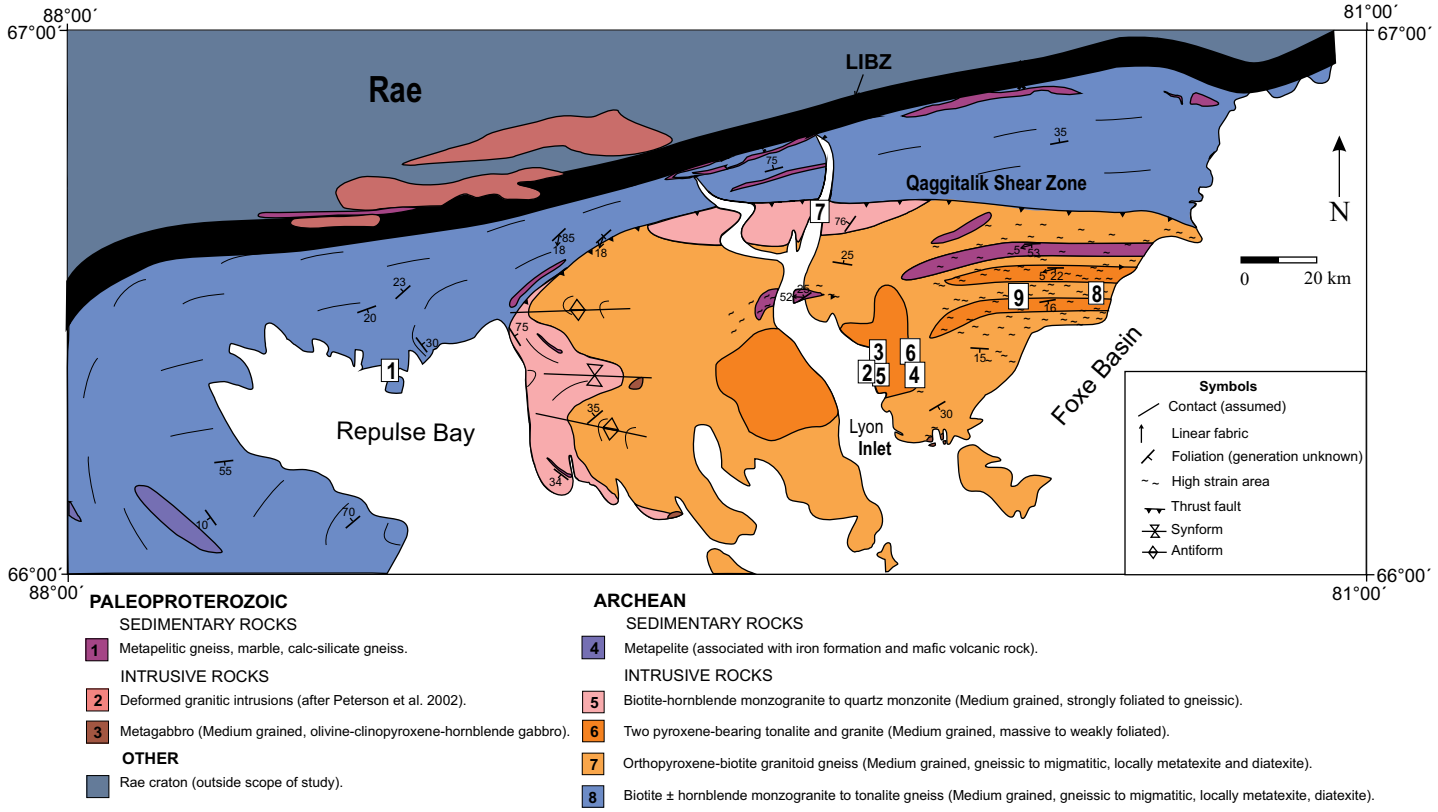

Figure 2. Geological map that denoted metamorphic domains of the study area of the Repulse Bay block (units 1 through 8; block extends to the south and west). Modified with sample locations after LaFlamme et al. (2014b). LIBZ – Lyon Inlet Boundary Zone.

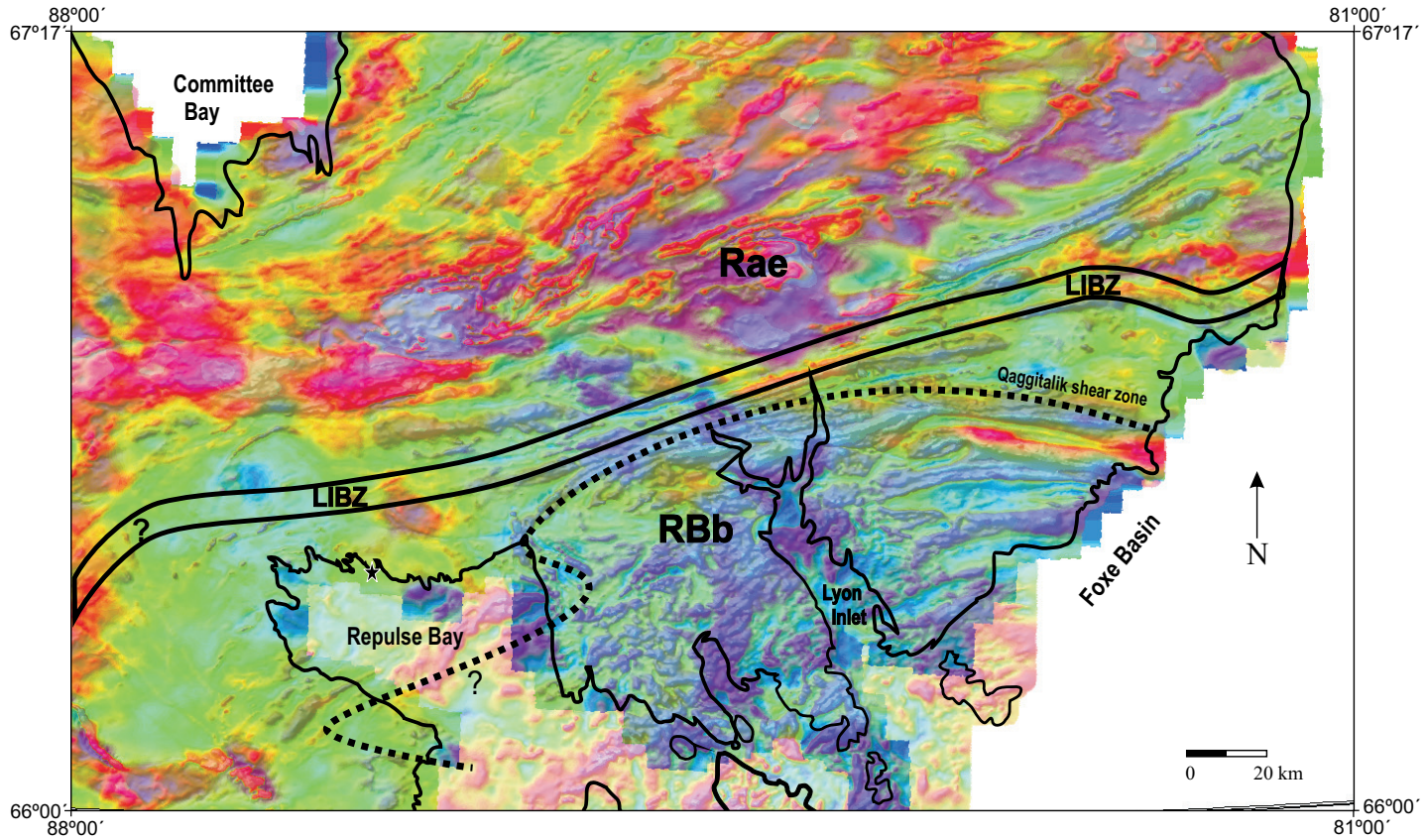

Figure 3. Combined airborne magnetic map and airborne radiometric map (equivalent U (eU); 800 m spacing) of the Repulse Bay block (RBb). Anomalously high magnetic properties in red and low in blue. High total U is in red, and low in blue. LIBZ – Lyon Inlet Boundary Zone.

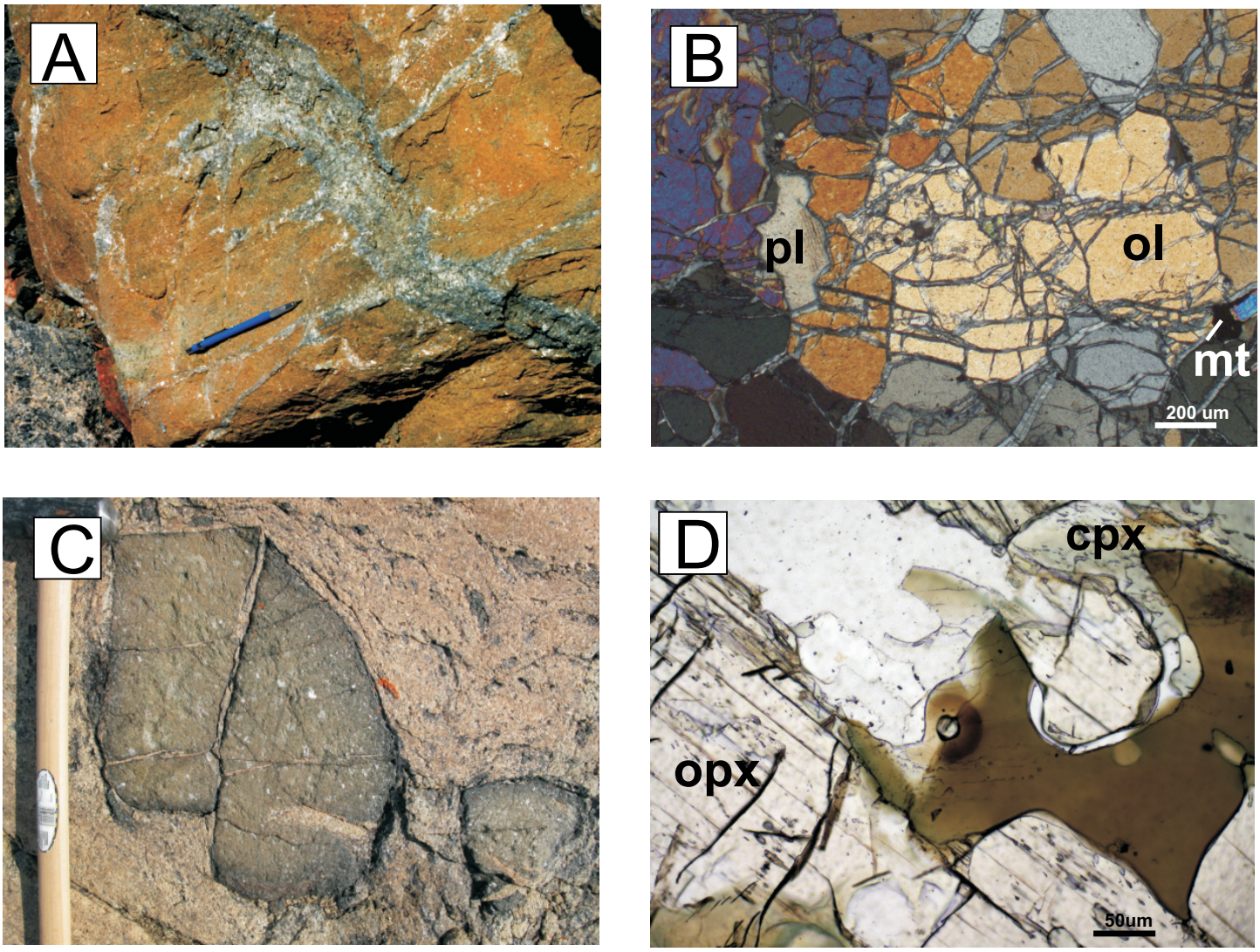

Figure 4. Representative pictures and photomicrographs of a dunite xenolith hosted TTG gneiss (A, B (crossed polars)) and a websterite xenolith hosted in enderbite (C, D (plane-polarized light)). Labels in Figure 4D are according to Whitney and Evans (2010).

defined by 5 to 10 cm thick compositional banding. Twenty percent of the unit takes the form of a stromatic metatexite migmatite, and locally as diatexite migmatite. This unit contains folded, dismembered, and boudinaged mafic dykes that are typically 1 to 2 m wide.

Within the eastern–central portion of the RBb, ca. 2.73–2.71 Ga biotite ± hornblende granodiorite and tonalite gneisses and migmatite, and sheets of clinopyroxene–hornblende metadiorite are exposed. In this region, hypersthene occurs as a prograde metamorphic mineral, replacing biotite. This unit is medium- to coarse-grained and yields a low (blue) signal in the combined aeromagnetic and total eU radiometric map (Fig. 3). Preserved xenocrystic zircon domains, Hf isotopic data, and zircon geochemistry reveal that ca. 2.86 Ga and ca. 2.73–2.71 Ga plutonism was derived from a ca. 3.25–3.10 Ga crust (LaFlamme et al. 2014a).

Charnockite and Granitoid Plutons

Hypersthene–augite–magnetite–biotite (± hornblende) enderbite with lesser charnockite (Unit 6) and biotite–hornblende ± augite granitoid (Unit 5) plutons intruded into, and commonly contain rafts of, the older TTG protoliths of the RBb. These plutons have been dated to be ca. 2.69–2.66 Ga (LaFlamme et al. 2014a). Charnockite plutons are massif-type and contain early igneous ortho- and clinopyroxene. Units 5 and 6 form large bodies throughout the southeastern portion of the RBb, forming a mottled high–low aeromagnetic signature, and a depleted (blue) eU radiometric signature (Fig. 3). These two units are homogeneous and massive in texture, becoming locally gneissic towards their outer margins. The foliation is defined by the alignment of biotite. Hafnium isotopic data and zircon trace element geochemistry reveal that this generation of magmatism was derived from both primitive and juvenile sources (LaFlamme et al. 2014a).

Ultramafic to mafic xenoliths typically occur within the plutons. Boudins of green dunite (Fig. 4A) composed of olivine + magnetite that is 10% altered to serpentine and phlogopite (Fig. 4B) are several metres in diameter. Based on their occurrence within lithologies preserving a depleted eU radiometric signal, these xenoliths are interpreted to outcrop within the plutons. The most common type of xenolith is websterite, which preferentially occurs in the enderbite portion of the pluton (Unit 6). Ultramafic websterite xenoliths (Fig. 4C) are up to 1 m in diameter, deep forest green in colour, medium grained,

Table 1. Analytical conditions for the geochemical analysis of olivine and pyroxene.

Mineral	Ablation mode	Crater Size (μm)	Ablation time (s)	Repetition Rate (Hz)	Fluence (J/cm^2)
Olivine	Linear Raster	48	30	10 (scan speed 5 μm/s)	5
Pyroxene	Drilling	124	40	5	10

and are composed of hypersthene–augite–plagioclase–magnetite with minor biotite and interstitial hornblende (Fig. 4D). Local exsolution of hypersthene occurred within the central portion of the augite grains. Monazite occurs as an accessory mineral. Mafic xenoliths are composed of hornblende with lesser amounts of biotite and clinopyroxene.

Metamorphism

The units of the RBb are polymetamorphosed, having undergone granulite-facies metamorphism twice since their formation (LaFlamme et al. 2014b). The earliest documented metamorphic event is localized and attributed to Neoarchean granulite-facies metamorphism associated with 2.69–2.66 Ga charnockitic plutonism in the lower to middle crust. This metamorphic event is discussed in further detail in this paper. Most recently, due to crustal thickening during the Paleoproterozoic Trans-Hudson orogeny, the units of the RBb underwent partial melting and ductile deformation at conditions of approximately 800°C and 9.5 kbar at ca. 1.82 Ga, followed by high temperature lateral extrusion (LaFlamme et al. 2014b).

METHODOLOGY

Whole Rock Chemical Compositions

Analyses were completed at Activation Laboratories Limited (Ancaster, Ontario, Canada) on rock powders prepared in a soft iron swingmill followed by lithium metaborate/tetraborate fusion and nitric acid dissolution of the fused bead then inductively coupled plasma–emission spectroscopy (ICP–ES) and ICP–mass spectrometry (MS). Major and trace elements were analysed by fusion ICP–ES in two separate batches. Each batch contained a method reagent blank, certified reference material and 17% replicates. Samples were mixed with a flux of lithium metaborate and lithium tetraborate and fused in an induction furnace. The melt was immediately poured into a solution of 5% nitric acid containing an internal standard, and mixed continuously until completely dissolved (~30 min). The samples were run for major oxides and selected trace elements (V, Cr, Co, Rb, Sr, Y, Zr, Nb, Cs, Ba, La, Ce, Pr, Nd, Sm, Eu, Gd, Tb, Dy, Ho, Er, Tm, Yb, Lu, Hf, Ta, Pb, Th, U, Be, Ni, Cu, Zn, Ga, Ge, As, Mo, Ag, In, Sn, Sb, W, Tl, Bi) on a Perkin Elmer Sciex ELAN 6000, 6100 or 9000 ICP–MS. Three blanks and five controls (three before sample group and two after) were analysed per group of samples. Duplicates were fused and analysed every 15 samples. The instrument was recalibrated every 40 samples. Calibration was performed using seven prepared USGS and CANMET certified reference materials. A total of four international standards were included as unknowns for quality control: NIM-D, NIM-N, MRG-1, SY-4.

Mineral Compositions

Major Elements

Major element analysis of mineral compositions for olivine and pyroxene was completed at the University of New Brunswick Microscopy and Microanalysis Facility by Energy Dispersive (X-ray) Spectrometry (EDS) using a JEOL6400 SEM equipped with an EDAX Genesis X-ray Microanalyser EDS operated at 1.5 nA and 15 kV with a focused beam. Spectra were collected for 60 s and spectrum background was removed by interpolation for each analysis. EDAX (Genesis) Energy Dispersive X-ray Analyser software was used to analyse and calibrate the energy spectrum in order to output the abundance of specific elements. RZAF (reverse ZAF) values (used to adjust beam current factor to account for the effect of atomic number, absorption within the sample detector and X-ray-induced fluorescence within the sample) were determined by comparing the measured and accepted values of a standard closely matching the unknown. Standards used for RZAF calibration were: 1, C.M. Taylor Company Multi-element standard mount No. 202-52 for diopside (AS1150-AB), and 2, Dunn SEM standard mount for olivine (1741) and orthopyroxene (alpine).

Trace Elements

Trace element geochemistry was completed by LA–ICP–MS at the University of New Brunswick, Department of Earth Sciences. Analyses were carried out using a Resonetics S-155 193 um ArF (excimer) laser ablation system coupled with a Agilent 7700x quadropole ICP–MS with two external rotary pumps and Iolite™ Trace Elements Data Reduction Scheme (Paton et al. 2011), running as a plug-in for Wavemetrics Igor Pro 6.22™. Quantitative measurements were collected for olivine (^{7}Li, ^{23}Na, ^{27}Al, ^{31}P, ^{43}Ca, ^{45}Sc, ^{47}Ti, ^{51}V, ^{52}Cr, ^{55}Mn, ^{59}Co, ^{60}Ni, ^{63}Cu, ^{66}Zn, ^{89}Y, ^{90}Zr, ^{93}Nb) and pyroxene (^{24}Mg, ^{29}Si, ^{43}Ca, ^{89}Y, ^{90}Zr, ^{93}Nb, ^{139}La, ^{140}Ce, ^{143}Nd, ^{147}Sm, ^{151}Eu, ^{155}Gd, ^{163}Dy, ^{166}Er, ^{173}Yb, ^{232}Th, ^{238}U). Dwell times for the individual analytes listed above were set between 0.01 and 0.05 s (approximately inversely proportional to the concentration in the target grain), for a total ICP–MS sweep time of about 0.5 s. To create ideal laser material coupling during ablation, conditions were varied for each mineral analysed in separate runs (Table 1).

The S-155 cell was pressurized with high purity He gas (at a rate of ~300 mL/min) and mixed in the cell with Ar (at a rate of 1000 mL/min). In each case, a background delay of 20 s was used. In the case of zircon, U–Pb ratios were analysed to ensure that trace elements were analysed from the magmatic domain of the grain. Concentration standard NIST-610 and one or two standards analysed as unknowns to ensure quality of data were included before and after each run using the same operating conditions. Standards analysed as unknowns included: GSE-1G, GORA-132G and GORA-128G. The ICP–MS was tuned using NIST-610 in order to maximize sensitivity while also monitoring oxide production ($^{248}ThO^+/^{232}Th^+ <$ 0.3%), doubly charged ions ($^{22}M^+/^{44}Ca^{++} <$ 0.4%), and plasma robustness ($^{238}U^+/^{232}Th^+ = 1.05$).

The total ICP–MS acquisition time was set to correspond to the total time to run through the predefined laser ablation sequence and the two instruments were operated simultaneously. To reduce the data Geostar laser log files and the Agilent time series data (cps versus time) were combined offline using the Iolite™ version 2.13 automatic integrations function, running as a plug-in for Wavemetrics Igor Pro 6.22™ (Paton et al. 2011). Independently measured (SEM–EDS) concentrations (elemental wt. %) of Mg in the minerals was used as an internal standard.

Elemental maps

Elemental (Fe, Mg, Ca, Mn) mapping of pyroxene was completed at the University of New Brunswick Microscopy and Microanalysis Facility on a JEOL733 electron probe microanalyser equipped with four wavelength dispersive spectrometers (WDS) and Geller dQuant automation software. The accelerating voltage was 15 kV and the amperage 100 nA.

RESULTS

The following section presents results from whole rock major and trace element (13 samples) and mineral (clinopyroxene, orthopyroxene, and olivine) chemical compositions. Appendix 1 lists the locations of samples analysed for whole rock and mineral chemical composition.

Whole Rock Major and Trace Element Compositions

The major and trace element composition of 13 samples from the RBb are described in this section and presented in Table 2. The results are presented in two divisions including ca. 2.69–2.66 Ga pyroxene and non-pyroxene bearing granitoid rocks (5 samples), and xenoliths hosted within the granitoid rocks (7 samples: 6 websterite, 1 gabbro). A single sample from a dunite xenolith is also presented.

Alteration and partial melting can obscure primary magmatic trends by redistributing mobile elements. Care was taken to choose samples that preserved an unaltered igneous texture. Figure 5 plots selected major and trace elements from the 13 samples against Zr and Mg# to identify differentiation trends. Zr is an element known to be incompatible in mafic melts and strongly partitioned into the residual melt during fractionation (Pearce and Norry 1979, also see Jenner 1996). The results yield a negative correlation between FeO and Zr and a positive correlation for SiO_2 and K_2O against Zr. Transitional elements (e.g. Co) behave in a relatively systematic manner. However, high field strength elements (HFSE; e.g. Ta) and REE (not shown) demonstrate scattered behaviour. Granitoid and xenolith lithologies show a pattern of increasing alkali (K_2O + Na_2O) and LILE (Ba + Sr) content, and a concave downwards pattern for the Al_2O_3 content with decreasing Mg#. Systematic trends suggest that these lithologies may be at least partially related by fractional crystallization processes. Two additional diagrams highlight the relationship between the granitoid and xenolith suites by crystal fractionation processes. The bivariate diagram Nb/Ta versus Zr/Hf plots two twin ratios of HFSE. Because each element in these ratios occurs in the same valence state, it is thought that both elements behave similarly during various geochemical processes. Figure 6A demonstrates a systematic trend between the two ratios, indicating a cogenetic relationship between both the granitoid and xenolith suites. Figure 6B (after Pearce and Norry 1979; Pearce 1982) is sensitive to crystal fractionation of olivine, clinopyroxene, and orthopyroxene (which causes a rise in Zr and Ti) versus magnetite, biotite, and amphibole (which causes a decrease in Zr and Ti). What is important to note is that both the granitoid and xenolith suites lie on a single trend line that indicates that they were likely formed by crystal fractionation processes.

Granitoid and xenolith lithologies plot in the subalkaline field (Fig. 7A) of the SiO_2 versus total alkalis diagram of Irvine and Baragar (1971) and dominantly in the magnesian field (Fig. 7B) of the $FeO_T/(FeO_T + MgO)$ versus SiO_2 field of Frost et al. (2001). The ca. 2.69–2.66 Ga granitoid lithologies are SiO_2-rich (63.6–71.4 wt. %), with high $Na_2O + K_2O$ contents (up to 8.5 wt.%) and have a Mg# = 13–24 (Mg# = 100 * molecular $MgO/(MgO + FeO_T)$). Websterite and gabbro xenoliths hosted in the 2.69–2.66 Ga granitoid lithologies are SiO_2-poor (49.7–54.5 wt. %), and have a Mg# = 41–66. Transition element contents are low in granitoid lithologies (Cr < 30 ppm; V < 76 ppm; Ni < 10 ppm) and high in mafic to ultramafic xenoliths (Cr: 370–1080 ppm; V: 32–236 ppm; Ni: 90–1090 ppm). LILE contents in granitoid lithologies are high (Ba + Sr = up to 2239 ppm). One sample from a dunite xenolith (composed of olivine (90%) + spinel (2%) + phlogopite (8%)) contains 40% SiO_2 and a Mg# of 81. Transition elements within the dunite xenolith are high (Cr: 2440 ppm, Ni: 2800 ppm).

The chondrite-normalized REE profiles (normalizing values after Sun and McDonough 1989; Fig. 8A) for granitoid rocks and xenolith lithologies are nearly parallel. REE patterns in granitoid lithologies are moderately to highly fractionated (La_N/Yb_N = 4–54), whereas, REE patterns in xenoliths are moderately fractionated (La_N/Yb_N = 1–3). The granitoid lithologies exhibit a slightly negative to slightly positive Eu anomaly (Eu_N/Eu_N^* = 1.1); whereas the xenoliths yield a moderately negative Eu anomaly (Eu_N/Eu_N^* = 0.6). The dunite xenolith is also moderately fractionated (La_N/Yb_N = 0.9), with moderate LREE contents (La_N = 1.3) and low HREE contents (Yb_N = 1.4).

An extended chondrite-normalized trace element plot (normalizing values after Sun and McDonough 1989; Fig. 8B) demonstrates that for all samples the elements Nb, Ta, and Ti are depleted relative to LILE. The same plot demonstrates that the elements Zr and Hf are enriched with respect to the medium rare earth elements (MREE) within the granitoid units and depleted in the websterite and gabbro xenoliths.

Mineral Compositions

The mineral chemical composition of orthopyroxene and clinopyroxene from a sample of an enderbite intrusion (10CXAL190A01) and a websterite xenolith (10CXAL134B01), as well olivine from a sample of a dunite xenolith (10CXAL249A01) were analysed for major elements by EDS and trace elements by LA–ICP–MS. Major and trace element geochemical compositions are presented in Table 3. Raw analytical data for pyroxene and olivine trace element compositions are presented in Appendices 2 and 3, respectively.

Clinopyroxene and orthopyroxene fall within a solid solution between diopside ($CaMgSi_2O_6$), hedenbergite ($CaFeSi_2O_6$), enstatite ($Mg_2Si_2O_6$), and ferrosilite ($Fe_2Si_2O_6$). In this case, clinopyroxene in the enderbite intrusions yields a composition

Table 2. Whole rock major and trace element geochemical compositions.

Sample[a]	L249A-01	L001B-03	L194B-01	L134B-01	L131B-01	L001B-02	L001B-01	L001C-01	L190A-01	D003A-01	L118A-01	N031A-01	L184A-01
Lithology[b]	dunite	web	web	web	web	web	web	gabbro	end	ch	gd	g	gd
Location	1	2	3	4	5	2	2	2	6	1	7	8	9
Easting[c]	545100	643251	652390	639402	638853	643251	643251	643251	652515	643251	631908	697030	681910
Northing[c]	7370000	7383655	7388158	7390775	7394339	7383655	7383655	7383655	7385280	7383655	7413757	7394330	7393372
Setting	xenolith	xenolith	xenolith	xenolith	xenolith	xenolith	xenolith	xenolith	main	main	main	main	main
Min. Ass.[d]	olivine	OCB	OCB	OCB	OCB	OCB	OCB	CB	OCBH	OCBH	BH	B	B
SiO_2	40.02	49.66	50.79	54.53	50.59	52.79	52.13	50.7	63.57	68.25	71.38	68.92	64.51
TiO_2	0.011	0.351	0.241	0.151	0.242	0.175	0.203	0.892	0.758	0.574	0.24	0.18	0.305
Al_2O_3	0.34	9.61	4.12	2.81	3.70	3.29	3.56	13.8	15.41	15.16	14.61	13.61	17.76
$Fe_2O_3(T)$	10.3	9.67	15.09	10.51	12.02	12.48	13.22	10.86	6.16	3.83	3.03	3.77	2.91
MnO	0.17	0.23	0.24	0.23	0.26	0.52	0.49	0.144	0.07	0.03	0.02	0.02	0.04
MgO	44.55	12.24	25.10	20.78	14.53	17.00	16.80	7.83	1.30	1.13	0.67	0.58	0.90
CaO	0.14	13.02	2.35	8.58	15.94	12.12	10.04	9.55	3.78	3.95	2.53	1.75	3.15
Na_2O	0.05	1.98	0.4	0.64	0.78	0.75	0.78	3.3	3.92	4.31	4.41	2.63	4.33
K_2O	0.15	0.69	0.39	0.41	0.3	0.54	0.68	1.19	2.79	1.16	2.09	5.46	4.15
P_2O_5	-	0.03	0.02	0.02	0.02	0.02	-	0.23	0.14	0.13	0.06	0.09	0.12
LOI	2.55	3.32	0.04	1.58	1.17	0.60	0.49	1.30	0.92	0.83	1.07	1.14	0.77
Total	98.29	100.80	98.78	100.24	99.56	100.30	98.39	99.80	98.81	99.34	100.10	98.15	98.96
Sc	4	55	20	21	12	12	15	34	13	4	2	1	3
Be	-	1	-	-	1	-	-	1	1	1	1	-	4
V	14	185	108	62	104	32	46	236	76	69	21	38	31
Cr	2440	650	1080	1580	1020	1000	740	370	-	30	-	-	-
Co	114	37	109	58	66	47	35	37	11	6	4	5	5
Ni	2800	190	870	1050	1090	910	650	90	-	-	-	-	-
Cu	-	-	40	-	190	-	-	50	40	30	40	80	10
Zn	160	110	120	140	240	250	200	80	610	500	420	680	40
Ga	1	10	7	8	11	11	8	18	22	19	19	17	24
Ge	1.2	2.5	1.7	2.3	2.9	3.3	2.5	1.8	1.4	0.8	0.9	1.1	1.5
As	-	-	-	-	-	-	-	-	10	-	6	15	-
Rb	10	6	15	19	7	19	19	14	44	10	48	153	136
Sr	5	102	72	34	45	40	47	359	242	434	332	327	392
Y	0.5	18	4.5	28.9	9.8	37.4	24.8	20.7	18.4	3.7	2.3	4	6.3
Zr	4	15	25	21	24	31	18	95	212	135	140	237	208
Nb	-	3.2	1.1	1.3	2.0	3.6	2.8	4.6	12.6	4.3	3.2	1.8	7.4
Mo	-	-	-	-	-	-	-	-	-	-	-	-	4
Ag	-	-	-	-	-	-	0.7	-	-	-	-	-	-
In	-	-	-	-	-	-	-	-	0.1	-	-	0.1	-
Sn	-	2	-	8	2	2	1	-	3	1	-	1	1
Sb	1.2	0.2	0.6	0.3	0.9	2.3	2	-	0.5	-	-	1	-
Cs	0.2	-	0.1	0.2	-	0.1	-	-	-	-	-	-	1.5
Ba	13	73	181	61	106	189	191	353	1051	435	460	1912	982
La	1.25	12.8	5.26	13.8	16.3	14.3	9.9	33.9	27.6	29.0	14.0	99.0	34.4
Ce	2.54	34.2	10.4	46.7	39.0	52.2	34.8	75.1	55.5	47.2	22.0	165	59.5
Pr	0.33	4.23	1.2	7.36	4.4	7.89	5.43	9.43	7.18	4.78	2.13	15.8	6.22
Nd	1.02	16.3	4.49	32.2	14.9	33.6	22.9	36.9	30.5	16.1	6.89	45.7	20.4
Sm	0.47	3.7	0.89	8.39	2.61	8.49	5.78	6.86	6.96	2.16	1.01	4.48	3.4
Eu	0.107	0.862	0.217	0.596	0.671	1.3	0.768	1.62	1.12	0.819	0.595	0.708	0.899
Gd	0.21	3.39	0.92	6.77	2.17	7.41	5.10	5.62	6.12	1.44	0.65	1.85	2.23
Tb	0.04	0.58	0.14	1.08	0.32	1.26	0.83	0.81	0.9	0.16	0.09	0.18	0.28
Dy	0.2	3.37	0.85	6.04	1.88	7.35	4.70	4.11	4.57	0.74	0.42	0.76	1.2
Ho	0.04	0.66	0.17	1.12	0.36	1.41	0.94	0.82	0.79	0.13	0.08	0.13	0.21

(Continued)

Table 2. Whole rock major and trace element geochemical compositions. *(Continued)*

Sample[a]	L249A-01	L001B-03	L194B-01	L134B-01	L131B-01	L001B-02	L001B-01	L001C-01	L190A-01	D003A-01	L118A-01	N031A-01	L184A-01
Lithology[b]	dunite	web	web	web	web	web	web	gabbro	end	ch	gd	g	gd
Location	1	2	3	4	5	2	2	2	6	1	7	8	9
Easting[c]	545100	643251	652390	639402	638853	643251	643251	643251	652515	643251	631908	697030	681910
Northing[c]	7370000	7383655	7388158	7390775	7394339	7383655	7383655	7383655	7385280	7383655	7413757	7394330	7393372
Setting	xenolith	xenolith	xenolith	xenolith	xenolith	xenolith	xenolith	xenolith	main	main	main	main	main
Min. Ass.[d]	olivine	OCB	OCB	OCB	OCB	OCB	OCB	CB	OCBH	OCBH	BH	B	B
Er	0.18	1.85	0.49	2.99	1.06	4.04	2.62	2.32	1.93	0.37	0.21	0.37	0.55
Tm	0.037	0.262	0.072	0.41	0.155	0.582	0.384	0.349	0.236	0.046	0.029	0.051	0.084
Yb	0.24	1.7	0.52	2.45	0.99	3.62	2.50	2.21	1.31	0.28	0.19	0.31	0.55
Lu	0.036	0.26	0.099	0.371	0.152	0.539	0.402	0.333	0.192	0.041	0.031	0.047	0.088
Hf	0.1	0.5	0.6	0.9	0.6	1.1	0.5	2.5	4.7	2.9	3.2	5.6	4.9
Ta	0.03	0.17	0.12	0.12	0.23	0.43	0.16	0.14	0.33	0.18	0.08	-	0.27
W	-	-	-	-	-	-	-	1.1	1.8	-	-	-	10.8
Tl	-	-	0.09	0.09	0.10	0.08	-	0.09	0.65	0.14	0.36	1.10	0.79
Pb	-	-	-	-	-	-	-	9	149	151	144	275	32
Bi	-	-	-	-	0.2	-	-	-	0.3	0.2	0.3	0.9	0.2
Th	0.53	0.87	1.8	3.67	0.52	3.02	0.97	2.5	0.43	1.1	1.04	42	5.4
U	0.09	0.11	0.22	0.21	0.05	0.29	0.16	0.26	0.46	0.25	0.22	0.98	2.44

[a] Concentration of oxides are reported in wt. % and trace elements in ppm.
[b] Lithology abbreviations: web – websterite, end – enderbite, ch – charnockite, gd – granodiorite, g – granite.
[c] UTM coordinates in NAD83.
[d] Mineral associations (Min. Ass.) denote the mafic mineral components of the unit: O – orthopyroxene, C – clinopyroxene, B – biotite, H – hornblende.
For sample locations, see Figure 2.

of XWo: 45.9, XEn: 36.7, and XFs: 17.4, whereas, in the websterite xenolith yields a composition of XWo: 47.3, XEn: 44.3 and XFe: 8.4. Orthopyroxene in the enderbite intrusion yields a composition of XWo: 1.2, XEn: 49.2, and XFs: 49.6, whereas, in the websterite xenolith yields a composition of XWo: 0.9, XEn: 75.7 and XFe: 23.5. Clinopyroxene preserves a high Mg# in the enderbite intrusion (Mg# = 66) and in the websterite xenolith (Mg# = 85).

In chondrite-normalized REE plots (normalizing values after Sun and McDonough 1989; Fig. 9A), orthopyroxene in both samples contains sub-parallel REE patterns that are enriched in HREE compared to LREE (La_N/Yb_N=0.03–0.60) when normalized to chondrite values (Sun and McDonough 1989), with a distinct negative Eu anomaly (Eu_N/Eu_N^* = 0.13–0.37). Clinopyroxene in both samples preserves a nearly flat REE profile (La_N/Yb_N=1.4–3.3), with a distinct negative Eu anomaly (Eu_N/Eu_N^* = 0.17–0.28). However, in the websterite xenolith the REE profile is slightly convex upwards, whereas in the enderbite intrusion, the pyroxene REE profile is slightly concave upwards. Furthermore, clinopyroxene in the websterite xenolith contains a much higher REE content than in the enderbite intrusion. In primitive mantle-normalized trace element diagrams (normalizing values after Sun and McDonough 1989; Fig. 9B) all pyroxene grains have a negative anomaly in Zr compared to MREE. Pyroxene in the enderbite sample is depleted in both Th and Nb, while in the websterite sample is only depleted in Nb. Two-pyroxene thermometry (after Brey and Köhler 1990) yields a crystallization *T* of about 800 ± 15°C for the enderbite pluton and 749 ± 15°C for the websterite xenolith (assuming 20 kbar/75 km depth). These results reflect the temperature at which Ca–Fe–Mg diffusion ceased (Frost and Frost 2008).

Olivine ($[Mg,Fe]_2SiO_4$) mineral geochemistry was completed on a sample of dunite xenolith (10CXAL249A). The olivine in this sample occurs as Fo_{90} and yields high concentrations of Ni (3800 ppm), Zn (158 ppm), and Co (164 ppm) and low concentrations of Cr (6 ppm).

DISCUSSION

Relationship Between Granitoid Plutons and Entrained Ultramafic Xenoliths

Systematic behaviour for many major, compatible trace, and LIL elements versus Zr, suggests that these elements behave isochemically. Even the mobile elements (those with either low or high ionic potential) were not redistributed during metamorphism (Kerrich and Wyman 1996). Although the dataset is compositionally limited, we infer from Figure 5 a transitional trend in these elements that indicates that the granitoid and xenolith lithologies are related, and are considered to be at least in part the product of crystal fractionation. The observed scattered behaviour in HFSE and REE, plotted in Figure 5, is generally consistent with having arisen through fractional crystallization of a melt undergoing simultaneous assimilation (e.g. Rudnick et al. 1986). Figure 6 further strengthens this claim by demonstrating the cogenetic relationship between the granitoid and xenolith suites.

Whole rock analyses reveal a subalkaline, magnesian suite of ca. 2.69–2.66 Ga granitoid lithologies. The entrained dunite, websterite, and gabbro xenoliths within charnockite and granitoid lithologies yield subparallel chondrite-normalized REE

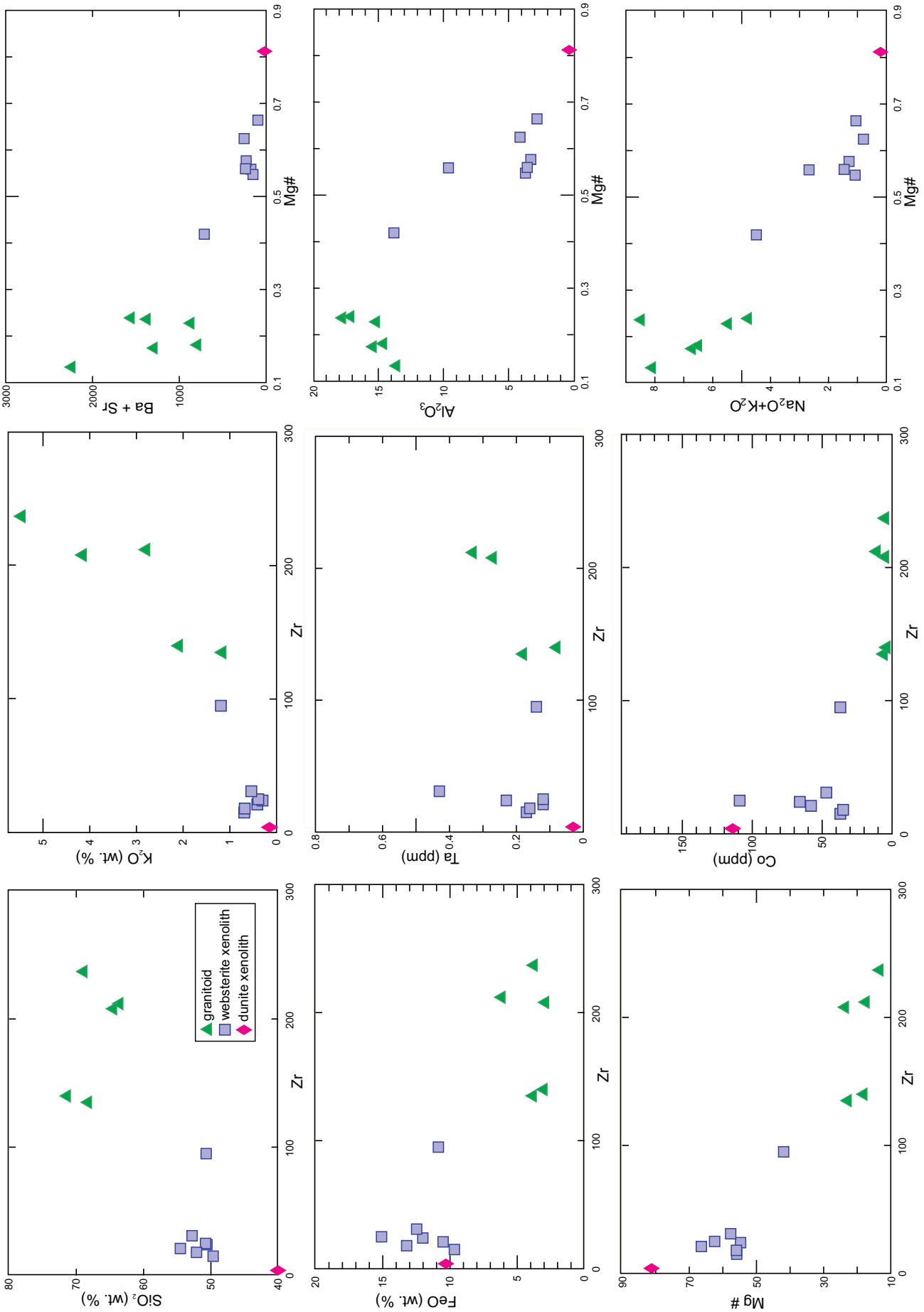

Figure 5. Selected major and trace element variation diagrams using Zr (ppm) and Mg# as a differentiation index.

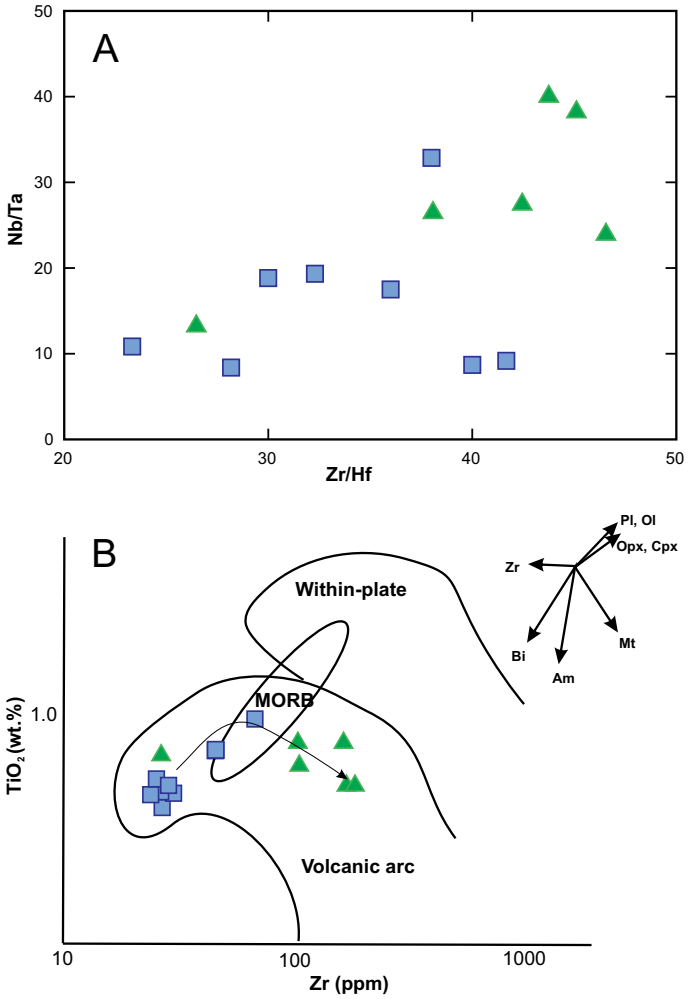

Figure 6. A) Bivariate diagram plotting Nb/Ta against Zr/Hf for the granitoid (triangles) and xenolith (squares) suites. B) Covariation diagram of TiO_2 versus Zr after Pearce and Norry (1979) to demonstrate that granitoid and xenolith suites lie on one trend line. Vector lines for olivine (Ol), plagioclase (pl), orthopyroxene (Opx), clinopyroxene (Cpx), magnetite (Mt), biotite (Bt), zircon (Zr), and amphibole (Am) after Pearce (1982).

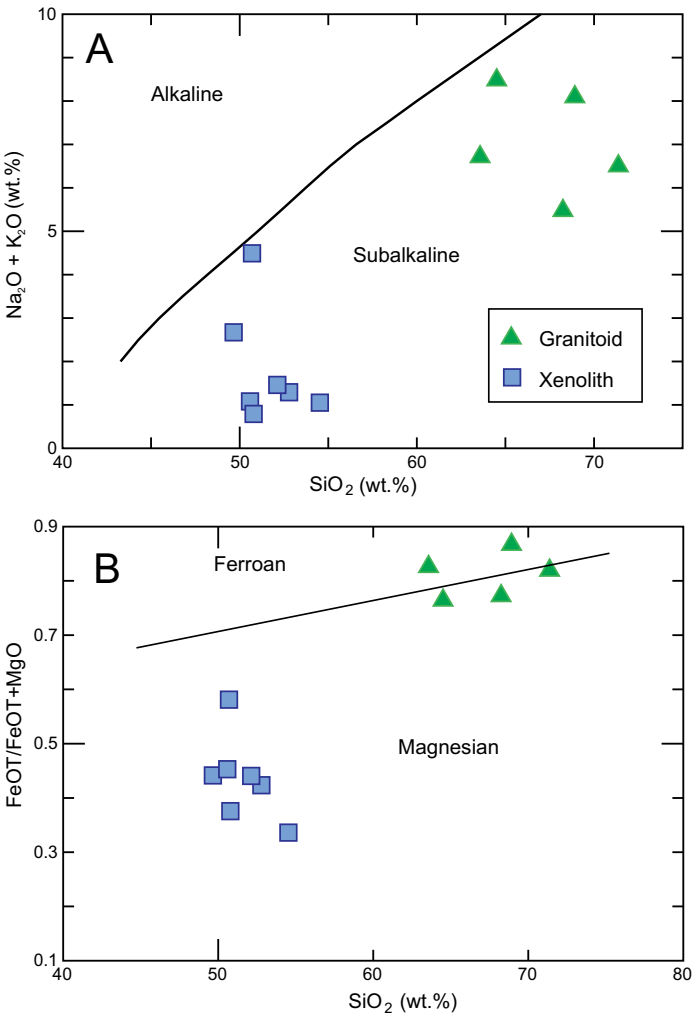

Figure 7. Repulse Bay block samples plotted on diagrams A) Na_2O+K_2O vs. SiO_2 (Irvine and Baragar 1971) and B) $FeO_T/(FeO_T + MgO)$ vs. SiO_2 (Frost et al. 2001).

patterns (Fig. 8A). These granitoid lithologies and xenoliths are moderately fractionated and exhibit LILE- and LREE-enriched, primitive mantle-normalized incompatible rare element patterns with moderate to significant Ta, Th, and Ti troughs (Fig. 8B). The Eu anomaly ranges from slightly negative to slightly positive indicating a progressive depletion in Eu^{2+} during plagioclase crystallization. The only distinct difference between xenoliths and granitoid lithologies is the concentration of primitive mantle-normalized Sr, Hf, and Zr ratios that are depleted compared to primitive mantle-normalized MREE ratios in websterite xenoliths (discussed below).

Pyroxene mineral compositions from an enderbite intrusion and websterite xenolith yield systematically parallel pyroxene trace element plots with only slight differences in primitive mantle-normalized Th and Nb concentrations, and in REE patterns in clinopyroxene. The clinopyroxene in the websterite xenolith has a convex-upward chondrite-normalized REE pattern. Both features are consistent with having formed as deep level cumulate crystals (Irving and Frey 1984; Deer et al. 1992).

When normalized against the primitive mantle, a dunite (olivine + phlogopite + magnetite) xenolith, occurring within the Neoarchean granitoid gneiss, displays a mantle-like signature including high Ni contents (2440 ppm) and high Mg# (81) in whole rock, and high forsterite content (Fo_{90}) and Ni content (4000 ppm) in olivine. These features are consistent with derivation from mantle melts (Sato 1977; Sano et al. 2002; de Hoog et al. 2010). Low Cr contents in olivine (6 ppm) compared to other mantle-derived lherzolite examples (de Hoog et al. 2010) is interpreted to reflect sequestering of Cr in phlogopite over olivine. The dunite xenolith also contains a whole rock signature which may be consistent with crustal contamination including LILE and LREE enrichment, and negative Nb, Ti and Y anomalies. However, based on a relatively low forsterite content in olivine compared to olivine found in typical subcontinental mantle lithosphere lherzolite xenoliths (Mg# in olivine ~93; e.g. Schmidberger and Francis 1999; Griffin et al. 2003, 2009), the dunite xenolith is interpreted to represent a cumulate-type magma, derived during Archean magmatism.

Given the decrease in Mg# and progressive increase in LILE and alkali content, it is possible that these lithologies record fractionation of a primitive magma during its passage through the mantle and the crust. The concave-down nature of Mg# vs. Al_2O_3 content is a feature consistent with the progressive fractional crystallization of clinopyroxene (e.g. Ohba

Table 3. Major and trace element mineral geochemical composition.

Sample[a] (10CXAL)	190A01	190A01	134B01	134B01	249A01
Lithology	enderbite	enderbite	websterite	websterite	dunite
Setting	main	main	xenolith	xenolith	xenolith
Mineral[b]	clinopyroxene	orthopyroxene	clinopyroxene	orthopyroxene	olivine
SiO_2	51.5	51.74	53.1	55.47	40.81
TiO_2	0.10	0.07	0.15	0.08	
Al_2O_3	1.33	0.91	1.91	0.98	
$Fe_2O_{3(T)}$	10.59	29.83	5.16	14.9	8.93
MnO	0.33	0.79	0.10	0.33	
MgO	12.5	16.61	15.35	26.93	48.92
CaO	21.75	0.58	22.81	0.42	
Na_2O	0.5	0.22	0.92	0.19	
K_2O	0.07	0.03	0.00	0.08	
Total	98.74	100.78	100.11	99.52	98.67
Si	184500	261400	240220	268800	
Ca	18920	5034	153878	3484	404
Y	15.95	16.30	77.41	2.60	0.06
Zr	0.260	0.235	29.705	0.447	0.112
Nb	0.042	0.013	0.090	0.011	0.020
La	10.750	0.578	19.703	0.232	
Ce	14.400	1.132	94.120	0.660	
Nd	5.880	0.611	86.570	0.515	
Sm	1.106	0.305	23.013	0.166	
Eu	0.097	0.022	1.335	0.014	
Gd	1.351	0.688	20.330	0.203	
Dy	2.468	2.346	16.818	0.352	
Er	2.459	2.603	7.779	0.376	
Yb	3.407	4.017	6.177	0.719	
Th	0.001	0.001	0.336	0.018	
U	0.003	0.001	0.135	0.013	
Li					3.9
Na					379
Al					10
P					19
Sc					15
Ti					7.8
V					0.48
Cr					128
Mn					1608
Co					163
Ni					3824.8
Cu					0.08
Zn					164

[a] Oxides are reported in wt. %, trace elements and Si, Ca are reported in ppm
[b] Mineral analysed

et al. 2009). Therefore, field, petrographic, and geochemical evidence exists in the RBb for large-scale fractional crystallization (e.g. magmatic layering, similar mineral assemblages between xenoliths and host lithologies, and similar whole rock and pyroxene trace element patterns). To account for the enrichment of fluid mobile elements like LREE, neither notable in the metasomatized mantle nor in slab melts, fractional crystallization processes are interpreted to have undergone concurrent assimilation with the solid wall rocks surrounding a magma chamber. The process is known as assimilation-fractional crystallization (DePaolo 1981). Therefore, based on similar mineralogy (orthopyroxene–clinopyroxene–biotite–plagioclase), petrographic features, and similar whole rock and pyroxene geochemical properties, the xenoliths and host charnockite and granitoid intrusions are interpreted to preserve a cogenate relationship rather than representing discrete magmatic events. The cumulate websterite xenoliths (now known as autoliths) may represent early crystallized units approaching the parental composition.

Sanukitoid Affinity of Neoarchean Intrusions

The presence of negative Nb, Ta, and Ti anomalies and enrichment of the LILE relative to the HFSE are characteristic features of volcanic arc magmas (Pearce 1982); however, these trace element compositions are not exclusive to arc magmatism. The retention of ~2% rutile in a mafic source can also generate these anomalies (Bédard 2006; Bédard et al. 2013). This 'arc-like' geochemical signature is also typical in Archean TTG and sanukitoid lithologies worldwide (e.g. Martin et al. 2005 and references therein). The sanukitoid suite is composed of Neoarchean granitoid lithologies that contain both an 'arc-like' and 'mantle-like' chemical signature that reflects their generation from a mantle peridotite source, rich in incompatible elements (Laurent et al. 2014 and references therein). Geochemically, the sanukitoid suite can vary depending on the physical conditions in which it was generated; however, the suite is always calc-alkaline, metaluminous, and commonly contains Mg# > 0.6, Ni > 100 ppm, Cr > 200 ppm, K_2O > 1%, Ba + Sr > 1000 ppm, enrichment in LREE, and little to no Eu anomaly (Stern et al. 1989).

In the RBb, websterite autoliths preserve a high Mg# (up to 0.66) and high Cr (650–1580 ppm) and Ni (90–1090 ppm) contents. Although the more differentiated granitoid lithologies do not preserve an obvious geochemical mantle signature, they do contain high alkali, Ba, and Sr contents, geochemical signatures that are interpreted to be indicative of mantle input (e.g. Walter 2003). The ca. 2.69–2.66 Ga granitoid rocks and autoliths are enriched in LREE and have a variable positive to negative Eu anomaly (Fig. 8). These features are consistent with the known geochemical properties of sanukitoid magmatism during ongoing fractional crystallization (e.g. Smithies and Champion 2000; Martin et al. 2005; Halla 2005; Heilimo et al. 2010; 2013; Laurent et al. 2013). Furthermore, the enderbite and websterite xenolith lithologies preserve an elevated Mg# in clinopyroxene (websterite xenolith = 85, enderbite intrusions = 66), similar to the Mg# in clinopyroxene in the Roaring River sanukitoid intrusion in the Superior Province (Stern and Hanson 1991) and the Panozero intrusion in the Karelian craton of the Baltic Shield (Mg# = 72–75; Lobach-Zhuchenko et al. 2008).

Melt Derivation

The Hf isotopic signature from ca. 2.69–2.66 Ga sanukitoid-type granitoid rocks in the RBb yields a wider range of initial εHf values (–7.1 to +1.0) than earlier ca. 2.73–2.71 Ga TTG-type magmatism (–4.8 to –2.4). This isotopic signature is a reflection of derivation of an isotopically juvenile source that interacted with an evolved crustal source. Based on the large

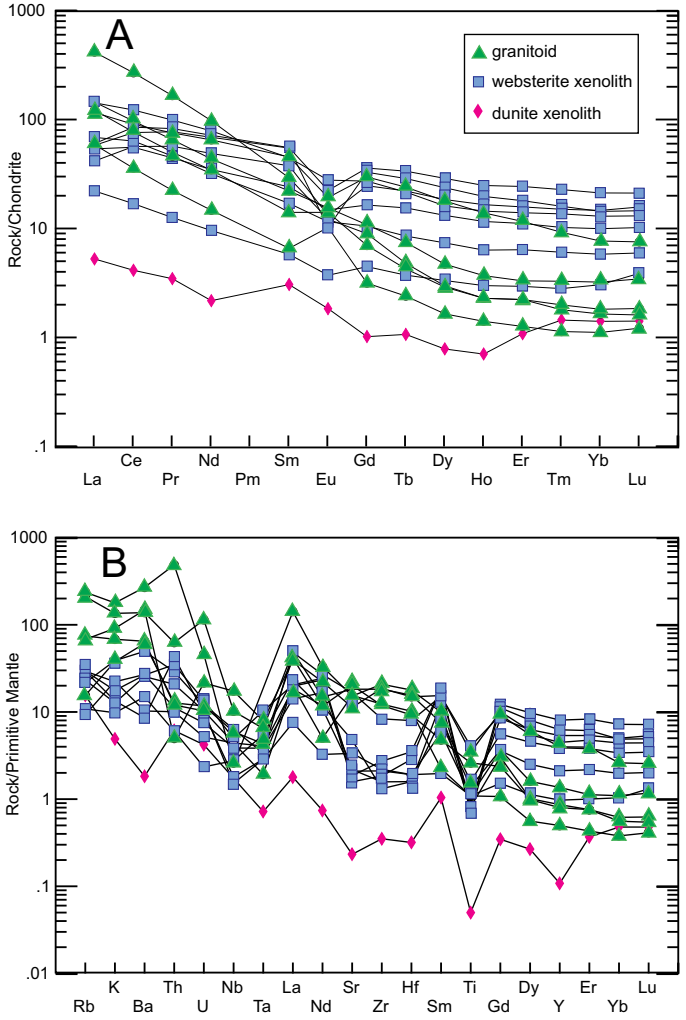

Figure 8. A) Chondrite-normalized REE plot (normalized values taken from Sun and McDonough 1989) for granitoid intrusions and xenoliths. B) Primitive mantle-normalized extended trace element diagram (primitive mantle-normalizing values taken from Sun and McDonough 1989).

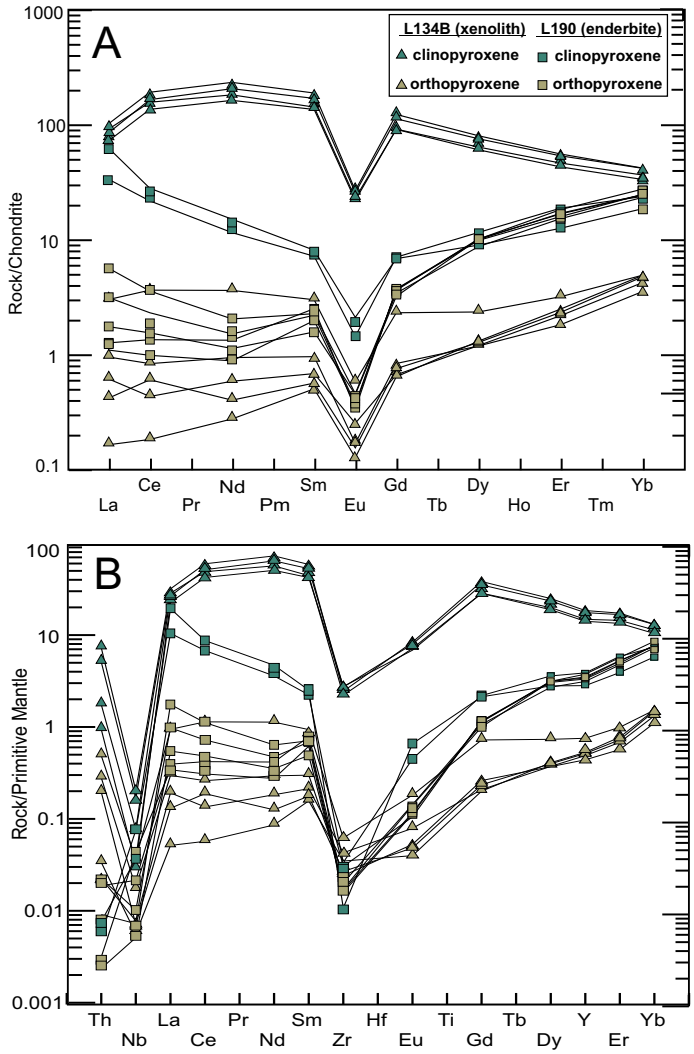

Figure 9. A) Chondrite-normalized REE plot (normalizing values taken from Sun and McDonough 1989) for orthopyroxene and clinopyroxene in enderbite intrusion and websterite xenolith. B) Primitive mantle-normalized extended trace element diagram (primitive mantle-normalizing values taken from Sun and McDonough 1989).

volume of exposed anhydrous magmatism and the geochemical signature of the cumulate-type websterite and dunite xenoliths, the juvenile source is interpreted to be derived directly from the primitive mantle.

Recycling of crust into the mantle occurs during accretion of island arcs at convergent margins. This type of accretion is proposed to have been the primary mechanism during amalgamation of the Slave and Superior cratons in the Archean (e.g. Ketchum et al. 2004; Davis et al. 2005). Based on a geochemical modelling of Sr, Nd, Hf, $\delta^{18}O$ values and trace elements, a number of authors have demonstrated that within a subduction zone setting, crustal reservoirs were the source of mantle enrichment to form the sanukitoid rocks in the Karelia, Baltic, Amazonia, Dharwar cratons, etc. (Fig. 10; Moyen et al. 2001; Lobach-Zhuchenko et al. 2005; de Oliveira et al. 2011; Heilimo et al. 2013). These sanukitoid intrusions are isotopically similar to comparable rocks in the Superior and Slave cratons of the Canadian Shield (Heilimo et al. 2013, and references therein), demonstrating that the same crustal formation processes were occurring within the Rae craton as well.

Because Zr and Hf are hosted by zircon in subduction zones (Rubatto and Hermann 2003), a residue containing accessory zircon, is likely controlling the Zr and Hf levels in websterite xenoliths. Metasomatism of the mantle by hydrous slab melts may have led to the enrichment of Zr and Hf (Rubatto and Hermann 2003) in the later cumulate products. In addition, the most evolved granitoid rocks contain the highest ferroan content, which are known to be derived from oxidizing slab melts that carry ferric iron in solution (Mungall 2002). Finally, the clinopyroxene chemical compositions demonstrate that REE were most abundant during the earlier stages of crystallization, which may indicate that the mantle was enriched in REE. These three features suggest that metasomatism of the primitive mantle by slab melts is an important component in Neoarchean magma generation.

The development of a metasomatically enriched lithosphere occurs by melting and hybridization of the mantle wedge with slab-derived crustal melts during subduction toward the end of the Archean (Moyen et al. 2001). An enriched (metasomatized) mantle is a prominent feature of the Neoarchean due to the effects of steeper subduction than in the earlier Archean. The breakdown of hydrous phases in sub-

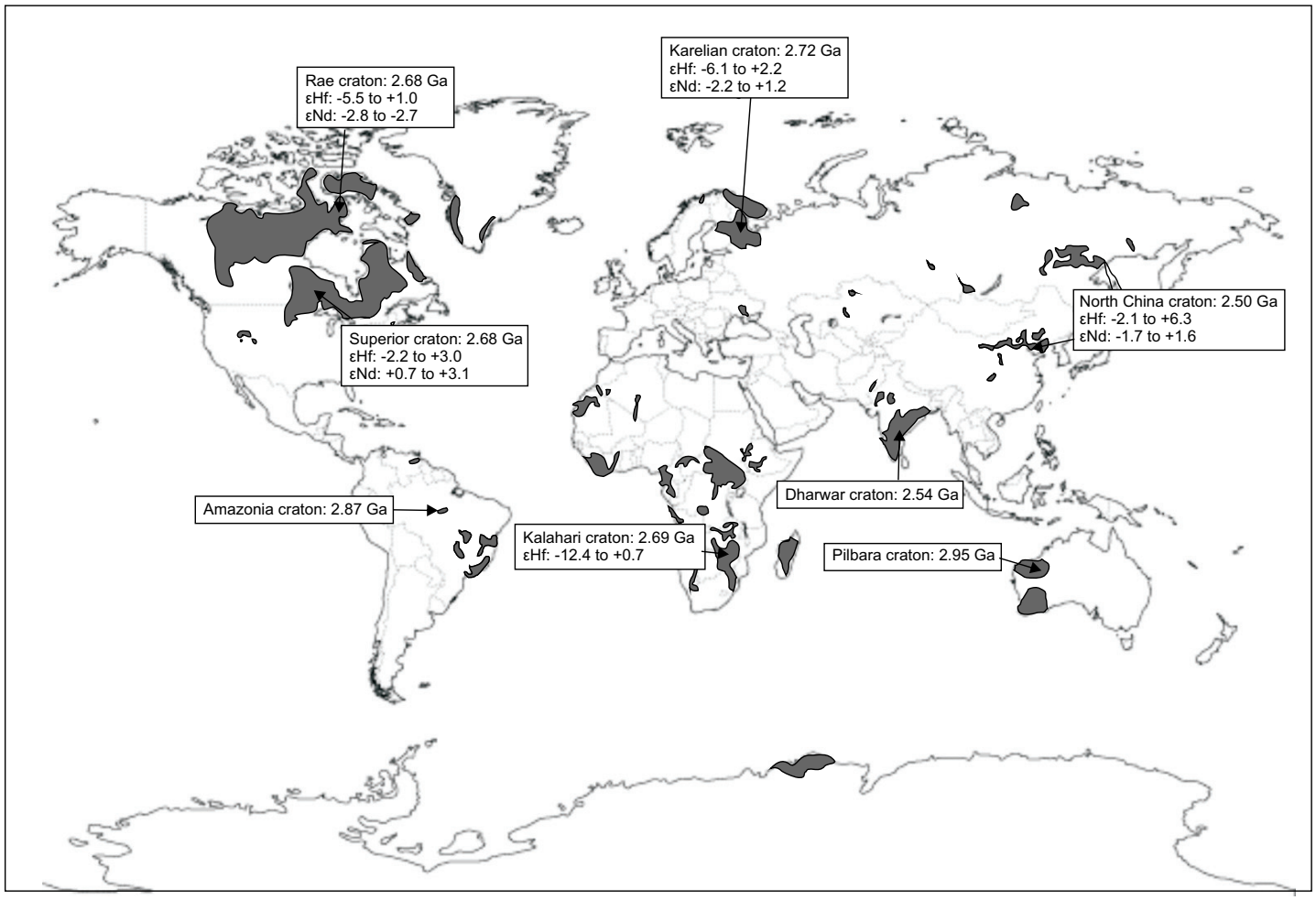

Figure 10. Location of some recognized sanukitoid magmatism worldwide. Global distribution of exposed Archean crust is in gray (modified after Bleeker 2003). Sanukitoid magmatism is found in the Karelian craton (Heilimo et al. 2013 and references therein), the Pilbara craton (Smithies and Champion 2000), the Superior craton (Stern and Hanson 1991; Davis et al. 2005), the Dharwar craton (Moyen et al. 2001 and references therein), the Kalahari craton (Zeh et al. 2009), the Amazonia craton (de Oliveira et al. 2009), the North China craton (Ma et al. 2013), and the Rae craton (this study).

ducting crust results in the formation of phlogopite and richterite in the upper mantle (Schmidt and Poli 1998). Thus, LILE enrichment within the mantle occurs by way of the sequestering of LILE in phlogopite, known to occur within a subduction zone setting at depth (Wyllie and Sekine 1982). Significant water and alkali contents existing in the mantle derived from slab melts may be the reason for the development of hydrous phases (interstitial biotite and amphibole) within the ultramafic autoliths and charnockitic intrusions (e.g. Ionov et al. 2002). For example, geochemical and isotopic evidence indicates a metasomatically modified mantle source in the nearby Hearne craton (Sandeman et al. 2003).

A number of mechanisms for sanukitoid melt derivation have been proposed in recent years to account for both mantle-derived and crust-contaminated geochemical and isotopic signatures. They include: 1) partial melting of a metasomatized mantle and assimilation of TTG crust (Smithies and Champion 2000; Moyen et al. 2001; de Oliveira et al. 2011); 2) partial melting of a metasomatized mantle hybridized by Archean sedimentary rocks (Heilimo et al. 2013) or fluids derived from Archean sedimentary rocks (Halla 2005); 3) an interplay among multiple processes including fractional crystallization, assimilation-fractional crystallization, and binary magma mixing (Laurent et al. 2013); 4) hybridization of TTG melts by assimilation of an olivine-bearing peridotite (Rapp et al. 2010); and 5) crystal fractionation through anatexis of lower crustal rocks (Qian and Hermann 2010). Laurent et al. (2014) pointed out that the global granitoid diversity associated with the sanukitoid suite reflects different petrogenetic processes occurring at mantle depths and, in particular, the specific nature and composition of the metasomatic agent. We propose here that the sanukitoid suite of the RBb was derived from a metasomatically enriched sub-continental lithospheric mantle that interacted with the base of the not yet refractory continental crust.

Conditions of Emplacement

The two-pyroxene thermometer of Brey and Köhler (1990) preserves Ca–Mg–Fe exchange temperatures that are much too low to reflect the crystallization temperature of the websterite xenoliths and enderbite intrusions. Based on the results from two-pyroxene thermometry and the homogeneous Fe and Mg content of pyroxenes preserved in the websterite xenolith (Fig. 11A) and enderbite intrusion (Fig. 11B), pyroxene thermometry is interpreted to have been reset by granulite-facies metamorphism during the Paleoproterozoic Trans-Hudson orogeny and exchange of Ca–Mg–Fe. It should also be

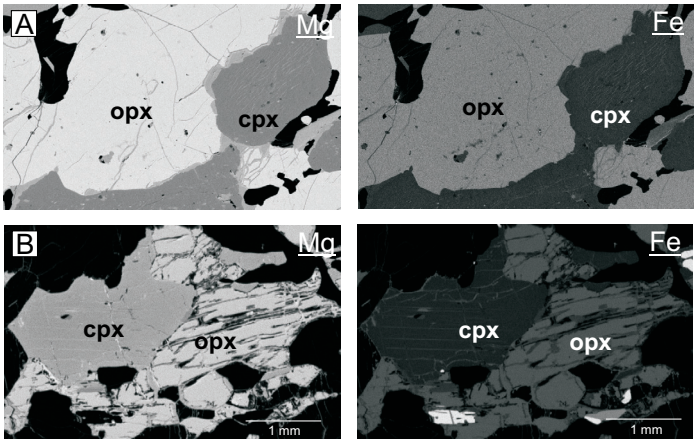

Figure 11. Magnesium and iron elemental maps by EMP analysis of pyroxenes in a websterite xenolith (A; 10CXAL134B) and enderbite intrusion (B; 10CXAL190A).

noted that erroneous *T* measurements for two-pyroxene thermometry have previously been reported for granulites devoid of spinel and olivine (e.g. Roach 2004).

TTG magmas form in different tectonic settings at melting pressures ranging from < 10 kbar to > 25 kbar, affecting residue mineralogy and trace element composition (Moyen and Stevens 2006; Moyen 2011; Nagel et al. 2012; Qian and Hermann 2013). Although sanukitoid magmas are known to be sourced from mantle that was metasomatized by melts, the nature of the sanukitoid series is strongly dependent on the pressure of magma generation (de Oliveira et al. 2011; Laurent et al. 2014). The sanukitoid suite from the RBb is relatively depleted in HREE compared to LREE contents in whole rock (see Fig. 8) indicative of garnet retention in the residue (Drummond and Defant 1990). This is in accord with the trace element zircon data presented by LaFlamme et al. (2014a) that demonstrates that both the ca. 2.73–2.71 Ga TTG gneiss and ca. 2.69–2.66 Ga granitoid rocks in the RBb formed from a source containing garnet.

Figure 12 demonstrates two typical Archean geotherms for a down-going oceanic plate in a subduction zone (after Foley 2008). The down-going amphibolite oceanic slab likely melted between the two geotherms in the 'garnet-present' field at *P*–*T* conditions of > 800°C and > 8 kbar to contribute (along with crustal reworking) to the intrusion of a ca. 2.73–2.71 Ga granitoid (granite, granodiorite, tonalite, trondhjemite) crust. These conditions are consistent with the findings of Moyen and Stevens (2006). The slab (now of a garnet–amphibole–pyroxenite composition) then melted again at $T > 1000$°C and $P >$ 11 kbar in the 'garnet-present' field contributing slab melt to the mantle. These conditions are in agreement with the high *T*/high *P* features of the RBb including: (1) the regional scale extent of the 2.69–2.66 Ga plutons; (2) the moderate HREE contents ($HREE_N$ = 10–177); and (3) ubiquitous presence of rutile needles in quartz throughout the intrusions (Sato and Santosh 2007).

Exsolution in plagioclase (in enderbite) and clinopyroxene (in entrained autoliths) as well as a variable Eu anomaly is evidence for very slow cooling following crystallization. Because charnockitic magmas are anhydrous and lack buoyancy, the accumulated crystal mush may rise slowly and ascend diapirically through the crust (Ashwal 1993; Bolle et al. 2000). Fractional crystallization during magma generation created a cumulate-type intrusion. Early crystallization products were ultramafic (orthopyroxene–clinopyroxene–plagioclase), whereas later more differentiated products were biotite and biotite–hornblende granite and granodiorite, a feature common to the sanukitoid suite (Laurent et al. 2014). The transition from dry to hydrated granitoid rocks is known to be complex due to fluids and heat involved in open system processes during magma ascent (Frost and Frost 2008) and therefore, does not preserve a typical layered intrusion.

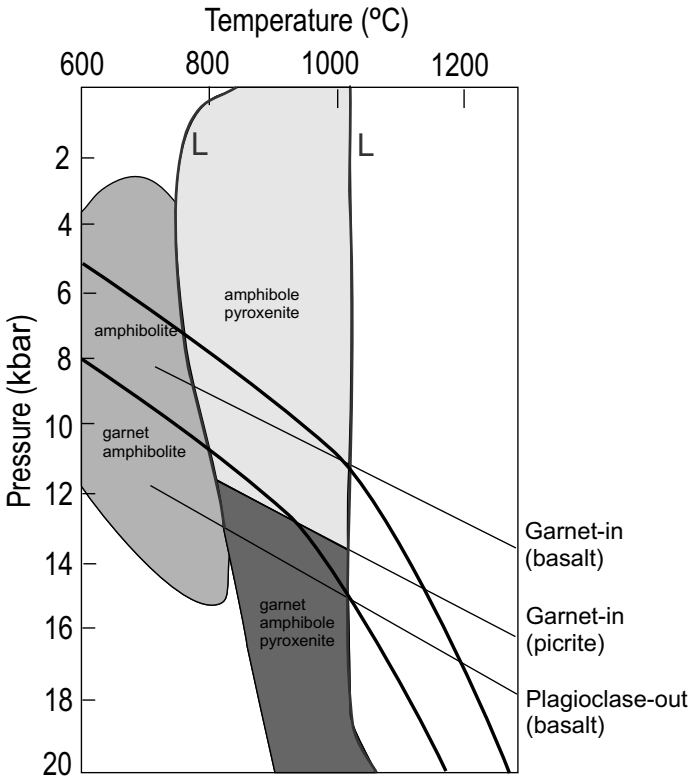

Figure 12. Two typical Archean geotherms for a down-going oceanic slab in an Archean subduction zone after Foley (2008). Amphibolite slab melting in the garnet-present field contributes to the intrusion of a ca. 2.73–2.71 Ga TTG-type crust. Melting of a garnet–amphibole pyroxenite slab contributes slab melts to the mantle to generate a ca. 2.69–2.66 Ga sanukitoid suite.

Regional Correlations

Giant high grade Neoarchean terranes are commonly exposed within the Superior Province, occurring at the margins of the craton or between granite–greenstone terranes (Percival et al. 1992). The Pikwitonei Granulite domain of the northwest Superior Province exposes anhydrous granulite intrusions that formed in the Mesoarchean (3.4–3.0 Ga) and Neoarchean (2.72–2.64 Ga). These lithologies were affected by a multistage metamorphic history at ca. 2716, 2694, 2680 and 2643 Ma, of which the generation of zircon at 2694 and 2680 Ma corresponds to amphibolite- and granulite-facies metamorphism, respectively (Heaman et al. 2011). Large scale Neoarchean plutons similar to those observed in the RBb have also been identified across Hudson Bay, in the Minto block of the northern Superior Province (Bédard 2003). The Minto block is host to Meso–Neoarchean amphibolite- to granulite-facies TTG gneiss, intruded by enderbite and granitoid plutons (Bédard 2003). These intrusions are also similar to those iden-

tified in the Baltic Shield, where a range of dehydrated to hydrated plutons intrude older gneisses and are host to ultramafic xenoliths (e.g. Lobach-Zhuchenko et al. 2005).

Based on a compilation of data from high grade terranes in the Superior Province including the Pikwitonei, Minto block, Split Lake block, Quetico, English River and Opatica domains, Heaman et al. (2011) demonstrated that Neoarchean magmatism and high grade (high *T*/low–moderate *P*) multi-stage metamorphism follows the development of 2.8–2.7 Ga granite–greenstone belts. Furthermore, Whalen et al. (2004) demonstrated that a compositional continuum exists between Neoarchean monzogranite to granodiorite plutonism and sanukitoid plutonism within the Superior Province, indicating that felsic granitoid rocks may be petrogenetically linked to mantle-derived magmatism. Therefore, crustal formation mechanisms in the RBb were synchronous and similar to those occurring in the Superior Province.

Neoarchean high grade igneous terranes have only been briefly described within the Rae craton as exemplified by the granulite domain of Boothia Peninsula mainland (Ryan et al. 2009). In this area, two pulses of magmatism are prominent at ca. 2.66 and 2.61–2.59 Ga, the second pulse being coeval with granulite-facies metamorphism and the intrusion of high-K granite (Hinchey et al. 2011). Here we demonstrate, however, that Neoarchean magmatism in the adjacent RBb spans a continuous time period from 2.73 to 2.66 Ga, with granulite-facies metamorphism being coeval with the intrusion of, and localized to lithologies surrounding, the ca. 2.69–2.66 Ga sanukitoid suite (see also LaFlamme et al. 2014b). Presently, there is no evidence for a 2.60 Ga metamorphic overprint within the RBb.

Implications for Neoarchean Magmatism

Subduction in the late Archean was likely unstable and not comparable to modern day subduction (see Bédard et al. 2013); however, it is the accepted geodynamic setting in which the petrographically variable Neoarchean lithologies (i.e. moderate to high pressure TTGs, sanukitoid intrusions, high-K granite) were formed (Laurent et al. 2014). Alternative mechanisms for the formation of Archean lithologies do exist but remain untested (see Bédard 2006). Conversely, many investigations lend support to the probability of Archean (especially in the Neoarchean) subduction. For instance, Hynes (2014) modelled mantle melting and the cooling of oceanic plates to determine that the resulting negative buoyancy of a subducting slab was in fact strong enough to initiate and sustain subduction in the warmer Archean era. Therefore, assuming subduction of oceanic crust was the mechanism by which Neoarchean TTG-type crust was generated (Smithies et al. 2003; Martin et al. 2005, 2010; see also Bédard 2006 and references therein), the Neoarchean marks a time when the Earth's thermal regime was high enough to induce melting of subducted oceanic crust, but was sufficiently low to generate small amounts of slab melts that were entirely consumed by hybridization with the overlying mantle wedge (e.g. Martin et al. 2005, 2010).

The phenomenon of mantle-derived, sanukitoid magmatism following the formation of granite–greenstone and TTG terranes is common in most Archean cratons worldwide (e.g. Dharwar craton, Moyen et al. 2001; Kalahari craton, Zeh et al. 2009; Fennoscandian Shield, Heilimo et al. 2013; Baltic Shield, Lobach-Zhuchenko et al. 2005, etc.; see Fig. 10). In many cases, the intrusion of regional-scale sanukitoid and high-K plutons occurred within tens of millions of years of the intrusion of TTG gneiss, and developed from a mixture of mantle and recycled crustal components (e.g. Lobach-Zhuchenko et al. 2008; Heilimo et al. 2013). This process is similar to A-type magmatism following subduction in post-Archean convergent plate margins (e.g. Turner et al. 1992; Laurent et al. 2014).

LaFlamme et al. (2014a, b) has demonstrated that Neoarchean magmatism occurred over ~ 63 m.y. within the RBb, between 2.73 and 2.66 Ga. Hafnium isotopic data and zircon geochemical compositions were used to distinguish between the two generations of magmatism. An earlier generation of magmatism formed granitoid gneiss, derived from a ca. 3.25–3.10 Ga mafic crustal substrate, and a later generation of magmatism was derived from a metasomatized primitive mantle that interacted with older crust. A prolonged period of magmatism in "modern style" plate tectonic collisional processes (e.g. Condie and Kröner 2008) is known to have occurred in post-Archean collisional orogens (e.g. Trans-Hudson, Grenville orogens). Similarly, plutonism has been shown to occur coevally with Archean craton-scale deformation and crustal thickening (e.g. Boily et al. 2009; Windley and Garde 2009). Based on Archean seismic reflection patterns, van der Velden et al. (2006) demonstrated that Neoarchean cratons are products of rigid plate behaviour much like in Proterozoic and Phanerozoic orogens, and therefore, behaved in a similar manner during plate collision.

Sanukitoid magmatism has been interpreted to occur following a period of TTG generation (Heilimo et al. 2011) in a style similar to anorogenic magmatism that follows subduction in a collisional environment (Manikyamba et al. 2012). Sanukitoid magmatism is interpreted to be generated by rifting and mantle upwelling related to slab break-off (e.g. Stevenson et al. 1999; Lobach-Zhuchenko et al. 2008; Heilimo et al. 2010). In the RBb, this observation is consistent with a period of magma generation at 2.73–2.71 Ga, followed by voluminous sanukitoid magmatism with negative Ta and Nb anomalies and a coincident depletion in Ti, Y, Yb concentrations in the RBb. Fractional crystallization of magma during slow ascent left behind large cumulate bodies resulting in differentiated anhydrous and hydrous granitoid plutons with entrained websterite and gabbroic xenoliths. Slow magmatic ascent coupled with significant differentiation has been described in Proterozoic orogens as resulting from the removal of an overthickened lithosphere following collapse of an orogen. Subsequent mantle-derived magmas evolved slowly at high *P* before ascending into the crust (McLelland et al. 2010). A similar setting is proposed for the generation of Neoarchean magmas in the RBb (Fig. 13).

Cratonization and Speculations on Kimberlite Emplacement

Globally, Neoarchean granitoid rocks came at a time that documented final stability of a crust that had previously undergone a high rate of recycling (e.g. Hawkesworth et al. 2010). A succession of melts resulted in chemical differentiation of the continental crust, and a change from an amphibolitic to a granulitic lower to middle crust (e.g. Fyfe 1973; Ivanic et al. 2012).

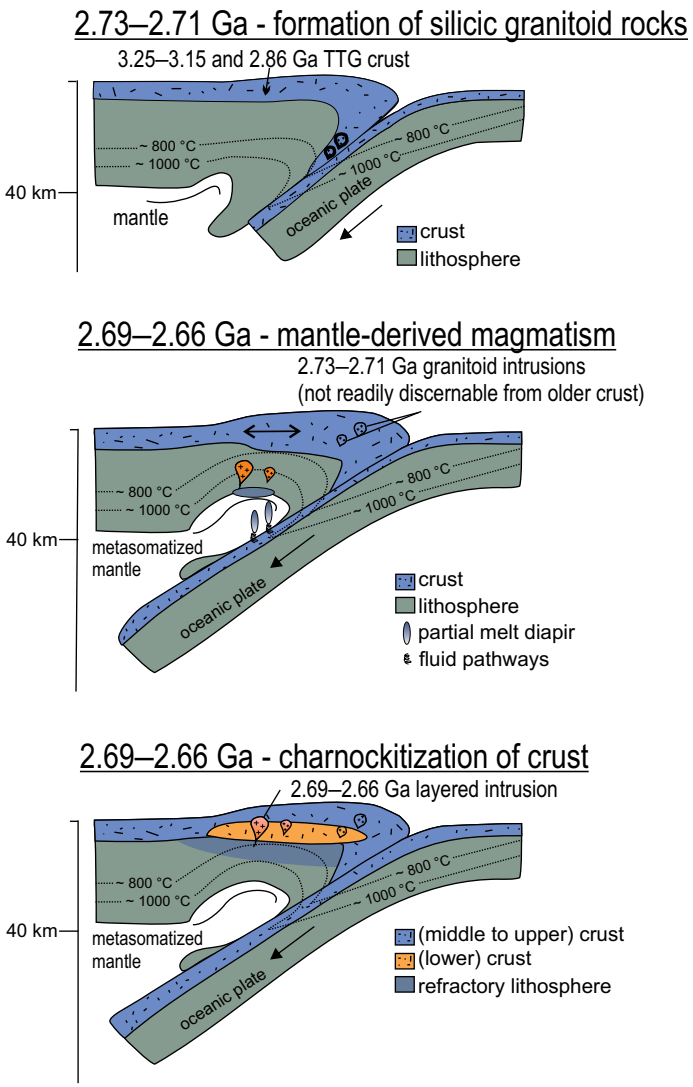

Figure 13. Tectonic setting of sanukitoid generation in the Repulse Bay block. Subduction-driven TTG generation at ca. 2.73–2.71 Ga. Extension, related to an over-thickened lithosphere at 2.69–2.66 Ga, drove mantle-derived magmatism. Colours correlate with the geological map depicted in Figure 2. Neoarchean subduction geotherms after Foley (2008).

The lower crust exposed in the central and southern portion of the RBb demonstrates a bull's eye pattern consisting of pyroxene-bearing ca. 2.73 Ga gneiss that surround the ca. 2.69 Ga dehydrated plutons (see Fig. 2). In these rocks orthopyroxene occurs as the product of a prograde reaction replacing biotite. Therefore, the generation of large volumes of charnockitic magma from a metasomatized depleted upper mantle left behind a granulitic crust and a refractory mantle that helped to stabilize a lithospheric keel in the Neoarchean. The subcontinental lithospheric mantle represents residues and/or cumulates from a high degree of melting at significant depths (e.g. Stevenson et al. 1999; Griffin et al. 2003) and, together with the melt-depleted lower to middle crust, is an important element in cratonization (Shirey et al. 2009). Therefore, voluminous Neoarchean dehydrated plutons may be indicative of an anomalously thick lithospheric keel.

Kimberlite emplacement requires a number of conditions: 1) a tectonically stable craton for at least 500 m.y. with a thick lithospheric keel (e.g. Pasteris 1984); 2) earlier extensive volcanism and/or intrusive magmatism and the addition of K, F, and S to the mantle by metasomatic processes (likely during subduction; e.g. Mitchell 1986; Harte et al. 1987; Shirey et al. 2013); and 3) an asthenospheric source component (Paton et al. 2009). This study suggests that Archean tectonic processes that resulted in fertilization and modification of the subcontinental lithospheric mantle and subsequent cratonization, may also have been critical in generating the perfect conditions for later kimberlite emplacement. Because sanukitoid magmatism occurs in ancient subduction zone settings, its presence may potentially be used as a tool to delineate ancient cratonic margins that have thick and metasomatized lithospheric keels. This statement is in agreement with the fact that the RBb is host to the largest kimberlite pipe in the eastern Canadian Arctic, which is situated proximal to sanukitoid magmatism.

CONCLUSIONS

Neoarchean magmatism in the RBb formed as regional scale ca. 2.73–2.71 Ga TTG-type plutonism and as ca. 2.69–2.66 Ga charnockite, enderbite and granitoid intrusions, host to websterite xenoliths. Based on the similar mineralogical assemblages, whole rock chemical composition of the 2.69–2.66 Ga granitoid intrusions and xenoliths, and similar trace element patterns of pyroxene, the lithologies are interpreted to be coeval and related in part by fractional crystallization. The mantle-like signature (high LILE, Mg#, MgO, Ni, Co) of the ca. 2.69–2.66 Ga lithologies are interpreted to indicate that Neoarchean magmatism was derived from partial melting of a primitive mantle source that was metasomatized by oceanic slab melts. Further crustal contamination occurred by way of interaction with lower crustal melts during magma generation and ascent, accounting for the geochemical and isotopic nature. Based on their chemical composition, the granitoid rocks and autoliths are interpreted to have intruded as a sanukitoid suite.

Neoarchean mantle-derived sanukitoid magmatism in the RBb, followed a period of TTG magmatism at 2.73–2.71 Ga in a subduction zone setting. Similar to post-Archean orogenesis, mantle-derived magmatism resulted from extension related to lithospheric removal beneath an over-thickened crust at depths of 35–40 km. The more buoyant felsic to intermediate anhydrous magmatism rose diapirically as a crystal mush to the middle crust. Sanukitoid magmatism in this region is unique in its preservation as a large scale cumulate intrusion ranging from ultramafic to felsic in composition. The formation of regional scale granulite in conjunction with granulite-facies metamorphism was integral in stabilizing a thick lithospheric keel beneath the RBb.

ACKNOWLEDGEMENTS

This research was funded by the Geological Survey of Canada under the Geomapping for Energy and Minerals program, and an NSERC Discovery Grant to C.R.M.M. Work was carried out as part of a Ph.D. thesis by the first author at the University of New Brunswick. Douglas Hall from the UNB Microscopy and Microanalysis Facility is thanked for help during major element data collection. Cliff Shaw is thanked for offering guidance on an earlier version of this paper. We are grateful to the Editor Brendan Murphy for insightful suggestions and to two anonymous reviewers for thorough and very helpful reviews.

REFERENCES

Ashwal, L.D., 1993, Anorthosites: Springer-Verlag, Berlin, 422 p., http://dx.doi.org/10.1007/978-3-642-77440-9.

Bédard, J.H., 2003, Evidence for regional-scale, pluton-driven, high-grade metamorphism in the Archaean Minto block, northern Superior Province, Canada: The Journal of Geology, v. 111, p. 183–205, http://dx.doi.org/10.1086/345842.

Bédard, J.H., 2006, A catalytic delamination-driven model for coupled genesis of Archean crust and sub-continental lithospheric mantle: Geochimica et Cosmochimica Acta, v. 70, p. 1188–1214, http://dx.doi.org/10.1016/j.gca.2005.11.008.

Bédard, J.H., Harris, L.B., and Thurston, P.C., 2013, The hunting of the snArc: Precambrian Research, v. 229, p. 20–48, http://dx.doi.org/10.1016/j.precamres.2012.04.001.

Berman, R.G., 2010, Metamorphic map of the western Churchill Province, Canada: Geological Survey of Canada Open File, 5279, 55 p., scale 1:2,500,000, http://dx.doi.org/10.4095/287320.

Berman, R.G., Sanborn-Barrie, M., Stern, R.A., and Carson, C.J., 2005, Tectonometamorphism at ca., 2.35 and 1.85 Ga in the Rae domain, Western Churchill Province, Nunavut, Canada: insights from structural, metamorphic and in situ geochronological analysis of the southwestern Committee Bay belt: The Canadian Mineralogist, v. 43, p. 409–442, http://dx.doi.org/10.2113/gscanmin.43.1.409.

Bethune, K.M., and Scammell, R.J., 2003, Geology, geochronology, and geochemistry of Archean rocks in the Eqe Bay area, north-central Baffin Island, Canada: constraints on the depositional and tectonic history of the Mary River Group of northeeastern Rae Province: Canadian Journal of Earth Sciences, v. 40, p. 1137–1167, http://dx.doi.org/10.1139/e03-028.

Bleeker, W., 2003, The late Archean record: a puzzle in ca. 35 pieces: Lithos, v. 71, p. 99–134, http://dx.doi.org/10.1016/j.lithos.2003.07.003.

Boily, M., Leclair, A., Maurice, C., Bédard, J.H., and David, J., 2009, Paleo- to Mesoarchean basement recycling and terrane definition in the northeastern Superior Province, Québec, Canada: Precambrian Research, v. 168, p. 23–44, http://dx.doi.org/10.1016/j.precamres.2008.07.009.

Bolle, O., Diot, H., and Duchesne, J.-C., 2000, Magnetic fabric and deformation in charnockitic igneous rocks of the Bjerkreim–Sokndal layered intrusion (Rogaland, Southwest Norway): Journal of Structural Geology, v. 22, p. 647–667, http://dx.doi.org/10.1016/S0191-8141(99)00183-2.

Brey, G.P., and Köhler, T., 1990, Geothermobarometry in four-phase lherzolites II. New thermobarometers, and practical assessment of existing thermobarometers: Journal of Petrology, v. 31, p. 1353–1378, http://dx.doi.org/10.1093/petrology/31.6.1353.

Condie, K.C., and Kröner, A., 2008, When did plate tectonics begin? Evidence form the geological record, *in* Condie, K.C., and Pease, V., *eds.,* When Did Plate Tectonics Begin on Planet Earth?: Geological Society of America Special Papers, v. 440, p. 281–294, http://dx.doi.org/10.1130/2008.2440(14).

Corrigan, D., Nadeau, L., Brouillette, P., Wodicka, N., Houlé, M.G., Tremblay, T., Machado, G., and Keating, P., 2013, Overview of the GEM Multiple Metals - Melville Peninsula project, central Melville Peninsula, Nunavut: Geological Survey of Canada, Current Research 2013-19, 17 p., http://dx.doi.org/10.4095/292862.

Davis, D.W., Amelin, Y., Nowell, G.M., and Parrish, R.R., 2005, Hf isotopes in zircon from the western Superior province, Canada: Implications for Archean crustal development and evolution of the depleted mantle reservoir: Precambrian Research, v. 140, p. 132–156, http://dx.doi.org/10.1016/j.precamres.2005.07.005.

Davis, W.J., Hanmer, S., Tella, S., Sandeman, H.A., and Ryan, J.J., 2006, U–Pb geochronology of the MacQuoid supracrustal belt and Cross Bay plutonic complex: Key components of the northwestern Hearne Subdomain, western Churchill Province, Nunavut, Canada: Precambrian Research, v. 145, p. 53–80, http://dx.doi.org/10.1016/j.precamres.2005.11.016.

de Hoog, J.C.M., Gall, L., and Cornell, D.H., 2010, Trace-element geochemistry of mantle olivine and application to mantle petrogenesis and geothermobarometry: Chemical Geology, v. 270, p. 196–215, http://dx.doi.org/10.1016/j.chemgeo.2009.11.017.

de Oliveira, M.A., Dall'Agnol, R., Althoff, F.J., and da Silva Leite, A.A., 2009, Mesoarchean sanukitoid rocks of the Rio Maria Granite-Greenstone Terrane, Amazonian craton, Brazil: Journal South American Earth Sciences, v. 27, p. 146–160, http://dx.doi.org/10.1016/j.jsames.2008.07.003.

de Oliveira, M.A., Dall'Agnol, R., and de Almeida, J.A.C., 2011, Petrology of the Mesoarchean Rio Maria Suite and the discrimination of sanukitoid series: Lithos, v. 127, p. 192–209, http://dx.doi.org/10.1016/j.lithos.2011.08.017.

Deer, W., Howie, R.A., and Zussman, J., 1992, An Introduction to the Rock-Forming Minerals (2 edition): Longman, London, 696 p.

DePaolo, D.J., 1981, Neodymium isotopes in the Colorado Front Range and crust-mantle evolution in the Proterozoic: Nature, v. 291, p. 193–196, http://dx.doi.org/10.1038/291193a0.

Drummond, M.S., and Defant, M.J., 1990, A model for trondhjemite-tonalite-dacite genesis and crustal growth via slab melting: Archean to modern comparisons: Journal of Geophysical Research, v. 95, p. 21503–21521, http://dx.doi.org/10.1029/JB095iB13p21503.

Foley, S., 2008, A trace element perspective on Archean crust formation and on the presence or absence of Archean subduction, *in* Condie, K.C., and Pease, V., *eds.,* When Did Plate Tectonics Begin on Planet Earth?: Geological Society of America Special Papers, v. 440, p. 31–50, http://dx.doi.org/10.1130/2008.2440(02).

Frisch, T., 2000, Precambrian geology of Ian Calder Lake, Cape Barclay, and part of Darby Lake map areas, south-central Nunavut: Geological Survey of Canada Bulletin, v. 542, 51 p.

Frost, B.R., and Frost, C.D., 2008, On charnockites: Gondwana Research, v. 13, p. 30–44, http://dx.doi.org/10.1016/j.gr.2007.07.006.

Frost, B.R., Barnes, C.G., Collins, W.J., Arculus, R.J., Ellis, D.J., and Frost, C.D., 2001, A geochemical classification for granitic rocks: Journal of Petrology, v. 42, p. 2033–2048, http://dx.doi.org/10.1093/petrology/42.11.2033.

Fyfe, W.S., 1973, The granulite facies, partial melting and the Archaean crust: Philosophical Transactions of the Royal Society of London, v. 273, p. 457–461, http://dx.doi.org/10.1098/rsta.1973.0011.

Griffin, W.L., O'Reilly, S.Y., Abe, N., Aulbach, S., Davies, R.M., Pearson, N.J., Doyle, B.J., and Kivi, K., 2003, The origin and evolution of Archean lithospheric mantle: Precambrian Research, v. 127, p. 19–41, http://dx.doi.org/10.1016/S0301-9268(03)00180-3.

Griffin, W.L., O'Reilly, S.Y., Afonso, J.C., and Begg, G.C., 2009, The composition and evolution of lithospheric mantle: a re-evaluation and its tectonic implications: Journal of Petrology, v. 50, p. 1185–1204. http://dx.doi.org/10.1093/petrology/egn033.

Halla, J., 2005, Late Archean high-Mg granitoids (sanukitoids) in the southern Karelian domain, eastern Finland; Pb and Nd isotopic constraints on crust-mantle interactions: Lithos, v. 79, p. 161–178, http://dx.doi.org/10.1016/j.lithos.2004.05.007.

Halla, J., van Hunen, J., Heilimo, E., and Hölttä, P., 2009, Geochemical and numerical constraints on Neoarchean plate tectonics: Precambrian Research, v. 174, p. 155–162, http://dx.doi.org/10.1016/j.precamres.2009.07.008.

Harte, B., Winterburn, P.A., and Gurney, J.J., 1987, Metasomatic phenomena in garnet peridotite facies mantle xenoliths from the Matsoku kimberlite pipe, Lesotho, *in* Menzies, M.A., and Hawkesworth, C.J., *eds.*, Mantle Metasomatism: Academic Press, London, p. 145–220.

Hartlaub, R.P., Chacko, T., Heaman, L.M., Creaser, R.A., Ashton, K.E., and Simonetti, T., 2005, Ancient (Meso- to Paleoarchean) crust in the Rae Province, Canada: Evidence from Sm–Nd and U–Pb constraint: Precambrian Research, v. 141, p. 137–153, http://dx.doi.org/10.1016/j.precamres.2005.09.001.

Hawkesworth, C.J., Dhuime, B., Pietranik, A.B., Cawood, P.A., Kemp, A.I.S., and Storey, C.D., 2010, The generation and evolution of the continental crust: Journal of the Geological Society, v. 167, p. 229–248, http://dx.doi.org/10.1144/0016-76492009-072.

Heaman, L.M., Böhm, Ch.O., Machado, N., Krogh, T.E., Weber, W., and Corkery, M.T., 2011, The Pikwitonei Granulite Domain, Manitoba: a giant Neoarchean high-grade terrane in the northwest Superior Province: Canadian Journal of Earth Sciences, v. 48, p. 205–245, http://dx.doi.org/10.1139/E10-058.

Heilimo, E., Halla, J., and Hölttä, P., 2010, Discrimination and origin of the sanukitoid series: Geochemical constraints from the Neoarchean western Karelian Province (Finland): Lithos, v. 115, p. 27–39, http://dx.doi.org/10.1016/j.lithos.2009.11.001.

Heilimo, E., Halla, J., and Huhma, H., 2011, Single-grain zircon U–Pb age constraints of the western and eastern sanukitoid zones in the Finnish part of the Karelian Province: Lithos, v. 121, p. 87–99, http://dx.doi.org/10.1016/j.lithos.2010.10.006.

Heilimo, E., Halla, J., Andersen, T., and Huhma, H., 2013, Neoarchean crustal recycling and mantle metasomatism: Hf–Nd–Pb–O isotope evidence from sanukitoids of the Fennoscandian shield: Precambrian Research, v. 228, p. 250–266, http://dx.doi.org/10.1016/j.precamres.2012.01.015.

Hinchey, A.M., Davis, W.J., Ryan, J.J., and Nadeau, L., 2011, Neoarchean high-potassium granites of the Boothia mainland area, Rae domain, Churchill Province: U–Pb zircon and Sm–Nd whole rock isotopic constraints: Canadian Journal of Earth Sciences, v. 48, p. 247–279, http://dx.doi.org/10.1139/E10-071.

Hoffman, P.F., 1988, United plates of America, the birth of a craton: Early Proterozoic assembly and growth of Laurentia: Annual Review of Earth and Planetary Sciences, v. 16, p. 543–603, http://dx.doi.org/10.1146/annurev.ea.16.050188.002551.

Hynes, A., 2014, How feasible was subduction in the Archean?: Canadian Journal of Earth Sciences, v. 51, p. 286–296, http://dx.doi.org/10.1139/cjes-2013-0111.

Ionov, D.A., Bodinier, J.-L., Mukasa, S.B., and Zanetti, A., 2002, Mechanisms and sources of mantle metasomatism: Major and trace element compositions of peridotite xenoliths from Spitsbergen in the context of numerical modelling: Journal of Petrology, v. 43, p. 2219–2259, http://dx.doi.org/10.1093/petrology/43.12.2219.

Irvine, T.N., and Baragar, W.R.A., 1971, A guide to the chemical classification of the

common volcanic rocks: Canadian Journal of Earth Sciences, v. 8, p. 523–548, http://dx.doi.org/10.1139/e71-055.

Irving, A.J., and Frey, F.A., 1984, Trace element abundances in megacrysts and their host basalts: Constraints on partition coefficients and megacryst genesis: Geochimica et Cosmochimica Acta, v. 48, p. 1201–1221, http://dx.doi.org/10.1016/0016-7037(84)90056-5.

Ivanic, T.J., Van Kranendonk, M.J., Kirkland, C.L., Wyche, S., Wingate, M.T.D., and Belousova, E.A., 2012, Zircon Lu–Hf isotopes and granite geochemistry of the Murchison Domain of the Yilgarn craton: Evidence for reworking of Eoarchean crust during Meo-Neoarchean plume-driven magmatism: Lithos, v. 148, p. 112–127, http://dx.doi.org/10.1016/j.lithos.2012.06.006.

Jenner, G.A., 1996, Trace element geochemistry of igneous rocks: geochemical nomenclature and analytical geochemistry, *in* Wyman, D.A., *ed.*, Trace Element Geochemistry of Volcanic Rocks: Applications for Massive Sulphide Exploration: Geological Association of Canada - Short Course Notes 12, p. 51–77.

Kerrich, R., and Wyman, D., 1996, Trace element systematics: an overview, *in* Wyman, D.A., *ed.,* Trace Element Geochemistry of Volcanic Rocks: Applications for Massive Sulphide Exploration: Geological Association of Canada - Short Course Notes 12, p. 1–50.

Ketchum, J.W.F., Bleeker, W., and Stern, R.A., 2004, Evolution of an Archean basement complex and its autochthonous cover, southern Slave Province, Canada: Precambrian Research, v. 135, p. 149–176, http://dx.doi.org/10.1016/j.precamres.2004.08.005.

LaFlamme, C., McFarlane, C.R.M., and Corrigan, D., 2014a, U–Pb, Lu–Hf and REE in zircon from 3.2 to 2.6 Ga Archean gneisses of the Repulse Bay block, Melville Peninsula, Nunavut: Precambrian Research, v. 252, p. 223–239, http://dx.doi.org/10.1016/j.precamres.2014.07.012.

LaFlamme, C., McFarlane, C.R.M., Corrigan, D., and Wodicka, N., 2014b, Origin and tectonometamorphic history of the Repulse Bay block, Melville Peninsula, Nunavut: exotic terrane or deeper level of the Rae craton?: Canadian Journal of Earth Sciences, v. 51, p. 1097–1122, http://www.nrcresearchpress.com/doi/abs/10.1139/cjes-2014-0040#.VJDVJCvF_Do.

Laurent, O., Martin, H., Doucelance, R., Moyen, J.-F., and Paquette, J.-L., 2011, Geochemistry and petrogenesis of high-K "sanukitoids" from the Bulai pluton, Central Limpopo Belt, South Africa: Implications for geodynamic changes at the Archaean–Proterozoic boundary: Lithos, v. 123, p. 73–91, http://dx.doi.org/10.1016/j.lithos.2010.12.009.

Laurent, O., Doucelance, R., Martin, H., and Moyen, J.-F., 2013, Differentiation of the late-Archaean sanukitoid series and some implications for crustal growth: Insights from geochemical modelling on the Bulai Pluton, Central Limpopo Belt, South Africa: Precambrian Research, v. 227, p. 186–203, http://dx.doi.org/10.1016/j.precamres.2012.07.004.

Laurent, O., Martin, H., Moyen, J.-F., and Doucelance, R., 2014, The diversity and evolution of late-Archean granitoids: Evidence for the onset of "modern-style" plate tectonics between 3.0 and 2.5 Ga: Lithos, v. 205, p. 208–235, http://dx.doi.org/10.1016/j.lithos.2014.06.012.

Lobach-Zhuchenko, S.B., Rollinson, H.R., Chekulaev, V.P., Arestova, N.A., Kovalenko, A.V., Ivanikov, V.V., Guseva, N.S., Sergeev, S.A., Matukov, D.I., and Jarvis, K.E., 2005, The Archaean sanukitoid series of the Baltic Shield: geological setting, geochemical characteristics and implications for their origin: Lithos, v. 79, p. 107–128, http://dx.doi.org/10.1016/j.lithos.2004.04.052.

Lobach-Zhuchenko, S.B., Rollinson, H., Chekulaev, V.P., Savatenkov, V.M., Kovalenko, A.V., Martin, H., Guseva, N.S., and Arestova, N.A., 2008, Petrology of a late Archaean, highly potassic sanukitoid pluton from the Baltic Shield: Insights into late Archaean mantle metasomatism: Journal of Petrology, v. 49, p. 393–420, http://dx.doi.org/10.1093/petrology/egm084.

Ma, X., Guo, J., Liu, F., Qian, Q., and Fan, H., 2013, Zircon U–Pb ages, trace elements, and Nd–Hf isotopic geochemistry of Guyang sanukitoids and related rocks: Implications for the Archean crustal evolution of the Yinshan Block, North China Craton: Precambrian Research, v. 230, p. 61–78, http://dx.doi.org/10.1016/j.precamres.2013.02.001.

Manikyamba, C., Kerrich, R., Polat, A., Raju, K., Satyanarayanan, M., and Krishna, A.K., 2012, Arc picrite-potassic adakitic-shoshonitic volcanic association of the Neoarchean Sigegudda greenstone terrane, western Dharwar craton: Transition from arc wedge to lithosphere melting: Precambrian Research, v. 212–213, p. 207–224, http://dx.doi.org/10.1016/j.precamres.2012.05.006.

Martin, H., and Moyen, J.-F., 2002, Secular changes in tonalite-trondhjemite-granodiorite composition as markers of the progressive cooling of Earth: Geology, v. 30, p. 319–322, http://dx.doi.org/10.1130/0091-7613(2002)030<0319:SCITTG>2.0.CO;2.

Martin, H., Smithies, R.H., Rapp, R., Moyen, J.-F., and Champion, D., 2005, An overview of adakite, tonalite-trondhjemite-granodiorite (TTG), and sanukitoid: relationships and some implications for crustal evolution: Lithos, v. 79, p. 1–24, http://dx.doi.org/10.1016/j.lithos.2004.04.048.

Martin, H., Moyen, J.-F., and Rapp, R., 2010, The sanukitoid series; magmatism at the Archaean–Proterozoic transition, *in* Clemens, J.D., *ed.,* Sixth Hutton Symposium on The Origin of Granites and Related Rocks: Geological Society of America Special Papers, v. 472, p. 15–33, http://dx.doi.org/10.1130/2010.2472(02).

McLelland, J.M., Selleck, B.W., Hamilton, M.A., and Bickford, M.E., 2010, Late- to post-tectonic setting of some major Proterozoic anorthosite-mangerite-charnockite-granite (AMCG) suites: The Canadian Mineralogist, v. 48, p. 729–750, http://dx.doi.org/10.3749/canmin.48.4.729.

Mitchell, R.H., 1986, Kimberlites: Mineralogy, Geochemistry, and Petrology: Springer, New York, 442 p., http://dx.doi.org/10.1007/978-1-4899-0568-0.

Moyen, J.-F., 2011, The composite Archaean grey gneisses: Petrological significance, and evidence for a non-unique tectonic setting for Archaean crustal growth: Lithos, v. 123, p. 21–36, http://dx.doi.org/10.1016/j.lithos.2010.09.015.

Moyen, J.-F., and Stevens, G., 2006, Experimental constraints on TTG petrogenesis: Implications for Archean geodynamics, *in* Benn, K., Mareschal, J.-C., and Condie, K.C., *eds.,* Archean Geodynamics and Environments: American Geophysical Union, Geophysical Monograph Series, v. 164, p. 149–175, http://dx.doi.org/10.1029/164GM11.

Moyen, J.-F., Martin, H., and Jayananda, M., 2001, Multi-element geochemical modelling of crust-mantle interactions during late-Archaean crustal growth; the Closepet Granite (South India): Precambrian Research, v. 112, p. 87–105, http://dx.doi.org/10.1016/S0301-9268(01)00171-1.

Mungall, J.E., 2002, Roasting the mantle: Slab melting and the genesis of major Au and Au-rich Cu deposits: Geology, v. 30, p. 915–918, http://dx.doi.org/10.1130/0091-7613(2002)030<0915:RTMSMA>2.0.CO;2.

Nagel, T.J., Hoffmann, J.E., and Münker, C., 2012, Generation of Eoarchean tonalite-trondhjemite-granodiorite series from thickened mafic arc crust: Geology, v. 40, p. 375–378, http://dx.doi.org/10.1130/G32729.1.

Ohba, T., Matsuoka, K., Kimura, Y., Ishikawa, H., and Fujimaki, H., 2009, Deep crystallization differentiation of arc tholeiite basalt magmas from northern Honshu arc, Japan: Journal of Petrology, v. 50, p. 1025–1046, http://dx.doi.org/10.1093/petrology/egp030.

Pasteris, J.D., 1984, Kimberlites: Complex mantle melts: Annual Review in Earth and Planetary Sciences, v. 12, p. 133–153, http://dx.doi.org/10.1146/annurev.ea.12.050184.001025.

Paton, C., Hergt, J.M., Woodhead, J.D., Phillips, D., and Shee, S.R., 2009, Identifying the asthenospheric component of kimberlite magmas from the Dharwar Craton, India: Lithos, v. 112, p. 296–310, http://dx.doi.org/10.1016/j.lithos.2009.03.019.

Paton, C., Hellstrom, J., Paul, B., Woodhead, J., and Hergt, J., 2011, Iolite: Freeware for the visualisation and processing of mass spectrometric data: Journal of Analytical Atomic Spectrometry, v. 26, p. 2508–2518, http://dx.doi.org/10.1039/c1ja10172b.

Pearce, J.A., 1982, Trace element characteristics of lavas from destructive plate boundaries, *in* Thorpe, R.S., *ed.,* Orogenic andesites and related rocks: John Wiley and Sons, Chichester, England, p. 528–548.

Pearce, J.A., and Norry, M.J., 1979, Petrogenetic implications of Ti, Zr, Y, and Nb variations in volcanic rocks: Contributions to Mineralogy and Petrology, v. 69, p. 33–47, http://dx.doi.org/10.1007/BF00375192.

Percival, J.A., and Mortensen, J.K., 2002, Water-deficient calc-alkaline plutonic rocks of northeastern Superior Province, Canada: significance of charnockitic magmatism: Journal of Petrology, v. 43, p. 1617–1650, http://dx.doi.org/10.1093/petrology/43.9.1617.

Percival, J.A., Mortensen, J.K., Stern, R.A., Card, K.D., and Bégin, N.J., 1992, Giant granulite terranes of northeastern Superior Province: the Ashuanipi complex and Minto block: Canadian Journal of Earth Sciences, v. 29, p. 2287–2308, http://dx.doi.org/10.1139/e92-179.

Peterson, T.D., van Breemen, O., Sandeman, H., and Cousens, B., 2002, Proterozoic (1.85–1.75 Ga) igneous suites of the Western Churchill Province: granitoid and ultrapotassic magmatism in a reworked Archean hinterland: Precambrian Research, v. 119, p. 73–100, http://dx.doi.org/10.1016/S0301-9268(02)00118-3.

Qian, Q., and Hermann, J., 2010, Formation of high-Mg diorites through assimilation of peridotite by monzodiorite magma at crustal depths: Journal of Petrology, v. 51, p. 1381–1416, http://dx.doi.org/10.1093/petrology/egq023.

Qian, Q., and Hermann, J., 2013, Partial melting of lower crust at 10–15 kbar: constraints on adakite and TTG formation: Contributions to Mineralogy and Petrology, v. 165, p. 1195–1224, http://dx.doi.org/10.1007/s00410-013-0854-9.

Rapp, R.P., Norman, M.D., Laporte, D., Yaxley, G.M., Martin, H., and Foley, S.F., 2010, Continent formation in the Archean and chemical evolution of the cratonic lithosphere: Melt-rock reaction experiments at 3–4 GPa and petrogenesis of Archean Mg-diorites (sanukitoids): Journal of Petrology, v. 51, p. 1237–1266, http://dx.doi.org/10.1093/petrology/egq017.

Rayner, N., Chakungal, J., and Sanborn-Barrie, M., 2011, New U–Pb geochronological results from plutonic and sedimentary rocks of Southampton Island, Nunavut: Geological Survey of Canada, Current Research 2011-5, 20 p.,

http://dx.doi.org/10.4095/287286.
Rayner, N., Sanborn-Barrie, M., and Chakungal, J., 2013, A 3.0 to 2.0 Ga plutonic record on Southampton Island, Nunavut: Geological Survey of Canada, Current Research 2013-6, 18 p., http://dx.doi.org/10.4095/292214.
Roach, I.C., 2004, Mineralogy, textures and P-T relationships of a suite of xenoliths from the Monaro Volcanic Province, New South Wales, Australia: Journal of Petrology, v. 45, p. 739–758, http://dx.doi.org/10.1093/petrology/egg108.
Rubatto, D., and Hermann, J., 2003, Zircon formation during fluid circulation in eclogites (Monviso, Western Alps): implications for Zr and Hf budget in subduction zones: Geochimica et Cosmochimica Acta, v. 67, p. 2173–2187, http://dx.doi.org/10.1016/S0016-7037(02)01321-2.
Rudnick, R.L., and Fountain, D.M., 1995, Nature and composition of the continental crust: A lower crustal perspective: Reviews in Geophysics, v. 33, p. 267–309, http://dx.doi.org/10.1029/95RG01302.
Rudnick, R.L., McDonough, W.F., McCulloch, M.T., and Taylor, S.R., 1986, Lower crustal xenoliths from Queensland, Australia: Evidence for deep crustal assimilation and fractionation of continental basalts: Geochimica et Cosmochimica Acta, v. 50, p. 1099–1115, http://dx.doi.org/10.1016/0016-7037(86)90391-1.
Ryan, J.J., Nadeau, L., Hinchey, A.M., James, D.T., Sandeman, H.A., Schetselaar, E.M., and Berman, R.G., 2009, Bedrock geology of the southern Boothia mainland area, Kitikmeot region, Nunavut: Current Research (Paper 2009-1), 21 p.
Sandeman, H.A., Cousens, B.L., and Hemmingway, C.J., 2003, Continental tholeiitic mafic rocks of the Paleoproterozoic Hurwitz Group, Central Hearne subdomain, Nunavut: insight into the evolution of the Hearne sub-continental lithosphere: Canadian Journal of Earth Sciences, v. 40, p. 1219–1237, http://dx.doi.org/10.1139/e03-035.
Sano, S., Oberhänsli, R., Romer, R.L., and Vinx, R., 2002, Petrological, geochemical and isotopic constraints on the origin of the Harzburg Intrusion, Germany: Journal of Petrology, v. 43, p. 1529–1549, http://dx.doi.org/10.1093/petrology/43.8.1529.
Sato, H., 1977, Nickel content of basaltic magmas: identification of primary magmas and a measure of the degree of olivine fractionation: Lithos, v. 10, p. 113–120, http://dx.doi.org/10.1016/0024-4937(77)90037-8.
Sato, K., and Santosh, M., 2007, Titanium in quartz as a record of ultrahigh-temperature metamorphism: the granulites of Karur, southern India: Mineralogical Magazine, v. 71, p. 143–154, http://dx.doi.org/10.1180/minmag.2007.071.2.143.
Schmidberger, S.S., and Francis, D., 1999, Nature of the mantle roots beneath the North American craton: Mantle xenolith evidence from Somerset Island kimberlites, Lithos, v. 48, p. 195–216, http://dx.doi.org/10.1016/S0024-4937(99)00029-8.
Schmidt, M.W., and Poli, S., 1998, Experimentally based water budgets for dehydrating slabs and consequences for arc magma generation: Earth and Planetary Science Letters, v. 163, p. 361–379, http://dx.doi.org/10.1016/S0012-821X(98)00142-3.
Shirey, S.B., and Hanson, G.N., 1984, Mantle-derived Archaean monzodiorites and trachyandesites: Nature, v. 310, p. 222–224, http://dx.doi.org/10.1038/310222a0.
Shirey, S.B., Ayer, J.A., and Wyman, D.A., 2009, Re-Os and PGE systematics of Neoarchean websterite xenoliths and diamondiferous lamprophyres of the Wawa area, Superior Province, Canada (abstract): Eos, Transactions, American Geophysical Union, Fall Meeting 2009, v. 90, Abstract # V13A-2003.
Shirey, S.B., Cartigny, P., Frost, D.J., Keshav, S., Nestola, F., Nimis, Pl, Pearson, D.G., Sobolev, N.V., and Walter, M.J., 2013, Diamonds and the geology of mantle carbon: Reviews in Mineralogy and Geochemistry, v. 75, p. 355–421, http://dx.doi.org/10.2138/rmg.2013.75.12.
Skulski, T., Sandeman, H., Sanborn-Barrie, M., MacHattie, T., Young, M., Carson, C., Berman, R., Brown, J., Rayner, N., Panagapko, D., Byrne, D., and Deyell, C., 2003, Bedrock geology of the Ellice Hills map area and new constraints on the regional geology of the Committee Bay area, Nunavu: Geological Survey of Canada, Current Research 2003-C22, 11 p.
Smithies, R.H., and Champion, D.C., 2000, The Archaean high-Mg diorite suite: Links to tonalite-trondhjemite-granodiorite magmatism and implications for early Archaean crustal growth: Journal of Petrology, v. 41, p. 1653–1671, http://dx.doi.org/10.1093/petrology/41.12.1653.
Smithies, R.H., Champion, D.C., and Cassidy, K.F., 2003, Formation of Earth's early Archaean continental crust: Precambrian Research, v. 127, p. 89–101, http://dx.doi.org/10.1016/S0301-9268(03)00182-7.
Stern, R.A., and Hanson, G.N., 1991, Archean high-Mg granodiorite: A derivative of light rare earth element-enriched monzodiorite of mantle origin: Journal of Petrology, v. 32, p. 201–238, http://dx.doi.org/10.1093/petrology/32.1.201.
Stern, R.A., Hanson, G.N., and Shirey, S.B., 1989, Petrogenesis of mantle-derived, LILE-enriched Archean monzodiorites and trachyandesites (sanukitoids) in southwestern Superior Province: Canadian Journal of Earth Sciences, v. 26, p. 1688–1712, http://dx.doi.org/10.1139/e89-145.
Stevenson, R., Henry, P., and Gariépy, C., 1999, Assimilation-fractional crystallization origin of Archean sanukitoid suites: Western Superior Province, Canada: Precambrian Research, v. 96, p. 83–99, http://dx.doi.org/10.1016/S0301-9268(99)00009-1.
Sun, S.-s., and McDonough, W.F., 1989, Chemical and isotopic systematics of oceanic basalts: implications for mantle composition and processes: Geological Society, London, Special Publications, v. 42, p. 313–345, http://dx.doi.org/10.1144/GSL.SP.1989.042.01.19.
Turner, S., Sandiford, M., and Foden, J., 1992, Some geodynamic and compositional constraints on "postorogenic" magmatism: Geology, v. 20, p. 931–934, http://dx.doi.org/10.1130/0091-7613(1992)020<0931:SGACCO>2.3.CO;2.
van Breemen, O., Pehrsson, S., and Peterson, T.D., 2007, Reconnaissance U–Pb SHRIMP geochronology and Sm–Nd isotope analyses from the Tehery-Wager Bay gneiss domain, western Churchill Province, Nunavut: Geological Survey of Canada, Current Research 2007-F2, 15 p.
van der Velden, A.J., Cook, F.A., Drummond, B.J., and Goleby, B.R., 2006, Reflections of the Neoarchean: A global perspective, *in* Benn, K., Mareschal, J.-C., and Condie, K.C., *eds.,* A Global Perspective in Archean Geodynamics and Environments: American Geophysical Union Geophysical Monograph Series, v. 164, p. 255–265, http://dx.doi.org/10.1029/164GM16.
Walter, M.J., 2003, Melt extraction and compositional variability in mantle lithosphere, *in* Holland, H.D., and Turekian, K.K., *eds.,* Treatise on Geochemistry: Volume 2: The Mantle and Core: Elsevier, p. 363–394, http://dx.doi.org/10.1016/B0-08-043751-6/02008-9.
Whalen, J.B., Percival, J.A., McNicoll, V.J., and Longstaffe, F.J., 2004, Geochemical and isotopic (Nd–O) evidence bearing on the origin of late- to post-orogenic high-K granitoid rocks in the Western Superior Province: implications for late Archean tectonomagmatic processes: Precambrian Research, v. 132, p. 303–326, http://dx.doi.org/10.1016/j.precamres.2003.11.007.
Whitney, D.L., and Evans, B.W., 2010, Abbreviations for names of rock-forming minerals: American Mineralogist, v. 95, p. 185–187, http://dx.doi.org/10.2138/am.2010.3371.
Windley, B.F., and Garde, A.A., 2009, Arc-generated blocks with crustal sections in the North Atlantic craton of West Greenland: Crustal growth in the Archean with modern analogues: Earth-Science Reviews, v. 93, p. 1–30, http://dx.doi.org/10.1016/j.earscirev.2008.12.001.
Wyllie, P.J., and Sekine, T., 1982, The formation of mantle phlogopite in subduction zone hybridization: Contributions to Mineralogy and Petrology, v. 79, p. 375–380, http://dx.doi.org/10.1007/BF01132067.
Zaleski, E., Davis, W.J., and Sandeman, H.A., 2001, Continental extension, mantle magmas and basement/cover relationships: Record - Australian Geological Survey Organisation 2001/37, p. 374–376.
Zeh, A., Gerdes, A., and Barton, J.M., Jr., 2009, Archean accretion and crustal evolution of the Kalahari Craton—the zircon age and Hf isotope record of granitic rocks from Barberton/Swaziland to the Francistown arc: Journal of Petrology, v. 50, p. 933–966, http://dx.doi.org/10.1093/petrology/egp027.

Received August 2014
Accepted as revised November 2014
First published on the web December 2014

Appendix 1: Location of samples used for analysis.

Sample	Easting[a]	Northing[a]
10CXAD003	643251.8	7383655.7
10CXAL001	643251.8	7383655.7
10CXAL118	631908.2	7413757.5
10CXAL131	638853.8	7394339.6
10CXAL134	639402.2	7390775.2
10CXAL184	681910.8	7393372.8
10CXAL190	652515.0	7385280.6
10CXAL249	545100.0	7370000.0
10CXAN031	697030.7	7394330.8

[a] NAD 1983; UTM Zone 16N

Appendix 2: Trace element geochemistry in pyroxene occurring in Archean enderbite and ultramafic autoliths reported in ppm.

Sample	Si	2SE	Ca	2SE	Y	2SE	Zr	2SE	Nb	2SE	La	2SE	Ce	2SE	Nd	2SE	Sm	2SE
10CXAL134B (UTM 639402.2E, 7390775.2N)																		
websterite xenolith in ca. 2.67 Ga enderbite																		
opx1	282000	1600	3400	180	2.09	0.04	0.28	0.02	0.013	0.003	0.214	0.025	0.484	0.045	0.42	0.04	0.14	0.02
cpx1b	242000	1100	149250	920	88.11	0.43	28.67	0.27	0.152	0.007	22.9	0.95	111	1.7	103.2	0.5	27.28	0.18
cpx2	240000	1000	161000	2000	70.66	0.85	32.25	0.40	0.024	0.003	16.26	0.35	78.84	0.97	71.9	0.9	19.64	0.27
opx2b	264000	1600	5110	160	3.60	0.08	0.73	0.03	0.027	0.004	0.677	0.082	2.11	0.15	1.60	0.09	0.44	0.03
opx3	266000	2200	3101	71	2.52	0.03	0.41	0.02	0.004	0.001	0.037	0.017	0.106	0.038	0.12	0.02	0.07	0.01
opx3b	267000	1700	2851	99	2.32	0.04	0.50	0.02	0.006	0.002	0.138	0.013	0.251	0.024	0.26	0.03	0.10	0.01
cpx4	244000	1100	159000	1100	83.59	0.53	31.9	0.29	0.057	0.005	19.1	0.31	95.74	0.65	90.9	0.4	24.53	0.19
opx4b	265000	1600	2960	110	2.46	0.03	0.31	0.08	0.005	0.001	0.094	0.022	0.35	0.11	0.18	0.03	0.08	0.01
cpx5	234880	680	146260	920	67.27	0.33	26.0	1.10	0.125	0.006	20.55	0.73	90.9	1.3	80.3	0.54	20.60	0.13
10CXAL190A (UTM 652515.0E, 7385280.6N; U-Pb concordant age: 2670 ± 11 Ma)																		
Orthopyroxene-clinopyroxene-biotite enderbite																		
opx1	250000	2500	4640	150	16.25	0.08	0.55	0.05	9.06	0.11	1.524	0.068	3.33	0.15	1.59	0.07	0.46	0.03
cpx1b	212000	1100	13960	280	13.64	0.22	0.28	0.02	17.2	2.2	3.77	0.18	7.02	0.52	3.73	0.12	1.17	0.07
cpx2	181000	2500	13300	2100	18.45	0.20	0.40	0.04	0.056	0.010	7.5	2.5	12.60	4.00	5.1	1.3	1.04	0.16
opx2b	270000	1400	4870	130	16.22	0.12	0.20	0.01	0.008	0.002	0.703	0.085	1.34	0.12	0.70	0.05	0.32	0.02
opx3	269000	1400	4880	110	16.68	0.12	0.36	0.03	0.016	0.003	0.284	0.013	0.78	0.03	0.59	0.04	0.36	0.03
opx3b	270000	3300	5380	210	14.90	0.09	0.24	0.01	0.005	0.002	1.262	0.087	2.07	0.11	0.90	0.05	0.33	0.02
opx4	249000	2000	5560	160	15.84	0.10	0.19	0.01	0.033	0.004	0.246	0.013	0.57	0.04	0.39	0.04	0.29	0.02
cpx4b	188000	1700	24540	520	13.45	0.15	0.13	0.02	0.027	0.006	14	1.1	16.20	1.20	6.66	0.47	1.17	0.07
opx5b	249000	1400	4480	140	17.85	0.24	0.20	0.01	0.004	0.001	0.393	0.045	0.90	0.07	0.5	0.04	0.23	0.02

Appendix 2: continued

Sample	Eu	2SE	Gd	2SE	Dy	2SE	Er	2SE	Yb	2SE	Th	2SE	U	2SE
10CXAL134B (UTM 639402.2E, 7390775.2N)														
websterite xenolith in ca. 2.67 Ga enderbite														
opx1	0.009	0.003	0.16	0.02	0.29	0.01	0.29	0.02	0.57	0.03	0.025	0.004	0.025	0.003
cpx1b	1.471	0.018	23.90	0.17	19.25	0.12	8.71	0.08	6.75	0.07	0.650	0.140	0.187	0.014
cpx2	1.206	0.029	17.80	0.28	15.36	0.22	7.27	0.10	5.87	0.11	0.084	0.022	0.088	0.004
opx2b	0.032	0.005	0.45	0.02	0.57	0.02	0.50	0.02	0.79	0.03	0.044	0.006	0.025	0.003
opx3	0.007	0.002	0.13	0.01	0.32	0.02	0.39	0.02	0.79	0.03	0.003	0.002	0.002	0.001
opx3b	0.014	0.003	0.13	0.02	0.29	0.02	0.34	0.01	0.68	0.02	0.002	0.001	0.005	0.001
cpx4	1.403	0.027	21.91	0.21	18.12	0.14	8.40	0.09	6.71	0.08	0.156	0.020	0.108	0.004
opx4b	0.009	0.002	0.15	0.01	0.31	0.01	0.37	0.01	0.77	0.03	0.017	0.008	0.011	0.002
cpx5	1.261	0.019	17.71	0.14	14.54	0.10	6.73	0.07	5.37	0.05	0.453	0.098	0.155	0.012
10CXAL190A (UTM 652515.0E, 7385280.6N; U-Pb concordant age: 2670 ± 11 Ma)														
Orthopyroxene-clinopyroxene-biotite enderbite														
opx1	0.030	0.004	0.84	0.04	2.42	0.06	2.59	0.04	3.99	0.07	-	-	0.013	0.005
cpx1b	0.076	0.011	1.44	0.09	2.37	0.06	2.03	0.06	2.85	0.09	-	-	0.004	0.001
cpx2	0.079	0.024	1.37	0.15	2.78	0.08	2.95	0.05	3.82	0.12	-	-	0.003	0.002
opx2b	0.021	0,003	0.71	0.03	2.44	0.05	2.63	0.04	3.95	0.06	-	-	-	-
opx3	0.019	0.002	0.73	0.04	2.41	0.04	2.66	0.04	3.97	0.07	-	-	-	-
opx3b	0.025	0.004	0.67	0.05	2.09	0.04	2.38	0.04	3.75	0.07	-	-	-	-
opx4	0.020	0.004	0.72	0.03	2.36	0.05	2.49	0.04	3.99	0.07	-	-	-	-
cpx4b	0.116	0.010	1.33	0.05	2.16	0.04	1.97	0.06	2.99	0.07	-	-	0.003	0.001
opx5b	0.025	0.004	0.63	0.04	2.43	0.05	2.86	0.07	4.43	0.09	-	-	-	-

Appendix 3: Trace element geochemistry in olivine reported in ppm.

Sample	Li	2SE	Na	2SE	Al	2SE	P	2SE	Ca	2SE	Sc	2SE	Ti	2SE	V	2SE	Cr	2SE
10CXAL249 (UTM 545100.0E, 7370000.0N)																		
dunite xenolith in ca. 2.72 Ga granitoid gneiss																		
L249_1	3.35	0.63	-	-	12.6	2.6	8.4	5.1	480	340	17.33	0.27	11.3	1.3	1.60	0.31	530	100
L249_2	4.95	0.51	48	18	5.6	1.5	24.7	5.9	540	350	16.59	0.32	9.1	1.1	0.28	0.09	36	16
L249_3	3.19	0.66	710	110	65.5	7.0	24.2	6.3	460	430	15.97	0.34	10.9	1.6	1.17	0.30	318	94
L249_4	2.82	0.72	-	-	2.0	1.1	11.5	6.6	310	370	15.31	0.30	7.5	1.5	0.17	0.08	24	5
L249_5	3.47	0.84	-	-	1.8	0.9	14.8	6.2	320	440	14.82	0.33	6.9	1.5	0.22	0.08	23	8
L249_6	3.85	0.63	-	-	1.1	1.1	19.8	5.3	660	390	13.86	0.28	7.5	1.1	0.11	0.08	20	11
L249_7	4.02	0.63	-	-	1.8	1.0	15.9	5.8	210	380	13.60	0.28	5.9	1.5	0.06	0.07	6.6	0.3
L249_8	3.89	0.75	-	-	1.6	1.2	26.5	6.5	370	410	13.73	0.28	5.4	1.4	0.11	0.06	5.7	0.3
L249_9	4.70	0.62	-	-	1.7	1.2	22.1	5.3	430	350	13.00	0.31	7.7	1.3	0.18	0.09	53	14
L249_10	4.43	0.75	-	-	7.4	2.7	23.4	6.5	260	380	12.80	0.30	6.0	1.3	0.94	0.38	260	130

Sample	Mn	2SE	Co	2SE	Ni	2SE	Zn	2SE	Y	2SE	Zr	2SE	Nb	2SE
L249_1	1515	10	164	2	3768	28	174.1	5.0	0.071	0.010	-	-	0.017	0.014
L249_2	1540	11	164	2	3738	32	151.6	2.9	0.058	0.008	0.05	0.02	0.015	0.013
L249_3	1592	15	163	2	3823	44	158.5	5.5	0.077	0.010	0.97	0.15	0.005	0.015
L249_4	1656	17	162	2	3804	43	162.2	4.1	0.035	0.007	-	-	0.002	0.014
L249_5	1532	16	162	2	3806	48	161.4	4.1	0.047	0.007	-	-	-	-
L249_6	1621	8	165	2	3859	26	165.3	2.9	0.069	0.011	-	-	0.045	0.014
L249_7	1723	15	163	2	3895	27	160.7	3.5	0.074	0.011	-	-	0.022	0.014
L249_8	1613	9	165	1	3916	29	165.9	3.6	0.062	0.011	-	-	0.024	0.016
L249_9	1634	10	165	1	3865	27	163.6	3.5	0.059	0.009	-	-	0.028	0.013
L249_10	1654	20	162	2	3774	56	173.5	7.1	0.055	0.009	-	-	0.023	0.015

ANDREW HYNES SERIES: TECTONIC PROCESSES

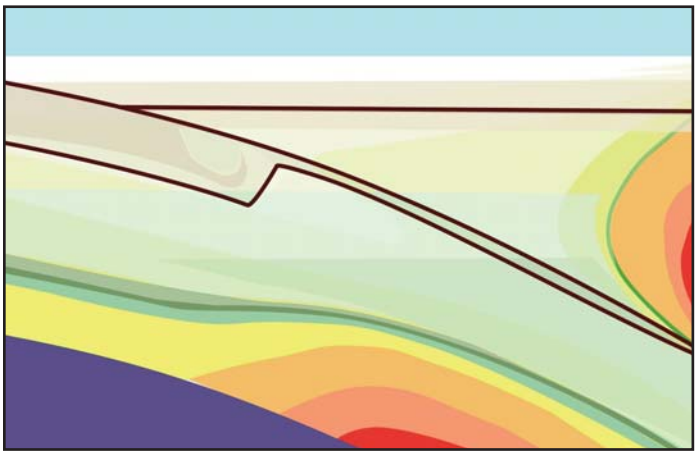

Geologic Setting of Eclogite-facies Assemblages in the St. Cyr Klippe, Yukon–Tanana Terrane, Yukon, Canada

M.B. Petrie[1], J.A. Gilotti[1], W.C. McClelland[1], C. van Staal[2], and S.J. Isard[1]

[1]Department of Earth and Environmental Sciences
University of Iowa, Iowa City, Iowa 52242, USA
E-mail: mbpetrie@gmail.com

[2]Natural Resources Canada
Geological Survey of Canada
Vancouver, British Columbia, V6B 5J3, Canada

SUMMARY

The St. Cyr area near Quiet Lake hosts well-preserved to variably retrogressed eclogite found as sub-metre to hundreds of metre-long lenses within quartzofeldspathic schist in south-central Yukon, Canada. The St. Cyr klippe consists of structurally imbricated, polydeformed and polymetamorphosed units of continental arc crust and ultramafic–mafic rocks. Eclogite-bearing quartzofeldspathic schist forms thrust slices in a 30 km long by 6 km wide, northwest-striking outcrop belt. The schist unit comprises metasedimentary and felsic intrusive rocks that are intercalated on the metre to tens of metres scale. Ultramafic rocks, serpentinite and associated greenschist-facies metagabbro form imbricated tectonic slices within the eclogite-bearing quartzofeldspathic unit, which led to a previously held hypothesis that eclogite was exhumed within a tectonic mélange. The presence of phengite and Permian zircon crystallized under eclogite-facies metamorphic conditions in the quartzofeldspathic host rocks indicate that the eclogite was metamorphosed *in situ* together with the schist as a coherent unit that was part of the continental arc crust of the Yukon–Tanana terrane, rather than a mélange associated with the subduction of oceanic crust of the Slide Mountain terrane. Petrological, geochemical, geochronological and structural similarities link St. Cyr eclogite to other high-pressure localities within Yukon, indicating the high-pressure assemblages form a larger lithotectonic unit within the Yukon–Tanana terrane.

RÉSUMÉ

La région de St-Cyr renferme des éclogites bien conservées à légèrement rétrogradées qui se présentent sous forme de lentilles allant de la fraction de mètre à quelques centaines de mètres de longueur, au sein d'un schiste quartzofeldspathique du centre-sud du Yukon au Canada. La klippe de St-Cyr est structurellement constituée d'unités imbriquées, polydéformées et polymétamorphisées de croûte d'arc continental et de roches ultramafiques à mafiques. Les schistes quartzofeldspathiques à lentilles d'éclogites forment des écailles de chevauchement d'une bande de 30 km de longueur par 6 km de largeur de direction nord-ouest. Les schistes sont constitués de roches métasédimentaires et de roches intrusives felsiques intercalées à des intervalles qui vont du mètre à quelques dizaines de mètres. Les roches ultramafiques, serpentinites et métagabbros au facies à schiste vert forment des écailles tectoniques imbriquées au sein de l'unité quartzofeldspathique à lentilles d'éclogite, d'où une précédente hypothèse voulant que les éclogites soient un produit d'exhumation à partir d'un mélange tectonique. La présence de phengite et de zircon permien cristallisé sous conditions métamorphiques du faciès à éclogite au sein de la roche hôte quartzofeldspathique indiquent que l'éclogite a été métamorphisée en place, avec le schiste comme unité cohérente du terrane de croûte d'arc continental de Yukon–Tanana, plutôt qu'un mélange associé à une subduction de croûte océanique du terrane de Slide Mountain. Des similarités pétrologiques, géochimiques, géochronologiques et structurales lient les éclogites de St-Cyr à d'autres lieux de hautes pressions au Yukon, ce qui indique que les

Geoscience Canada, v. 42, http://www.dx.doi.org/10.12789/geocanj.2015.42.073 pages 327–350
GC Data Repository: Andrew Hynes Series: Tectonic Processes.

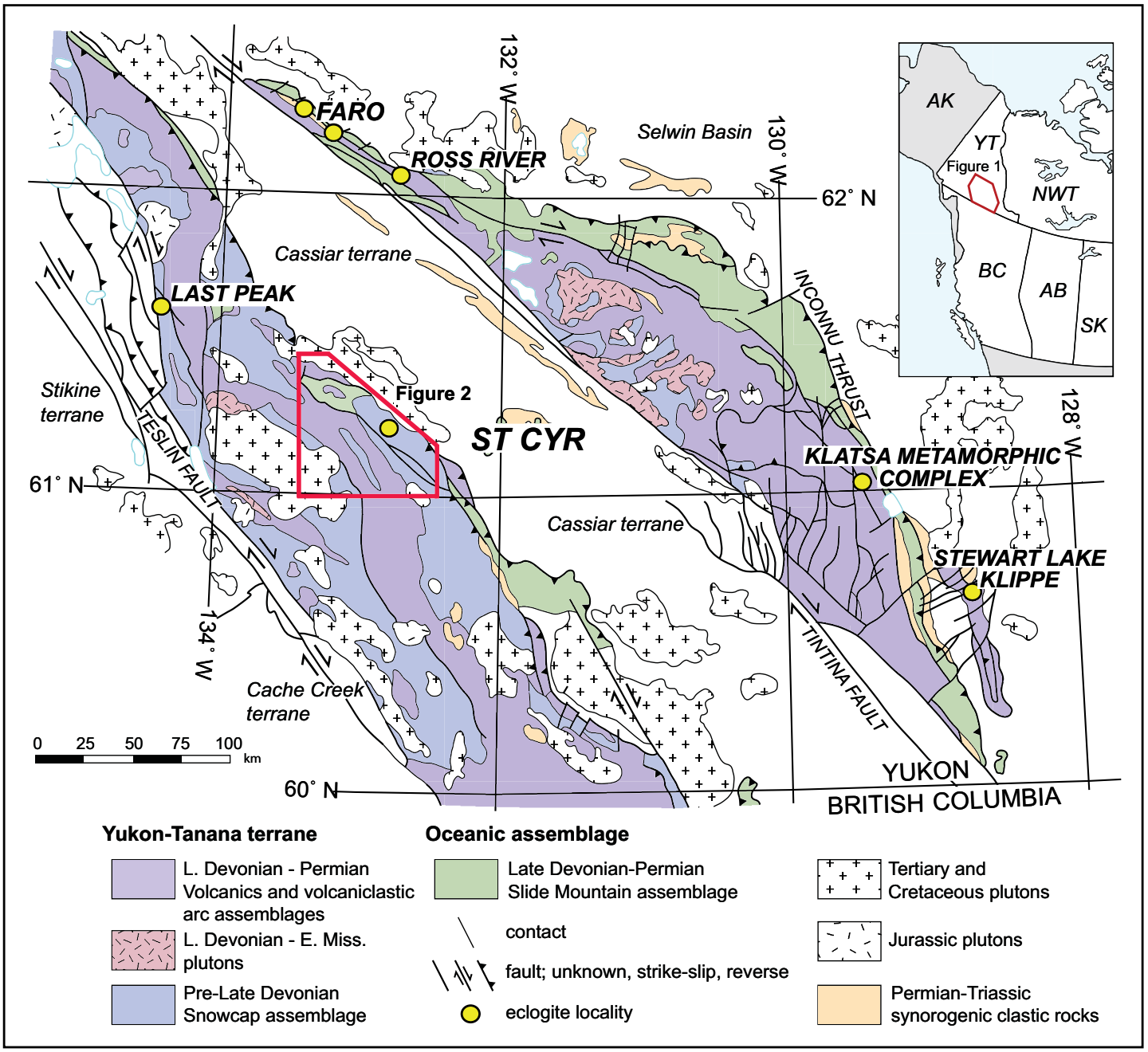

Figure 1. Regional geologic map of the Yukon-Tanana and Slide Mountain terranes in south-central Yukon (modified from Colpron et al. 2006a).

assemblages de hautes pressions forment une unité lithotectonique plus grande au sein du terrane de Yukon–Tanana.

INTRODUCTION

High-pressure metamorphic assemblages formed in Pacific-type convergent margins, such as the iconic Franciscan complex (Ernst 2015), are found along the western North American margin from Alaska to Mexico (Erdmer et al. 1998). The Yukon–Tanana terrane in the Canadian Cordillera preserves both Mississippian and Permian high-pressure rocks. In southeastern Yukon (Fig. 1), strongly retrogressed, Early Mississippian eclogite-facies rocks are preserved as pods within a tectonic mélange in the Klatsa metamorphic complex (Devine et al. 2006), the Simpson Range (Creaser et al. 1999) and the Stewart Lake klippe (Erdmer 1987; Erdmer et al. 1998). These high-pressure rocks are inferred to have formed during east-directed subduction of Panthalassa beneath the western edge of the Yukon–Tanana arc and then were transported eastward in Mesozoic thrust sheets (Erdmer et al. 1998; Devine et al. 2006). In contrast, in south-central Yukon, well-preserved, Late Permian eclogite and glaucophane schist is exposed within quartzofeldspathic schist (Erdmer and Helmstaedt 1983; Erdmer 1987, 1992; Erdmer et al. 1998). Traditionally, the eclogite was assumed to have formed within the Slide Mountain terrane, a mid- to Late Paleozoic ocean basin that developed between the Yukon–Tanana arc and the western margin of North America (e.g. Tempelman-Kluit 1977, 1979; Monger et al. 1982; Wheeler et al. 1991; Colpron et al. 2006a, 2007).

The St. Cyr area is the least known of four localities that preserve Permian eclogite in the Yukon–Tanana terrane (Figs. 1, 2, and 3; Erdmer 1992). Eclogite, garnet amphibolite, and low-grade mafic and ultramafic rocks in the St. Cyr klippe, previously mapped as part of a tectonic mélange, were considered to have formed within the Slide Mountain oceanic crust during subduction of the back-arc region (Tempelman-Kluit 1979; Erdmer 1992). However, Erdmer et al. (1998) recognized that the Permian eclogite occurrences, including the St. Cyr localities, are hosted by quartzofeldspathic schist that seems to share a common metamorphic history. Mafic and ultramafic rocks of the Slide Mountain terrane, in contrast, are of much lower metamorphic grade and lack the muscovite and quartz-rich host rocks typical of the eclogite-bearing units at St. Cyr, Faro, Ross River, and Last Peak (Fig. 1; e.g. Wheeler et al. 1991; Colpron et al. 2006a). Because the Permian eclogite is preserved within structurally coherent units prior to peak metamorphism (Erdmer et al. 1998), it is not part of a chaotic distribution typical of a mélange. This discovery has led to our hypothesis that the Permian eclogite-bearing rocks are a crustal component of the Yukon–Tanana composite arc.

This study documents the extent of high-pressure metamorphism in the St. Cyr area and establishes the protoliths of eclogite and quartzofeldspathic schist in order to place these rocks into a regional tectonic context. Field relationships, petrology and mineral chemistry show that the occurrence of eclogite in the St. Cyr area is widespread and that the eclogite is part of a coherent unit of quartzofeldspathic schist that correlates with the Yukon–Tanana terrane, rather than the Slide Mountain terrane. U–Pb geochronology of metatonalite samples tie the protolith to the Klinkit phase of Yukon–Tanana arc building, and yields Permian metamorphic ages for the eclogite-facies event.

REGIONAL GEOLOGIC SETTING

The Yukon–Tanana terrane extends from Alaska to British Columbia, and constitutes a major component of the Peri-Laurentian allochthons within the northern Canadian Cordillera (Fig. 1; Colpron et al. 2006a, 2007). The terrane comprises a mid- to Late Paleozoic composite arc–forearc system built upon a sliver(s) of continental crust rifted from western Laurentia (Nelson et al. 2013 and references therein). Three Late Devonian to Late Permian, unconformity-bounded, geochronologically and geochemically distinct volcanic and volcaniclastic assemblages are built upon pre-Early Devonian metasedimentary basement known as the Snowcap assemblage (Fig. 1; Mortensen 1992; Piercey et al. 2002, 2006, 2012; Colpron et al. 2006a; Piercey and Colpron 2009). The Snowcap assemblage is a heterogeneous mix of psammitic, pelitic and calc-silicate schist, quartzite, marble and amphibolite (Colpron et al. 2006a, 2006b; Piercey and Colpron 2009). These rocks are typically polydeformed and polymetamorphosed up to amphibolite-facies conditions (Colpron et al. 2006a; Berman et al. 2007; Piercey and Colpron 2009; Staples et al. 2013). Mafic amphibolite in the Snowcap assemblage displays normal mid-ocean ridge basalt (N-MORB), enriched mid-ocean ridge basalt (E-MORB), or ocean island basalt (OIB) signatures consistent with emplacement in a continental rift setting (Nelson and Friedman 2004; Colpron et al. 2006b; Piercey and Colpron 2009). The Snowcap metasedimentary section is characterized by Precambrian detrital zircon populations consistent with a western North American provenance (Piercey and Colpron 2009). Snowcap rocks are commonly intruded by deformed Late Devonian to Early Mississippian tonalite, granodiorite and granite bodies.

The Late Devonian to Early Mississippian Finlayson assemblage, the oldest arc assemblage, is characterized by mafic to felsic metavolcanic and metaplutonic rocks of arc and back-arc affinities (Murphy et al. 2006; Piercey et al. 2006, 2012). The assemblage also includes ultramafic rocks, carbonaceous pelite, quartzite, volcaniclastic rocks and minor marble (Mortensen 1992; Colpron et al. 2006a; Murphy et al. 2006). The Finlayson assemblage is unconformably overlain by the Mississippian to Early Permian Klinkit assemblage, consisting of variably metamorphosed mafic to intermediate calc-alkaline volcanic and volcaniclastic rocks with minor alkali basalt, limestone/marble and conglomerate (Simard et al. 2003; Nelson and Friedman 2004; Murphy et al. 2006; Roots et al. 2006). The Klondike assemblage, the youngest assemblage in the Yukon–Tanana terrane, consists of Middle to Late Permian felsic calc-alkaline metavolcanic and metaplutonic rocks and minor mafic rocks (Mortensen 1990; Dusel-Bacon et al. 2006).

Yukon–Tanana arc rocks are thought to have co-evolved with the opening of a marginal basin represented by an oceanic assemblage of chert, argillite and mafic volcanic rocks (Fig. 1; Mortensen 1992; Nelson 1993; Nelson et al. 2006; Colpron et al. 2006a; Piercey et al., 2006, 2012). This marginal basin was originally termed the Anvil Ocean by Tempelman-Kluit (1979).

The remnants of this basin are preserved today in a discontinuous belt along the eastern edge of the Yukon–Tanana terrane and called the Slide Mountain terrane (Wheeler and McFeely 1991; Mortensen 1992; Pigage 2004; Colpron et al. 2006a; Piercey et al. 2012). In southeastern Yukon, the Slide Mountain terrane is found as fault-bounded slivers of oceanic lithosphere preserved between the Yukon–Tanana terrane and the underlying North American margin. Representative assemblages of the Slide Mountain terrane include unmetamorphosed to greenschist-facies basalt, gabbro, leucogabbro, and variably serpentinized ultramafite, as well as deep-water sedimentary sequences such as chert and argillite (Tempelman-Kluit 1979; Colpron 2006; Colpron et al. 2006a; Murphy et al. 2006; Nelson et al. 2006; Piercey et al. 2012). Other sedimentary rocks found within the Slide Mountain terrane include siltstone, limestone, epiclastic sandstone and conglomerate, and phyllitic chert. Basalt typically display MORB geochemical signatures (Piercey et al. 2006), and together with the ultramafic rocks, is interpreted as a unit of oceanic crust and mantle (Murphy et al. 2006; Piercey et al 2012). Two important characteristics of the Slide Mountain terrane are that metamorphic grade is usually greenschist facies or lower and it is not known to contain muscovite–quartz schist (Wheeler et al. 1991; Colpron et al. 2006a; Piercey et al. 2012).

Blueschist- and eclogite-facies rocks are known from several localities in the Yukon–Tanana terrane (Fig. 1; Erdmer 1992; Mortensen 1992; Erdmer et al. 1998; Devine et al. 2006). The Simpson Range and Stewart Lake areas contain retrogressed eclogite that records evidence of mid-Mississippian high-pressure metamorphism (Creaser et al. 1999). In the

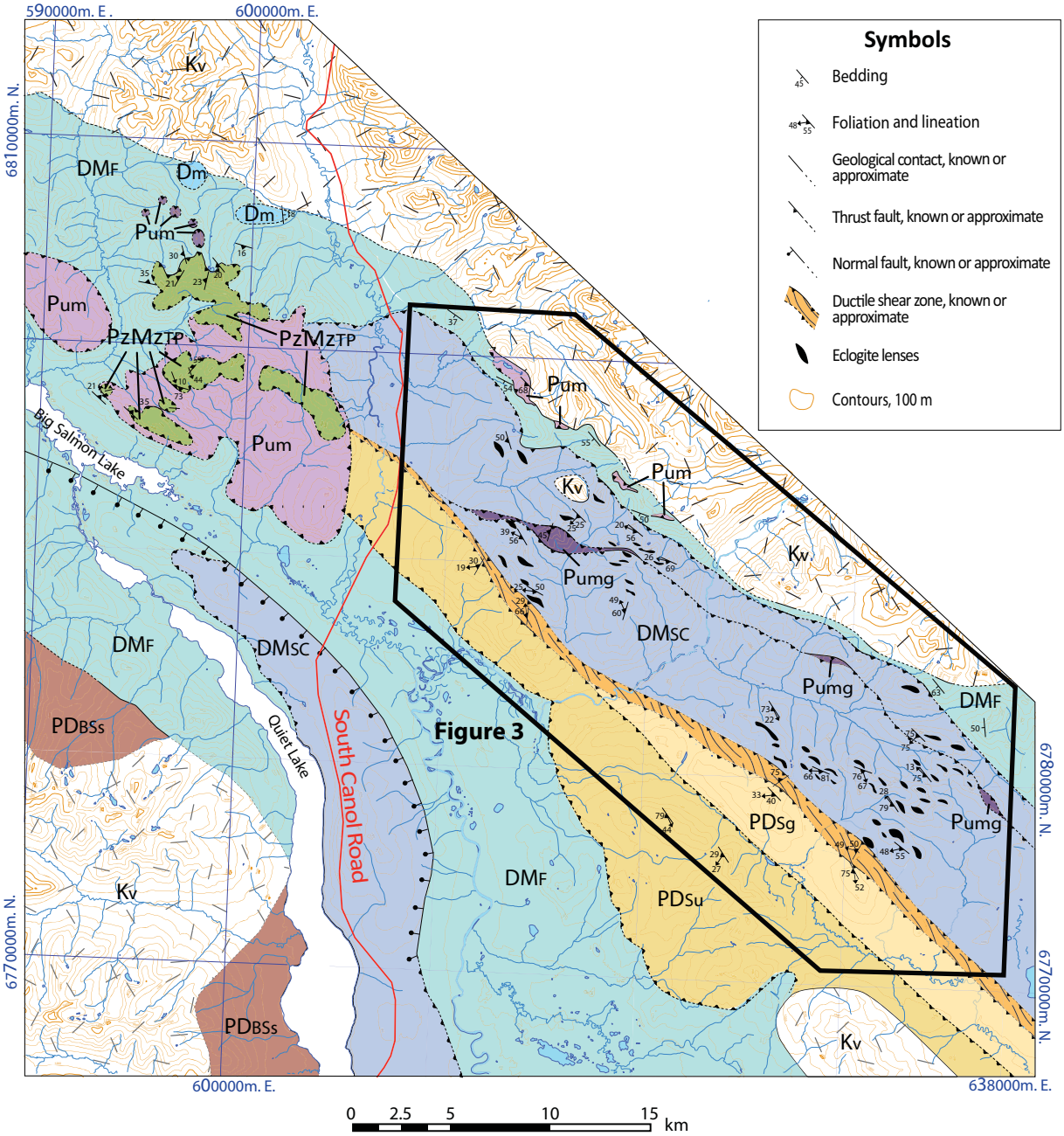

Legend

Cretaceous
Nisutlin Batholith
Kv quartz monzonite intrusion & porphyry dykes

Paleozoic-Mesozoic
Tower Peak assemblage
PzMzTP green, massive, non-foliated to weakly foliated, contains pyroxene, plagioclase, +/- chlorite, +/- epidote

thrust contact

Paleozoic
Pum serpentinized ultramafic rocks & gabbro

thrust contact

Pre-Earliest Devonian - Neoproterozoic
Snowcap Assemblage
PDSu undifferentiated schist, minor quartzite & marble
PDSg garnet-mica schist

Paleozoic
Pumg serpentinized ultramafic rocks & gabbro

thrust contact

Post-Earliest Devonian
St. Cyr Eclogite-Bearing Unit
DMSC undifferentiated quartzofeldspathic rocks (metaigneous & metasedimentary) hosting eclogite & retrogressed eclogite lenses

thrust contact

Late Devonian - Early Mississippian
Finlayson Assemblage
Dm marble
DMF phyllite, siltstone, slate

Proterozoic
Big Salmon Complex
PBSs flaser marble

Figure 2. Geologic map of the Quiet Lake region, modified from Colpron (2006) and Tempelman-Kluit (2012), based on mapping by Isard (2014) and this study.

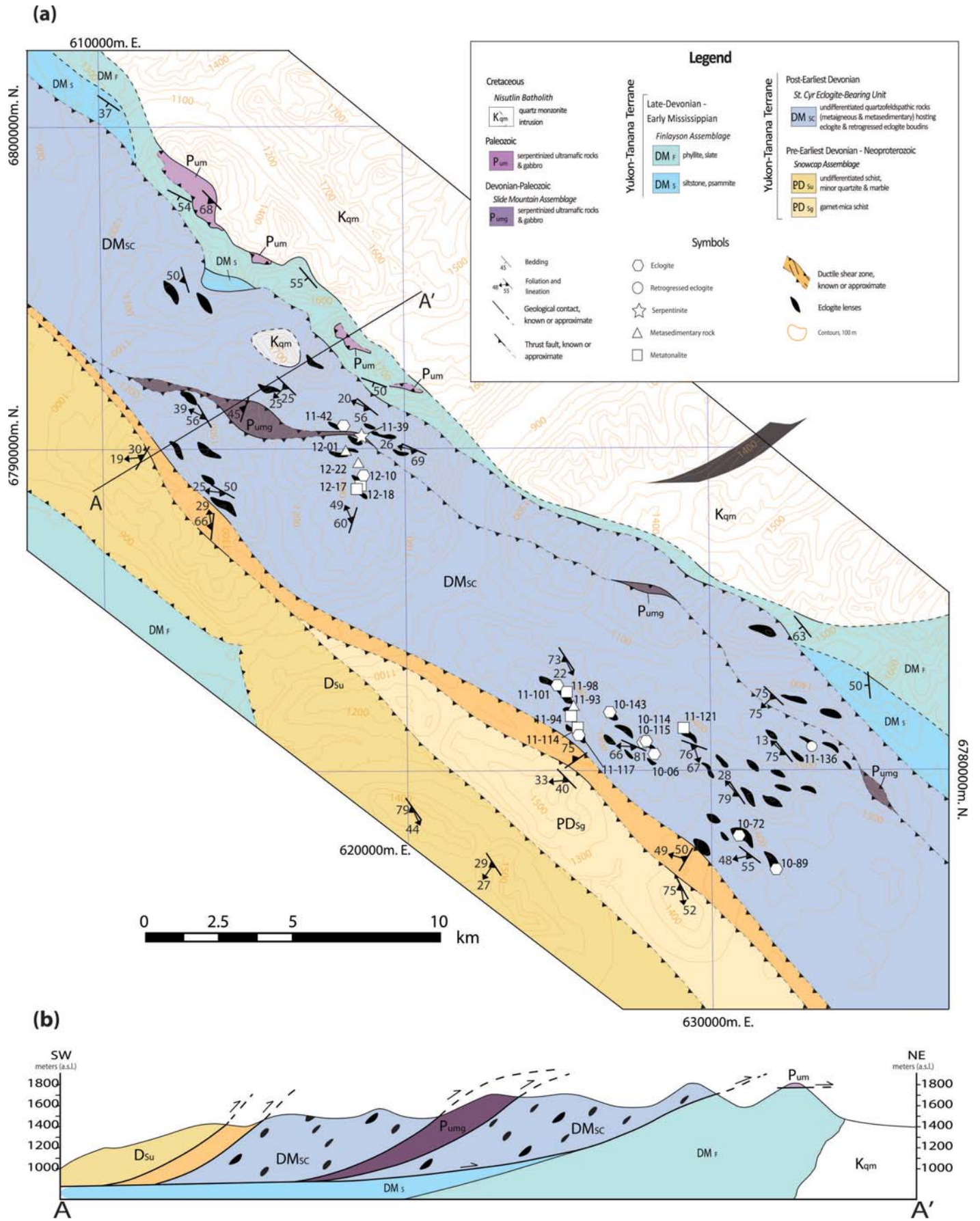

Figure 3. (a) Geologic map and (b) cross-section (vertical = horizontal scale) of the St. Cyr study area. UTM coordinates for samples shown on the map are found in Table DR-1.

southern Campbell Range, omphacite inclusions in zircon from garnet amphibolite are the only petrological evidence of high-pressure metamorphism within the Klatsa complex (Devine et al. 2006). These high-pressure mafic bodies are interpreted to have formed in a tectonic mélange with serpentinized ultramafic and gabbroic rocks and low-grade basalt, chert, limestone and chlorite-schist interpreted to be derived from Yukon–Tanana terrane basement and early Yukon–Tanana arc rocks (Erdmer 1987; Erdmer et al. 1998; Devine et al. 2006). In addition to the St. Cyr area, Permian age high-pressure rocks are found at Ross River, Faro and Last Peak (Erdmer and Armstrong 1989; Creaser et al. 1997; Erdmer et al. 1998). At these localities, eclogite and variably retrogressed equivalent rocks form metre- to tens of metres-sized lenses or structurally conformable layers hosted by greenschist-, blueschist-, or amphibolite-facies schist and quartzite (Erdmer and Helmstaedt 1983; Erdmer 1987; Erdmer et al. 1998). Structural fabrics shared by the eclogite and the host rocks led to the suggestion that they were in contact prior to peak metamorphism (Erdmer and Helmstaedt 1983; Erdmer 1987; Creaser et al. 1997; Erdmer et al. 1998).

GEOLOGY OF THE ST. CYR AREA

The eclogite-bearing rocks of the St. Cyr area are located southeast of the South Canol Road and 14 km northeast of Quiet Lake (Figs. 2 and 3). The area is bounded to the northeast by the Nisutlin Batholith. Eclogite, garnet amphibolite and moderately metamorphosed mafic and ultramafic rocks were previously interpreted as large blocks within a tectonic mélange assigned to the Slide Mountain terrane (Tempelman-Kluit 1979; Erdmer 1992). Fallas (1997) showed that eclogite and retrogressed eclogite are intercalated with quartzofeldspathic tectonites of both sedimentary and igneous origin, and that high-pressure metamorphism was much more widespread than previously known. Fallas (1997) also recognized the shared penetrative fabric displayed by quartzofeldspathic schist and eclogite.

Eclogite-Bearing Quartzofeldspathic Schist

Quartzofeldspathic schist hosting eclogite in the St. Cyr area occurs in at least two thrust slices in a 30 km long by 6 km wide, northwest-striking belt of metasedimentary and felsic metaigneous rocks that are intercalated on the metre to hundreds of metres scale. The quartzofeldspathic rocks were mapped as one unit because it was not always possible to distinguish between the two protoliths due to the strong foliation, fine grain size and poor exposure. Eclogite and retrogressed eclogite are found as sub-metre to hundreds of metres scale lenses surrounded by the quartzofeldspathic schist (Figs. 3 and 4). Both eclogite and the host rocks display schistosity in eclogite-facies assemblages. Schistosity in eclogite is defined by compositional layering and grain-shape-preferred orientation of omphacite and amphibole, whereas phengitic white mica defines the planar fabric of the schist. Lenses of eclogite are flattened parallel to the schistosity in the host rocks. Most commonly, schistosity in the mafic boudins is subparallel to the schistosity in the adjacent host rocks. In other cases, schistosity is discordant to the planar fabric in host rocks; some mafic boudins are massive or display complex internal folding. Contacts between eclogite lenses and the surrounding host rocks range from sharp to gradational. Adjacent to contacts with the metasedimentary rocks, the mafic boudins preserve plagioclase melt stringers, which may be derived from prograde dehydration melting of the metasedimentary rocks or decompression melting of the metasedimentary rocks related to the boudinage of the high-pressure mafic rocks.

Quartzofeldspathic schist with an igneous origin include meta-quartz diorite, metatonalite and metatrondhjemite. Host rocks derived from sedimentary protoliths include mica- and garnet-bearing quartzite, garnet–mica schist and feldspar–quartz–mica schist. The schist is fine-grained and exhibits amphibolite- or greenschist-facies assemblages. Contacts between the metaigneous rocks and the metasedimentary rocks do not show evidence of faulting or strain localization and are assumed to be pre-metamorphic.

Schistosity of the quartzofeldspathic rocks is defined by the alignment of mica (including phengite) and, less commonly, grain-shape-preferred orientation of quartz. Intensity of fabric development is moderate to strong with few areas of localized strain. Schistosity in the upper and lower eclogite-bearing thrust sheets is dominantly northwest-striking and moderately to steeply southwest-dipping (Fig. 5). Poles to foliation in the upper sheet lie on a great circle and are interpreted to represent a later phase of regional-scale folding with an axis that plunges moderately to the northwest (Fig. 5a). Several macroscopic, open to isoclinal folds with moderately to steeply plunging, northwest-trending fold axes were observed, parasitic to the larger-scale fold; however, the data are inconclusive as to whether they form part of a regional synform, like that mapped by Tempelman-Kluit (1979, 2012), thus we did not include a synform in our cross-section. Quartz and plagioclase stretching lineations plunge moderately to steeply in the down-dip direction of the foliation plane, parallel to the fold axes (Fig. 5a). Lineations in the lower thrust sheet plunge shallowly to moderately toward the northwest or southeast (Fig. 5b).

Non-Eclogite-bearing Metasedimentary Units

In the southwestern part of the St. Cyr area, rocks with lithologic, metamorphic and detrital zircon signatures correlative with the Snowcap assemblage (Gilotti et al. 2013) are found in the hanging wall of a shear zone, structurally above eclogite-bearing quartzofeldspathic schist (PDsu and PDsg in Fig. 3). The rocks are divided into two lithostratigraphic units inferred to be separated by a northwest-striking thrust fault (Fig. 3). From west to east they include: (1) interlayered garnet–white mica schist, chlorite schist, quartz–white mica schist, with minor biotite schist, quartzite, calc-silicate and carbonate, and (2) garnet–white mica schist. The rocks are medium- to coarse-grained, variably deformed and exhibit amphibolite-facies metamorphism locally retrograded to greenschist-facies assemblages. The schistosity, defined by the planar alignment of micas, strikes northwest and dips moderately to steeply southwest (Fig. 5c). Quartz, mica and plagioclase stretching lineations are variable, plunging shallowly to the south and moderately to the northwest and southeast (Fig. 5c). Some garnet within the schist shows S-shaped spiral inclusion trails.

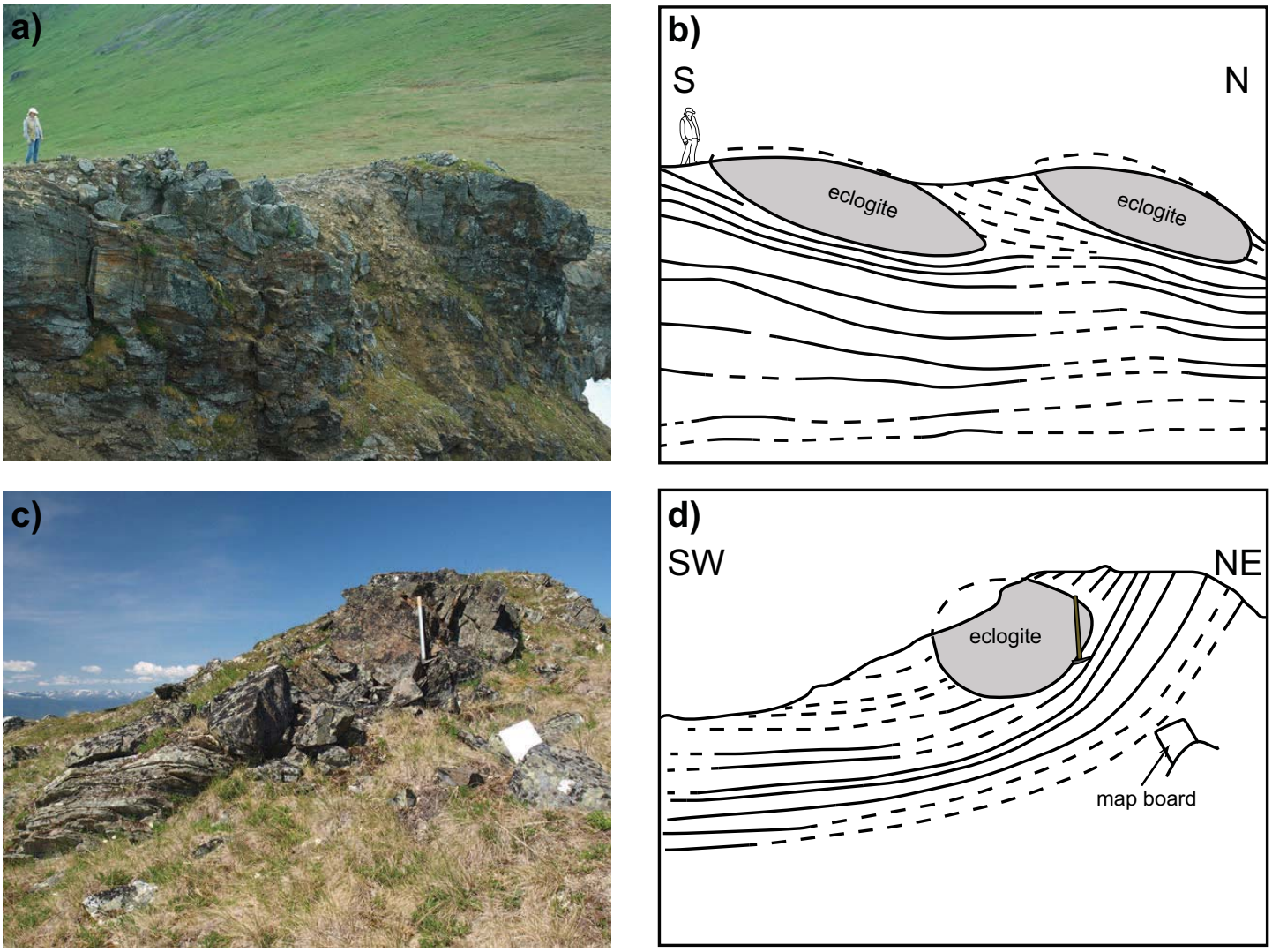

Figure 4. (a) and (c) Field photographs of eclogite boudins within the quartzofeldspathic host rocks. (a) Person for scale. (c) Hammer for scale is 80 cm long. (b) and (d) Line drawings showing the eclogite boudins and the trace of the foliation in the host rocks.

Shear Zone Between Eclogite-bearing Schist and Eclogite-free Schist

Eclogite-free metasedimentary rocks of Snowcap affinity lie structurally above a 400 m-thick shear zone separating this unit from underlying eclogite-bearing quartzofeldspathic schist (Figs. 2 and 3). The northwest-striking shear zone contains a mixture of metre-sized lenses of variably metamorphosed mafic, ultramafic, carbonate and undifferentiated quartzofeldspathic rocks in a matrix dominated by metapsammite. At least one lens of eclogite of indeterminate size was identified within the shear zone. The ultramafic rocks are pervasively serpentinized and mafic blocks are composed of greenschist-facies metagabbro. Quartzofeldspathic blocks contain garnet-bearing and garnet-free schist interpreted to be derived from sedimentary and felsic igneous protoliths, respectively. The metapsammitic matrix is composed of greenschist-facies phyllite and quartzite (Fig. 6). Outcrop-scale shear bands show a top-to-the-northeast thrust sense (Fig. 6a and b).

Foliation in the metapsammitic matrix is defined by the planar alignment of phyllosilicate minerals. Foliation strikes northwest or northeast and dips moderately to steeply to the southwest, northwest and northeast (Fig. 5d). Quartz, mica and plagioclase stretching lineations plunge down-dip or moderately to steeply northwest (Fig. 5d). These rocks are complexly folded on the centimetre to metre scale, with randomly oriented, but steeply plunging fold axes (Fig. 6c and d).

Low-Grade Mafic and Ultramafic Rocks

Mafic and ultramafic rocks form a structurally imbricated panel within the eclogite-bearing quartzofeldspathic unit (Pumg; Fig. 3). The ultramafic rocks form prominent orange peaks on high ridges throughout the field area (Fig. 7a). These fault-bounded bodies range in size from a few square metres to several hundred square metres and include both greenschist-facies gabbro to leucogabbro and intact, variably serpentinized ultramafic rocks composed of olivine + clinopyroxene. Powder X-ray diffraction analysis of serpentinite sample 11-39 on a D8 Advance Bruker instrument housed within the Department of Chemistry, University of Iowa, shows that lizardite is the main serpentine mineral, and as such indicates metamorphic temperatures < 300°C (Evans et al. 2013). Lizardite was also identified in the northwestern portion of the St. Cyr klippe, northwest of South Canol Road (Isard and Gilotti 2014). Within the centres of the panels, metamor-

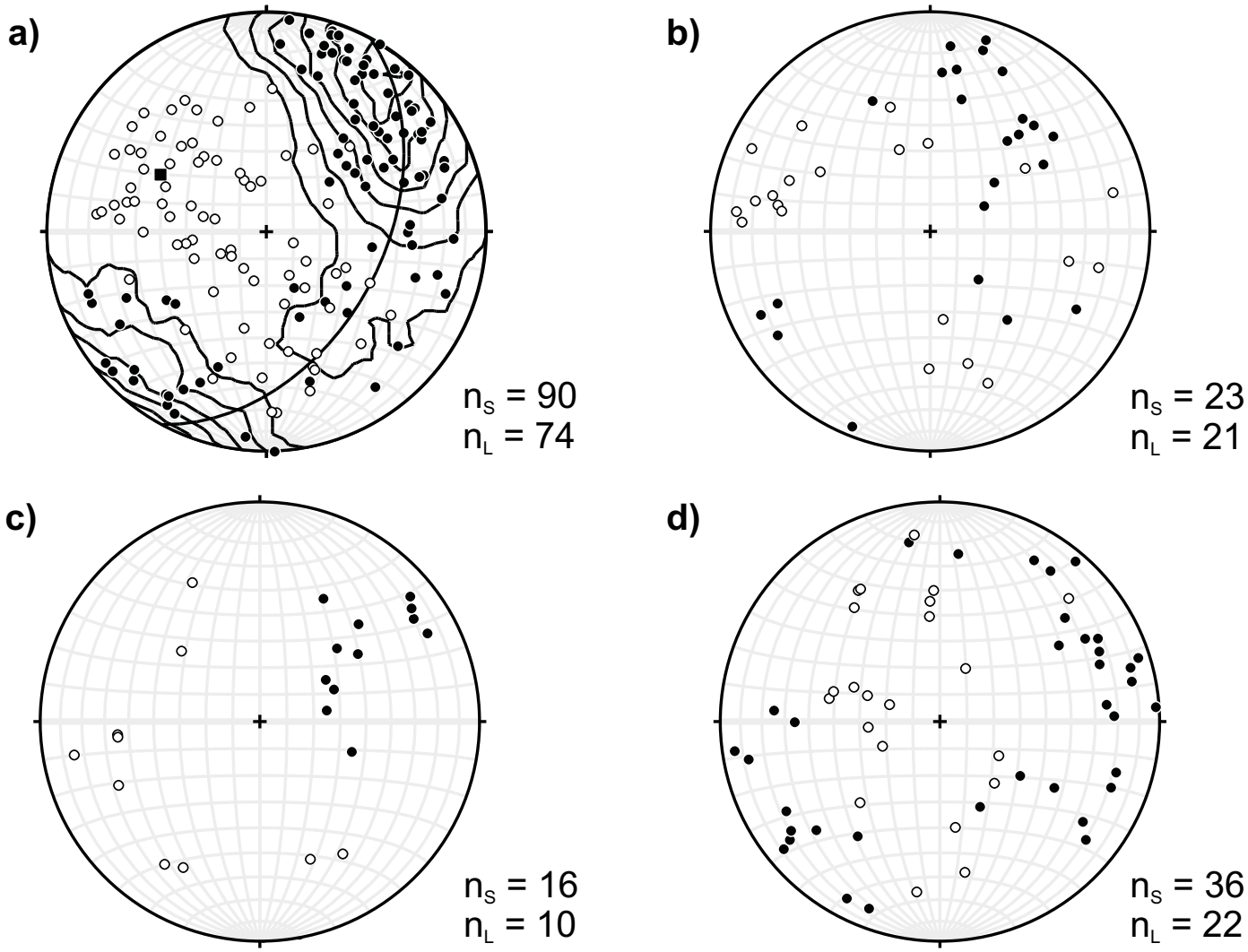

Figure 5. Lower hemisphere, equal area stereonet of poles to foliation (filled circles) and lineations (open circles) in the field area. (a) Upper thrust sheet of eclogite-bearing quartzofeldspathic schist. Poles to foliations plot along a great circle whose pole (black square) gives the regional fold axis at 298°/45°. (b) Lower thrust sheet of eclogite-bearing quartzofeldspathic schist. (c) Non-eclogite-bearing schist assigned to the Snowcap assemblage. (d) Shear zone between eclogite-bearing and non-eclogite-bearing schist.

phosed gabbro and leucogabbro is massive and exhibits igneous textures (Fig. 7b), with leucogabbro intruded into the surrounding gabbro and ultramafic rocks (Fig. 7c). Adjacent to the fault contacts, ultramafic rocks are moderately to strongly foliated, dipping steeply to the southwest; the degree of deformation increases with the degree of serpentinization and proximity to the faults. Although the mafic and ultramafic protoliths are inferred to be largely Paleozoic in age, this interpretation is complicated by the recovery of unexpected Mesozoic zircon from several units on both sides of the South Canol Road (Isard 2014; W.C. McClelland unpublished data).

Finlayson Assemblage and Nisutlin Batholith

The footwall of the St. Cyr klippe (Fig. 3) contains siliciclastic and minor carbonate rocks of the Finlayson assemblage, the oldest volcanic and volcaniclastic arc assemblage of the Yukon–Tanana terrane (Colpron et al. 2006a). The contact with the overlying eclogite-bearing schist is sharp, and both schist and clastic sedimentary rocks are brecciated. The siliciclastic rocks in the footwall consist of an interlayered package of phyllite, siltstone, shale, with minor psammite overlain by thickly-bedded psammite, quartzite, marble and minor siltstone. A detrital zircon population from marble in the footwall yielded a maximum depositional age of 368 Ma, supporting the interpretation that the footwall is part of the Finlayson assemblage of the Yukon–Tanana terrane (Isard 2014). The low-grade metasedimentary rocks in the footwall contain a pervasive, moderately southwest-dipping cleavage.

The Early to mid-Cretaceous Nisutlin Batholith cuts rocks of both the Finlayson assemblage and St. Cyr klippe (Tempelman-Kluit 1977; Colpron 2006). Intrusion of medium- to coarse-grained, biotite quartz monzonite produced a 100 m-thick contact aureole that metamorphosed the Finlayson sedimentary rocks to andalusite-bearing hornfels (Fallas et al. 1999). A small 1x1 km satellite pluton of the Nisutlin Batholith intruded quartzofeldspathic schist in the central-eastern portion of the field area, pinning movement on the basal thrust of the St. Cyr klippe as pre-Cretaceous in age.

Structural Interpretation

The Snowcap assemblage, the St. Cyr eclogite-bearing unit and the mafic–ultramafic rocks form a series of thrust slices, inter-

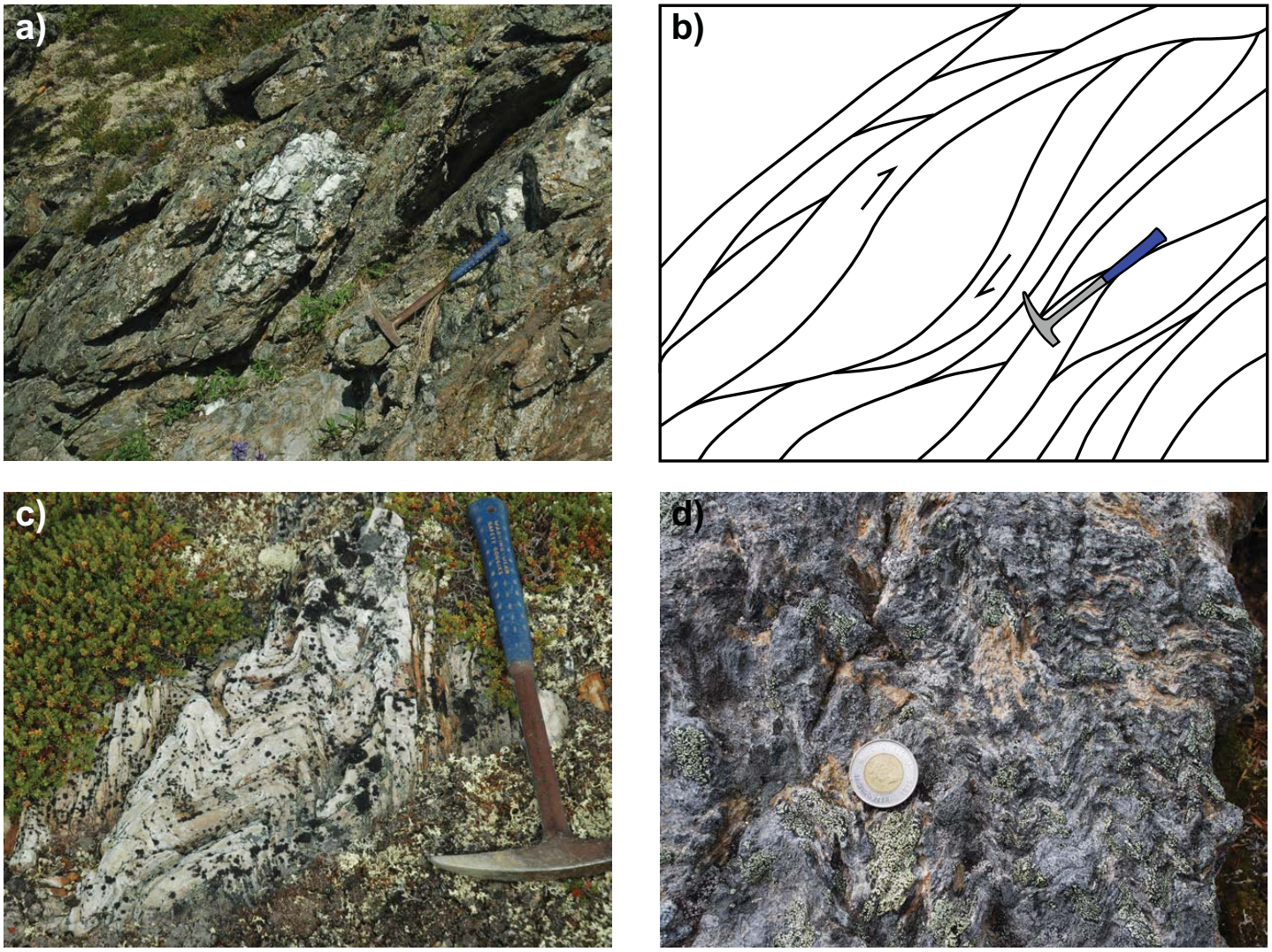

Figure 6. Field photographs of the metapsammitic matrix of the shear zone. (a) View of the southwest-dipping foliation from the northwestern portion of the field area. Hammer for scale is 42 cm long. (b) Line drawing of photo in (a) illustrating an anastomosing foliation and top-to-the-northeast direction of movement. (c) Folded quartzite; hammer is 42 cm long. (d) Crenulations within a micaceous quartzite. Coin for scale is 2.8 cm in diameter.

preted as an imbricate stack (see cross-section A–A' in Fig. 3). The ductile shear zone with top-to-the-northeast sense of shear clearly places slices of Snowcap assemblage over eclogite-bearing schist. However, the eclogite-bearing unit forms two distinct, southwest-dipping slices that are separated by a younger thrust carrying the mafic and ultramafic rocks, which potentially contain Mesozoic gabbro. The imbricate stack is overlain by a composite klippe of mafic, ultramafic and serpentinite lithologies and the uppermost Tower Peak unit – a low-grade metabasalt (Fig. 2; Isard 2014). Both the Tower Peak and mafic–ultramafic units exhibit brittle structures, including fault gouge and cataclasite, and are metamorphosed in the greenschist facies. Mesozoic zircon has also been recovered from the Tower Peak metabasalt (Isard 2014). We have chosen to map the two mafic–ultramafic units separately (Figs. 2 and 3; Pum and Pumg) based on their structural level, but we acknowledge that they could share the same protolith.

The imbricate slices and the uppermost klippe appear to have a common footwall dominated by phyllite (Fig. 2). Templeman-Kluit (1979, 2012) mapped the entire structure as the St. Cyr klippe, but this interpretation hinges on the nature of the southwestern contact between the upper slice of the Snowcap assemblage (PDSu; Fig. 2) and the phyllite. We did not observe an exposure of this key contact; therefore, we kept the relationship shown in the previous map that requires a sub-horizontal thrust beneath the imbricate slices. We cannot confirm that the entire structure is a klippe, but the alternative interpretation of Finlayson assemblage thrust over Snowcap assemblage would require a thrust within the current footwall (DMF) northwest of Tower Peak, which was also not observed (Fig. 2).

PETROLOGY OF ECLOGITE AND QUARTZOFELDSPATHIC HOST ROCKS

Eclogitic rocks from two localities near the South Canol Road were first described by Erdmer (1992); additional localities were noted by Fallas et al. (1998). Here, we document the pervasive nature of high-pressure metamorphism of both the mafic lenses and the quartzofeldspathic host rocks in the St. Cyr area. Omphacite, garnet, quartz and rutile comprise the representative high-pressure assemblage for mafic rocks, whereas the presence of phengite and garnet is the most com-

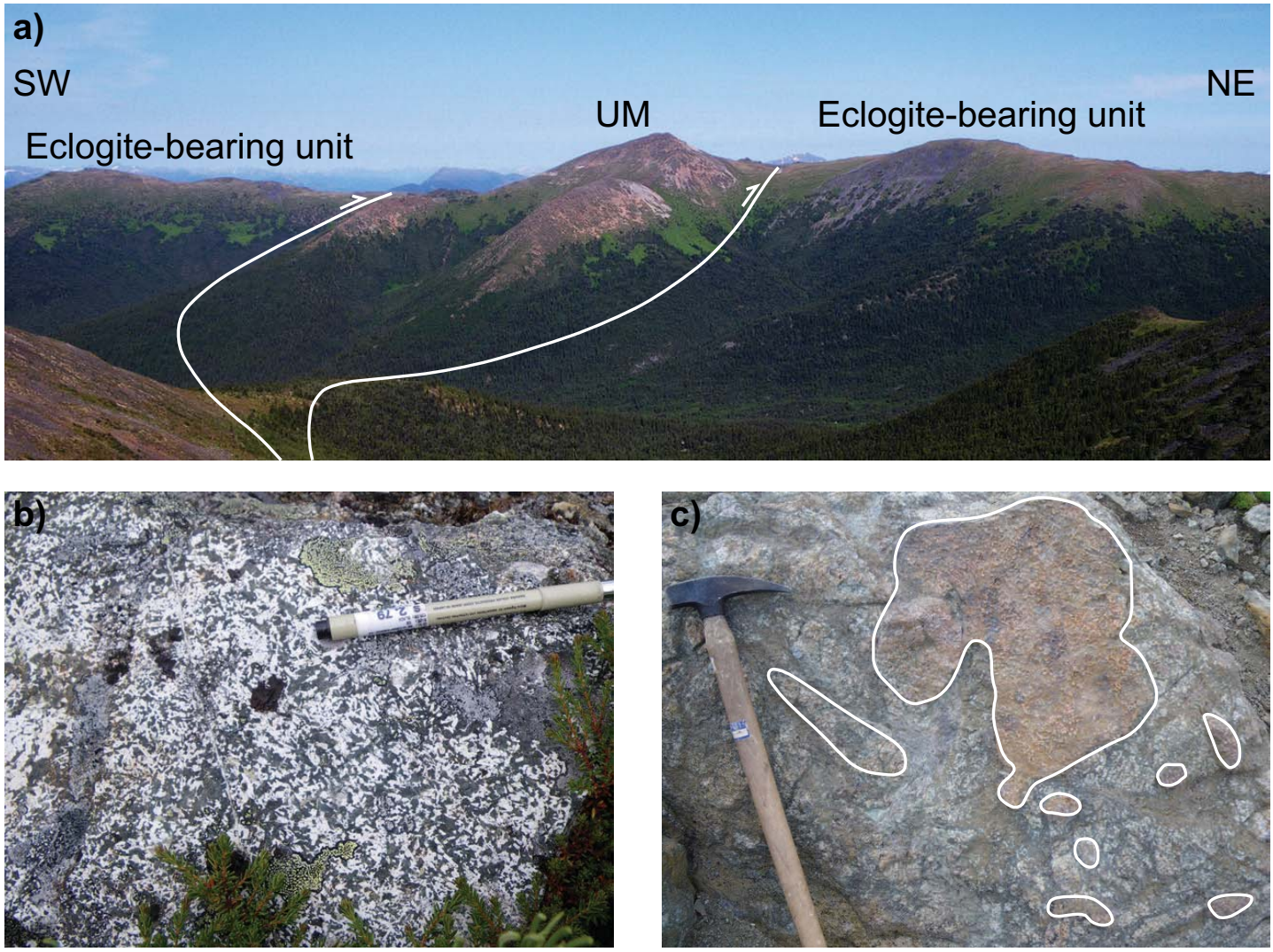

Figure 7. Field photographs of low-grade mafic and ultramafic rocks imbricated within the St. Cyr eclogite-bearing unit. (a) View of a large, orange-weathering ultramafic body (UM) in the central portion of the field area. This photo looks northwest at the cross-section line in Figure 3b. White lines mark thrust boundaries. (b) Outcrop of leucogabbro preserving intrusive igneous texture. Pen for scale is 13.5 cm long. (c) Outcrop of leucogabbro intrusion with ultramafic enclaves (outlined in white). Hammer for scale is 80 cm long.

pelling evidence of high-pressure metamorphism in quartzofeldspathic schist. Both assemblages display an amphibolite-facies to greenschist-facies overprint.

Eclogite and Retrogressed Eclogite

Well-preserved eclogite contains a peak mineral assemblage of omphacite + garnet + quartz + rutile ± phengite ± amphibole, with epidote, apatite and zircon as accessory phases (Fig. 8). Omphacite forms pale green, 200–800 μm equant grains or elongate porphyroblasts. Garnet is typically idioblastic and fine-grained, ≤ 300 mm in diameter. Where present as a peak phase, brownish-green amphibole constitutes subidioblastic, 300–900 μm grains in equilibrium with omphacite or idioblastic inclusions in garnet (Fig. 8b). Rutile is present in the matrix and included within garnet. Other inclusions observed in garnet are omphacite, quartz, titanite, plagioclase, diopside, augite, phengite, muscovite, epidote, ilmenite and calcite; these inclusions are generally confined to the garnet cores. Quartz occurs as either 100–300 μm long grains with undulose-extinction and subgrains, or < 100 μm polycrystalline aggregates with undulose- to flat-extinction and 120° triple-junctions.

Eclogite shows progressive retrogression from fresh eclogite to garnet amphibolite. In the transition zones between preserved eclogite and garnet amphibolite, omphacite-rich and amphibole-rich layers are commonly interleaved. In the least retrogressed samples, omphacite is replaced by fine-grained, lobate symplectites of diopside + plagioclase or amphibole + plagioclase (Fig. 8c and d). Phengite is commonly replaced by fine-grained, blocky symplectites of biotite and plagioclase. Other retrograde features include rutile rimmed by ilmenite, ilmenite surrounded by titanite and garnet rimmed by biotite. In moderately retrogressed samples, garnet is subhedral, with embayed edges converted to biotite, and inclusions of quartz, amphibole, rutile, clinopyroxene and phengite. In samples with ≥ 10 modal percent clinopyroxene, amphibole forms medium, light greenish-brown, subidioblastic to idioblastic grains, with long dimensions that help define the schistosity. In samples with trace amounts of clinopyroxene, the clinopyroxene is typically small (< 50 μm) and surrounded by extremely fine-grained amphibole + plagioclase symplectite. The symplectite

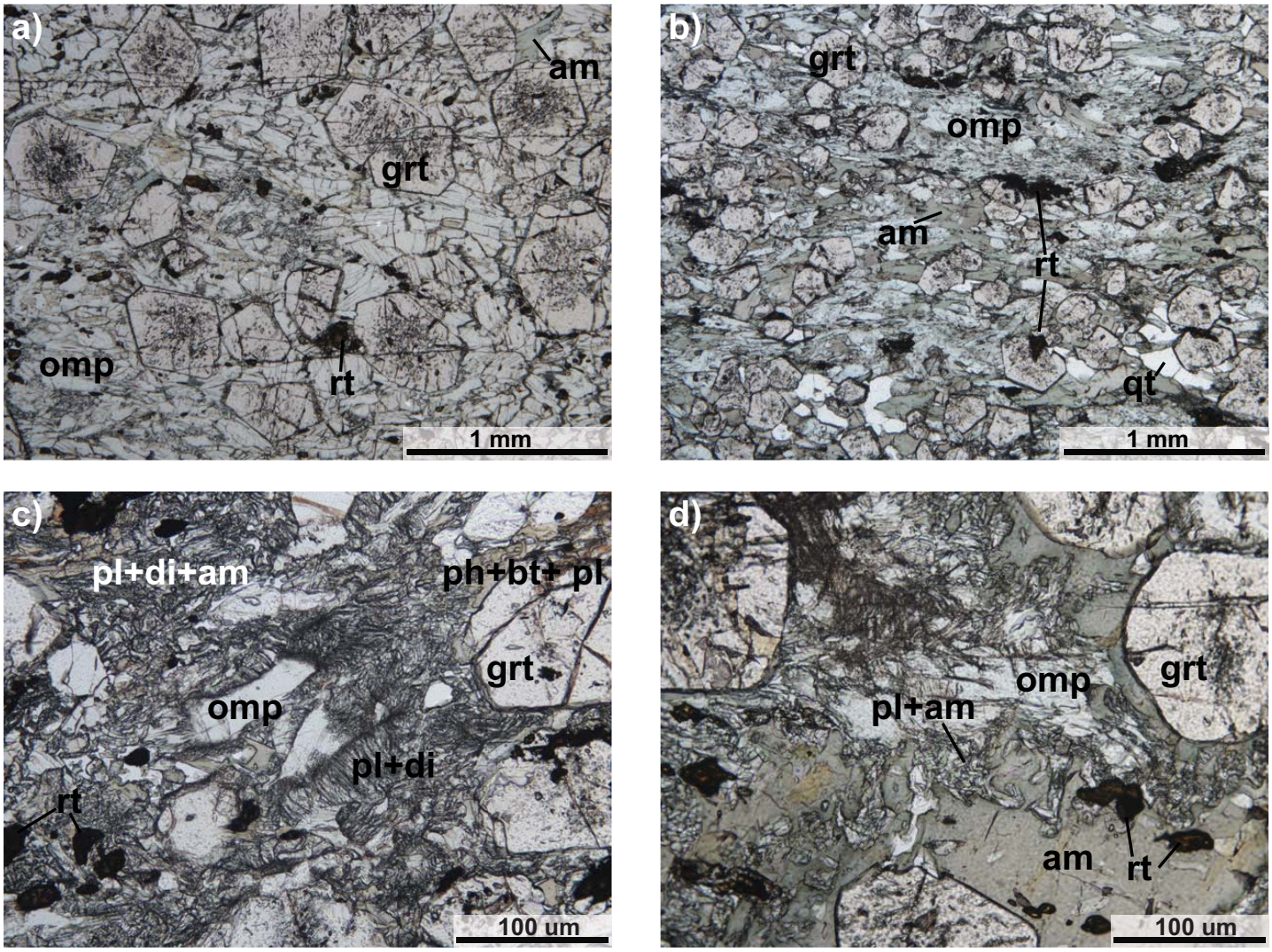

Figure 8. Photomicrographs of eclogite in the St. Cyr klippe. (a) Well-preserved eclogite sample 11-101 with a peak assemblage of omphacite, garnet and rutile. (b) Well-preserved eclogite sample 10-89 with a peak assemblage of omphacite, garnet, quartz, amphibole and rutile. (c) Retrogressed eclogite sample 12-10 showing omphacite altering to lobate symplectite of plagioclase + diopside, which is in turn replaced by amphibole. (d) Retrogressed eclogite sample 10-06 with omphacite partially converted to plagioclase + amphibole. Plane polarized light. am = amphibole, bt = biotite, di = diopside, grt = garnet, omp = omphacite, pl = plagioclase, qt = quartz, rt = rutile.

creates a cloudy appearance along the grain boundaries of larger amphibole grains. Completely retrogressed eclogite consists of amphibole + garnet + plagioclase ± quartz ± biotite ± ilmenite ± titanite. Retrograde amphibole is pale bluish-green, 200–800 μm, with a grain-shape-preferred orientation parallel to the foliation, and straight grain boundaries devoid of any symplectite. Quartz and amphibole are common inclusions in garnet.

Quartzofeldspathic Schist

Quartzofeldspathic schist is derived from both igneous and sedimentary protoliths. The mineral assemblage of metaigneous schist is quartz, garnet, phengite and plagioclase, with or without biotite, clinozoisite, or apatite (Fig. 9a and b). Rutile, apatite, ilmenite and K-feldspar are common accessory phases. Metasedimentary protoliths are distinguished from metaigneous rocks by a higher modal percent of quartz, garnet, micas and a lack of K-feldspar. In both lithologies, quartz exhibits undulose-extinction, subgrains and lobate grain boundaries – evidence for dynamic recrystallization over a range of temperatures (~300–500°C; e.g. Stipp et al. 2002). Coarse-grained biotite is pale reddish-brown to dark greenish-brown and is commonly altered to chlorite. Biotite is also a typical retrograde phase after phengite.

In metaigneous rocks (Fig. 9a and b), phengite grains are either 300–800 μm in length, isolated grains within the matrix, or occur as < 50 μm, idioblastic, randomly-oriented crystals replacing plagioclase. Garnet is present as subidioblastic porphyroblasts with embayed boundaries altered to chlorite. Titanite forms inclusions in garnet or overgrowths on ilmenite or rutile. Clinozoisite is 100–400 μm long and exhibits embayed grain boundaries. Epidote forms < 50 μm lobes replacing clinozoisite and plagioclase, which consists of 500–1000 μm grains with embayed boundaries and multiple phases of albite growth and deformation twins.

In metasedimentary rocks (Fig. 9c and d), 100–600 μm phengite is a common matrix phase. Garnet forms isolated, subidioblastic to rounded porphyroblasts or aggregates of small, ≤ 100 μm, grains within plagioclase and contains inclusions of quartz, phengite and biotite. In the most retrogressed

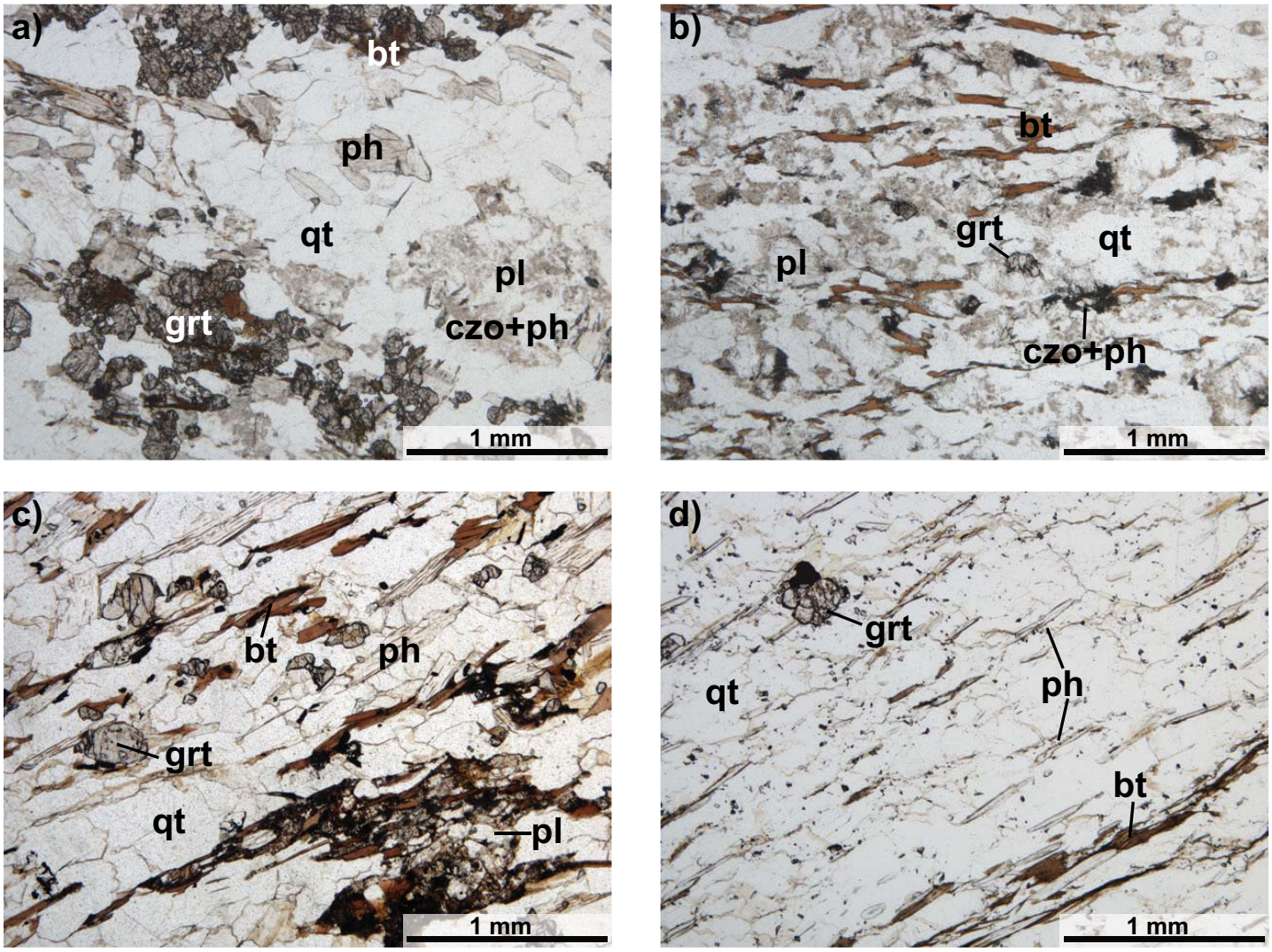

Figure 9. Photomicrographs of the quartzofeldspathic host rocks. (a) Garnet-bearing, phengite + biotite-bearing metatonalite sample 11-121. Plagioclase is replaced by fine-grained phengite and clinozoisite. (b) Foliated metatonalite sample 11-98. This sample has more biotite than sample 11-121 and phengite occurs within or adjacent to plagioclase. (c) Sample 11-93, garnet–mica schist with phengite. (d) Garnet–phengite quartzite sample 12-01. Plane-polarized light. bt = biotite, czo = clinozoisite, grt = garnet, ph = phengite, pl = plagioclase, qt = quartz.

samples, garnet is fractured and replaced by chlorite or biotite. In quartzite, the long axes of garnet grains lie in the schistosity defined by the grain-shape-preferred orientation of micas. Titanite forms medium, idioblastic grains within the matrix. Plagioclase is found as elliptical porphyroclasts with embayed or lobate grain boundaries. Quartz in plagioclase-rich samples is also preserved as porphyroclasts, surrounded by a finer grained quartz + mica matrix.

MINERAL CHEMISTRY

Mineral composition was determined for nine eclogite, three metatonalite and three metasedimentary rocks in order to characterize the high-pressure phases. UTM coordinates for the analyzed samples are shown in Table DR-1[1], and representative mineral compositions are given in Tables 1, 2, DR-2, DR-3, and DR-4. Mineral chemistry was determined using a CAMECA SX-100 electron microprobe at the University of California, Davis. Analytical conditions include 15 kV acceleration voltage, 5–20 nA beam current and a beam diameter of 1–10 mm. Major element concentrations are shown as weight % oxides (wt.%). Amphibole nomenclature is after Hawthorne et al. (2012), pyroxene nomenclature is after Morimoto (1989) and epidote nomenclature follows Armbruster et al. (2006). Mineral abbreviations are from Whitney and Evans (2010).

Clinopyroxene

Clinopyroxene composition is plotted in Figure 10 and representative analyses are given in Table 1. Clinopyroxene analyses were normalized to four cations per formula unit ($M2M1Si_2O_6$) and the Fe^{2+}/Fe^{3+} ratio was obtained from the charge balance. Cations were assigned to the M1 and M2 sites according to the procedure described in Morimoto (1989).

[1]Electronic supplementary materials (Tables DR-1 through -8), are available at the GAC's open source GC Data Repository, Andrew Hynes Series link, at http://www.gac.ca/wp/?page_id=306.

Table 1. Representative clinopyroxene composition in eclogite.

Sample	10-115	12-10	11-42	12-10	11-117	11-42	11-117	11-42
Mineral	Omp in matrix	Omp in matrix	Omp in matrix	Cpx within symplectite	Cpx within symplectite	Cpx adj to am+pl symplectite	Omp incl in garnet	Cpx incl in garnet
Analysis #	3/1	2/1	12/1	6/1	5/1	9/1	4/1	3/1
SiO_2	55.866	54.393	53.995	51.107	53.655	53.150	55.152	52.887
TiO_2	0.060	0.203	0.082	0.322	0.075	0.187	0.178	0.147
Al_2O_3	10.262	9.723	4.726	7.697	1.679	3.960	9.981	1.487
Cr_2O_3		0.045		0.033	0.009			
FeO	5.520	5.189	7.108	6.441	11.260	7.441	6.436	9.679
MnO	0.000	0.048	0.175	0.048	0.177	0.173	0.078	0.408
MgO	8.049	9.334	11.433	12.757	10.673	12.043	8.142	12.205
CaO	13.457	16.073	19.398	18.837	21.570	20.841	13.560	23.113
Na_2O	6.780	5.207	2.865	2.296	1.416	2.290	6.398	0.409
K_2O	0.000		0.005			0.017	0.001	0.100
Wt % total	99.994	100.215	99.787	99.538	100.514	100.102	99.926	100.435
Mineral formulas based on 6 oxygens								
Si	1.992	1.949	1.980	1.867	2.005	1.949	1.977	1.976
Ti	0.002	0.005	0.002	0.009	0.002	0.005	0.005	0.004
Al	0.431	0.411	0.204	0.331	0.074	0.171	0.422	0.065
Cr		0.001		0.001	0.000			
Fe^{3+}	0.050	0.041	0.036	0.080	0.014	0.084	0.059	0.009
Fe^{2+}	0.114	0.114	0.182	0.117	0.338	0.145	0.134	0.293
Mn	0.000	0.001	0.005	0.001	0.006	0.005	0.002	0.013
Mg	0.428	0.499	0.625	0.695	0.595	0.658	0.435	0.680
Ca	0.514	0.617	0.762	0.737	0.864	0.819	0.521	0.925
Na	0.469	0.362	0.204	0.163	0.103	0.163	0.445	0.030
K	0.000		0.000			0.001	0.000	0.005
End Member for Ca-Na Pyroxenes (Morimoto 1989)								
Quad	0.50	0.60	0.76	0.75	0.88	0.77	0.51	0.96
Jd	0.45	0.35	0.20	0.17	0.10	0.15	0.43	0.03
Ae	0.05	0.04	0.04	0.08	0.01	0.08	0.06	0.01
Quad Cpx for Ws-En-Fs plot								
Wo				0.45	0.48	0.48		0.49
En				0.43	0.33	0.39		0.36
Fs				0.12	0.19	0.13		0.16

am – amphibole, cpx – clinopyroxene, omp – omphacite, pl - plagioclase.

Omphacite (i.e. sodic clinopyroxene with a jadeite component between 20–80 mol %) was confirmed in all nine eclogite samples. In general, $Jd_{35–49}$ in grain cores decreases to $Jd_{20–30}$ at grain rims, which are adjacent to symplectites. Diopside is found within symplectites or at grain rims adjacent to amphibole–plagioclase symplectites with a jadeite content ranging from $Jd_{10–18}$. Idioblastic clinopyroxene inclusions in garnet are diopside ($Jd_{2–8}$) or omphacite ($Jd_{20–43}$).

Amphibole

Taramite, kataphorite and winchite [Si = 6.16–7.21 atoms per formula unit (apfu), Ca = 1.13–1.49 apfu, $^{[A]}$(Na+K) = 0.34–0.86 apfu] are found as matrix grains in equilibrium with omphacite (Fig. 11; Table DR-2). Symplectitic amphibole is more calcic than the matrix amphibole, and is pargasitic with Si = 6.30–7.19 apfu, Ca = 1.50–2.28 apfu, $^{[A]}$(Na+K) = 0.48–0.90 apfu. Both Na–Ca and Ca amphibole are included in garnet. These include taramite and katophorite [Si = 6.00–6.72 apfu, Ca = 1.50–1.31 apfu, $^{[A]}$(Na+K) = 0.53–0.88 apfu] as sodic phases, and sadanagite, pargasite and magnesiohornblende [Si = 5.87–6.89 apfu, Ca = 1.51–1.79 apfu, $^{[A]}$(Na+K) = 0.34–0.81 apfu] as calcic phases.

Garnet

Garnet in eclogite exhibits a rather narrow compositional range of almandine–pyrope–grossular–spessartine solid solution from $Alm_{50–61}Prp_{7–21}Grs_{17–34}Sps_{0.5–6.8}$ (Table DR-3). Garnet is typical of type C eclogite, which is defined by Coleman et al. (1965) as crustally derived, relatively low-temperature eclogite. Garnet displays both prograde and sector zoning (Fig. 12). Prograde compositional zoning exhibits a core to rim decrease in Mn and Ca. In some cases, Ca zonation is more complex, rising away from the core before decreasing at the rim. Sector zoning is developed in the intermediate domain between a distinct core and outer rim, and is thought to be due to either the heterogeneous distribution of Mg and Fe on the {110} faces

Table 2. Representative phengite composition.

Rock type	Eclogite			Metatonalite		Metasedimentary rock		
Sample	11-117	10-115	10-115	11-94	12-18	11-93	11-93	12-22
Mineral	Ph in matrix core	Ph in matrix rim	Ph incl in Grt	Ph in matrix	Ph repl Pl	Ph in matrix	Ph incl in Grt	Ph repl Pl
Analysis #	1/13	3/1	1/1	1/5	1/1	7/1	1/1	7/1
SiO_2	49.642	48.466	49.049	47.900	50.863	48.283	46.879	48.283
TiO_2	0.879	0.974	0.995	0.811	0.054	1.310	1.518	0.000
Al_2O_3	27.241	27.593	28.004	30.459	27.479	29.088	32.298	28.680
FeO	2.356	2.274	2.488	1.683	2.188	3.416	1.746	2.035
MnO	0.011	0.011	0.000	0.000	0.000	0.034	0.000	0.069
MgO	3.319	3.374	3.556	2.278	2.325	2.730	2.064	2.940
CaO	0.011	0.030	0.014	0.029	0.128	0.000	0.003	0.077
Na_2O	0.630	0.524	0.688	0.307	2.104	0.496	0.717	0.739
K_2O	10.289	9.945	9.853	10.506	8.482	9.892	9.826	9.721
BaO		0.876		0.630	0.617	0.610	0.856	0.683
Wt % total	94.378	94.067	94.647	94.603	94.240	95.859	95.907	93.227
Mineral formulas based on 11 oxygens								
Si	3.353	3.304	3.301	3.234	3.422	3.240	3.127	3.306
Ti	0.045	0.050	0.050	0.041	0.003	0.066	0.076	0.000
Al	2.168	2.217	2.221	2.423	2.179	2.300	2.538	2.314
Fe^{2+}	0.133	0.130	0.140	0.095	0.123	0.192	0.097	0.116
Mn	0.001	0.001	0.000	0.000	0.000	0.002	0.000	0.004
Mg	0.334	0.343	0.357	0.229	0.233	0.273	0.205	0.300
Ca	0.001	0.002	0.001	0.002	0.009	0.000	0.000	0.006
Na	0.082	0.069	0.090	0.040	0.274	0.065	0.093	0.098
K	0.886	0.865	0.846	0.905	0.728	0.847	0.836	0.849
Ba		0.023		0.017	0.016	0.016	0.022	0.018

grt – garnet, ph – phengite, pl - plagioclase.

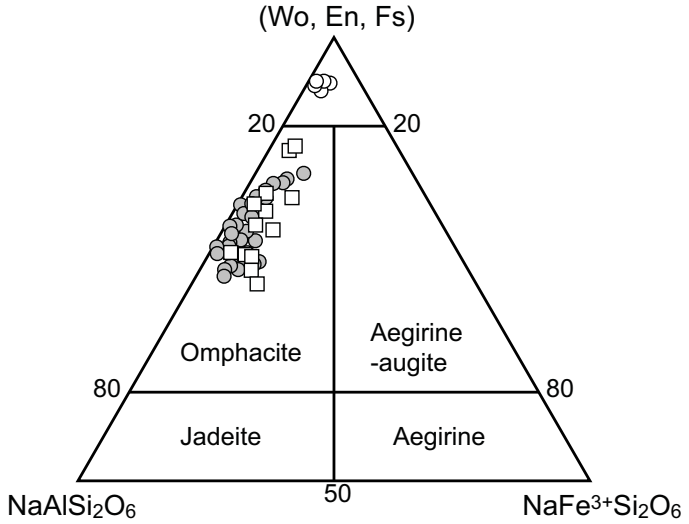

Figure 10. Ternary plots (after Morimoto 1989) of omphacite composition in the matrix (grey circles), included in garnet (open squares), and diopside in symplectite (open circles). Wo, En, Fs = wollastonite (Fe: $CaSiO_3$) + enstatite (En: $MgSiO_3$) + ferrosilite (Fs: $FeSiO_3$).

of garnet or a rapid increase in temperature (Shirahata and Hirajima 1995; Kleinschmidt et al. 2008). Sector zoning is most pronounced in the Mg component, where Mg decreases early in growth history, only to steeply increase at the rim. Mn shows less well-defined sector variation in some samples. The ~30 μm-wide rim of the grain is characterized by a slight increase in Mn, and decrease in Fe and Ca.

Garnet in quartzofeldspathic schist is much more compositionally complex than that in the eclogite (Table DR-3). Grains display highly variable zoning patterns in metasedimentary and metaigneous schist, and even between garnet grains in the same sample. This may reflect the original bulk rock composition or some of the garnet could be detrital. Zoning along rims and cracks indicates that garnet has been affected by element diffusion after peak metamorphism. In general, garnet in metatonalite is a solid solution in the range $Alm_{39–54}Prp_{1.2–25}Grs_{29–51}Sps_{2.7–7.1}$. Although pyrope content reaches 25 mol%, most contains less than 2 mol%. Metatonalite garnet displays two types of zoning: (1) homogeneous cores with <20 μm wide retrograde rims where Fe and Mn increase and Mg decreases, and (2) prograde zoning with a core to rim increase in Mg and decrease in Fe, Ca and Mn without a retrograde rim. Garnet composition in the metasedimentary rocks is $Alm_{54–69}Prp_{6–21}Grs_{10–29}Sps_{0.5–21}$. These garnet grains are irregularly zoned and tend to be more Mn-rich than garnet in metatonalite; they generally exhibit a core to rim decrease in Fe and Mg and increase in Mn and Ca. At the outermost rims (<20 μm from the edge) Fe and Mg show significant decreas-

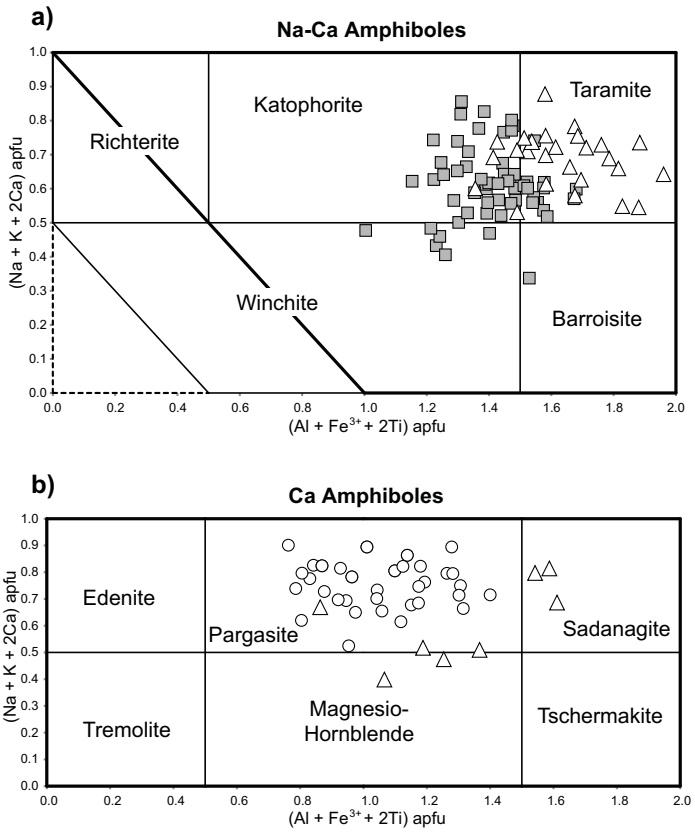

Figure 11. Amphibole composition; diagrams after Hawthorne et al. (2012). (a) Na–Ca amphibole in the matrix (grey squares) and included in garnet (open triangles). (b) Ca-amphibole in symplectites (open circles) and as garnet inclusions (open triangles).

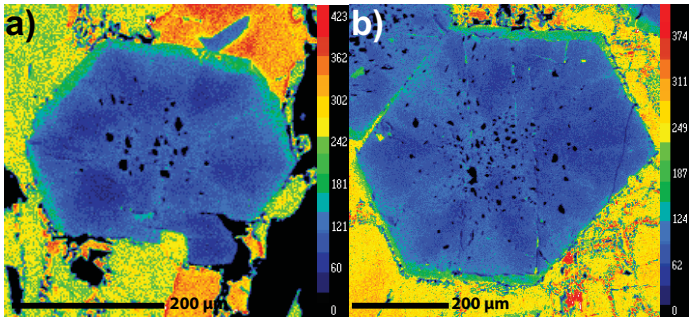

Figure 12. Mg X-ray maps in sector-zoned garnet from the St. Cyr klippe. Eclogite samples (a) 10-143 and (b) 10-06. Warm colors represent higher elemental concentrations.

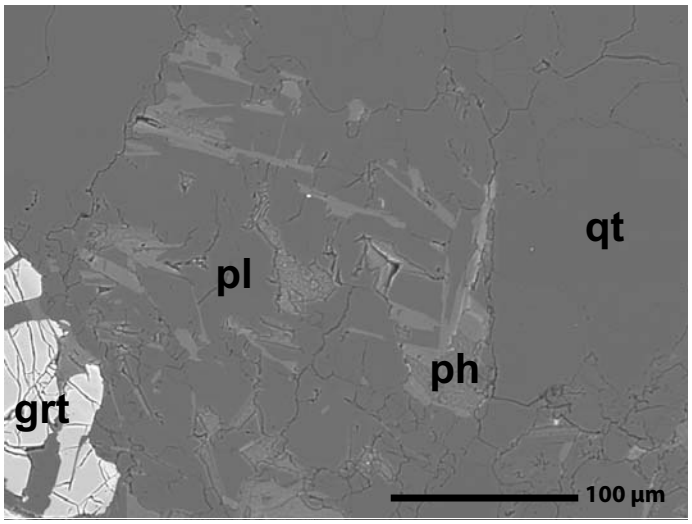

Figure 13. Backscattered electron SEM image of fine-grained phengite replacing plagioclase within metatonalite sample 12-18.

es in concentration. For example, Fe decreases as much as 39 mol% from the adjacent analysis in the core of the grain, whereas Ca and Mn substantially increase – 22 mol% in the case of Ca. Along cracks, Mg decreases, Ca and Mn increase and Fe remains unchanged.

Phengite

White mica is muscovite to phengite (Si apfu > 3.2) in chemical composition. Phengite was found in three eclogite samples as matrix grains and included in garnet. In the matrix, white mica composition ranges from 3.12 to 3.67 Si apfu (Table 2). Inclusions in garnet have Si contents as high as 3.32 apfu. Although most of the phengite is homogeneous, a few grains in each sample display a decrease in Mg, Ba and Si within 25–10 µm of the grain rim. Matrix phengite was identified in all six of the analyzed quartzofeldspathic host rocks, where it is irregularly zoned, with the highest values of Si generally concentrated in grain cores. With decreasing Si, Ba and Mg also decrease. In metatonalite, matrix white mica contains 3.07 to 3.45 Si apfu, and the fine grains of phengite that replace plagioclase contain up to 3.48 Si apfu (Fig. 13; Table 2). In metasedimentary rocks, Si concentrations are 3.04 to 3.34 apfu, which is lower than the Si content in metatonalite, possibly a reflection of different bulk composition. White mica inclusions in garnet in metasedimentary rocks are muscovite, with Si values between 2.99 and 3.13 apfu.

Other Phases

Representative compositions of biotite, plagioclase, K-feldspar and epidote are presented in Table DR-4. Biotite that has completely replaced phengite in the matrix of eclogite is relatively homogeneous (Si = 2.79–2.87 apfu, X_{Mg} [Mg/(Mg+Fe)] = 0.54–0.63, TiO_2 = 2.70–3.74 wt.%). Biotite in garnet has a similar X_{Mg} (0.53–0.68), but is richer in Si (2.97–3.07 apfu) and much lower in TiO_2 (0.14–0.16 wt.%) than matrix grains. Biotite in symplectites with plagioclase shows much wider compositional variations with respect to Si (2.66–3.27 apfu) and TiO_2 (0.86–3.69 wt.%), but displays a similar X_{Mg} (0.48–0.49). In metatonalite, biotite matrix and symplectite grains are homogeneous (Si = 2.75–2.80 apfu, X_{Mg} = 0.49–0.51, TiO_2 = 1.63–1.76 wt.%). Biotite in metasedimentary rocks has a range of Si (2.72–2.89 apfu) and X_{Mg} (0.48–0.52) similar to metatonalite biotite, but with a wider range in TiO_2 (1.20–2.31 wt.%). Plagioclase in eclogite is albite–oligoclase ($An_{2–22}$) in symplectites with clinopyroxene and where it is included in garnet. In symplectites with phengite, plagioclase is oligoclase ($An_{9–30}$). Plagioclase in metatonalite and metasedimentary rocks is also albite–oligoclase, ranging from $An_{2–26}$ and $An_{3–32}$, respectively. These ranges fall within the peristerite miscibility gap, and both albite and oligoclase occur as intergrowths in matrix grains within each sample. K-feldspar was identified in one sample as fine grains adjacent to plagioclase in the range $An_{0.5–3}$. Epidote is found in both eclogite and

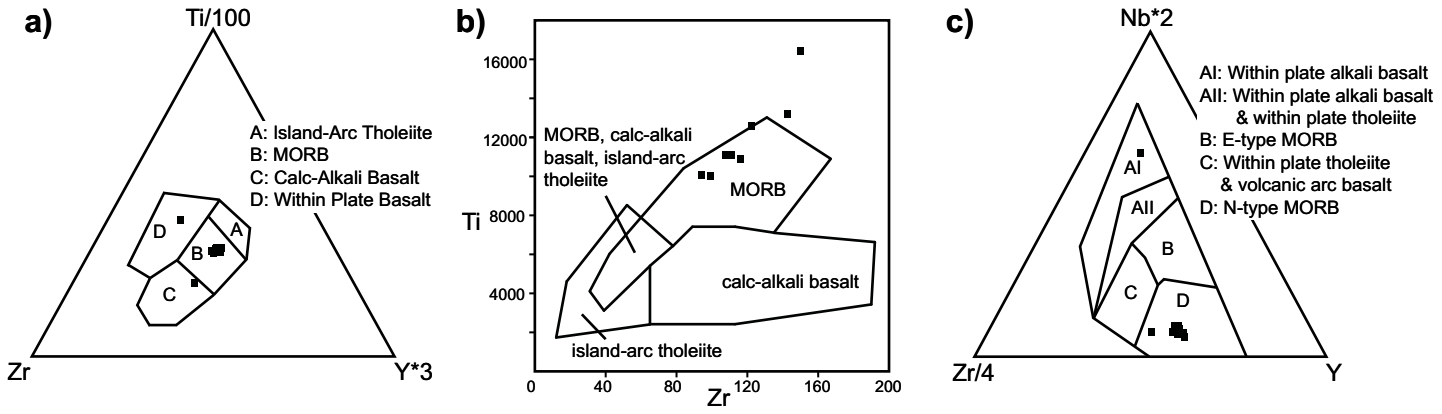

Figure 14. Trace element discrimination diagrams for eclogite to identify the protolith and its tectonic setting in the St. Cyr klippe. (a) and (b) trace element discrimination diagrams of Ti–Zr–Y and the Ti–Zr, respectively, from Pearce and Cann (1973). (c) Nb–Zr–Y plot from Meschede (1986). The protolith is primarily normal mid-oceanic ridge basalt (N-MORB).

metatonalite, and clinozoisite is present in metasedimentary rocks. In eclogite, the pistacite component [$Ca_2Al_2Fe^{3+}Si_3O_{12}(OH)$] in epidote in the matrix and included in garnet lies between 23–35 mol% and 10–34 mol%, respectively. In metatonalite, epidote after plagioclase has a pistacite component of 20–29 mol%. Clinozoisite from one metasedimentary sample is 0.04 to 5 mol% in pistacite content.

GEOCHEMISTRY

Whole rock major and trace element concentrations for ten eclogite samples were analyzed by X-ray fluorescence and inductively coupled plasma mass spectrometry, respectively, at the GeoAnalytical Laboratory of Washington State University, Pullman, WA, following conventional procedures (Johnson et al. 1999). Bulk composition (Table DR-5) reveals that the eclogite is basaltic in composition. SiO_2 content is 45.2–51.1 wt.%, with TiO_2 = 1.7–2.7 wt.% and Na_2O = 2.5–4.0 wt.%. Trace element discrimination diagrams (Fig. 14) show that most of the St. Cyr eclogite samples fall in the mid-ocean ridge basalt (MORB) field of the Ti–Zr–Y and the Ti–Zr plot (Pearce and Cann 1973) and the normal type MORB (N-MORB) field in the Nb–Zr–Y plot (Meschede 1986). The primitive mantle trace element-normalized plot (Fig. 15) shows that the eclogite compositions broadly correlate with N-MORB (Sun and McDonough 1989).

ZIRCON U–PB GEOCHRONOLOGY AND TRACE ELEMENT GEOCHEMISTRY OF METATONALITE

U–Pb dates of zircon from four metatonalite samples were obtained in an effort to determine the age of the protolith and high-pressure metamorphism. The four samples were chosen based on their close proximity to eclogite lenses. Cathodoluminescence (CL) images of zircon (Fig. 16) guided the choice of analytical spots. U–Pb data is presented in Tables DR-6, DR-8 and Figure 17, and trace element data is in Table DR-7 and Figure 18.

Analytical Methods

Zircon grains were separated from 1–3 kg samples by standard physical separation techniques and mounted in 2.54 cm epoxy rounds, which were polished to expose grain interiors. CL, transmitted light and reflected light images were used to characterize zircon domains, identify internal growth zones and

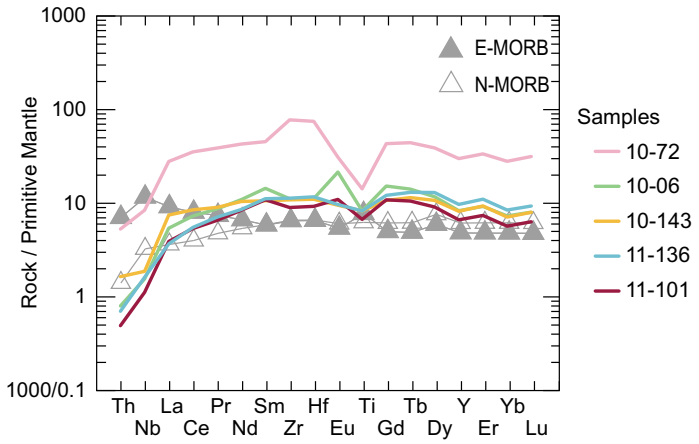

Figure 15. Primitive mantle-normalized plot based on Sun and McDonough (1989) for eclogite and retrogressed eclogite in the St. Cyr klippe. Normal mid-ocean ridge basalt (N-MORB) and enriched mid-ocean ridge basalt (E-MORB) are shown for reference (Sun and McDonough 1989).

select spot locations for analysis (Fig. 16).

U–Th–Pb isotopes and trace element data were measured on three samples (11-94, 11-114, and 12-17) using the sensitive high-resolution ion microprobe-reverse geometry (SHRIMP–RG) mass spectrometer at the U.S. Geological Survey – Stanford University ion probe facility, Stanford, California. Calibration of U was based on zircon standard Madagascar Green (MAD; 4196 ppm U; Barth and Wooden 2010). Isotopic ratios were calibrated by replicate analysis of zircon standard R33 (421 Ma, Black et al. 2004; Mattinson 2010), which was rerun after every fourth analysis. The analytical routine followed Barth and Wooden (2006, 2010). Uncertainties in the isotopic ratios are reported at the 1σ level. Ages are assigned based on the weighted mean of $^{206}Pb/^{238}U$ ages corrected for common Pb using the ^{207}Pb correction method (Williams 1998). Uncertainties in the weighted mean ages discussed below are reported at the 95% confidence level. The weighted mean ages are equivalent within uncertainty to concordia ages calculated in Squid 1.13 (Ludwig 2005). Age calculations and Tera-Wasserburg diagrams (Fig. 17) were generated with the Isoplot 3 program of Ludwig (2003).

Trace element data for Y, REE and Hf were collected simultaneously with the U, Th and Pb analyses. The following peaks were measured: ^{89}Y, ^{139}La, ^{140}Ce, ^{146}Nd, ^{147}Sm, ^{153}Eu,

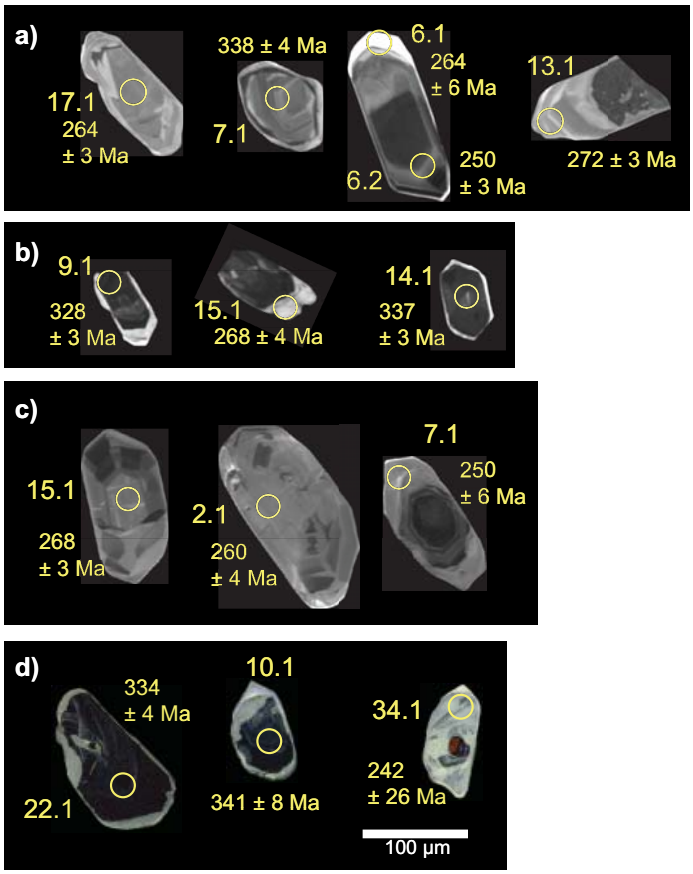

Figure 16. Representative cathodoluminescence (CL) images of zircon in (a) 11-94, (b) 11-114, and (c) 12-17. (d) Representative color CL images of zircon in 11-98. Ellipses indicate SHRIMP-RG U–Pb and trace element analysis spots labeled by grain and spot number.

$^{157}Gd^{16}O$, $^{163}Dy^{16}O$, $^{166}Er^{16}O$, $^{172}Yb^{16}O$, $^{90}Zr_2{}^{16}O$, $^{180}Hf^{16}O$, ^{206}Pb, $^{232}Th^{16}O$, $^{238}U^{16}O$. Data reduction of elemental concentrations used zircon standards CZ3 and MAD (Mazdab and Wooden 2006; Mazdab 2009). Chondrite-normalized REE plots (Fig. 18) use the chondrite REE abundances of Anders and Grevesse (1989) multiplied by a factor of 1.36 (Korotev 1996). Chondrite-normalized values for Pr were calculated by interpolation ($Pr_{(N)} = La_{(N)}{}^{0.33} \times Nd_{(N)}{}^{0.67}$). Eu and Ce anomalies are based on $Eu_{(N)}/Eu^*$ and $Ce_{(N)}/Ce^*$ with Eu* and Ce* calculated as geometric means (e.g. $Eu^* = (Sm_{(N)} \times Gd_{(N)})^{0.5}$).

The fourth metatonalite sample (11-98) was analyzed by laser ablation inductively coupled mass spectrometry (LA–ICP–MS) at the University of Arizona LaserChron Center using a spot size of 30 µm. Analytical procedures followed Gehrels et al. (2006, 2008). Common Pb corrections were made using ^{204}Hg-corrected ^{204}Pb measurements for each analysis, and initial Pb compositions of Stacey and Kramers (1975). U and Th concentrations and Pb/U fractionation were calibrated against the Arizona Laserchron Center Sri Lanka (SL) zircon standard (563.5 ± 3.2 Ma; ~518 ppm U and 68 ppm Th; Gehrels et al. 2008). Standards were analyzed at the beginning, end, and after every 5 grains for the primary standard (SL) and after every 15 grains for the secondary standard (R33).

Metatonalite Sample 11-94

Sample 11-94 was collected several metres away from an approximately two metre diameter eclogite boudin in the south-central part of the field area (Fig. 3). It is a medium-grained, moderately foliated metatonalite schist, with an estimated mode of 50% quartz, 30% plagioclase, 15% phengite and 5% biotite. Accessory phases include epidote, apatite, garnet and titanite. Plagioclase is replaced by very fine grains of phengite, epidote and K-feldspar. Isolated garnet is replaced by chlorite along rims and fractures. Phengite is partially replaced by biotite, which is in turn overprinted by chlorite.

Zircon in sample 11-94 is elongate, euhedral to subrounded, with complex cores and rims (Fig. 16). Some oscillatory zoned, subrounded cores are surrounded by CL-dark mantles and homogeneous CL-light grey rims (e.g. grain 7 in Fig. 16a). Other euhedral cores are zoned but appear patchy and are overgrown by thicker coarsely-zoned rims (Fig. 16a, grain 17). Grains with round, CL-dark, mottled cores display coarsely-zoned rims that are moderately luminescent in CL (Fig. 16a, grain 13). The analyzed cores and rims can be divided into three populations defined by variations in trace element composition. Eight core analyses, with ^{207}Pb-corrected $^{206}Pb/^{238}U$ ages ranging from 303 to 349 Ma, are characterized by steep HREE (Yb/Gd = 6–41), ΣREE = 308–2136, negative Eu and positive Ce anomalies (Eu/Eu* = 0.2–0.6 and Ce/Ce* = 2–35) and Th/U ratios of 0.1–0.3, all typical of igneous zircon (Hoskin and Schaltegger 2003). Two cores have elevated light REE (LREE; Fig. 18a) indicating probable modification of the original trace element signature. The remaining six cores give a weighted mean $^{206}Pb/^{238}U$ age of 331 ± 4 Ma (mean square weighted deviation, MSWD = 1.5), which we interpret as the igneous crystallization age. Eight core and rim analyses show a strong depletion of ΣREE (32–61), a pronounced flattening of the HREE pattern (Yb/Gd = 2–13), no negative Eu anomaly (Fig. 18a) and Th/U ratios ranging from 0.004 to 0.01. These are all characteristics consistent with the growth or recrystallization of zircon during high-pressure metamorphism in the presence of garnet (Rubatto 2002; Rubatto and Hermann 2007). The ^{207}Pb-corrected $^{206}Pb/^{238}U$ ages from zircon displaying a flat HREE pattern range from 249 to 284 Ma. Assuming the older two analyses reflect mixing with protolith zircon and the two younger ages reflect Pb-loss or continued recrystallization, the remaining grains with flat HREE patterns and low REE abundance give a weighted mean $^{206}Pb/^{238}U$ age of 268 ± 4 Ma (MSWD = 1.1). The final group includes five oscillatory zoned or patchy cores and three metamorphic rims that have elevated ΣREE (129–837) and steep HREE (Yb/Gd = 37–822) compared to grains with flat HREE signatures, but similarly low Th/U (0.002–0.003) values and no negative Eu anomaly (Fig. 18a). Metamorphic ^{207}Pb-corrected $^{206}Pb/^{238}U$ ages from zircon with steep HREE range from 259 to 271 Ma. Assuming the youngest analysis reflects Pb-loss, seven analyses from zircon with steep HREE give a weighted mean $^{206}Pb/^{238}U$ age of 266 ± 3 Ma (MSWD = 1.7). The age difference between metamorphic zircon with flat versus steep HREE patterns is not distinguishable. Pooling ages from both groups of metamorphic zircon gives a weighted mean $^{206}Pb/^{238}U$ age of 266 ± 3 Ma (MSWD = 1.4), which is interpreted as the best estimate for high-pressure metamorphism (Fig. 17a). Grains with flat HREE patterns are inferred to be slightly older than zircon with steep patterns based on textural evidence: the core of grain 6 has a flat HREE pattern whereas the rim displays a steep HREE pattern (Fig. 16a). The change in REE abundance

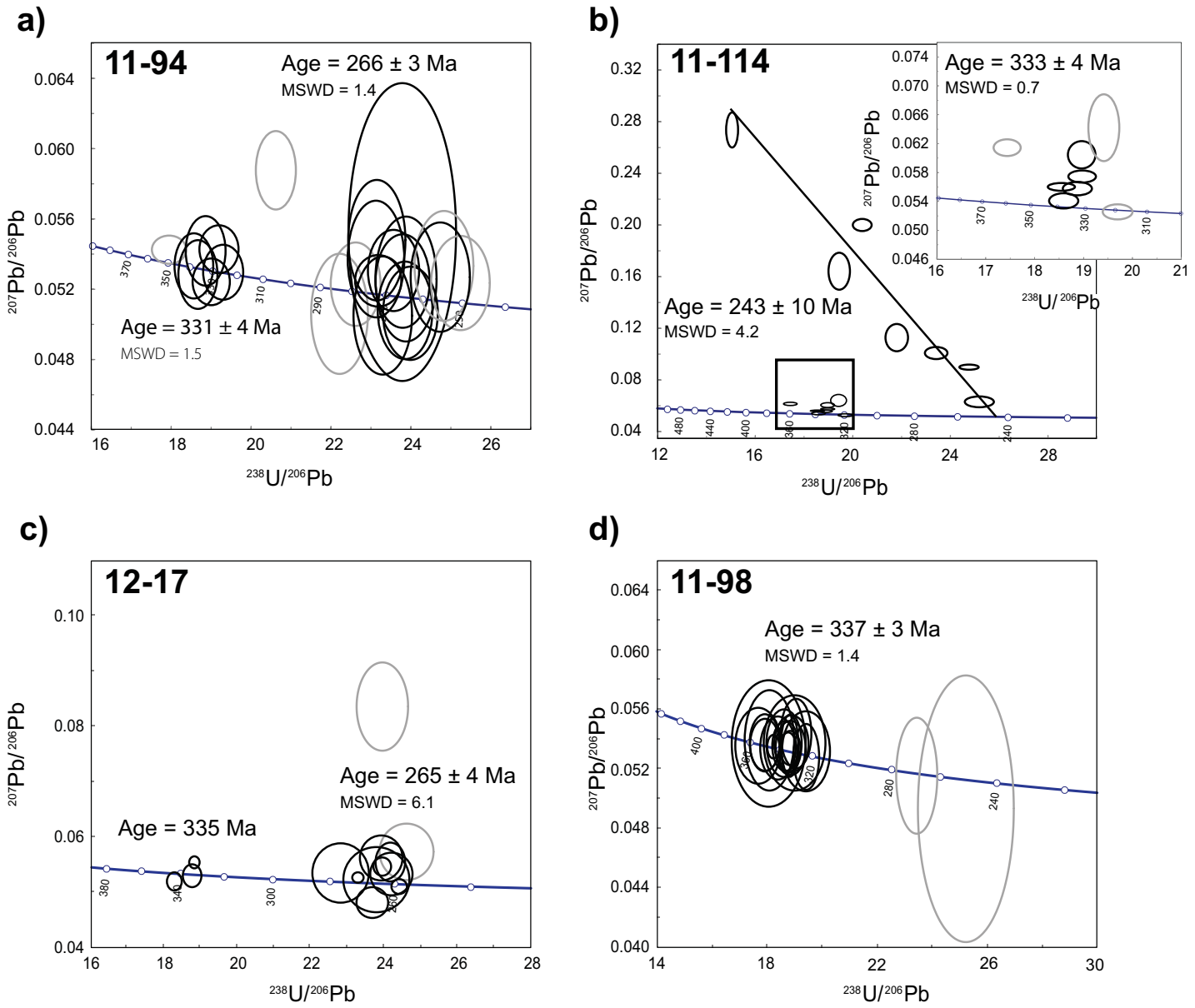

Figure 17. Terra–Wasserburg plots of SHRIMP-RG U–Pb data from metatonalite samples (a) 11-94, (b) 11-114, (c) 12-17 and (d) 11-98. Data are 1σ error ellipses uncorrected for common Pb. Black ellipses are used in calculating concordia ages. Errors are reported at the 95% confidence level. (a) Weighted mean ages were calculated for 11-94. (b) A concordia age was calculated for the crystallization age of sample 11-114 and an intercept age of 243 ± 10 Ma was calculated for the metamorphic age. (c) A weighted mean was calculated for the crystallization and high-pressure metamorphic ages of 12-17. (d) The igneous crystallization age is interpreted to be 337 ± 3 Ma.

and HREE pattern is interpreted to reflect the breakdown of garnet during continued high-pressure metamorphism, but additional analysis is required to confirm this hypothesis.

Metatonalite Sample 11-114

Sample 11-114 was collected adjacent to an eclogite boudin in the south-central part of the field area (Fig. 3). It is a fine- to medium-grained, metatonalite schist composed of approximately 50% quartz, 20% plagioclase and 30% white mica; titanite and apatite are accessory phases. Plagioclase is replaced by fine grains of white mica. Unlike sample 11-94, this sample lacks garnet altogether. Retrograde microstructures include white mica replaced by biotite, and biotite replaced by chlorite. A well-developed schistosity is defined by the planar alignment of phyllosilicate grains.

Zircon in sample 11-114 preserves CL-dark cores with faint oscillatory zoning overgrown by CL-bright rims (Fig. 16b). Seven cores with ^{207}Pb-corrected ^{206}Pb/^{238}U ages spanning 303–338 Ma have characteristic igneous trace element patterns, including steep HREE patterns (Yb/Gd = 7-17), ΣREE = 724–1170, Th/U = 0.1–0.4, a positive Ce anomaly (Ce/Ce* = 3–22) and a modestly developed negative Eu anomaly (Eu/Eu* = 0.3; Fig. 18b). Five of those cores give a ^{206}Pb/^{238}U concordia age of 333 ± 4 Ma (MSWD = 0.7; Fig. 17b), although two cores have elevated LREE patterns (Fig. 16b), indicating possible partial resetting of the protolith U–Pb systematics. The age of CL-dark cores is interpreted as the age of the protolith, which is within error of the 331 ± 4 Ma age of oscillatory zoned and patchy cores in sample 11-94.

Cl-bright rims give ^{207}Pb-corrected ^{206}Pb/^{238}U ages between

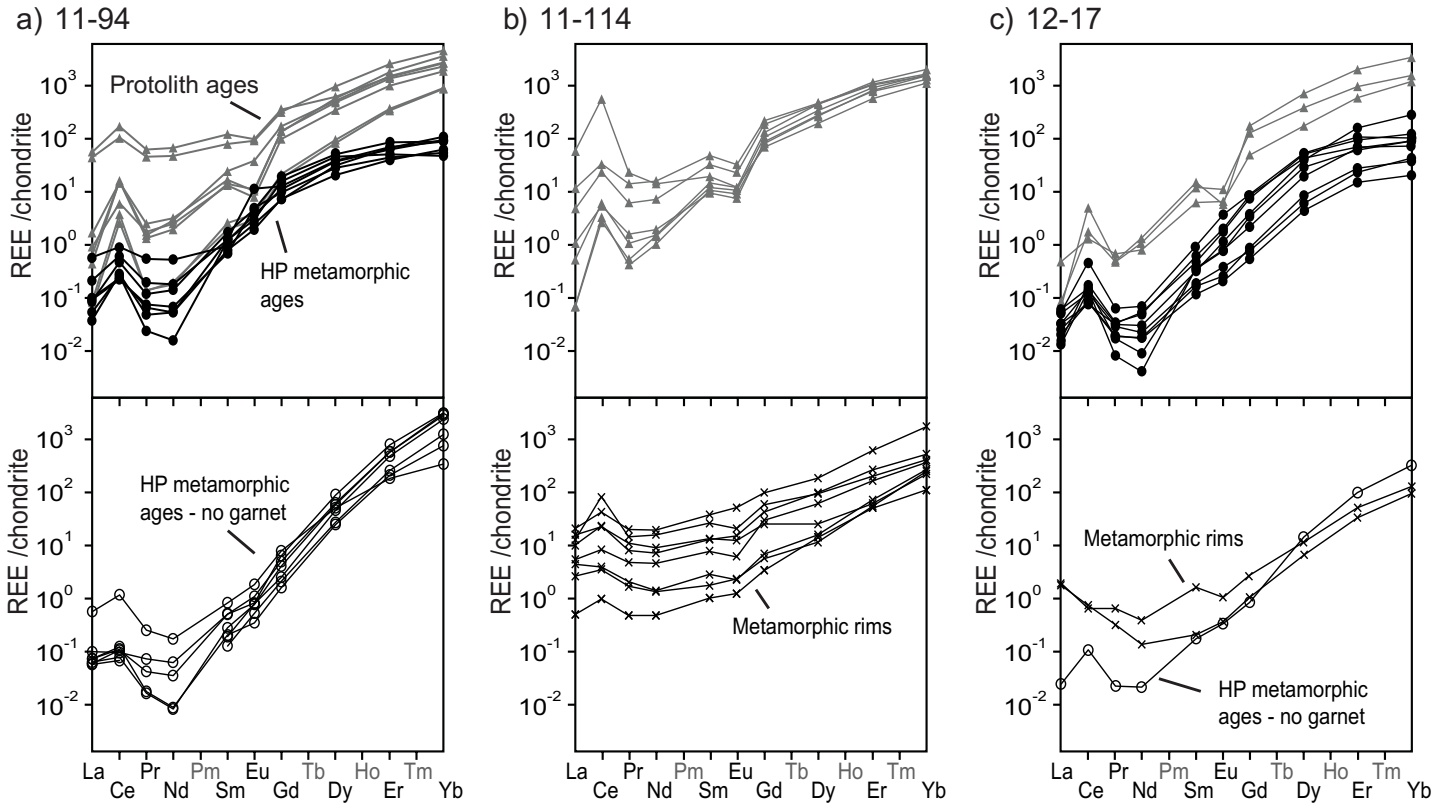

Figure 18. Chondrite-normalized REE patterns for different age populations of zircon grains from metatonalite samples (a) 11-94, (b) 11-114, and (c) 12-17. Normalization uses chondrite abundances from Anders and Grevesse (1989) multiplied by 1.36 (Korotev 1996). Ages are divided into igneous crystallization ages (light grey triangles) and metamorphic ages (open black circles – high-pressure with steep HREE patterns; filled black circles – high-pressure with flat HREE patterns; black crosses – metamorphic with high LREEs).

356–243 Ma, overlapping in part with the ages of the cores. The rims have variable trace element signatures with generally more elevated ΣREE (49–832), steeper HREE (Yd/Gd = 6–39) patterns and Th/U ratios ranging from igneous core values of 0.3 to 0.004 (Fig. 18b). In addition, the rims trend toward smaller or no negative Eu anomalies and depressed Ce anomalies (Fig. 18b). The steep HREE patterns for metamorphic zircon are interpreted to reflect the lack of garnet in the sample. Three-dimensional linear regression of the seven youngest rim ages with relatively high common Pb values defines a lower intercept of 243 ± 10 Ma (MSWD = 4.2). Assuming high-pressure metamorphism at 266 ± 3 Ma based on sample 11-94, the relatively high MSWD of 4.2 for regression of the rim analyses is interpreted to reflect dispersion in the analyses resulting from a complex history of post-high-pressure metamorphic overgrowths or disturbance of U–Pb systematics of the protolith zircon during exhumation.

Metatonalite Sample 12-17

Sample 12-17 was collected directly above a contact with metasedimentary schist in the central portion of the field area (Fig. 3). This fine-grained metatonalite schist contains about 60% plagioclase, 15% quartz, 10% epidote, 9% biotite and 6% white mica, with garnet, titanite and apatite as accessory phases. Plagioclase is replaced by small white mica grains and lobate symplectites of epidote. Retrograde features include white mica replaced by biotite, and biotite replaced by chlorite. A moderately developed schistosity is defined by the planar alignment of phyllosilicate grains.

Zircon in sample 12-17 is elongate and euhedral or subrounded, and preserves complexly zoned dark- to medium-grey cores surrounded by CL-bright rims (Fig. 16c). Zircon cores are dark, and oscillatory zoned or homogeneous (grain 7.1 in Fig. 16c), while others are mottled or patchy (Fig. 16c, grain 2.1). Still other cores are sector-zoned, a common zoning pattern preserved in zircon grown in the eclogite facies (Fig. 16c, grain 15.1; Corfu et al. 2003). Analysis of three oscillatory zoned cores give ^{207}Pb-corrected ^{206}Pb/^{238}U ages ranging from 332 to 343 Ma. Trace element patterns are characterized by steep HREE (Yb/Gd = 12–23), high ΣREE = 3141–10,278, negative Eu and positive Ce anomalies (Eu/Eu* = 0.1–0.3 and Ce/Ce* = 2–33) and Th/U ratios typical of igneous zircon ranging from 0.2–0.4. The three cores give a weighted mean ^{206}Pb/^{238}U age of 335 ± 14 Ma (MSWD = 6.9). The U–Pb ages and systematics, as well as the trace element signature defined by the three core analyses, are consistent with the protolith ages and signatures determined for the other samples. Accordingly, a protolith age of ca. 335 Ma is inferred for metatonalite sample 12-17.

Ten mottled, patchy, or sector-zoned cores give ^{207}Pb-corrected ^{206}Pb/^{238}U ages ranging from 255 to 276 Ma. These cores display depleted ΣREE values (94–697), Th/U values in the range of 0.001–0.02 and lack a negative Eu anomaly (Eu/Eu* = 0.001–0.02) as is typical of high-pressure metamorphic zircon. The middle (M)REE patterns are relatively steep, but most analyses show flattening of the HREE patterns (Yb/Gd = 8–454; Fig. 18c). The ten zircon cores give a weighted mean ^{206}Pb/^{238}U age of 265 ± 4 Ma (MSWD = 6.1).

The large spread in ages and high MSWD indicate the calculated age incorporates multiple unresolved components. Two CL-bright rims (grain 7.1 in Fig. 16c) gave the youngest ages and record low Th/U (0.01–0.004), depleted ΣREE values (185–277), steep HREE patterns (Yb/Gd = 49–96) and minor negative Eu anomalies (0.5–0.8). The relatively high common Pb and elevated LREE patterns (Fig. 18c) suggest these analyses may be affected by alteration and the ages were therefore excluded from calculation of the weighted mean $^{206}Pb/^{238}U$ age. Exclusion of additional analyses to reduce the observed MSWD of 6.1 is possible. For example, exclusion of analyses 9.1 and 14.1 based on the interpretation that the slightly older ages reflect mixed protolith and metamorphic domains yields a revised age of 262 ± 2 Ma with a more reasonable MSWD = 1.4. There is, however, no evidence from the CL images or trace element chemistry that justify this exclusion. Alternatively, younger analyses may be excluded assuming they represent post-high-pressure metamorphism or Pb-loss in order to bring the MSWD to acceptable levels. In the absence of clear textural or chemical evidence for defining subgroups of data, the age of 264 ± 5 Ma, which is consistent with the age of high-pressure metamorphism determined for sample 11-94, is viewed as the best estimate for eclogite-facies metamorphism for this sample. The range in ages and consequent high MSWD are attributed to unresolved complexities in the zircon systematics.

Metatonalite Sample 11-98

Sample 11-98 is a fine-grained metatonalite schist collected several metres away from a large eclogite boudin in the south-central part of the field area (Fig. 3). The sample is composed of ~ 40% quartz, 35% plagioclase, 10% biotite, 10% epidote and 5% white mica; garnet, ilmenite titanite and apatite are accessory phases. Plagioclase is replaced by fine grains of white mica and epidote. White mica is replaced by biotite, biotite is replaced by chlorite, and a well-developed schistosity is defined by the planar alignment of phyllosilicate grains.

Zircon in 11-98 is elongate and euhedral, and preserves dark- to medium-grey, oscillatory zoned cores surrounded by CL-bright rims (Fig. 16d). The majority of analyses give $^{206}Pb/^{238}U$ ages ranging from 323 to 365 Ma with two analyses yielding younger ages of 251 and 269 Ma (Fig. 17d). The young ages are interpreted to record Pb-loss, growth or recrystallization associated with metamorphism as observed in samples 11-94, 11-114 and 12-17. The 25 older zircon grains give a weighted mean $^{206}Pb/^{238}U$ age of 337 ± 3 Ma (MSWD = 1.4), which is similar to the igneous crystallization ages of the other three samples and interpreted as the protolith age for this sample.

DISCUSSION

The St. Cyr klippe is a complex collection of thrust slices that records contrasting geologic histories. The imbricate stack includes a slice of greenschist-facies oceanic-like crust and serpentinized mantle, and thrust sheets of different units of the Yukon–Tanana terrane. Two imbricate panels of amphibolite-facies quartzofeldspathic schist form part of the Snowcap assemblage, which constitutes the basal substrate to the arc assemblages (e.g. Colpron et al. 2006a). Snowcap assemblage rocks are thrust on top of at least two slices of eclogite-bearing quartzofeldspathic schist that are dominated by Yukon–Tanana arc material. Igneous crystallization ages for metatonalite samples (337 to 331 Ma) fall within the Little Salmon Cycle (as defined by Piercey et al. 2006) of the Klinkit phase of Yukon–Tanana arc activity (342 to 314 Ma; Nelson et al. 2006 and references therein). Felsic metaigneous and metavolcanic rocks of similar age are found in the Yukon–Tanana terrane in the Fortymile River assemblage in eastern Alaska, the Tatlmain Plutonic Suite and Little Salmon Formation in the Glenlyon area of central Yukon, and the Ram Creek and Big Salmon complexes in the Wolf Lake–Jennings River area of southern Yukon–northern British Columbia (Nelson and Friedman 2004; Colpron et al. 2006b; Dusel-Bacon et al. 2006; Roots et al. 2006).

Whole-rock composition of eclogite indicates that its protolith was N-MORB-like tholeiitic basalt. Primitive basalt is found throughout the Yukon-Tanana arc, from initial arc formation in the Mid- to Late Devonian through the Late Permian (Colpron et al. 2006a; Nelson et al. 2006). In addition, the penetrative fabrics shared by eclogite and the host rocks and widespread high-pressure metamorphism contrast with the low-grade, weakly deformed oceanic pelagic sedimentary rocks that are common to the Slide Mountain terrane (Wheeler et al. 1991; Colpron et al. 2006a; Piercey et al. 2012). Therefore, we conclude that the eclogite is derived from the Yukon–Tanana terrane, rather than the Slide Mountain terrane.

The eclogite-bearing quartzofeldspathic rocks at St. Cyr record evidence of high-pressure metamorphism consistent with that of other Permian high-pressure rocks in the Yukon–Tanana terrane (e.g. Erdmer et al. 1998). Trace element signatures of metamorphic zircon in metatonalite samples 11-94 and 12-17 indicate their formation under garnet-present, plagioclase-absent pressure–temperature conditions, consistent with eclogite-facies paragenesis. These zircon grains record a high-pressure metamorphic age of 266 ± 3 to 265 ± 4 Ma, which agrees with the SIMS ages (271–267 Ma) determined for eclogite (Petrie 2014) and the U–Pb TIMS zircon age of 266 ± 0.6 Ma derived from eclogite (Fallas et al. 1998). These dates are also within error of a U–Pb zircon age interpreted to record the high-pressure metamorphism of eclogite at Last Peak (269 ± 2 Ma; Creaser et al. 1997), and corroborate other Permian eclogite-facies assemblages attributed to the Yukon–Tanana terrane.

The St. Cyr klippe is significant in that it represents a glimpse into Late Permian high-pressure metamorphism in the Yukon–Tanana terrane. Taken as a whole, the Yukon–Tanana terrane is a complex polymetamorphic terrane, recording multiple ages and pressure–temperature ranges of peak metamorphism. For example, in the Stewart River area, titanite and monazite ages suggest that Yukon-Tanana arc and Snowcap assemblage rocks were metamorphosed during deformation at relatively low-pressure conditions between 365 and 350 Ma and at medium-pressure conditions at ~ 265 Ma (Berman et al. 2007). These rocks were further overprinted by regional Cretaceous plutonism and Jurassic–Cretaceous metamorphism during deformation and exhumation (Berman et al. 2007; Staples et al. 2013). In the St. Cyr area, the majority of $^{40}Ar/^{39}Ar$ muscovite cooling ages (Fallas et al. 1998) fall between 263 Ma and 235 Ma, further demonstrating that high-pressure rocks in the St. Cyr klippe escaped the regionally pervasive Jurassic and Cretaceous metamorphic overprint recorded in other

Yukon–Tanana terrane rocks.

Eclogite in the St. Cyr klippe is remarkably well preserved, and comparison of the petrological and chemical signatures to the three other eclogite localities suggests a genetic link. In the St. Cyr klippe, omphacite ($Jd_{20–49}$) and phengite (up to 3.67 Si apfu) compositions overlap with those of eclogite in Ross River, Faro and Last Peak (Erdmer 1987; Erdmer et al. 1998; Perchuk et al. 1999; Perchuk and Gerya 2005; Ghent and Erdmer 2011). Phengite in the host quartzofeldspathic schist contains values of Si between 3.20 and 3.48, which is slightly higher than the Si content of phengite in garnet–mica schist at Last Peak (3.20 to 3.38 Si apfu; Hansen 1992). Eclogite at Ross River is hosted by quartzofeldspathic garnet–mica- and glaucophane-bearing schist (Erdmer 1987; Erdmer and Armstrong 1989; Ghent and Erdmer 2011), at Faro by glaucophane-bearing and garnet–mica schist that contains phengite (Perchuk et al. 1999; Perchuk and Gerya 2005), and at Last Peak, by hornblende, biotite, and phengite-bearing schist (Erdmer and Helmstaedt 1983; Erdmer et al. 1998). These rocks bear a resemblance to the host rocks in the St. Cyr klippe, although the amphibole is less sodic at St. Cyr. At each of the three other localities, the peak eclogite-facies assemblage is omphacite + garnet + quartz, which is the dominant peak assemblage at St. Cyr (Creaser et al. 1997; Erdmer et al. 1998). Phengite is confirmed in eclogite from Ross River and Faro (Erdmer 1987; Perchuk et al. 1999). Like eclogite at St. Cyr, during the transition from eclogite to garnet amphibolite, omphacite was replaced primarily by calcic amphibole, such as pargasite, and albitic plagioclase (Erdmer and Helmstaedt 1983; Erdmer 1987; Creaser et al. 1997; Perchuk et al. 1999). Geochemically, the MORB signature recorded in the major and trace element geochemistry of St. Cyr eclogite is consistent with the geochemical signatures of eclogite at all three localities (Erdmer and Helmstaedt 1983; Creaser et al. 1999; Pigage 2004; Ghent and Erdmer 2011). Thus, the Permian eclogites in the Yukon–Tanana terrane are not isolated occurrences, but form part of a regional high-pressure lithotectonic assemblage.

When eclogite was first identified in the St. Cyr area, the high-pressure mafic rocks were assumed to have formed at depth and returned to the surface within a tectonic mélange (e.g. Erdmer 1987). The results of our investigation show that the basaltic protolith of the eclogite existed within the quartzofeldspathic host rocks of the Yukon–Tanana terrane prior to subduction, and experienced the same metamorphic history. Thus, the high-pressure assemblage in the St. Cyr klippe represents slices of coherent continental arc crust subducted to high-pressure conditions in Permian time. The idea of emplacement of exotic slivers versus metamorphism *in situ* of high-pressure rocks was something of a controversy in high-pressure and ultrahigh-pressure (UHP) terranes, such as the Western Gneiss Region in Norway and the Dabie-Sulu UHP terrane in China (e.g. Smith 1984; Wang and Liou 1991). The argument was largely due to the rare preservation of the pre- versus post-metamorphic field relationships between eclogite and the host rocks, as well as retrograde overprinting of the host rocks that erased the evidence of UHP metamorphism (Andersen et al. 1991; Zhang et al. 1995). Numerous studies on the eclogite-bearing host rocks in these localities have shown that those rocks have in fact been subjected to coeval high-pressure and UHP metamorphism (Wang and Liou 1991; Zhang et al. 1995; Wain 1997; Carswell et al. 2003; Liu et al. 2005; Butler et al. 2013), and hence they represent coherent slices of continental crust. Eclogite in the St. Cyr klippe also formed *in situ* with the enveloping high-pressure, Yukon–Tanana derived schist, and thus constitutes coherent slices of Yukon–Tanana terrane arc-derived rocks.

CONCLUSIONS

The St. Cyr klippe consists of variably metamorphosed and deformed, structurally imbricated units of Yukon–Tanana continental arc crust and ultramafic–mafic rocks of possible oceanic affinity. However, the absence of any other rocks typical of the Slide Mountain terrane argues that these rocks did not form part of this oceanic assemblage. Quartzofeldspathic schist derived from the Yukon–Tanana terrane host sub-metre to hundreds of metres scale lenses of well-preserved eclogite and retrogressed eclogite. The presence of phengite and high-pressure zircon in quartzofeldspathic schist shows that eclogite was metamorphosed *in situ* with its host rock during the Late Permian. This confirms that the eclogite-bearing unit consists of slices of coherent arc crust, and that the eclogite is not part of a tectonic mélange. The petrological, geochemical, geochronological, and structural relationships between eclogite and the host rocks in the St. Cyr klippe are shared with similar high-pressure assemblages found in the Yukon–Tanana terrane at Faro, Ross River and Last Peak. These mutual relationships suggest that Permian high-pressure assemblages form part of a larger high-pressure lithotectonic assemblage within the Yukon–Tanana terrane.

ACKNOWLEDGEMENTS

This work is based primarily on fieldwork performed by Petrie during the 2010, 2011 and 2012 field seasons as part of a PhD dissertation. We would like to thank Jacob Stewart and Dylan Cook for their exemplary work as field assistants. We are grateful to the Yukon Geological Survey for their logistical support. Sarah Roeske and Nick Botto assisted with the electron microprobe analyses, and Joe Wooden helped with collection and interpretation of U/Pb–trace element data at the USGS-SHRIMP laboratory. This study was supported by National Science Foundation grant EAR-1118834 to Gilotti, Geological Survey of Canada funding to van Staal, and a Geological Society of America Student Research Grant, an Alliances for Graduate Education and the Professoriate Fellowship and Department of Earth and Environmental Sciences, University of Iowa, funds to Petrie. We thank Maurice Colpron and Dan Gibson for their helpful reviews, and Brendan Murphy for his editorial work.

REFERENCES

Anders, E., and Grevesse, N., 1989, Abundances of the elements: Meteoritic and solar: Geochimica et Cosmochimica Acta, v. 53, p. 197–214, http://dx.doi.org/10.1016/0016-7037(89)90286-X.

Andersen, T.B., Jamtveit, B., Dewey, J.F., and Swensson, E., 1991, Subduction and eduction of continental crust: major mechanisms during continent-continent collision and orogenic extensional collapse, a model based on the south Norwegian Caledonides: Terra Nova, v. 3, p. 303–310, http://dx.doi.org/10.1111/j.1365-3121.1991.tb00148.x.

Armbruster, T., Bonazzi, P., Akasaka, M., Bermanec, V., Chopin, C., Gieré, R., Heuss-Assbichler, S., Liebscher, A., Menchetti, S., Pan, Y., and Pasero, M., 2006, Recommended nomenclature of epidote-group minerals: European Journal of Mineralogy, v. 18, p. 551–567, http://dx.doi.org/10.1127/0935-1221/2006/0018-0551.

Barth, A.P., and Wooden, J.L., 2006, Timing of magmatism following initial convergence at a passive margin, southwestern U.S. Cordillera, and ages of lower crustal magma sources: The Journal of Geology, v. 114, p. 231–245, http://dx.doi.org/10.1086/499573.

Barth, A.P., and Wooden, J.L., 2010, Coupled elemental and isotopic analyses of polygenetic zircons from granitic rocks by ion microprobe, with implications for melt evolution and the sources of granitic magmas: Chemical Geology, v.

277, p. 149–159, http://dx.doi.org/10.1016/j.chemgeo.2010.07.017.
Berman, R.G., Ryan, J.J., Gordey, S.P., and Villeneuve, M., 2007, Permian to Cretaceous polymetamorphic evolution of the Stewart River region, Yukon-Tanana terrane, Yukon, Canada: *P-T* evolution linked with *in situ* SHRIMP monazite geochronology: Journal of Metamorphic Geology, v. 25, p. 803–827, http://dx.doi.org/10.1111/j.1525-1314.2007.00729.x.
Black, L.P., Kamo, S.L., Allen, C.M., Davis, D.W., Aleinikoff, J.N., Valley, J.W., Mundil, R., Campbell, I.H., Korsch, R.J., Williams, I.S., and Foudoulis, C., 2004, Improved $^{206}Pb/^{238}U$ microprobe geochronology by the monitoring of a trace-element-related matrix effect; SHRIMP, ID-TIMS, ELA-ICP-MS and oxygen isotope documentation for a series of zircon standards: Chemical Geology, v. 205, p. 115–140, http://dx.doi.org/10.1016/j.chemgeo.2004.01.003.
Butler, J.P., Jamieson, R.A, Steenkamp, H.M, and Robinson, P., 2013, Discovery of coesite– eclogite from the Nordøyane UHP domain, Western Gneiss Region, Norway: field relations, metamorphic history, and tectonic significance: Journal of Metamorphic Geology, v. 31, p. 147–163, http://dx.doi.org/10.1111/jmg.12004.
Carswell, D.A., Brueckner, H.K., Cuthbert, S.J., Mehta, K., and O'Brien, P.J., 2003, The timing of stabilisation and the exhumation rate for ultra-high pressure rocks in the Western Gneiss Region of Norway: Journal of Metamorphic Geology, v. 21, p. 601–612, http://dx.doi.org/10.1046/j.1525-1314.2003.00467.x.
Coleman, R.G., Lee, D.E., Beatty, L.B., and Brannock, W.W., 1965, Eclogites and eclogites: Their differences and similarities: Geological Society of America Bulletin, v. 76, p. 483–508, http://dx.doi.org/10.1130/0016-7606(1965)76[483:EAETDA]2.0.CO;2.
Colpron, M., 2006, Tectonic assemblage map of Yukon-Tanana and related terranes in Yukon and northern British Columbia: Yukon Geologic Survey, Open File 2006–1, scale: 1:1,000,000.
Colpron, M., Nelson, J.L., and Murphy, D.C., 2006a, A tectonostratigraphic framework for the pericratonic terranes of the northern Canadian Cordillera, *in* Colpron, M., and Nelson, J.L., *eds.*, Paleozoic Evolution and Metallogeny of Pericratonic Terranes at the Ancient Pacific Margin of North America, Canadian and Alaskan Cordillera: Geological Association of Canada, Special Paper 45, p. 1–23.
Colpron, M., Mortensen, J.K., Gehrels, G.E., and Villeneuve, M., 2006b, Basement complex, Carboniferous magmatism and Paleozoic deformation in Yukon-Tanana terrane of central Yukon: Field, geochemical and geochronological constraints from Glenlyon map area, *in* Colpron, M., and Nelson, J.L., *eds.*, Paleozoic Evolution and Metallogeny of Pericratonic Terranes at the Ancient Pacific Margin of North America, Canadian and Alaskan Cordillera: Geological Association of Canada, Special Paper 45, p. 131–151.
Colpron, M., Nelson, J.L., and Murphy, D.C., 2007, Northern Cordilleran terranes and their interactions through time: GSA Today, v. 17, p. 4–10, http://dx.doi.org/10.1130/GSAT01704-5A.1.
Corfu, F., Hanchar, J.M., Hoskin, P.W.O., and Kinny, P., 2003, Atlas of zircon textures, *in* Hanchar, J.M., and Hoskin, P.W.O., *eds.*, Zircon: Reviews in Mineralogy and Petrology: American Mineralogist, v. 53, p. 469–500, http://dx.doi.org/10.2113/0530469.
Creaser, R.A., Erdmer, P., Stevens, R.A., and Grant, S.L., 1997, Tectonic affinity of Nisutlin and Anvil assemblage strata from the Teslin tectonic zone, northern Canadian Cordillera: Constraints from neodymium isotope and geochemical evidence: Tectonics, v. 16, p. 107–121, http://dx.doi.org/10.1029/96TC03317.
Creaser, R.A., Goodwin-Bell, J-A.S., and Erdmer, P., 1999, Geochemical and Nd isotopic constraints for the origin of eclogite protoliths, northern Cordillera: implications for the Paleozoic tectonic evolution of the Yukon-Tanana terrane: Canadian Journal of Earth Sciences, v. 36, p. 1697–1709, http://dx.doi.org/10.1139/e99-070.
Devine, F., Carr, S.D., Murphy, D.C., Davis, W.J., Smith, S., and Villeneuve, M., 2006, Geochronological and geochemical constraints on the origin of the Klatsa metamorphic complex: Implications for Early Mississippian high-pressure metamorphism within Yukon-Tanana terrane, *in* Colpron, M., and Nelson, J.L., *eds.*, Paleozoic Evolution and Metallogeny of Pericratonic Terranes at the Ancient Pacific Margin of North America, Canadian and Alaskan Cordillera: Geological Association of Canada, Special Paper, 45, p. 107–130.
Dusel-Bacon, C., Hopkins, M.J., Mortensen, J.K., Dashevsky, S.S., Bressler, J.R., and Day, W.C., 2006, Paleozoic tectonic and metallogenic evolution of the pericratonic rocks of east-central Alaska and adjacent Yukon, *in* Colpron, M., and Nelson, J.L., *eds.*, Paleozoic Evolution and Metallogeny of Pericratonic Terranes at the Ancient Pacific Margin of North America, Canadian and Alaskan Cordillera: Geological Association of Canada, Special Paper 45, p. 25–74.
Erdmer, P., 1987, Blueschist and eclogite in mylonitic allochthons, Ross River and Watson Lake areas, southeastern Yukon: Canadian Journal of Earth Sciences, v. 24, p. 1439–1449, http://dx.doi.org/10.1139/e87-136.
Erdmer, P., 1992, Eclogitic rocks of the St. Cyr klippe, Yukon, and their tectonic significance: Canadian Journal of Earth Sciences, v. 29, p. 1296–1304, http://dx.doi.org/10.1139/e92-103.
Erdmer, P., and Armstrong, R.L., 1989, Permo–Triassic isotopic dates for blueschist, Ross River area, Yukon: Exploration and Geological Services Division, Yukon, Indian and Northern Affairs Canada, Yukon Geology, 2, p. 33–36.
Erdmer, P., and Helmstaedt, H., 1983, Eclogite from central Yukon: a record of subduction at the western margin of ancient North America: Canadian Journal of Earth Sciences, v. 20, p. 1389–1408, http://dx.doi.org/10.1139/e83-126.
Erdmer, P., Ghent, E.D., Archibald, D.A., and Stout, M.Z., 1998, Paleozoic and Mesozoic high-pressure metamorphism at the margin of ancestral North America in central Yukon: Geological Society of America Bulletin, v. 110, p. 615–629, http://dx.doi.org/10.1130/0016-7606(1998)110<0615:PAMHPM>2.3.CO;2.
Ernst, W.G., 2015, Franciscan geologic history constrained by tectonic/olistostromal high-grade metamafic blocks in the iconic Californian Mesozoic–Cenozoic accretionary complex: American Mineralogist, v. 100, p. 6–13, http://dx.doi.org/10.2138/am-2015-4850.
Evans, B.W., Hattori, K., and Baronnet, A., 2013, Serpentinite: What, Why, Where?: Elements, v. 9, p. 99–106, http://dx.doi.org/10.2113/gselements.9.2.99.
Fallas, K.M., 1997, Preliminary constraints on the structural and metamorphic evolution of the St. Cyr Klippe, south-central Yukon: LITHOPROBE Slave-Northern Cordillera Lithospheric Evolution (SNORCLE) Transect Meeting Report, March 7–9, 1997, University of Calgary, AB, v. 56, p. 90–95.
Fallas, K.M., Erdmer, P., Archibald, D.A., Heaman, L.M., and Creaser, R.A., 1998, The St. Cyr Klippe, south-central Yukon: an outlier of the teslin tectonic zone?: LITHOPROBE Slave- Northern Cordillera Lithospheric Evolution (SNORCLE) Transect Meeting Report, March 6–8, 1998, Simon Fraser University, BC, p. 131–138.
Fallas, K.M., Erdmer, P., Creaser, R.A., Archibald, D.A., and Heaman, L.M., 1999, New terrane interpretation for the St. Cyr Klippe, south-central Yukon: LITHOPROBE Slave-Northern Cordillera Lithospheric Evolution (SNORCLE) Transect Meeting Report, March 5–7, 1999, University of Calgary, AB, v. 69, p. 130–137.
Gehrels, G.E., Valencia, V., and Pullen, A., 2006, Detrital zircon geochronology by laser ablation multicollector ICPMS at the Arizona Laserchron Center; Geochronology: Emerging Opportunities, Paleontological Society Short Course: Paleontological Society Papers, v. 12, p. 67–76.
Gehrels, G.E., Valencia, V.A., and Ruiz, J., 2008, Enhanced precision, accuracy, efficiency and spatial resolution of U–Pb ages by laser ablation-multicollector-inductively coupled plasma- mass spectrometry: Geochemistry Geophysics Geosystems, v. 9, Q03017, http://dx.doi.org/10.1029/2007GC001805.
Ghent, E., and Erdmer, P., 2011, Very high-pressure epidote eclogite from Ross River area, Yukon, Canada, records deep subduction, *in* Dobrzhinetskaya, L.F., Faryad, S.W., Wallis, S., and Cuthbert, S., *eds.*, Ultrahigh-pressure Metamorphism: 25 Years after the Discovery of Coesite and Diamond: Elsevier, Burlington, MA, p. 441–457, http://dx.doi.org/10.1016/B978-0-12-385144-4.00013-8.
Gilotti, J.A., McClelland, W.C., Petrie, M.B., and van Staal, C., 2013, Interpreting subduction polarity from eclogite-bearing slices in accretionary orogens - a cautionary note from the Yukon-Tanana terrane (Abstract): Geological Society of America, Annual Meeting, 2013, Abstracts, p. 442.
Hansen, V.L., 1992, *P-T* evolution of the Teslin suture zone and Cassiar tectonites, Yukon, Canada: evidence for A- and B-type subduction: Journal of Metamorphic Geology, v. 10, p. 239–263, http://dx.doi.org/10.1111/j.1525-1314.1992.tb00081.x.
Hawthorne, F.C., Oberti, R., Harlow, G.E., Maresch, W.V., Martin, R.F., Schumacher, J.C., and Welch, M.D., 2012, Nomenclature of the amphibole supergroup: American Mineralogist, v. 97, p. 2031–2048, http://dx.doi.org/10.2138/am.2012.4276.
Hoskin, P.W.O., and Schaltegger, U., 2003, The composition of zircon and igneous and metamorphic petrogenesis, *in* Hanchar, J.M., and Hoskin, P.W.O., *eds.*, Zircon: Reviews in Mineralogy and Petrology, American Mineralogist, v. 53, p. 27–62, http://dx.doi.org/10.2113/0530027.
Isard, S.J., 2014, Origin of the Tower Peak unit, St. Cyr area, Canadian Cordillera: Unpublished MSc Thesis, University of Iowa, Iowa City, IA, 130 p.
Isard, S.J., and Gilotti, J.A., 2014, Geology and jade prospects of the northern St. Cyr klippe (NTS 105F/6), Yukon, *in* MacFarlane, K.E., Nordling, M.G., and Sack, P.J., *eds.*, Yukon Exploration and Geology: Yukon Geologic Survey, p. 69–77.
Johnson, D.M., Hooper, P.R., and Conrey, R.M., 1999, XRF Analysis of rocks and minerals for major and trace elements on a single low dilution Li-tetraborate fused bead: JCPDS- International Center for Diffraction Data, v. 41, p. 843–867.
Kleinschmidt, G., Heberer, B., and Läufer, A.L., 2008, Pre-Alpine sector-zoned garnets in the southeastern Alps: Zeitschrift der Deutschen Gesellschaft für Geowissenschaften, v. 159, p. 565–573, http://dx.doi.org/10.1127/1860-1804/2008/0159-0565.
Korotev, R.L., 1996, A self-consistent compilation of elemental concentration data

for 93 geochemical reference samples: Geostandards Newsletter, v. 20, p. 217–245, http://dx.doi.org/10.1111/j.1751-908X.1996.tb00185.x.

Liu, F., Liou, J.G., and Xu, Z., 2005, U–Pb SHRIMP ages recorded in the coesite-bearing zircon domains of paragneisses in the southwestern Sulu terrane, eastern China: New Interpretation: American Mineralogist, v. 90, p. 790–800, http://dx.doi.org/10.2138/am.2005.1677.

Ludwig, K.R., 2003, User's manual for Isoplot 3.00: a geochronological toolkit for Microsoft Excel: Berkeley Geochronology Center Special Publication, 4, p. 70.

Ludwig, K.R., 2005, Squid version 1.13b: A user's manual: Berkley Geochronology Center Special Publication, 2, p. 1–22.

Mattinson, J.M., 2010, Analysis of the relative decay constants of ^{235}U and ^{238}U by multi-step CA-TIMS measurements of closed-system natural zircon samples: Chemical Geology, v. 275, p. 186–198, http://dx.doi.org/10.1016/j.chemgeo.2010.05.007.

Mazdab, F.K., 2009, Characterization of flux grown trace-element-doped titanite using the high-mass-resolution ion microprobe (SHRIMP-RG): Canadian Mineralogist, v. 47, p. 813–831, http://dx.doi.org/10.3749/canmin.47.4.813.

Mazdab, F.K., and Wooden, J.L., 2006, Trace element analysis in zircon by ion microprobe (SHRIMP-RG): Technique and applications: Geochimica et Cosmochimica Acta, v. 70, A405, http://dx.doi.org/10.1016/j.gca.2006.06.817.

Meschede, M., 1986, A method of discriminating between different types of mid-ocean ridge basalts and continental tholeiites with the Nb-Zr-Y diagram: Chemical Geology, v. 56, p. 207– 218, http://dx.doi.org/10.1016/0009-2541(86)90004-5.

Monger, J.W.H., Price, R.A., and Tempelman-Kluit, D.J., 1982, Tectonic accretion and the origin of the two major metamorphic and plutonic welts in the Canadian Cordillera: Geology, v. 10, p. 70–75, http://dx.doi.org/10.1130/0091-7613(1982)10<70:TAATOO>2.0.CO;2.

Morimoto, N., 1989, Nomenclature of pyroxenes: Canadian Mineralogist, v. 27, p. 143–156, http://dx.doi.org/10.2465/minerj.14.198.

Mortensen, J.K., 1990, Geology and U–Pb geochronology of the Klondike District, west-central Yukon Territory: Canadian Journal of Earth Sciences, v. 27, p. 903–914, http://dx.doi.org/10.1139/e90-093.

Mortensen, J.K., 1992, Pre-Mid-Mesozoic tectonic evolution of the Yukon-Tanana terrane, Yukon and Alaska: Tectonics, v. 11, p. 836–853, http://dx.doi.org/10.1029/91TC01169.

Murphy, D.C., Mortensen, J.K., Piercey, S.J., Orchard, M.J., and Gehrels, G.E., 2006, Mid- Paleozoic to early Mesozoic tectonostratigraphic evolution of Yukon-Tanana and Slide Mountain terranes and affiliated overlap assemblages, Finlayson Lake massive sulphide district, southeastern Yukon, *in* Colpron, M., and Nelson, J.L., *eds.*, Paleozoic Evolution and Metallogeny of Pericratonic Terranes at the Ancient Pacific Margin of North America, Canadian and Alaskan Cordillera: Geological Association of Canada, Special Paper, 45, p. 75–105.

Nelson, J.L., 1993, The Sylvester Allochthon: upper Paleozoic marginal-basin and island-arc terranes in northern British Columbia: Canadian Journal of Earth Sciences, v. 30, p. 631–643, http://dx.doi.org/10.1139/e93-048.

Nelson, J., and Friedman, R., 2004, Superimposed Quesnel (late Paleozoic–Jurassic) and Yukon- Tanana (Devonian–Mississippian) arc assemblages, Cassiar Mountains, northern British Columbia: Field, U–Pb, and igneous petrochemical evidence: Canadian Journal of Earth Sciences, v. 41, p. 1201–1235, http://dx.doi.org/10.1139/e04-028.

Nelson, J.L., Colpron, M., Piercey, S.J., Dusel-Bacon, C., Murphy, D.C., and Roots, C.F., 2006, Paleozoic tectonic and metallogenetic evolution of pericratonic terranes in Yukon, northern British Columbia and eastern Alaska, *in* Colpron, M., and Nelson, J.L., *eds.*, Paleozoic Evolution and Metallogeny of Pericratonic Terranes at the Ancient Pacific Margin of North America, Canadian and Alaskan Cordillera: Geological Association of Canada, Special Paper 45, p. 323–360

Nelson, J.L., Colpron, M., and Israel, S., 2013, The Cordillera of British Columbia, Yukon, and Alaska: Tectonics and Metallogeny: Society of Economic Geologists Special Publication, v. 17, p. 53–109.

Pearce, J.A., and Cann, J.R., 1973, Tectonic setting of basic volcanic rocks determined using trace element analyses: Earth and Planetary Science Letters, v. 19, p. 290–300, http://dx.doi.org/10.1016/0012-821X(73)90129-5.

Perchuk, A.L., and Gerya, T.V., 2005, Dynamics of subsidence and exhumation of eclogites of the Yukon-Tanana terrane, (Canadian Cordilleras), according to petrological reconstructions and geodynamic modeling: Petrologiya, v. 13, p. 280–294.

Perchuk, A., Philippot, P., Erdmer, P., and Fialin, M., 1999, Rates of thermal equilibration at the onset of subduction deduced from diffusion modeling of eclogitic garnets, Yukon-Tanana terrane, Canada: Geology, v. 27, p. 531–534, http://dx.doi.org/10.1130/0091-7613(1999)027<0531:ROTEAT>2.3.CO;2.

Petrie, M.B., 2014, Evolution of eclogite facies metamorphism in the St. Cyr klippe, Yukon– Tanana terrane, Yukon, Canada: Unpublished Ph.D. Thesis, University of Iowa, Iowa City, IA, 168 p.

Piercey, S.J., and Colpron, M., 2009, Composition and provenance of the Snowcap assemblage, basement to the Yukon-Tanana terrane, northern Cordillera: Implications for Cordilleran crustal growth: Geosphere, v. 5, p. 439–464, http://dx.doi.org/10.1130/GES00505.1.

Piercey, S.J., Mortensen, J.K., Murphy, D.C., Paradis, S., and Creaser, R.A., 2002, Geochemistry and tectonic significance of alkalic mafic magmatism in the Yukon-Tanana terrane, Finlayson Lake region, Yukon: Canadian Journal of Earth Sciences, v. 39, p. 1729–1744, http://dx.doi.org/10.1139/e02-090.

Piercey, S.J., Nelson, J.L., Colpron, M., Dusel-Bacon, C., Simard, R.-L., and Roots, C.F., 2006, Paleozoic magmatism and crustal recycling along the ancient Pacific margin of North America, northern Cordillera, *in* Colpron, M., and Nelson, J.L., *eds.*, Paleozoic Evolution and Metallogeny of Pericratonic Terranes at the Ancient Pacific Margin of North America, Canadian and Alaskan Cordillera: Geological Association of Canada, Special Paper 45, p. 281–322.

Piercey, S.J., Murphy, D.C., and Creaser, R.A., 2012, Lithosphere-asthenosphere mixing in a transform-dominated late Paleozoic backarc basin: Implications for northern Cordilleran crustal growth and assembly: Geosphere, v. 8, p. 716–739, http://dx.doi.org/10.1130/GES00757.1.

Pigage, L.C., 2004, Bedrock geology compilation of the Anvil District (parts of NTS 105K/2, 3, 5, 6, 7 and 11), central Yukon: Yukon Geological Survey Bulletin 15, p. 103.

Roots, C.F., Nelson, J.L., Simard, R.-L., and Harms, T.A., 2006, Continental fragments, mid- Paleozoic arcs and overlapping late Paleozoic arc and Triassic sedimentary rocks in the Yukon- Tanana terrane of northern British Columbia and southern Yukon, *in* Colpron, M., and Nelson, J.L., *eds.*, Paleozoic Evolution and Metallogeny of Pericratonic Terranes at the Ancient Pacific Margin of North America, Canadian and Alaskan Cordillera: Geological Association of Canada, Special Paper 45, p. 153–177.

Rubatto, D., 2002, Zircon trace element geochemistry: partitioning with garnet and the link between U–Pb ages and metamorphism: Chemical Geology, v. 184, p. 123–138, http://dx.doi.org/10.1016/S0009-2541(01)00355-2.

Rubatto, D., and Hermann, J., 2007, Zircon behaviour in deeply subducted rocks: Elements, v. 3, p. 31–35, http://dx.doi.org/10.2113/gselements.3.1.31.

Shirahata, K., and Hirajima, T., 1995, Chemically sector-zoned garnet in Sanbagawa schists: its mode of occurrence and growth timing: Journal of Mineralogy, Petrology and Economic Geology, v. 90, p. 69–79, http://dx.doi.org/10.2465/ganko.90.69.

Simard, R.-L., Dostal, J., and Roots, C.F., 2003, Development of late Paleozoic volcanic arcs in the Canadian Cordillera: an example from the Klinkit Group, northern British Columbia and southern Yukon: Canadian Journal of Earth Sciences, v. 40, p. 907–924, http://dx.doi.org/10.1139/e03-025.

Smith, D.C., 1984, Coesite in clinopyroxene in the Caledonides and its implications for geodynamics: Nature, v. 310, p. 641–644, http://dx.doi.org/10.1038/310641a0.

Stacey, J.S., and Kramers, J.D., 1975, Approximation of terrestrial lead isotope evolution by a two-stage model: Earth and Planetary Science Letters, v. 26, p. 207–221, http://dx.doi.org/10.1016/0012-821X(75)90088-6.

Staples, R.D., Gibson, H.D., Berman, R.G., Ryan, J.J., and Colpron, M., 2013, A window into the Early to mid-Cretaceous infrastructure of the Yukon-Tanana terrane recorded in multi-stage garnet of west-central Yukon, Canada: Journal of Metamorphic Geology, v. 31, p. 729–753, http://dx.doi.org/10.1111/jmg.12042.

Stipp, M., Stünitz, H., Heilbronner, R., and Schmid, S.M., 2002, The eastern Tonale fault zone: a 'natural laboratory' for crystal plastic deformation of quartz over a temperature range from 250 to 700°C: Journal of Structural Geology, v. 24, p. 1861–1884, http://dx.doi.org/10.1016/S0191-8141(02)00035-4.

Sun, S.–s., and McDonough, W.F., 1989, Chemical and isotopic systematics of oceanic basalts: implications for mantle composition and processes: Geological Society, London, Special Publications, v. 42, p. 313–345, http://dx.doi.org/10.1144/GSL.SP.1989.042.01.19.

Tempelman-Kluit, D.J., 1977, Geology of Quiet Lake and Finlayson Lake map areas, Yukon Territory: Geological Survey of Canada, Open File 486, 3 maps, scale: 1: 250,000, http://dx.doi.org/10.4095/129286.

Tempelman-Kluit, D.J., 1979, Transported cataclasite, ophiolite and granodiorite in the Yukon: evidence of arc-continent collision: Geological Survey of Canada, Paper, 79-14, 27 p., http://dx.doi.org/10.4095/105928.

Tempelman-Kluit, D.J., 2012, Geology of Quiet Lake and Finlayson Lake map areas, south-central Yukon – An early interpretation of bedrock stratigraphy and structure: Geological Survey of Canada, Open File 5487, 103 p., http://dx.doi.org/10.4095/291931.

Wain, A., 1997, New evidence for coesite in eclogite and gneisses: Defining an ultra-high-pressure province in the Western Gneiss Region of Norway: Geology, v. 25, p. 927–930, http://dx.doi.org/10.1130/0091-7613(1997)025<0927:NEFCIE>2.3.CO;2.

Wang, X., and Liou, J.G., 1991, Regional ultrahigh-pressure coesite-bearing eclogitic terrane in central China: Evidence from country rocks, gneiss, marble, and metapelite: Geology, v. 19, p. 933–936, http://dx.doi.org/10.1130/0091-7613(1991)019<0933:RUPCBE>2.3.CO;2.

Wheeler, J.O., and McFeely, P., 1991, Tectonic map of the Canadian Cordillera and adjacent parts of the USA: Geological Society of Canada, "A" Series Map 1712A, scale: 1:2,000,000, http://dx.doi.org/10.4095/133549.

Wheeler, J.O., Brookfield, A.J., Gabrielse, H., Monger, J.W.H., Tipper, H.W., and Woodsworth, G.J., 1991, Terrane map of the Canadian Cordillera: Geological Survey of Canada, "A" Series Map 1713A, scale: 1:2,000,000, http://dx.doi.org/10.4095/133550.

Whitney, D.L., and Evans, B.W., 2010, Abbreviations for names of rock-forming minerals: American Mineralogist, v. 95, p. 185–187, http://dx.doi.org/10.2138/am.2010.3371.

Williams, I.S., 1998, U–Th–Pb geochronology by ion microprobe, *in* McKibben, M.A., Shanks III, W.C., and Ridley, W.I., *eds.*, Applications of microanalytical techniques to understand mineralizing processes: Reviews in Economic Geology, v. 7, p. 1–35.

Zhang, R.Y., Hirajima, T., Banno, S., Cong, B., and Liou, J.G., 1995, Petrology of ultrahigh-pressure rocks from the southern Su-Lu region, eastern China: Journal of Metamorphic Geology, v. 13, p. 659–675, http://dx.doi.org/10.1111/j.1525-1314.1995.tb00250.x.

Received December 2014
Accepted as revised May 2015

For access to Petrie et al. (2015) electronic supplementary materials (Tables DR-1 through -8), please visit GAC's open source GC Data Repository, the Andrew Hynes Series: Tectonic Processes link at http://www.gac.ca/wp/?page_id=306.

SERIES

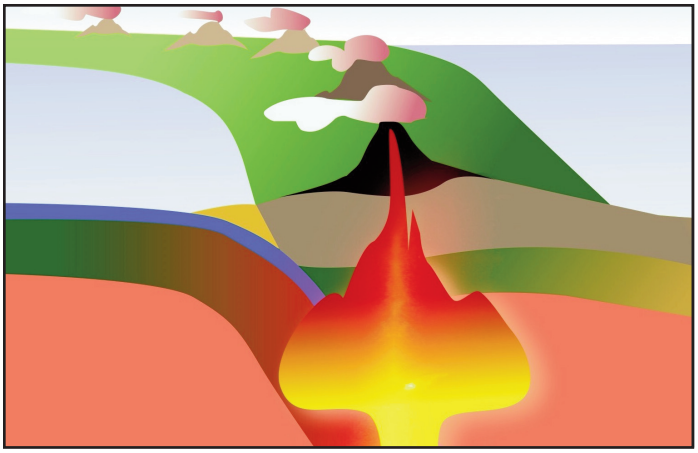

Igneous Rock Associations 18. Transition Metals in Oceanic Island Basalt: Relationships with the Mantle Components

John D. Greenough and Kevin MacKenzie

Department of Earth and Environmental Sciences
SCI 216, University of British Columbia, Okanagan
3333 University Way,
Kelowna, British Columbia, V1V 1V7, Canada
Email: john.greenough@ubc.ca

SUMMARY

Incompatible elements and isotopic ratios identify three end-member mantle components in oceanic island basalt (OIB); EM1, EM2, and HIMU. We estimate compatible to mildly incompatible transition metal abundance trends (Ni, Co, Fe, Cu, Cr, V, Mn, Sc, and Zn) in 'primitive' basalt suites (Mg# = Mg/(Mg + 0.9*Fe) atomic = 0.72) from 12 end-member oceanic islands by regressing metals against Fe/Mg ratios in sample suites, and solving for concentrations at Mg/Fe = 1 (Mg# = 0.72). Using the transition metal estimates, exploratory statistics reveal that islands 'group' based on mantle component type even when La/Yb ratios are used to compensate metal concentrations for percentage melting. Higher chalcophile Zn (and Pb, earlier work) in EM1 and EM2 compared to HIMU, and higher Cr (3+) and Sc in HIMU relative to EM1, support views that HIMU represents subduction-processed ocean floor basalt. Incompatible elements, ratios and isotopes indicate that EM1 is Archean, EM2 is Proterozoic or younger, and both are related to sediment subduction. As found with incompatible elements, EM1 and EM2 show similar 'compatible' element concentrations, but lower (multivalence) Cr, Fe and Mn in EM1 could indirectly reflect increasing oxidation of subducted sediment between the Archean and Proterozoic. Alternatively, changes in subduction processes that yielded peak continental formation in the Neoarchean, and craton-suturing in the Paleoproterozoic may account for EM1–EM2 differences. EM1 shows similar or lower Cr, Ni and Co compared to HIMU and EM2 suggesting that economic viability of layered intrusions, which have extreme EM1-like signatures, is unrelated to high metals in EM1 mantle sources, but that high % melting appears important. Because core-concentrated transition metals correlate with mantle component type, lithospheric recycling apparently controls their concentrations in OIB and core-mantle interaction may be unimportant.

RÉSUMÉ

Les éléments incompatibles et les rapports isotopiques permettent de délimiter trois termes extrêmes de composants mantéliques dans des basaltes insulaires océaniques (OIB), soit EM1, EM2, et HIMU. Nous estimons les tendances d'abondance de métaux de transition (Ni, Co, Fe, Cu, Cr, V, Mn, Sc, and Zn) compatibles à modérément incompatibles dans des suites de basaltes « primitifs » (Mg# = Mg/(Mg + 0,9*Fe) rayon atomique = 0,72) sur 12 termes extrêmes de matériaux insulaires océaniques, par régression des concentrations des métaux sur les rapports Fe/Mg dans des échantillons des suites, la détermination étant définie au rapport Mg/Fe = 1 (Mg# = 0,72). L'utilisation d'une approche statistique exploratoire sur les estimations de métaux de transition montre que la composition des îles se « regroupent » en fonction du type de composition du manteau, cela même lorsque les ratios La/Yb sont utilisés pour compenser les concentrations de métaux pour déterminer le pourcentuel de fusion. Le caractère plus chalcophile du Zn (et Pb, travail antérieur) dans EM1 et EM2 comparé à HIMU, et la plus grande teneur en Cr (3+) et Sc dans HIMU par rapport à EM1, accréditent l'idée que HIMU représente le basalte de subduction des fonds océaniques. Les éléments incompatibles, les ratios et les isotopes montrent que EM1 est archéen, que EM2 est protérozoïque ou plus jeune, et que les deux sont liés à la subduction sédimentaire. Comme constaté pour les éléments incompatibles, EMI et EM2 affichent une compatibilité similaire des concentrations en éléments « compatibles », toutefois une concentration inférieure en Cr (multivalent), Fe et Mn dans EM1 pourrait refléter indirectement une oxydation croissante des sédiments subduits entre l'Archéen et le Protérozoïque. Par

Geoscience Canada, v. 42, http://www.dx.doi.org/10.12789/geocanj.2015.42.071 pages 351–367
GC Data Repository: Igneous Rock Associations

ailleurs, les changements dans les mécanismes de subduction qui ont mené à un maximum de formation continentale au Néoarchéen et à des épisodes de sutures cratoniques au Paléoprotérozoïque, peuvent expliquer les différences entre EM1 et EM2. La teneur similaire ou inférieure en Cr, Ni et Co de EM1 par rapport à HIMU et EM2 permet de croire que la viabilité économique des intrusions stratifiées – lesquelles montrent des signatures extrêmes EM1 – est sans rapport avec les sources mantéliques à fortes teneurs en métaux, mais que le fort pourcentuel de fusion qui importerait. Parce que la concentration du noyau en métaux de transition correspond avec le type de composant du manteau, c'est le recyclage lithosphérique qui contrôle apparemment leurs concentrations dans l'OIB, et l'interaction noyau-manteau pourrait être sans importance.

Traduit par le Traducteur

INTRODUCTION

Incompatible elements and the small number of their radiogenic isotopic ratios have been paramount to providing a picture for evolution of the Earth's mantle. The prevailing view is that melt extraction of incompatible elements from the mantle has led to formation of incompatible-element depleted mid-ocean-ridge basalt (MORB) mantle (DMM), continental crust enriched in these elements, and 3+ oceanic island basalt (OIB) end-member mantle components bearing subduction-recycled materials including: enriched mantle 1 (EM1; sediment), enriched mantle 2 (EM2; sediment), and high Mu (high μ = high U/Pb = HIMU; subduction-processed MORB) (Zindler and Hart 1986; Sun and McDonough 1989; Hofmann 1997; Bennett 2003; Hofmann 2003; Greenough et al. 2007). The oceanic islands with the most extreme isotopic and trace element concentrations, representing each of the mantle components, are well established (e.g. Zindler and Hart 1986; Hofmann 2003; Greenough et al. 2005b, 2007; see METHODS for caveats about individual samples, and chemical variation at individual islands). However, most incompatible element ratios and radiogenic isotopic ratios are unlikely to be sensitive to processes that would impact transition metals (Fe, Cu, V, etc.) in basalt including source region mineralogy (e.g. Sobolev et al. 2005; Gurenko et al. 2009; Le Roux et al. 2011), subduction-recycled Fe/Mn-rich pelagic sediment in mantle sources (e.g. Scherstén et al. 2004), core-formation, or core-interaction processes involving deep mantle plumes (e.g. Humayun et al. 2004; Brandon and Walker 2005; Qin and Humayun 2008). Theoretically, siderophile (Goldschmidt classification) and ferrophile elements (elements important in mantle and crustal Fe–Mg-bearing phases) can help distinguish between hypotheses.

Studies of incompatible elements (e.g. Ba, Rb, Nb, La) in OIB source regions use ratios of similarly incompatible elements to minimize the impact of differentiation and the percentage of melting, and these ratios have been used for chemical characterization of the end-member mantle components (Allègre et al. 1995; Greenough et al. 2005b, 2007). Far fewer studies have used *compatible* elements to describe mantle heterogeneity because it has been challenging to deal with the effects of differentiation, the percentage of melting, and oxygen fugacity, but this is changing (e.g. Lee et al. 2005, 2010, 2012; Le Roux et al. 2010, 2011).

Our objective is to evaluate the hypothesis that the first-row transition elements Ni, Co, Fe, Cu, Cr, V, Mn, Sc, and Zn, which are variably 'compatible' to somewhat incompatible, have concentrations in OIB magmas and source regions that are correlated with mantle component type. We regressed each element against Mg/Fe ratios in basaltic suites from twelve oceanic islands representing the most extreme examples of each of the end-member mantle components. The regressions compensate for differentiation and yield estimates of average element concentrations in 'primary' magmas. Incorporating proxies for the percentage of melting (e.g. La/Yb ratios) allows us to appraise the effect of melting on element concentrations. As many of these elements are siderophile or chalcophile, they were likely concentrated in the core during differentiation. Therefore, we also use our regressions to test the hypothesis that compatible element concentrations in OIB reflect core–mantle interaction. However, in contrast with the well-established, geochemistry-based data that characterize basalts from each of the mantle components, available seismic tomography information, for the depth of origin of OIB-forming 'plumes,' has comparatively low 'resolution' making it challenging to conclusively test the core–mantle interaction hypothesis.

METHODS

Data Selection and Preparation

All raw data used in the paper were downloaded from the GEOROC web site (Sarbas and Nohl 2008) and are given in an Electronic Supplementary Materials file*, ESM Table-1. To estimate transition metal abundances in primary (undifferentiated) basaltic magmas, we regressed metal data for oceanic island basalts against Mg/Fe (wt. %) ratios (MacKenzie 2008). Twelve islands were used in this experiment, all identified as representatives of the end-member mantle components based on Sr, Nd, and Pb isotopic data (e.g. Zindler and Hart 1986; Hofmann 2003) and average trace element ratio data (e.g. Allègre et al. 1995; Greenough et al. 2005b, 2007). Islands used include EM1: Aitutaki, Gough, Heard, Kerguelen, and Pitcairn, EM2: São Miguel, Tahiti, Tutuila, and Upolu, and HIMU: Mangaia, St. Helena, and Tubuai. We recognize that the average isotopic and trace element ratio signature is not as strong for some islands as others within one component group. For example, average Pitcairn (an EM1 island) $^{143}Nd/^{144}Nd$ and $^{87}Sr/^{86}Sr$ ratios are higher and lower (respectively) than all other EM1 islands used in the study (i.e. least EM1-like; Greenough et al. 2005b) but they are distinct from all non-EM1 oceanic islands. Another issue is that there is chemical variability in basalt from any one island, but based on averaged isotopic and trace element data, each island listed above shows characteristics representative of the associated component source type. This is important because there are far more samples with transition metal data than with isotopic data, and those with isotopic data do not necessarily have complementary trace element or transition metal data. We use incompatible element data (incompatible element ratios) to confirm that the average composition of samples used to represent each island classifies it according to component type, and then test the hypothesis that transition metal concentrations in primary basalt occurrences also correlate with component type. Thus, we suggest that the regression analysis

approach used here (see details below) will yield useful 'average' approximations of transition metal concentrations in primary magmas for each island and test the hypothesis that concentrations are related to component type. We acknowledge that this approach, which necessarily uses multiple samples, may not yield the most extreme source composition at one island, but should provide useful average transition metal data for each end-member island.

Many compatible to mildly incompatible, siderophile, chalcophile, and/or ferromagnesian mineral-associated elements were considered for analysis but elements such as Au and the platinum group elements (PGE) were eliminated because there were no data for ≥ 25% of the islands. Our study focuses on elements that are likely to have high concentrations in the core, such that core–mantle interaction should result in these elements being unrelated to the patterns seen in incompatible trace element ratios and lithophile element isotopic ratios that have been ascribed to lithosphere recycling. McDonough (2003) estimated that the core contains 93% of the planet's inventory of Ni and Co, 87% of the Fe, 60–65% of the Cu and Cr, 50% of V and ~10% of the Mn. Ferrophile Sc and chalcophile Zn were included in the study because they are controlled by Fe-bearing minerals (Sc) and possibly sulphides (Zn) in the mantle and crust, and although they are *not* considered significantly enriched in the core (McDonough 2003), they provide context for interpreting information from the other elements. Although some of these elements are rarely considered in studies on mantle chemical heterogeneity, all may be useful in evaluating relationships with mantle component type and unlike the PGE, they are commonly reported in geochemical studies of basaltic rocks.

After downloading the major element and trace element whole-rock data from the GEOROC website, several filters were used to screen the island data sets prior to statistical analysis. All rocks (analyses) had associated major element data determined by X-ray fluorescence (XRF) on glass discs, atomic absorption spectroscopy (AA) or emission spectroscopy. Most trace elements were determined by ICP–MS (inductively coupled plasma–mass spectrometry) or INA (instrumental neutron activation), with XRF on pressed powder pellets commonly used to determine Ni, Cr and chalcophile elements such as Cu and Zn. A small percentage of trace element data come from emission spectroscopy. Trace element precision and accuracy are generally between 5 and 10%. Over 95% of trace element data are post-1970 but a few samples with earlier major element analyses contribute to assessments of Mn concentrations; we note that those used survived the regression screening process described in the next paragraph. As a check on data quality the major elements were summed and samples with values outside of the 98–102% range were omitted; and analyses that were normalized to 100% in the literature were eliminated. Similarly, only samples with loss on ignition (or total H_2O) < 4 wt. % were kept, to avoid issues related to alteration. Finally, when doing the regression analyses to estimate transition metal concentrations in primary magmas from each end-member island, outliers and high-leverage samples were eliminated (see section Statistical Methods). Despite the above quality-control procedures, not all data will have the same precision and accuracy, and there may be systematic biases. In the case of Mn, analyses are not of as high quality as the data reported in Humayun et al. (2004) for a small number of samples mostly from Hawaii. However, the large size of the data sets available from repositories such as GEOROC helps counter some of these problems (e.g. precision and inter-lab bias) because data come from numerous labs; the study involves nearly 700 rocks, and over 5000 analyses of 9 elements. Secondly, exploratory statistics are used to uncover patterns in the chemical data and samples, using all data simultaneously. If patterns emerge that are clearly relatable to well-established geological factors (e.g. if islands have overall transition metal geochemistry that is tied to the type of mantle component) then these patterns are unlikely to be fortuitous. Thirdly, any patterns that do emerge from such large data sets are likely to be of planetary importance and it is difficult to use small data sets to uncover large-scale patterns. As suggested by Le Roux et al. (2010) who looked at Fe/Zn/Mn relationships in OIB, there is little alternative but to try using the available world-wide data set at this time.

Highly differentiated samples were not used. The degree of differentiation was estimated from Mg# values [Mg# = Mg/(Mg+(0.9*Fe^t)) atomic] which decrease with differentiation because Mg enters octahedral sites in Fe–Mg silicates in preference to Fe (Basaltic Volcanism Study Project 1981). Samples with Mg# < 0.4 were omitted. Iron is reported in the literature various ways. All iron was recalculated as FeO^t (total Fe as wt. % FeO). Although samples bearing accumulated ferromagnesian phases could have Mg# values ≥ 0.4 despite a magma Mg# < 0.4, the regression procedure used to estimate transition element abundances in primary magmas eliminated outliers and high-leverage samples. Thus, if phenocryst accumulation had a significant impact on trace element composition, the sample was eliminated when the regression analyses were performed (see section Statistical Methods).

In preparation for statistical analysis, Mg/Fe^t ratios (wt. % of cations) were calculated and used as the independent variable in the regression analyses. Transition metal abundances were estimated from the regression analyses assuming primary magmas have a Mg/Fe^t ratio of 1.0. This ratio translates into a Mg# value of 0.72, and primary magmas formed in equilibrium with ~Fo_{90} olivine should show Mg# values between 0.70 to 0.72 with an exchange coefficient value ($K_D{}^{Mg\text{-}Fe}{}_{Ol\text{-}Liq} = (X^{Mg}{}_{Liq}/X^{Mg}{}_{Ol})/(X^{Fe2+}{}_{Liq}/X^{Fe2+}{}_{Ol})$) = 0.3 (Roeder and Emslie 1970). Olivine is by far the dominant mineral found in mantle xenoliths and it generally has a composition close to Fo_{90} (*ibid*). Recent experiments have shown that $K_D{}^{Mg\text{-}Fe}{}_{Ol\text{-}Liq}$ is dependent on temperature, olivine composition and melt composition but the observation that it tends to be close to 0.3 in natural systems is because the effects of these parameters cancel out (Toplis 2005; Matzen et al. 2011). Thus, these authors noted that a $K_D{}^{Mg\text{-}Fe}{}_{Ol\text{-}Liq}$ value of 0.3 (Mg# = 0.72 atomic and Mg/Fe^t = 1 wt. %) is a convenient reference point for general petrological studies. The debate about whether primary basaltic magmas can originate from non-olivine sources spans decades (Basaltic Volcanism Study Project 1981) and although a common view is that magmas form in the presence of olivine, there is no unanimous agreement (e.g. Kogiso et al. 2003; Keshav et al. 2004, 2006; Sobolev et al. 2005; Lustrino 2006). We note that there are a few, non-cumulus samples present in the majority of island suites (8 of 12 suites) that have Mg# values between 0.69 and 0.71 (Table 1) suggesting that ~0.70 is a

Table 1: Estimates of transition metal concentrations in primary magmas for 12 oceanic islands representing EM1, EM2, and HIMU mantle components.

Island	Aitutaki	Gough	Heard	Kerguelen	Pitcarin	São Miguel	Tahiti	Tutuila	Upolu	Mangaia	St Helena	Tubuai
Type	EM1	EM1	EM1	EM1	EM1	EM2	EM2	EM2	EM2	HIMU	HIMU	HIMU
Depth	~2800	Unseen	~2800	~2800	Unseen	~2800	~2800	~2800	~2800	~2800	Unseen	~2800
Plot Abbrev.	Ai	Go	He	Ke	Pi	Sa	Ta	Tu	Up	Ma	St	Tb
Transition metal estimates												
Cr	256	444	669	309	606	957	823	1041	754	1146	870	1099
Ni	283	417	506	363	427	328	435	500	567	471	366	362
Co	53	71	116	71	38	46	79	98	62	86	74	76
Sc		25	27	28		29	74		20	52	56	51
V		195	286	396	187	283	301	236	217	205	427	255
Zn	95	100	106	147	90	86	124	93	115	79	84	88
Cu	44	45	77	41	83	94	71	67	58	218	97	135
Mn	1221	1117	1244	1265	739	1308	1363	1336	1213	1432	1016	1394
Fe	76855	85325	91466	84593	47904	98612	96639	91292	103299	90441	93851	88753
Fe/Mn	63	76	74	67	65	75	71	68	85	63	92	64
Zn/Fe (*104)	12.4	11.7	11.6	17.3	18.8	8.7	12.9	10.1	11.2	8.8	9.0	9.9
Percentage of melting proxies												
La/Yb	38.8	23.8	27.1	27.7	22.1	21.1	22.0	11.7	23.4	18.6	22.0	29.9
Nb/Y	2.29	1.75	1.80	0.93	1.30	2.13	1.65	0.75	1.60	1.84	2.04	2.77
Maximum Mg/Fe ratio and Mg#												
Mg/Fe	0.94	0.87	0.97	0.92	0.48	0.96	0.97	0.93	0.76	0.81	0.81	0.91
Mg#	0.71	0.69	0.71	0.70	0.55	0.71	0.71	0.70	0.66	0.67	0.67	0.70

Notes: All concentrations in ppm. Type = Mantle component type. Plot Abbrev. = Abbreviated island name on plots.
Transition metal estimates = regression results at Mg/Fe (ratio in wt. % of cations with Fe = total Fe) = 1 = Mg# (Mg/(Mg + 0.9*Fe total) atomic) = 0.72.
Percentage of melting proxies = element ratios that are dominantly controlled by the percentage of melting.
Maximum Mg/Fe and Mg# = maximum values of Mg/Fe ratio and Mg# (both defined above) in each island data set.
Depth = imaged plume depth from Montelli et al. (2006). Unseen = there is no evidence for a plume.
Note that for 'unseen' Gough there is no obvious low velocity zone in this area.
Both Pitcairn and St. Helena are somewhat isolated oceanic islands. Neither is associated with a 'plume' low velocity zone.
Tubuai is 650 km S of Tahiti but within the low velocity zone centred on Tahiti. Tubuai depth is for the Tahiti plume though on a different hot-spot trace.

common upper value for a primary magma regardless of the source mineralogy (see also Greenough et al. 2005b). A final point is that any study of transition metals in OIB has to make assumptions (usually using Mg/Fe ratios or Mg concentrations) about what constitutes a primary or primitive magma and consider how element concentrations or ratios are impacted by melting and differentiation (e.g. Humayun et al. 2004; Le Roux et al. 2010). This paper assumes that primary magmas have Mg# values between 0.69 and 0.72.

Fifty incompatible element ratios were calculated from pairs of similarly incompatible elements (elements separated by < 10 elements in the Sun and McDonough (1989) incompatibility list) following procedures outlined by Greenough et al. (2005b, 2007). These ratios are used to confirm the geochemical character or mantle component type of islands in the Transition Metals and Mantle Components section of the paper.

Ratios for Nb/Y and La/Yb (i.e. ratios from element pairs with very different incompatibility) act as proxies for the percentage of melting. Although theoretically impacted by source composition, they are overwhelmingly controlled by the percentage of melting as surmised by Kay and Gast (1973) and Pearce and Cann (1973), and Pearce (1996) used Nb/Y ratios to separate basalt occurrences into alkaline and tholeiitic clans. Both Allègre et al. (1995) and Greenough et al. (2007) used exploratory statistical methods and trace element ratios (12 and 135, respectively) to show that ratios sort oceanic basalt into groupings that correspond with the isotope-defined mantle components. However, both studies found that ratios calculated from element pairs that have distinctly different incompatibility provide little or no information on source type. Further, Greenough et al. (2007) showed that all extremely dissimilarly incompatible element ratios (i.e. calculated from elements separated by ≥ 20 elements in the Sun and McDonough (1989) list) are highly correlated with one another, which is what is predicted if the percentage of melting controls ratio values. La and Yb are separated by ~25 elements on the Sun and McDonough (1989) list and we conclude that ratio values dominantly reflect the percentage of melting and provide a useful proxy for the percentage of melting.

The final step in the preparation of the dataset was to average the major elements, trace elements and incompatible element ratios for each individual island though these data are not used to estimate transition metal concentrations in 'primary' magmas from each island.

Statistical Methods

Linear regression was used to estimate transition element concentrations in 'primitive' magmas (Mg# = 0.72 = (Mg/(Mg + 0.9*Fe^{total}) atomic) = Mg/Fe^{total} wt. % of cations = 1.00) in each

end-member mantle component oceanic island. Default algorithms in SYSTAT v. 13 software identified outliers and high-leverage samples and in an iterative procedure, up to 20% of the data, for any one transition metal from one island, was eliminated to minimize the impact of outliers and high-leverage samples on the regression analyses. Anomalous data can come from human mistakes (sample mix-ups in the field, analytical errors, typographical errors, etc.) or natural processes (phenocryst accumulation, sample alteration, etc.) all of which can escape the major element total and LOI screens. The outlier and high-leverage sample screening eliminated those samples, but in general over 90% of the samples were retained in making primary-magma element concentration estimates from the regression analysis.

Next, we employed a powerful 'exploratory' statistical method, multidimensional scaling (MDS), and SYSTAT v. 13 software, to find the 'big picture' relationships between the islands using all the regression-derived transition metal data simultaneously. Exploratory data analysis techniques such as MDS and principal component analysis (PCA) cannot use information about possible sample relationships/groupings to influence results; sample relationships on plots simply reflect the geochemical data describing individual samples. MDS resembles PCA but is known for its ability to summarize variance in a small number of dimensions (Wilkinson et al. 1992; Borg and Groenen 1997, p. 1–14). Other advantages over PCA are that sample groups with small differences are not amalgamated, and the algorithms do not attempt to 'statistically' define sample groups. Thus the geochemist can look for groupings that reflect processes (e.g. % melting) or resemble groupings known about from other geochemical data (e.g. mantle components based on isotopes). However, MDS does not preserve the absolute distance between samples and without statistical grouping, output does not identify and weight geochemical parameters (i.e. individual transition metals and their concentrations) that create groups in PCA.

MDS produces 'maps' of island relationships with relative positioning given by Dimension 1 and Dimension 2 coordinates. Similar objects (islands) plot close together on a MDS diagram ('map') and dissimilar objects plot far apart. Matrices of island-versus-island Pearson correlation coefficients were used as distance measures that act as input for the MDS calculations. If the elements (transition metals from regression analysis) in each island were plotted against analogous concentrations in all other islands, two islands with identical transition metal abundances would produce a perfectly straight correlation line and yield a correlation coefficient of 1. These two islands would tend to plot atop one another on a MDS diagram but the correlation coefficients are only approximations of how similar two islands are. As an analogy, given a geographic map, accurate distance measurements from three points to a fourth determine the position of the fourth point. In the case of the OIB, the position of each island on the MDS 'map,' which is based on island-versus-island Pearson correlation coefficients calculated from the regression-determined transition metal concentrations, is over-determined because with 12 islands, there are 11 distances from one island to the other 11. The position of the 12th island is over-determined and the job of the MDS algorithms (the loss function) is to optimally place each island on the 'map,' relative to all other islands, given that the Pearson correlation coefficients, measuring geochemical 'distances' between islands, are only 'estimates.' Calculations proceeded as follows: 1) All elements were z-scored (standardized) to put them on the same scale so that each contributed equally to assessments of similarity; 2) a matrix of island-versus-island correlation coefficients was calculated from the z-scored data; and 3) this matrix was used along with linear MDS and a Kruskal loss function (SYSTAT default) to create the diagrams. MDS can also be used to compare the behaviour of chemical data; for example, when Ni is high are there other elements that tend to be high, or elements that behave the opposite of Ni? To compare chemical data, a matrix of element-versus-element correlation coefficients was calculated from z-scored data (step 2 above).

RESULTS/DATA

The linear regressions gave equations for lines through the transition metal-versus-Mg/Fe data for each island, and solving the equations for a Mg/Fe ratio of 1 (i.e. Mg# = 0.70) yielded the concentrations of nine transition metals in hypothetical primitive basalt from 12 oceanic islands (Table 1). Raw data for these regressions appears in Electronic Supplementary Materials[1] ESM Table-1, and plots of all regressions are given in ESM Table-2, with information on the regression lines (slope, intercept, probabilities = p-values) in ESM Table-3.

The results involved ~100 regressions that utilized over 600 rock samples. Every regression was plotted, visually inspected, and linearity confirmed (see caveats below) though some elements at some islands did not change in concentration with changing Mg/Fe. This confirmation of linearity is important because one could argue that changes in the phases or proportions of phases precipitating during differentiation could produce curved or kinked Mg/Fe-versus-element plots resulting in inaccurate estimates of element concentrations at Mg/Fe = 1. Complicated scenarios where a phase was precipitated/removed from a magma, and then added back in (e.g. xenolith addition), resulting in a magma Mg/Fe ratio resembling that from before the phase was removed, are possible. However, if the process resulted in the sample plotting significantly off the Mg/Fe-versus-transition metal regression line, our screening procedure that eliminated outliers ensured that the sample was removed. We conclude that, regardless of what minerals, mineral compositions or proportions of minerals are responsible for the linear relationships, they provide useful approximations of element concentrations in a 'primary' magma.

Figure 1 shows a few typical regressions (see ESM Table-2 for all plots). Averages (there are 12 islands) of the percentage errors on regression estimates for elements range from 6.3 (Fe) to 23 (Cu; see ESM Table-3) and average p-values (probabilities) on the correlation coefficients are between 0.004 and 0.027 (see ESM Table-3) indicating that the correlations tend

[1] Electronic supplementary materials (ESM Tables 1 through 4), are available at the GAC's open source GC Data Repository, Igneous Rock Associations link, at http://www.gac.ca/wp/?page_id=306.

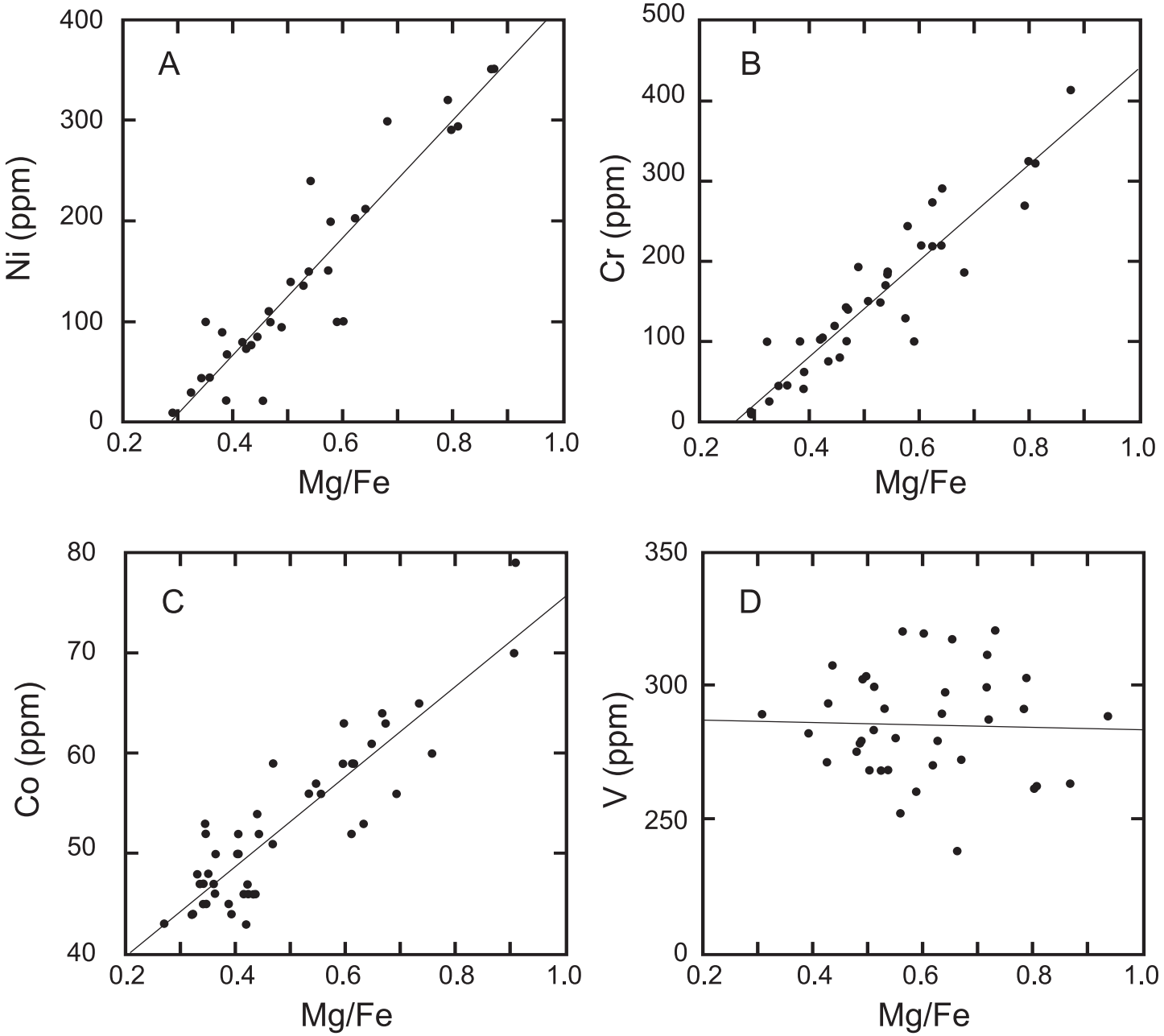

Figure 1. Example plots of transition metals (ppm) plotted against Mg/Fe (metal wt. % with Fe = total Fe) in selected oceanic islands. Data are those used to estimate Ni and Cr in 'primary' Gough basalt (A, B), Co for Tubuai (C) and V for São Miguel (D). Correlation coefficients for A, B, C, and D are 0.95, 0.91, 0.89, and 0.03 with p-values < 0.001 for Ni, Cr, and Co and 0.85 for V. Standard error of estimates are 34.7, 37.0, 3.60, and 20.2 respectively. Lines on the diagrams represent the least-squares regressions. All of the ~100 Mg/Fe regressions are shown in Electronic Supplementary Materials ESM Table-2. See text for discussion.

to be strong and estimates of element concentrations should yield useful approximations of transition metal abundances in primary magmas. Some elements show little change in concentration with changing Mg/Fe and so slopes on the regressions approach zero. An example is V in São Miguel basalt (Fig.1D; correlation coefficient, r = 0.03) and others can be identified with the % slope values in ESM Table-3. A low (absolute value) % slope indicates that the element is at the boundary between being compatible (decreases with diminishing Mg/Fe) and incompatible during differentiation. The data set for Kerguelen shows weaknesses with a few elements (Co, V, Cu) represented by only three samples in the regressions (ESM Table -3). Similarly, Co, V, Zn and Cu are only represented by three samples in the Tutuila data set. Most islands have a few samples with Mg/Fe values greater than 0.80 (Mg# > 0.67) (Table 1 and ESM Table-3) which provide assurance that the regression results can be extrapolated to a Mg/Fe ratio of 1.0. Eight of the twelve islands have samples within the range for a primary magma (Mg/Fe ≥ 0.87 or Mg# between 0.69 and 0.72). Just as importantly, these data show that primitive magmas with geochemistry consistent with pre-differentiation formation from Fo_{90} olivine-bearing peridotite exist on most islands. Upolu and Pitcairn have the lowest maximum Mg/Fe ratios of 0.76 and 0.48 (respectively; Mg# = 0.66, 0.55) and thus required the most extrapolation to estimate primary magma compositions. Irrespective of what the statistical data

suggest (e.g. high r, low p, small estimated percentage error; see ESM Table-3) the results for these islands need to be treated with more caution.

Le Roux et al. (2011) gave average Ni, Co, Zn, Mn, and Fe in EM1 (Pitcairn), and EM2 (Samoan Islands) and HIMU (Austral-Cook Islands) apparently derived from information in Jackson and Dasgupta (2008). Most values are within 10% of average EM1, EM2 and HIMU using data in Table 1, with two ~ 15% different, and three 20–25% different. Thus our results are quite similar, but more detailed comparisons are difficult because the results here are more comprehensive.

The Mg/Fe regression results (e.g. Fig. 1) compensate for differentiation in estimating transition metal abundances in primary magmas, but differences in element concentrations between islands and/or the mantle component types EM1, EM2, HIMU may be impacted by the percentage of melting. Figure 2 shows four example elements (Ni, Cr, Zn and Cu) plotted against average La/Yb (a proxy for the percentage of melting) for each island, confirming that concentrations can be affected by the percentage of melting. Results for all nine elements are summarized as follows. Ni, Cr (Fig. 2) and Mn show moderately strong to weak negative correlations with La/Yb (r = -0.60, -0.61 and -0.29 with p = 0.029, 0.026, and 0.34; respectively). Zinc provides an example of a modestly positive correlation, and Cu shows no significant correlation with La/Yb (Fig. 2). Correlation coefficients for V, Fe, Zn, Co, Sc, and Cu are 0.55 0.45, 0.41, 0.34 0.09 and 0.03 with p = 0.07, 0.13, 0.16, 0.26, 0.81 and 0.92 (respectively).

DISCUSSION

Element Relationships and Percentage Melting

Element behaviour during melting was qualitatively assessed using MDS. Each element in Table 1 was z-scored to put it on the same scale, a matrix of element-versus-element Pearson correlation coefficients was prepared, and this matrix used to create a multidimensional scaling (MDS) 'map' (Fig. 3). Proxies for the percentage of melting (La/Yb, Nb/Y and their inverse ratios; e.g. Kay and Gast 1973; Pearce and Cann 1973) were included in all steps of the MDS calculations. Objects (elements or element ratios) showing the strongest antithetic behaviour tend to plot across the X-axis (Dimension 1) of MDS diagrams. Objects showing weaker antithetic behaviour and generally reflecting a subsidiary process, plot along the Y-axis (Dimension 2). Simple X-Y plots of La/Yb versus Yb/La or Nb/Y versus Y/Nb will yield perfect negative correlations (r = –1). Thus, La/Yb and Yb/La should occur on opposite sides of a MDS diagram along Dimension 1, and La/Yb and Nb/Y (as well as Yb/La and Y/Nb) should plot close together if controlled by the percentage of melting. Figure 3 shows this is the case. Slight separation of La/Yb and Nb/Y (they do not plot exactly atop one another) is consistent with source composition having some effect on the plotting position of the two ratios. Significantly, Ni occurs close to and between Y/Nb and Yb/La on the opposite side of the diagram from La/Yb and Nb/Y. We conclude that Ni is strongly compatible and as the percentage of melting goes up, Ni concentrations increase, and La/Yb and Nb/Y ratios go down. Other apparently compatible elements on the left-side of Figure 3 include Co and Cr. Most other transition metals plot between values of 0 and 1 along Dimension 1 suggesting they are slightly incompatible, but they are also affected by a secondary process, such as source region composition, that causes them to plot along Dimension 2 with Zn behaving antithetically to Cu and Sc (Fig. 3). Possible causes for these Zn–Cu–Sc relationships are examined below, where origins of the mantle components are discussed.

Transition metal concentrations in Table 1 were regressed against average La/Yb ratios using all islands regardless of whether they were EM1, EM2 or HIMU islands. The data produce clear, highly significant ($p < 0.06$) trends for Ni and Cr (Fig. 2); separate regressions by individual mantle type do not appear to be justified. Table 2 gives all regression results (slope, intercept, correlation coefficient, probability) and shows that apart from Ni and Cr, most elements are moderately to poorly correlated with La/Yb. Negative slopes indicate compatible behaviour and positive slopes modest incompatibility, though an alternative interpretation is that temperature affects bulk partitioning coefficients. Bulk partitioning coefficients cannot be determined without many assumptions but, taking the regression results at face value, *relative* compatibility or incompatibility of elements during melting can be estimated by using the regression equations to calculate an enrichment or depletion factor. The column labelled 'Factor' in Table 2 gives the ratio of the concentration of an element at La/Yb = 10 divided by the concentration of the element at La/Yb = 40, for compatible elements, with the concentrations determined from the overall regression equations. Similarly, for somewhat incompatible elements Factor was calculated from the concentration at La/Yb = 40 divided by that at La/Yb = 10. The Factor values were assigned + and – signs depending on whether the element was incompatible or compatible. These Factor values suggest that Cr, Sc, Cu, Ni, Co, Fe, and Mn are compatible (decreasing compatibility in that order), and Zn and V may show modest incompatibility. Lee et al. (2005) indicated that V and Sc should show somewhat similar compatibility during melting of spinel lherzolite but in the presence of garnet, the case for OIB, they note that Sc will become more compatible.

We caution that the low correlation coefficients with high p-values (≥ 0.5) for many of these regressions suggest the estimates of relative compatibility or incompatibility are crude. However, a similar analysis of relative compatibility performed on the Mg/Fe regressions indicates decreasing compatibility during differentiation in the order Cr, Ni, Sc, Cu, Co Fe, V, Mn, Zn with a change from compatible to incompatible around Fe and V. Thus, to a first approximation, the inferred order of compatibility is very similar during melting and differentiation.

Lee et al. (2012) reviewed Cu concentrations in arc magmas and MORB and modelled the effect of source Cu and S concentration, mineral modes and oxygen fugacity ($f(O_2)$) on magma Cu concentrations. Their results suggest that the oxygen fugacity in MORB and arc sources must be low enough to keep S in the S^{2-} state, which stabilizes sulphide phases and makes Cu compatible, because both have low, nearly identical primary magma Cu concentrations (60–70 and 50–90 ppm, respectively). As noted above, taken at face value, the La/Yb regression suggests that Cu is overall compatible (Fig. 2; Table 2), indicating that, like MORB and arc sources, $f(O_2)$ is low enough to stabilize sulphide phases. Further, our mean concentrations for Cu in EM1 and EM2 magmas (58 and 73 ppm, respectively) are essentially identical to those for MORB and

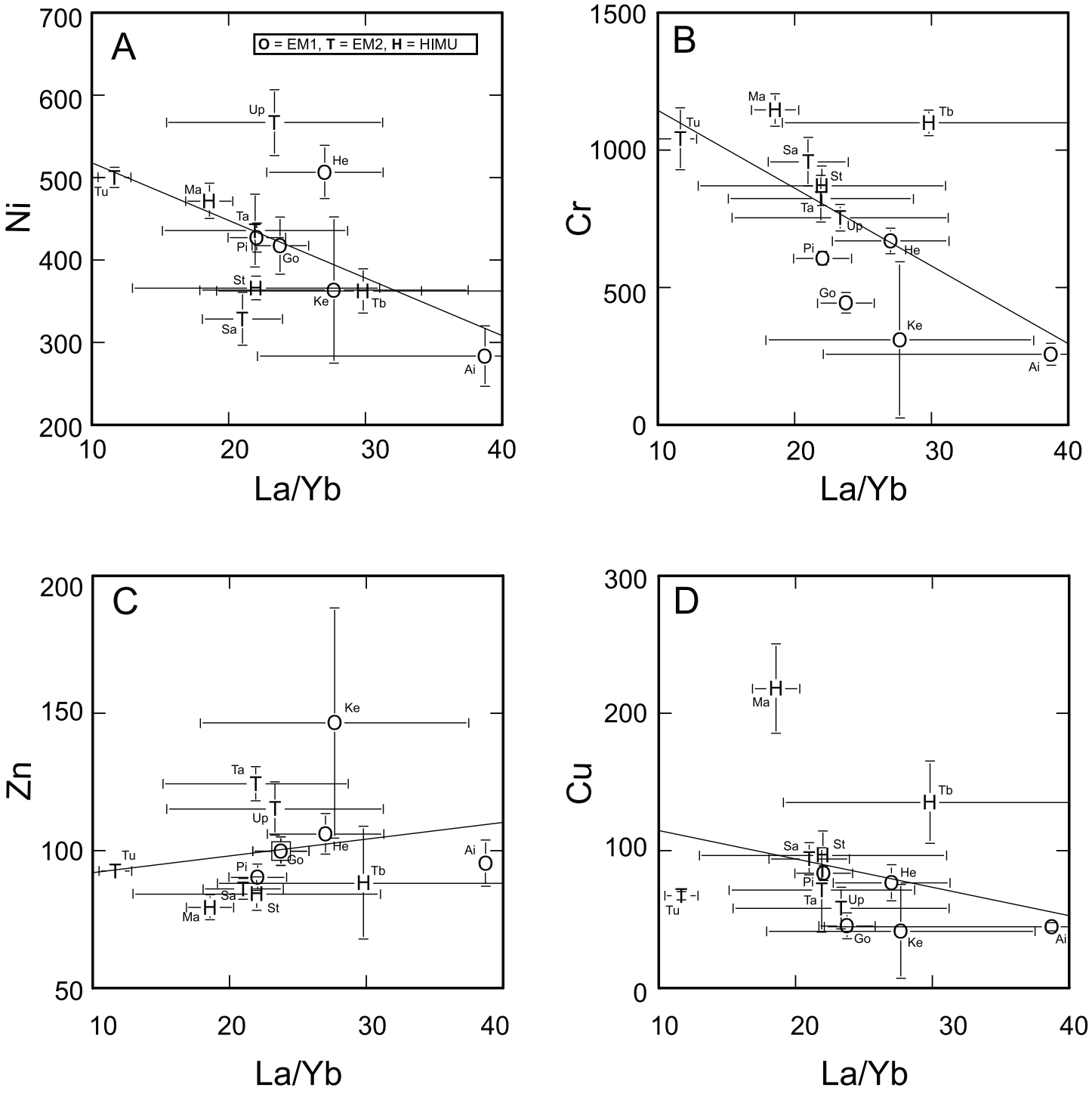

Figure 2. Example plots of estimated primary magma concentrations of transition metals (from Mg/Fe regressions; e.g. Figure 1) in end-member OIB plotted against La/Yb, a proxy for the percentage of melting. Error bars on data points represent the standard deviation on the mean La/Yb ratio for each island and the standard error of estimate on transition metal concentrations from the Mg/Fe regressions (ESM Table-3). Symbols: O = EM1, T = EM2, and H = HIMU. Island symbols are: Aitutaki = Ai, Gough = Go, Herd = He, Kerguelen = Ke, Mangaia = Ma Pitcairn = Pi, São Miguel = Sa, St. Helena = St, Tahiti = Ta, Tubuai = Tb, Tutuila = Tu, Upolu = Up. Lines represent linear least squares regression through data with r = -0.56, -0.62, 0.21, -0.28 and p = 0.06, 0.03, 0.52, and 0.39 for Ni, Cr, Zn and Cu, respectively.

arc magmas. However, the HIMU average is much higher (150 ppm), consistent with either higher source Cu concentrations, or a more oxidized source (S as SO_4^{2-}). Only three HIMU islands are included in the study, but Figure 2D indicates Cu is compatible during melting even for these islands consistent with their sources having high Cu concentrations as opposed to being oxidized.

It is possible that the La/Yb regression slopes reflect temperature effects on bulk partition coefficients. Le Roux et al. (2011) measured olivine/melt and orthopyroxene/melt partitioning coefficients indicating that Mn, Fe, Co, Ni and possibly also Zn become less compatible with increasing temperature but calculated bulk peridotite/melt coefficients suggesting that Fe and Zn show little temperature dependence, with Mn sub-

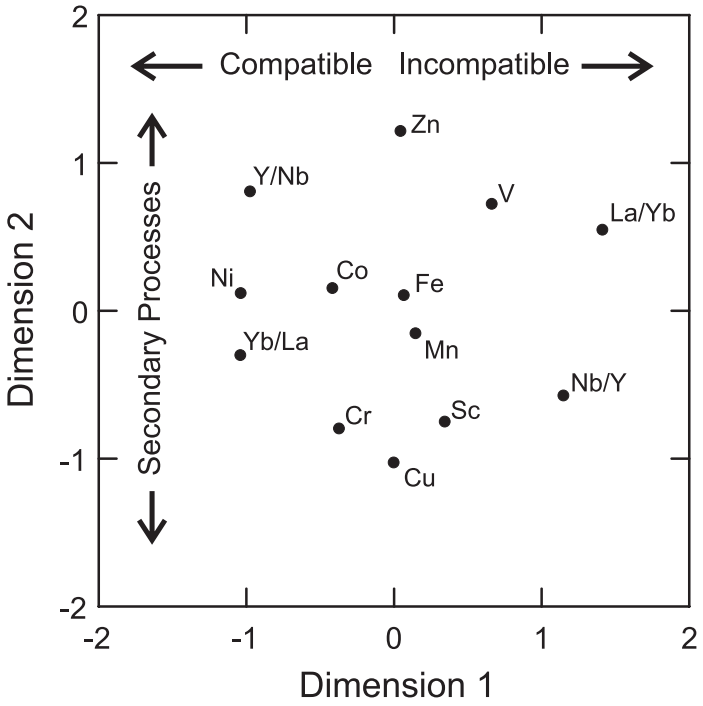

Figure 3. Multidimensional scaling diagram illustrating relationships between transition metal abundances and proxies for the percentage melting (La/Yb and Nb/Y and their inverses) in primary (Mg/Fe wt. % = 1) oceanic island basalts. Dimension 1 and Dimension 2 can be thought of as 'map coordinates.' Objects (e.g. two elements) that plot close together will have a high element-versus-element correlation coefficient. Compatible elements (e.g. Ni) plot toward the left whereas less-compatible to modestly incompatible elements plot somewhat to the right along Dimension 1. Some secondary process or processes (e.g. source region compositional variation) causes elements to spread out along Dimension 2. See text for discussion. To produce the diagram, elements and ratios were z-scored and a matrix of element (or ratio)-versus-element correlation coefficients were prepared and processed in SYSTAT MDS software using a Kruskal loss function and linear multidimensional scaling. Diagram uses data from Table 1.

tly more compatible, and Co less compatible, with increasing temperature. Assuming that temperature increases with depth, and given the strong positive correlation between La/Yb and pressure (Greenough et al. 2005b), lower concentrations for most metals at high La/Yb could reflect increased compatibility at higher temperatures. Given the information from Le Roux et al. (2011) for a minor impact of temperature on bulk D values, the simplest explanation for any metal concentration correlations with La/Yb from this study is that they reflect the percentage of melting.

Estimates were made for transition metal concentrations in a primary magma with a La/Yb ratio of 10 (Table 2), a value that divides tholeiitic from alkaline OIB (Greenough et al. 2005a, b) and all islands here are at least subtly alkaline (La/Yb $\geq$ 10; Fig. 2). The La/Yb-adjusted concentrations were calculated by moving an element's island concentration (Table 1) parallel to the overall La/Yb versus element regression slope in Table 2, to a La/Yb value of 10.

Using these data, a MDS diagram was prepared (not shown) but unlike Figure 3 it reveals a 'random' distribution of the La/Yb-adjusted transitional metals, none of which plot close to indicators of melting percentage (e.g. La/Yb). Thus, the normalization procedure discussed above removed any clear dependence of metal abundance estimates on the percentage of melting. The compatible behaviour of Cr, Ni and

Table 2: La/Yb regression results and transition metal concentrations in primary oceanic island basalts adjusted to a common La/Yb ratio of 10.

Island transition metal concentrations at La/Yb = 10.[b]													Regression coefficients and statistics[a]				
Island	Aitutaki	Gough	Heard	Kerguelen	Pitcairn	São Miguel	Tahiti	Tutuila	Upolu	Mangaia	St. Helena	Tubuai	S^i	C^i	r	p	Factor
Is. Abbrev.	Ai	Go	He	Ke	Pi	Sa	Ta	Tu	Up	Ma	St	Tb					
Type	EM1	EM1	EM1	EM1	EM1	EM2	EM2	EM2	EM2	HIMU	HIMU	HIMU					
Cr	1072	835	1153	812	949	1271	1162	1090	1133	1391	1211	1662	-28.3	1428	-0.624	0.030	-3.89
Ni	484	513	625	487	511	405	519	512	660	531	450	501	-6.97	586	-0.556	0.060	-1.68
Co	76	83	130	86	47	55	89	99	73	93	84	92	-0.813	92.0	-0.246	0.441	-1.41
Sc		44	49	52		44	89		37	63	72	77	-1.31	71.5	-0.258	0.503	-3.05
V		136	213	320	135	236	250	229	159	168	376	170	4.28	175	0.263	0.433	1.59
Zn	78	91	96	136	83	79	117	91	107	74	77	76	0.609	86.0	0.205	0.522	1.20
Cu	104	74	112	78	108	117	96	71	86	236	122	176	-2.06	136	-0.275	0.387	-2.16
Mn	1252	1132	1262	1284	752	1319	1376	1338	1227	1441	1029	1415	-1.06	1246	-0.036	0.910	-1.03
Fe	89464	91374	98947	92369	53206	103453	101883	92045	109163	94221	99129	97456	-438	97940	-0.203	0.528	-1.16

Notes:
[a] S^i = regression slope for element i. C^i = regression constant (y intercept) for element i. r = correlation coefficient. p = probability..
[a] Regression equation is $T^i = S^*La/Yb + C^i$ where T^i = concentration of Transition element i at specified La/Yb ratio.
[a] Factor = the multiplying factor for the element between La/Yb = 10 and La/Yb = 40 from regression equation. + = positive slope; – = negative.
[b] Estimates of all element concentrations (ppm) except Cu and Sc used island element concentrations and La/Yb ratios in Table 1 with Cu and Sc concentrations in this table the same as in Table 1.
[b] Estimates were made using the slopes (S) given above, equations discussed in the text, and a La/Yb ratio of 10.

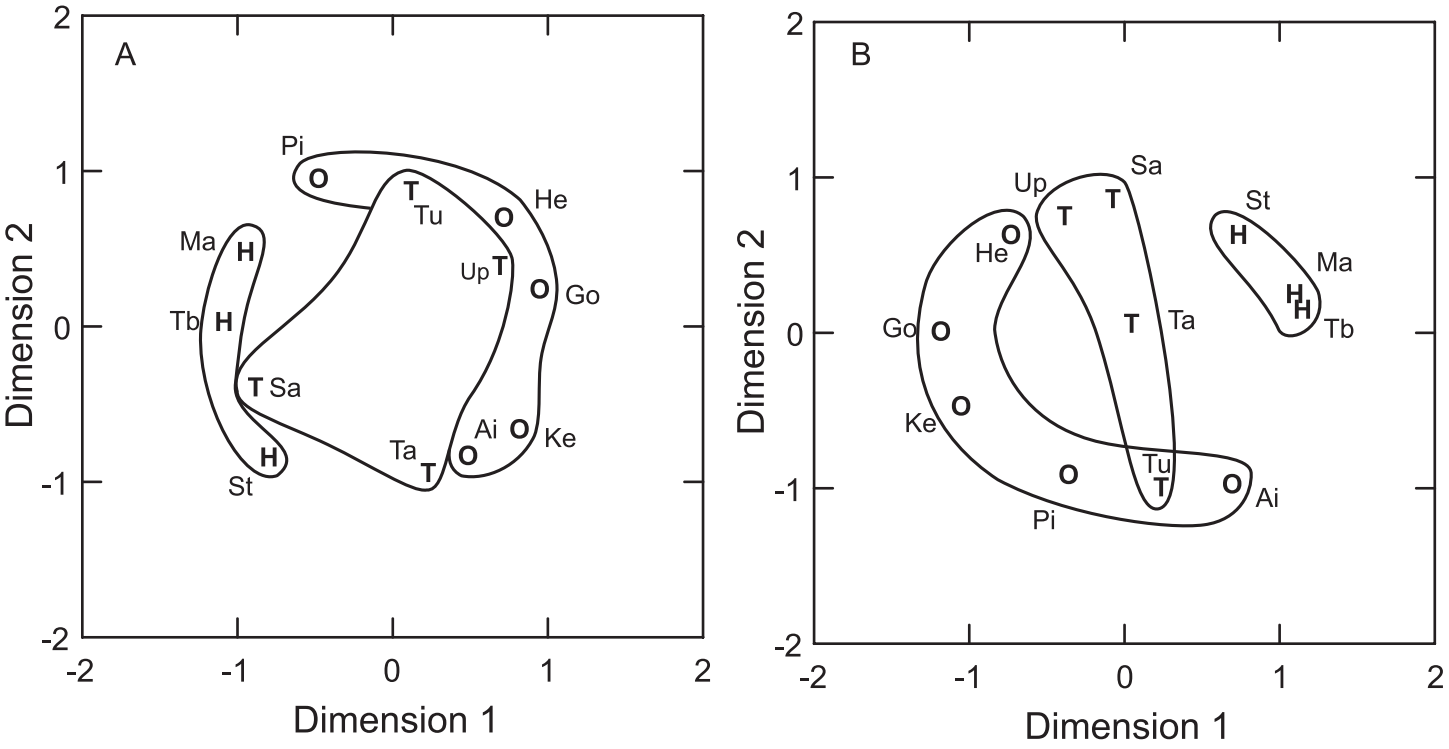

Figure 4. Multidimensional scaling (MDS) diagrams showing island relationships based on A) estimated transition metal abundances for each island (Table 1) and B) similarly incompatible element ratios (SIER; ratios and data in ESM Table-4). For each plot, Dimension 1 and Dimension 2 resemble map coordinates. Islands that plot close together would have a high island-versus-island correlation coefficient using the transition metal data (Fig. 4A) or SIER (Fig. 4B). Hand-drawn fields emphasize that EM1, EM2 and HIMU islands (symbols O, T and H respectively) tend to fall in the same area of each plot. To prepare the diagrams, transition elements (4A) and SIER ratios (4B) were z-scored and matrices of sample-versus-sample correlation coefficients prepared and processed in SYSTAT MDS software using a Kruskal loss function and linear multidimensional scaling. Island abbreviations are Aitutaki = Ai, Gough = Go, Herd = He, Kerguelen = Ke, Mangaia = Ma, Pitcairn = Pi, São Miguel = Sa, St. Helena = St, Tahiti = Ta, Tubuai = Tb, Tutuila = Tu, Upolu = Up.

Co during melting means that primary tholeiitic OIB (La/Yb ~ 5; e.g. Mauna Loa average, Greenough et al. 2005b) will have higher Cr, Ni and Co concentrations than the alkali basalt examples in this study (extrapolate Ni and Cr trends in Fig. 2). The following section looks at patterns in the transition metal data related to mantle component type keeping in mind the impact of melting.

Transition Metals and the Mantle Components

A problem with analyzing multi-element geochemical data sets using inferential statistics is that it is all too easy to find some element or combination of elements that fortuitously confirms pre-conceived notions about how samples should be related. The advantage of starting the analysis with an exploratory statistical tool such as MDS is that all element data can be used simultaneously to uncover the dominant relationships between samples (islands). In addition, the software does not know one island from another, and patterns that emerge are purely a reflection of relationships in the input data and are unlikely to be fortuitous. Once the dominant relationships have been ascertained, it is possible to use inferential techniques with more confidence to understand the causes of these relationships.

The MDS diagram in Figure 4A shows overall island relationships using all estimated transition metal abundances in primary magmas (Table 1) unadjusted for the percentage of melting. To prepare Figure 4A, Table 1 data were z-scored (each element put on the same scale), a matrix of sample-versus-sample Pearson correlation coefficients calculated, and these data used with linear regression and a Kruskal loss function to yield Figure 4A. As shown, EM1 appears distinct from HIMU but EM2 islands are less distinct and plot between or overlap onto fields for EM1 and HIMU. Another MDS diagram (not shown) was prepared from the La/Yb-adjusted transition metal abundances (Table 2) but it is very similar to Figure 4A. Reasons why the La/Yb-adjusted and unadjusted data sets lead to similar MDS diagrams include: 1) the percentage of melting impacts the most compatible and most incompatible element concentrations, but some, or most elements are relatively unaffected (neither strongly incompatible or compatible); 2) nearly 80% of the islands, have somewhat similar La/Yb ratios that fall between 20 and 30 and thus these islands formed from similar percentages of melting; 3) 'similarity' between islands was determined using Pearson correlation coefficients; primary basalt from two islands formed from identical source regions but from somewhat different percentages of melting will show different concentrations for many elements, but this does not mean that they will not be highly correlated. In other words the use of correlation coefficients as a distance measure mitigates the impact of the percentage of melting. Due to the fewer assumptions associated with the derivation of the 'primary magma' compositions in Table 1, subsequent discussion focuses on these data.

The organization of islands by component type based on the transition metal data (Fig. 4A) resembles results if similarly incompatible element ratios (SIER) are used to compare islands (Fig. 4B) with MDS methods detailed in Greenough et al. (2007). Elements with similar bulk distribution coefficients

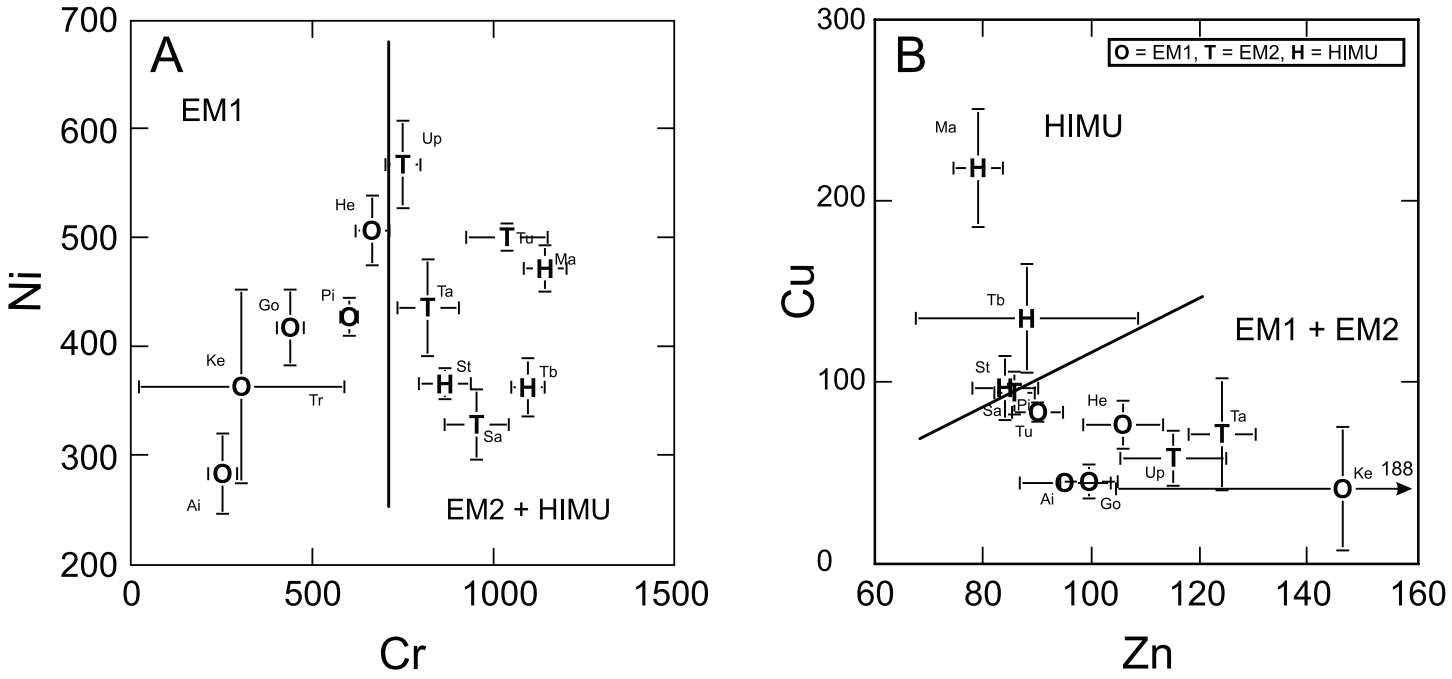

Figure 5. Discrimination diagrams separating end-member mantle component islands (symbols: O = EM1, T = EM2, H = HIMU). Hand-drawn lines suggest dividing lines between data for component island types. Error bars represent the standard error of estimate from Mg/Fe regressions. Island abbreviations are Aitutaki = Ai, Gough = Go, Herd = He, Kerguelen = Ke, Mangaia = Ma, Pitcairn = Pi, São Miguel = Sa, St. Helena = S,; Tahiti = Ta, Tubuai = Tb, Tutuila = Tu, Upolu = Up. All concentrations are in ppm. Plots derived from data in Table 1 with standard error of estimate values given in Electronic Supplementary Materials ESM Table-3.

(i.e. separated by ≤ 10 elements in the Sun and McDonough (1989) relative incompatibility list) should have ratios in magmas that approach mantle source values, and the ratios will not vary with the percentage of melting. Ratios are also minimally impacted by differentiation. If the ratio for two similarly incompatible elements varies between islands, the variation probably reflects differences in source region composition. The fifty ratios used here (ESM Table-4 which also gives ratio calculation procedures), involving 22 incompatible elements, were identified in Greenough et al. (2005b) as useful for distinguishing OIB mantle components. Figure 4B shows that these SIER separate EM1, EM2 and HIMU basalts but like the transition metals, EM2 tends to be intermediate between EM1 and HIMU. Based on Figure 4A and 4B, it appears that patterns in transition metal abundances are dominantly tied to mantle component type and thus likely related to recycling of lithospheric materials back into the mantle.

Chromium effectively separates EM1 from EM2 and HIMU islands (Fig. 5A). Copper–Zn relationships separate HIMU from EM1 and EM2 (Fig. 5B). Other than Cr, the only elements that tend to distinguish EM1 and EM2 are Fe and possibly Mn. Scandium can also effectively separate EM1 from HIMU. Nickel, Co and V concentrations are similar in all three groups. Thus, the distinctions between the mantle components are subtle and it is only when all data are assessed simultaneously (Fig. 4A) that clear patterns emerge. The situation is similar with SIER where individual ratio-versus-ratio plots do not, in general, unambiguously separate end member islands (Greenough et al. 2005b, 2007) but use of many ratios simultaneously distinguishes the mantle components on MDS plots (Fig. 4B).

Origins of the Mantle Components

Proposals for origin of the end-member mantle components (HIMU, EM1, EM2, DMM = Depleted MORB mantle, FOZO = Focal Zone) are well discussed in the literature (Zindler and Hart 1986; Sun and McDonough 1989; Hart et al. 1992; Hofmann 1997; Hilton et al. 1999; Bennett 2003; Hofmann 2003; Jackson and Dasgupta 2008). A popular hypothesis suggests that HIMU sources contain subduction-processed ocean floor basalt (Hofmann 2003; Greenough et al. 2005b, 2007). EM1 and EM2 tend to be ascribed to sediment subduction but the signatures are strongest in basalt that formed from melting subcontinental lithosphere (Hawkesworth et al. 1986; Weaver 1991; Milner and le Roex 1996; Greenough and Kyser 2003). The time of formation of the mantle components is poorly constrained but Said and Kerrich (2010) and Manikyamba and Kerrich (2011) have shown that HIMU existed since the Neoarchean and may still be forming. EM1 appears to be Archean, whereas EM2 may be Proterozoic or younger (Tatsumi 2000; Greenough and Kyser 2003; Greenough et al. 2005b, 2007).

The transition metal-based MDS results (Fig. 4A) show OIB islands group based on mantle component type. Average transition metal concentrations for EM1, EM2 and HIMU (Table 3) are shown on primitive mantle-normalized diagrams in Figure 6. T-tests comparing individual mean compositions of EM1, EM2 and HIMU islands indicate that Zn is lower in HIMU compared to EM1 ($p = 0.08$) and EM2 ($p = 0.11$), supporting hypotheses that HIMU sources have been depleted in chalcophile elements (Pb, Zn) as a result of element extraction from ocean floor basalt during subduction processing and transfer of these elements to the continental lithosphere (Hofmann 1997, 2003). The model suggests that high-field-strength elements (e.g. U, Th) were not transferred by this process.

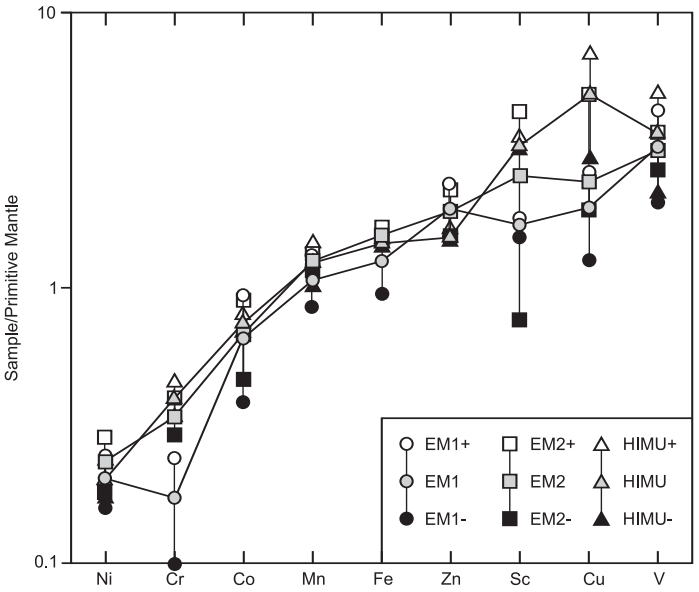

Figure 6. Primitive mantle normalized patterns for averaged primary magma EM1, EM2 and HIMU transition metal concentrations (Table 3). Elements are organized along the x-axis based on average enrichment compared to primitive mantle. Error bars (e.g. EM1+ and EM1-) represent the standard deviation on mean metal concentrations (Table 3) for each island type. Note the log scale on the Y axis. Primitive mantle normalizing values are from McDonough (2003).

However, chalcophile Cu appears higher in HIMU sources compared to EM1 ($p = 0.12$) and EM2 ($p = 0.16$; Fig. 6) perhaps because it was not as efficiently extracted from the ocean floor source as Zn. Chromium tends to have a 3+ charge and it might be predicted that, like other high-field-strength elements (U, Th) it should be enriched in HIMU sources (not transferred to the lithosphere). The t-tests and Figure 6 show that this is the case when comparisons are made with EM1 sources ($p = 0.004$), but EM2 is not distinctive ($p = 0.24$). Similarly, Sc is higher in HIMU compared to EM1 ($p = 0.0006$). To conclude, comparing EM1 and EM2 transition metal abundances to those in HIMU supports the hypothesis that HIMU represents subduction-processed lithosphere now part of the convecting oceanic mantle.

Nickel, Co, and V are similar in primary magmas from all three types of source regions but t-tests indicate that Cr ($p = 0.004$), Fe (0.05) and Mn (0.13) (Fig. 6) are lower in EM1 compared to EM2 (Fig. 6; Table 3). Assuming that both are sediment signatures superimposed on subcontinental lithosphere and EM1 is Archean and EM2 Proterozoic (or younger), differences in Cr, Fe and Mn could reflect how elements were transferred between the subducting slab and overlying lithosphere. High Archean heat flow resulted in continent-forming melt transfer from the slab whereas cooler Proterozoic processes yielded fluid transfer to the overlying mantle lithosphere in association with the major craton-stitching orogenic events *circa* 1.8 Ga (Hoffman 1988; Drummond and Defant 1990). Melt transfer may have more efficiently removed Cr, Fe and Mn from subducted sediment during the Archean leaving EM1 sources depleted in these elements.

Alternative explanations for differences in Cr, Mn and Fe between EM1 and EM2 include differences in mantle oxidation state or the proportions of garnet and clinopyroxene in source regions. These elements have multiple valence states,

Table 3: Average transition metal concentrations in primary EM1, EM2 and HIMU.

Island	Av. EM1	SD	Av. EM2	SD	Av. HIMU	SD
Cr	457	180	894	130	1038	148
Ni	399	83	458	102	400	62
Co	70	30	71	22	79	6.1
Sc	27	2	41	29	53	2.7
V	266	98	259	40	296	117
Zn	108	23	105	18	84	4.5
Cu	58	20	73	15	150	62
Mn	1117	219	1305	66	1281	230
Fe	77228	17194	97461	4971	91015	2597

Notes: Number of islands for EM1, EM2 and HIMU, most elements = 5, 4, and 3.
Exceptions: Sc = 3 EM1 and 3 EM2; and V = 4 EM1 due to no data for some islands.
All concentrations are in ppm of the metal.

and magmatic concentrations may reflect increasing oxidation (e.g. Holland 1984; Rouxel et al. 2005) of subducted sediment between the Archean (EM1) and Proterozoic (EM2). Le Roux et al. (2010) theorized that high source region $f(O_2)$ should result in low magmatic Zn/Fe and high Fe/Mn. Lee et al. (2010) looked at Zn/Fe in more detail and concluded that primitive arc magmas, primitive MORB, and mantle peridotite have Zn/Fe * 10^4 ratios between 8 and 11 consistent with an upper mantle $f(O_2)$ value between FMQ-1 and FMQ+1 (log units) as found by other studies (Lee et al. 2005, 2012; Mallmann and O'Neill 2009). Our Zn/Fe ratios (mean of all values, Table 1 = 11.9; Fig. 7) are identical to those for OIB reported by Le Roux et al. (2010; Zn/Fe * 10^4 = 9.6–13.9) though Kerguelen and Pitcairn (17 and 19) are high. The mean for EM1 (14.4) is higher than the mean for EM2 (10.7; $p = 0.08$) and HIMU (9.2) potentially consistent with lower $f(O_2)$ in EM1 sources. However, mean Fe/Mn ratios for EM1, EM2 and HIMU are similar (68, 75 and 73, respectively) and assuming restricted variability in mantle $f(O_2)$ (e.g. Mallmann and O'Neill 2009; Lee et al. 2010, 2012), high Zn/Fe in EM1 does not appear related to oxidation. Following arguments in Le Roux et al. (2010) to explain higher Zn/Fe in OIB compared to MORB, it may be that EM1 sources have high Zn/Fe, or be more garnet- and/or clinopyroxene-rich compared with HIMU and EM2.

Comments on Metallogenesis

A few (< 20) large intrusions supply most of the world's Ni, Co, Cr, and PGE (platinum-group elements) (e.g. Best 2003, p. 331). They may be ore-bearing because they formed from magmas with 'compatible' element concentrations maximized by high percentages of melting, or other factors (e.g. sulphur fugacity) may have impacted deposit formation (e.g. Lee 1996; Naldrett 2005; Mungall and Naldrett 2008). They are noritic (Kerrich et al. 2005) and bear extreme EM1-like Ba/La and Rb/Ba signatures (Zhang et al. 2008; Said and Kerrich 2010; Greenough et al. 2011) that contrast with uneconomic intrusions bearing HIMU and EM2 signatures (Zhang et al. 2008). The regression results (Table 2) predict high Cr, Ni and Co (1300, 570 and 90 ppm, respectively) in high % melting, rift or

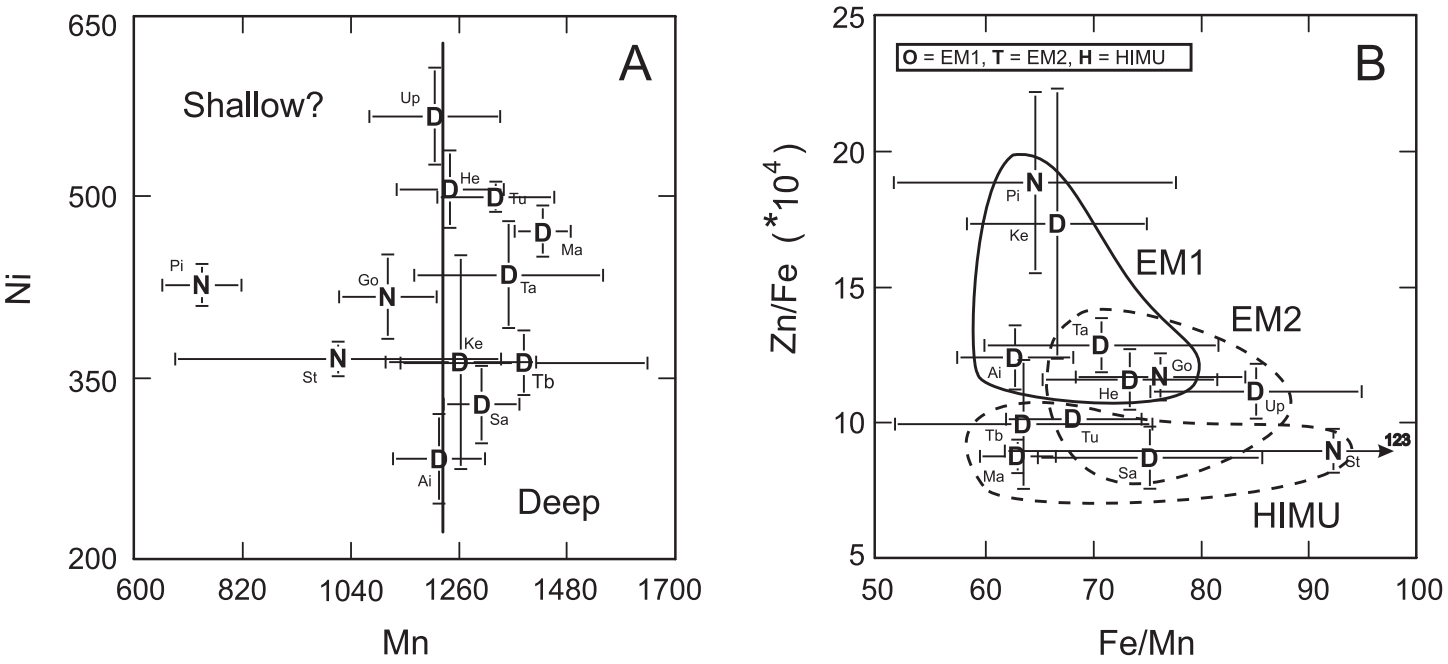

Figure 7. Plots of Mn versus Ni (A) and Fe/Mn versus Zn/Fe (* 10^4) (B) in studied OIB. Sample symbols are D = Deep plume and N = Not 'seen' (shallow?) from the Montelli et al. (2006) seismic tomography study. In B) hand-drawn fields circle EM1, EM2 and HIMU islands as labeled. Island abbreviations are Aitutaki = Ai, Gough = Go, Herd = He, Kerguelen = Ke, Mangaia = Ma, Pitcairn = Pi, São Miguel = Sa, St. Helena = St, Tahiti = Ta, Tubuai = Tb, Tutuila = Tu, Upolu = Up. Mn and Ni in ppm with Fe/Mn and Zn/Fe ratios calculated from ppm data (Table 1). Error bars come from the standard error of estimate values given in Electronic Supplementary Materials ESM Table-3.

superplume magmas (e.g. La/Yb = 2). The Cr and Ni values resemble those in picritic Deccan basalt (1500 and 665 ppm, respectively) and olivine-rich Karroo basalt (960 and 800 ppm, respectively; primary magmas; Basaltic Volcanism Study Project 1981, p. 409–432). Thus, our results confirm that for Ni, Cr and Co, economic potential is enhanced by a high % melting but they do not support EM1 sources having anomalously high concentrations of these elements. In the case of Cr, EM1 sources may have lower concentrations than either HIMU or EM2. Thus other EM1 characteristics, such as sulphur availability or solubility and/or magma oxygen fugacity may lead to element scavenging and concentration to form ore deposits.

Mineralogical and Lithological Composition of the Mantle

Elements discussed here have been used to test for core–mantle interaction, a sediment contribution to the sources of some enriched-mantle component magmas, and olivine-free (pyroxenite) mantle source lithologies. Sobolev et al. (2005) argued that high Ni content in Hawaiian olivine reflects precipitation from high Ni magmas generated from low melting point eclogite (recycled basaltic oceanic crust) after reaction with peridotite to produce pyroxenite. Pyroxenite melts variably mixed with peridotite melts yielding magmas with high Ni contents because olivine-free pyroxenite would have a lower bulk crystal/liquid partitioning coefficient than magmas from sources bearing olivine. Sobolev et al. (2007) expanded on the model. Gurenko et al. (2009) tested it using Canary Islands basalt where some rocks have extreme HIMU signatures that should show the high-Ni signature well. Extreme HIMU signatures, reflected in high $^{206}Pb/^{204}Pb$ and $^{207}Pb/^{204}Pb$ isotopic ratios are commonly ascribed to source enrichment in aged, recycled, oceanic basaltic crust that will form eclogite at pressure. Using modified equations by Sobolev et al. (2007) to predict the relative proportions of peridotite and pyroxenite involved in melting, Gurenko et al. (2009) concluded that the isotopically most extreme HIMU Canary Islands samples come from peridotite, as opposed to pyroxenite-rich sources. Herzberg (2011) used existing experimental major element data, Ni and Mn data, numerical models for predicting source mineralogy/lithology, magma composition and olivine compositions, and a solid-state, recycled crust-mantle peridotite reaction model for production of pyroxenite (different from Sobolev et al. 2005, 2007 and Gurenko et al. 2009 cited above) to conclude that Ni, Ca, Mn, and Fe/Mn data for olivine phenocrysts from Hawaii and the Canary Islands support the pyroxenite source model.

Our results do not show any clear difference in the Ni content of magmas from each of the mantle components and thus provide no support for the idea that HIMU (eclogite/pyroxenite-rich) sources produce high-Ni magmas. Similarly, Sobolev et al. (2007) predicted that pyroxenite-derived melts will have higher Fe/Mn ratios and higher Si than peridotite-derived melts. Although our Fe/Mn ratio for St. Helena is high, the other two HIMU islands have among the lowest Fe/Mn ratios (Table 1). A study of the major element composition of end-member mantle component OIB (Jackson and Dasgupta 2008) concluded that HIMU islands have lower Si contents and the low Si does not appear related to high-pressure melting. Thus, overall, these observations do not support a pyroxenite or olivine-free-source model.

Wang and Gaetani (2008) did Ni partitioning coefficient experiments and concluded that reaction of an eclogite-derived melt with olivine (peridotite) can yield Si-enriched melts with moderate Ni contents that precipitate high-Ni olivine. They argued that an olivine-free 'hybrid' pyroxenite source, as proposed by Sobolev et al. (2005), is not required to

explain high-Ni contents in Hawaiian lavas. Gurenko et al. (2009) argued that the Wang and Gaetani (2008) results cannot account for variations in Fe/Mn ratios but as noted above, there is no clear support for olivine-free sources from Fe/Mn ratios. Humayun et al. (2004) and Qin and Humayun (2008) recognized the potential utility of Fe/Mn ratios for testing hypotheses on the origin of OIB but were concerned about the analytical integrity of existing data sets for resolving arguments. Their high-precision Fe and Mn measurements were used to argue for high Fe in OIB. This was ascribed to core–mantle interaction but they could not rule out the possibility that mantle pyroxenite (model by Sobolev et al. 2005, 2007) influences or controls ratios. The seven samples they analyzed from Tahiti (EM2) have an average Fe/Mn ratio of 67 (ratio here = 71) and the three from St. Helena (HIMU) gave a low average ratio (57) compared to what we obtained (92; Table 1) but their St. Helena ratio resembles the ratios of other HIMU-type islands studied here (Mangaia = 63; Tubiai = 64; Table 1). Perhaps pyroxenite is important in the generation of HIMU OIB, but based on the predictions from the afore-mentioned experiments, our data do not appear to support the hypothesis because critical elements (Ni, Fe, Mn) and ratios (Fe/Mn) are not substantially different for other types of OIB (EM1; EM2). A caveat is that EM1 and EM2 may represent other types of pyroxenite sources modified by the addition of subducted sediment or by addition of metasomatic fluids bearing a subducted sediment signature.

Le Roux et al. (2010) drew attention to the potential significance of high Zn/Fe ratios in some OIB compared to MORB, and argued that because ratios cannot be fractionated during peridotite melting, either some OIB originates from peridotite sources with high Zn/Fe, or it comes from lithologies (e.g. eclogite) with bulk Zn/Fe (solid source/melt) partitioning coefficients less than one. A follow-up study (Le Roux et al. 2011) measured mineral/melt partitioning coefficients for Mn, Co, Ni and Zn in olivine, orthopyroxene, and clinopyroxene, and integrated published results for garnet. These data were used to predict Mn/Fe, Zn/Fe, Mn/Zn and Co/Fe ratio behaviour during partial melting of primitive mantle peridotite, MORB-like eclogite and mixtures of the two. The modeling yielded maximum Zn/Fe and minimum Ni/Co and Co/Fe ratios for pure peridotite melting and they concluded that many OIB have element ratios that deviate from what is predicted from melting pure peridotite sources. Issues are that Zn/Fe ratios predict that MORB dominantly have peridotite sources, but they have Ni/Co and Co/Fe that imply a substantial eclogite component in their sources and Ni/Co values suggest more eclogite than in most OIB sources (Le Roux et al. 2011, their figure 7). Comparing our data with their modeling results, many of our end-member islands, including all HIMU have Zn/Fe that supports a pure peridotite source. A significant eclogite component (≥ 30%) is implied using our Ni/Co and Co/Fe ratios and EM1 and EM2 islands tend to have a higher eclogitic percentage than HIMU islands. Balta et al. (2011) did melting experiments on peridotite at 3 GPa under hydrous conditions and demonstrated that Mn can be compatible in garnet and that solid/liquid partitioning coefficients are impacted by temperature and melt composition. These observations predict the potential for large variations in magma Mn content and Fe/Mn ratios that only involve peridotite melting. The study demonstrates the challenges of modeling (e.g. Le Roux et al. 2011), where there are many variables that can impact results. Similarly, isotopes and incompatible element ratios tell us that the end member OIB sources are chemically different and that assumptions about constant transition metal concentrations for peridotite and eclogite may not be valid. Our results suggest that the end-member mantle components are apparently distinct in terms of some transition metal abundances. Thus modeling of these elements to predict the relative importance of eclogite versus peridotite in sources will apparently require better information on source chemical composition.

Implications for Core-Mantle Interaction

Estimates by McDonough (2003) suggest that 93% to 50% of the Earth's Ni, Co, Fe, Cu, and Cr occur in the core. Thus 'mantle plume' basalt sources could be enriched in these elements if they exchanged matter with the core. The seismic tomography techniques of Montelli et al. (2004, 2006) purport to see ~35 narrow plume-like structures, most originating at the base of the lower mantle with only two confined to the upper mantle. Plumes of shallow origin cannot have interacted with the core. Table 1 shows depths-of-origin for plumes studied here (Montelli et al. 2004, 2006) and most originate from ~2800 km (base of the lower mantle). Islands Tubuai and Tahiti occur on different hot-spot traces but within the same low-velocity anomaly (see Table 1 notes). Plumes associated with Gough, St. Helena and Pitcairn islands were not 'seen' possibly reflecting inadequacies in the distribution of epicentres and seismic stations (Kerr 2003; Montelli et al. 2004), the plumes are extinct, or they are so narrow they escaped imaging. Assuming that un-imaged plumes are shallow, inspection of the transition metal-based MDS diagram (Fig. 4A) reveals that the three islands (symbols; St, Go and Pi) plot randomly. With the exception of Mn (Fig. 7A), none of the elements separate un-imaged (shallow?) plumes from imaged deep-plume islands. Although Mn concentrations are higher in islands associated with imaged deep plumes, core–mantle interaction is unlikely to control mantle Mn because the core has 10% of the planet's Mn budget and lower concentrations (0.03 wt. %) than in the mantle (0.10 wt. %; McDonough 2003). Humayun et al. (2004) proposed that high Fe/Mn in Hawaiian OIB compared to MORB and Iceland basalt (a 'shallow' plume; Montelli et al. 2006) suggests core–mantle interaction by the Hawaiian plume. However, islands underlain by deep plumes do not show high Fe/Mn ratios (Fig. 7B).

Our results suggest that 'incompatible' transition metal abundances correlate with mantle component source type (Fig. 4) and thus dominantly reflect recycling of lithosphere. Tungsten, Tl and Os isotopic studies support recycling of lithospheric materials back into the mantle, with little or no evidence for core-mantle interaction (Schaefer et al. 2002; Scherstén et al. 2004; Brandon and Walker 2005; Nielsen et al. 2006, Willbold et al. 2009; Nebel et al. 2010). Thus our results support arguments against core–mantle interaction and suggest that transition metal concentrations are probably controlled by lithospheric recycling.

SUMMARY COMMENTS AND CONCLUSIONS

Radiogenic and stable isotopes along with incompatible trace element ratios firmly establish the existence of the mantle components (Zindler and Hart 1986; Weaver 1991; Eiler et al. 1997; Hofmann 2003; Greenough et al. 2007). Because the vast amount of the previous work is based on lithophile elements, the components are unlikely to be products of processes involving the core. Given the importance of subduction today and through Earth history, the mantle components probably reflect lithospheric recycling processes (*ibid.*). Beyond these generalizations, detailed information on the composition of the components is lacking and therefore their origin, and what they represent (e.g. sediment, ocean floor basalt, continental crust, etc.) remains speculative. Results here suggest that the first-row transition metals in OIB also reflect these lithospheric recycling processes because they dominantly correlate with well-established information on component type for the end-member islands used in the study. Chromium, Zn, Cu, and Fe appear particularly correlated with component type but most elements make contributions to distinguishing one or more of the components. Three of these (Mn, Zn and Sc) are probably not important core constituents. Although results are not shown, discriminant analysis confirms that various combinations of Cr, Ni, Co, Fe, Cu, and V (important core constituents; McDonough 2003) separate islands by component type. Of these elements, Ni makes the least contribution to separation because average concentrations are similar for each component type. Unless core–mantle interaction resulted in somewhat uniform Ni concentrations in all island-forming plumes it is not obvious that this lack of relationship between Ni and component type provides any substantial support for core–mantle interaction. The work by Humayun et al. (2004) implies that element ratios may be more sensitive tests of core–mantle interaction. Accordingly, 21 least compatible and more compatible element ratios were calculated from elements that are adjacent, or within three elements of one another in the list (moderately incompatible to most compatible: Zn, Mn, V, Fe, Co, Cu, Sc, Ni, and Cr). These ratios were used with MDS to compare the 'similarity' of islands and, like element concentrations, they separate EM1 from HIMU but show EM2 as intermediate. The plot is not shown because it is essentially the same as obtained with element concentrations (Fig. 4A). Although the results here do not preclude core–mantle interaction, the simplest conclusion is that, apart from percentage melting and differentiation, the dominant controls on first-row transition metals in OIB are the processes responsible for forming the mantle components.

ACKNOWLEDGEMENTS

Ideas for derivation of transition metal abundances in primary OIB magmas stemmed from a study of French Polynesia basalt with J. Dostal. MacKenzie refined methods in a B.Sc. Honours thesis at University of British Columbia, Okanagan. J.B. Balta provided a helpful review of an early version of the manuscript. Reviews by C.-T.A. Lee and an anonymous reviewer led to numerous improvements. R. Corney did the drafting. This work was funded by a NSERC Discovery grant to JDG and made possible by the GEOROC data base.

REFERENCES

Allègre, C.J., Schiano, P., and Lewin, E., 1995, Differences between oceanic basalts by multitrace element ratio topology: Earth and Planetary Science Letters, v. 129, p. 1–12, http://dx.doi.org/10.1016/0012-821X(94)00235-Q.

Balta, J.B., Asimow, P.D., and Mosenfelder, J.L., 2011, Manganese partitioning during hydrous melting of peridotite: Geochimica et Cosmochimica Acta, v. 75, p. 5819–5833, http://dx.doi.org/10.1016/j.gca.2011.05.026.

Basaltic Volcanism Study Project, 1981, Basaltic Volcanism on the Terrestrial Planets: Pergamon Press Inc., New York, 1286 p.

Bennett, V.C., 2003, Compositional evolution of the mantle, *in* Carlson, R.W., *ed.,* Volume 2: The Mantle and Core, Treatise on Geochemistry: Elsevier-Pergamon, Oxford, p. 493–519, http://dx.doi.org/10.1016/B0-08-043751-6/02013-2.

Best, M.G., 2003, Igneous and Metamorphic Petrology, 2nd Edition: Blackwell Science Ltd., Malden, MA, USA, 729 p.

Borg, I., and Groenen, P., 1997, Modern Multidimensional Scaling, Theory and Applications: Springer-Verlag, New York, 472 p., http://dx.doi.org/10.1007/978-1-4757-2711-1.

Brandon, A.D., and Walker, R.J., 2005, The debate over core-mantle interaction: Earth and Planetary Science Letters, v. 232, p. 211–225, http://dx.doi.org/10.1016/j.epsl.2005.01.034.

Drummond, M.S., and Defant, M.J., 1990, A model for trondhjemite-tonalite-dacite genesis and crustal growth via slab melting: Archean to modern comparisons: Journal of Geophysical Research, v. 95, p. 21503–21521, http://dx.doi.org/10.1029/JB095iB13p21503.

Eiler, J.M., Farley, K.A., Valley, J.W., Hauri, E.H., Craig H., Hart, S.R., and Stolper, E.M., 1997, Oxygen isotope variations in ocean island basalt phenocrysts: Geochimica et Cosmochimica Acta, v. 61, p. 2281–2293, http://dx.doi.org/10.1016/S0016-7037(97)00075-6.

Greenough, J.D., and Kyser, T.K., 2003, Contrasting Archean and Proterozoic lithospheric mantle: Isotopic evidence from the Shonkin Sag sill (Montana): Contributions to Mineralogy and Petrology, v. 145, p. 169–181, http://dx.doi.org/10.1007/s00410-002-0435-9.

Greenough, J.D., Dostal, J., and Mallory-Greenough, L.M., 2005a, Oceanic Island Volcanism I: Mineralogy and Petrology: Geoscience Canada, v. 32, p. 29–45.

Greenough, J.D., Dostal, J., and Mallory-Greenough, L.M., 2005b, Oceanic Island Volcanism II: Mantle Processes: Geoscience Canada, v. 32, p. 77–90.

Greenough, J.D., Dostal, J., and Mallory-Greenough, L.M., 2007, Incompatible element ratios in French Polynesia basalts: describing mantle component fingerprints: Australian Journal of Earth Sciences, v. 54, p. 947–958, http://dx.doi.org/10.1080/08120090701488271.

Greenough, J.D., Kamo, S.L., Theny, L., Crowe, S.A., and Fipke, C., 2011, High precision U–Pb age and geochemistry of the mineralized (Ni–Cu–Co) Suwar intrusion, Yemen: Canadian Journal of Earth Sciences, v. 48, p. 495–514, http://dx.doi.org/10.1139/E10-067.

Gurenko, A.A., Sobolev, A.V., Hoernle, K.A., Hauff, F., and Schmincke, H.-U., 2009, Enriched, HIMU-type peridotite and depleted recycled pyroxenite in the Canary plume: A mixed-up mantle: Earth and Planetary Science Letters, v. 277, p. 514–524, http://dx.doi.org/10.1016/j.epsl.2008.11.013.

Hart, S.R., Hauri, E.H., Oschmann, L.A., and Whitehead, J.A., 1992, Mantle plumes and entrainment: Isotopic evidence: Science, v. 256, p. 517–520, http://dx.doi.org/10.1126/science.256.5056.517.

Hawkesworth, C.J., Mantovani, M.S.M., Taylor, P.N., and Palacz, Z., 1986, Evidence from the Parana of south Brazil for a continental contribution to Dupal basalts: Nature, v. 322, p. 356–359, http://dx.doi.org/10.1038/322356a0.

Herzberg, C., 2011, Identification of source lithology in the Hawaiian and Canary Islands: Implications for origins: Journal of Petrology, v. 52, p. 113–146, http://dx.doi.org/10.1093/petrology/egq075.

Hilton, D.R., Grönvold, K., Macpherson, C.G., and Castillo, P.R., 1999, Extreme $^{3}He/^{4}He$ ratios in northwest Iceland: constraining the common component in mantle plumes: Earth and Planetary Science Letters, v. 173, p. 53–60, http://dx.doi.org/10.1016/S0012-821X(99)00215-0.

Hoffman, P.F., 1988, United plates of America, the birth of a craton: Early Proterozoic assembly and growth of Laurentia: Annual Reviews Earth and Planetary Sciences, v. 16, p. 543–603, http://dx.doi.org/10.1146/annurev.ea.16.050188.002551.

Hofmann, A.W., 1997, Mantle geochemistry: the message from oceanic volcanism: Nature, v. 385, p. 219–229, http://dx.doi.org/10.1038/385219a0.

Hofmann, A.W., 2003, Sampling mantle heterogeneity through oceanic basalts: isotopes and trace elements, *in* Carlson, R.W., *ed.,* Volume 2: The Mantle and Core, Treatise on Geochemistry: Elsevier-Pergamon, Oxford, p. 1–44, http://dx.doi.org/10.1016/B0-08-043751-6/02123-X.

Holland, H.D., 1984, The Chemical Evolution of the Atmosphere and Oceans: Princeton University Press, Princeton, NJ, 582 p.

Humayun, M., Qin, L., and Norman, M.D., 2004, Geochemical evidence for excess iron in the mantle beneath Hawaii: Science, v. 306, p. 91–94, http://dx.doi.org/10.1126/science.1101050.

Jackson, M.G., and Dasgupta, R., 2008, Compositions of HIMU, EM1, and EM2 from global trends between radiogenic isotopes and major elements in oceanic island basalts: Earth and Planetary Science Letters, v. 276, p. 175–186, http://dx.doi.org/10.1016/j.epsl.2008.09.023.

Kay, R.W., and Gast, P.W., 1973, The rare earth content and origin of alkali-rich basalts: The Journal of Geology, v. 81, p. 653–682, http://dx.doi.org/10.1086/627919.

Kerr, R.A., 2003, Mantle plumes both tall and short?: Science, v. 302, p. 1643, http://dx.doi.org/10.1126/science.302.5651.1643.

Kerrich, R., Goldfarb, R.J., and Richards, J.P., 2005, Metallogenic provinces in an evolving geodynamic framework: Economic Geology 100th Anniversary Volume, p. 1097–1136.

Keshav, S., Gudfinnsson, G.H., Sen, G., and Fei, Y., 2004, High-pressure melting experiments on garnet clinopyroxenite and the alkalic to tholeiitic transition in ocean-island basalts: Earth and Planetary Science Letters, v. 223, p. 365–379, http://dx.doi.org/10.1016/j.epsl.2004.04.029.

Keshav, S., Bizimis, M., Gudfinnsson, G.H., Sen, G., and Fei, Y., 2006, Response to the comment by M. Lustrino on "High-pressure melting experiments on garnet clinopyroxenite and the alkalic–tholeiitic transition in ocean-island basalts" by Keshav et al. [Earth and Planetary Science Letters, v. 223, p. 365–379 (2004)]: Earth and Planetary Science Letters, v. 241, p. 997–999, http://dx.doi.org/10.1016/j.epsl.2005.10.023.

Kogiso, T., Hirschmann, M.M., and Frost, D.J., 2003, High-pressure partial melting of garnet pyroxenite: possible mafic lithologies in the source of ocean island basalts: Earth and Planetary Science Letters, v. 216, p. 603–617, http://dx.doi.org/10.1016/S0012-821X(03)00538-7.

Lee, C.A., 1996, A review of mineralization in the Bushveld Complex and some other Layered Intrusions, *in* Cawthorn, R.G., *ed.,* Layered Intrusions: Elsevier, NY, p. 103–145, http://dx.doi.org/10.1016/S0167-2894(96)80006-6.

Lee, C.-T.A., Leeman, W.P., Canil, D., and Li, Z.-X.A., 2005, Similar V/Sc systematics in MORB and arc basalts: Implications for the oxygen fugacities of their mantle source regions: Journal of Petrology, v. 46, p. 2313–2336, http://dx.doi.org/10.1093/petrology/egi056.

Lee, C.-T.A., Luffi, P., Le Roux, V., Dasgupta, R., Albaréde, F., and Leeman, W.P., 2010, The redox state of arc mantle using Zn/Fe systematics: Nature, v. 468, p. 681–685, http://dx.doi.org/10.1038/nature09617.

Lee, C.-T.A., Luffi, P., Chin, E.J., Bouchet, R., Dasgupta, R., Morton, D.M., Le Roux, V., Yin, Q.-z., and Jin, D., 2012, Copper systematics in arc magmas and implications for crust-mantle differentiation: Science, v. 336, p. 64–68, http://dx.doi.org/10.1126/science.1217313.

Le Roux, V., Lee, C.-T.A., and Turner, S.J., 2010, Zn/Fe systematics in mafic and ultramafic systems: Implications for detecting major element heterogeneities in the Earth's mantle: Geochimica et Cosmochimica Acta, v. 74, p. 2779–2796, http://dx.doi.org/10.1016/j.gca.2010.02.004.

Le Roux, V., Dasgupta, R., and Lee, C.-T.A., 2011, Mineralogical heterogeneities in the Earth's mantle: Constraints from Mn, Co, Ni and Zn partitioning during partial melting: Earth and Planetary Science Letters, v. 307, p. 395–408, http://dx.doi.org/10.1016/j.epsl.2011.05.014.

Lustrino, M., 2006, Comment on "High-pressure melting experiments on garnet clinopyroxenite and the alkalic to tholeiitic transition in ocean-island basalts" by Keshav et al. [Earth and Planetary Science Letters, v. 223 (2004), p. 365–379]: Earth and Planetary Science Letters, v. 241, p. 993–996, http://dx.doi.org/10.1016/j.epsl.2005.10.024.

MacKenzie, K., 2008, A New Perspective on the Core Mantle Interaction Debate: Unpublished B.Sc. Honors Thesis, University of British Columbia – Okanagan, BC, 29 p.

Mallmann, G., and O'Neill, H.St.C., 2009, The crystal/melt partitioning of V during mantle melting as a function of oxygen fugacity compared with some other elements (Al, P, Ca, Sc, Ti, Cr, Fe, Ga, Y, Zr and Nb): Journal of Petrology, v. 50, p. 1765–1794, http://dx.doi.org/10.1093/petrology/egp053.

Manikyamba, C., and Kerrich, R., 2011, Geochemistry of alkaline basalts and associated high-Mg basalts from the 2.7 Ga Penakacherla Terrane, Dharwar craton, India: An Archean depleted mantle-OIB array: Precambrian Research, v. 188, p. 104–122, http://dx.doi.org/10.1016/j.precamres.2011.03.013.

Matzen, A.K., Baker, M.B., Beckett, J.R., and Stolper, E.M., 2011, Fe–Mg partitioning between olivine and high-magnesian melts and the nature of Hawaiian parental liquids: Journal of Petrology, v. 52, p. 1243–1263, http://dx.doi.org/10.1093/petrology/egq089.

McDonough, W.F., 2003, Compositional model for the Earth's core, *in* Carlson, R.W., *ed.,* Volume 2: The Mantle and Core, Treatise on Geochemistry: Elsevier-Pergamon, Oxford, p. 547–568, http://dx.doi.org/10.1016/B0-08-043751-6/02015-6.

Milner, S.C., and le Roex, A.P., 1996, Isotope characteristics of the Okenyenya igneous complex, northwestern Namibia; constraints on the composition of the early Tristan plume and the origin of the EM1 mantle component: Earth and Planetary Science Letters, v. 141, p. 277–291, http://dx.doi.org/10.1016/0012-821X(96)00074-X.

Montelli, R., Nolet, G., Dahlen, F.A., Masters, G., Engdahl, E.R., and Hung, S.-H., 2004, Finite-frequency tomography reveals a variety of plumes in the mantle: Science, v. 303, p. 338–343, http://dx.doi.org/10.1126/science.1092485.

Montelli, R., Nolet, G., Dahlen, F.A., and Masters, G., 2006, A catalogue of deep mantle plumes: New results from finite-frequency tomography: Geochemistry, Geophysics, Geosystems, v. 7, Q11007, http://dx.doi.org/10.1029/2006GC001248.

Mungall, J.E., and Naldrett, A.J., 2008, Ore deposits of the Platinum-group elements: Elements, v. 4, p. 253–258, http://dx.doi.org/10.2113/GSELEMENTS.4.4.253.

Naldrett, A.J., 2005, A history of our understanding of magmatic Ni-Cu sulphide deposits: The Canadian Mineralogist, v. 43, p. 2069–2098, http://dx.doi.org/10.2113/gscanmin.43.6.2069.

Nebel, O., Vroon, P.Z., Wiggers de Vries, D.F., Jenner, F.E., and Mavrogenes, J.A., 2010, Tungsten isotopes as tracers of core–mantle interactions: The influence of subducted sediments: Geochimica et Cosmochimica Acta, v. 74, p. 751–762, http://dx.doi.org/10.1016/j.gca.2009.10.017.

Nielsen, S.G., Rehkämaper, M., Norman, M.D., Halliday, A.N., and Harrison, D., 2006, Thallium isotopic evidence for ferromanganese sediments in the mantle source of Hawaiian basalts: Nature, v. 439, p. 314–317, http://dx.doi.org/10.1038/nature04450.

Pearce, J.A., 1996, A user's guide to basalt discrimination diagrams, *in* Wyman, D.A. *ed.,* Trace Element Geochemistry of Volcanic Rocks: Applications for Massive Sulphide Exploration: Geological Association of Canada, Short Course Notes 12, p. 79–113.

Pearce, J.A., and Cann, J.R., 1973, Tectonic setting of basic volcanic rocks determined using trace element analyses: Earth and Planetary Science Letters, v. 19, p. 290–300, http://dx.doi.org/10.1016/0012-821X(73)90129-5.

Qin, L., and Humayun, M., 2008, The Fe/Mn ratio in MORB and OIB determined by ICP–MS: Geochimica et Cosmochimica Acta, v. 72, p. 1660–1677, http://dx.doi.org/10.1016/j.gca.2008.01.012.

Roeder, P.L., and Emslie, R.F., 1970, Olivine-liquid equilibrium: Contributions to Mineralogy and Petrology, v. 29, p. 275–289, http://dx.doi.org/10.1007/BF00371276.

Rouxel, O.J., Bekker, A., and Edwards, K.J., 2005, Iron isotope constraints on the Archean and Paleoproterozoic ocean redox state: Science, v. 307, p. 1088–1091, http://dx.doi.org/10.1126/science.1105692.

Said, N., and Kerrich, R., 2010, Magnesian dyke suites of the 2.7 Ga Kambalda Sequence, Western Australia: Evidence for coeval melting of plume asthenosphere and metasomatised lithospheric mantle: Precambrian Research, v. 180, p. 183–203, http://dx.doi.org/10.1016/j.precamres.2010.04.003.

Sarbas, B., and Nohl, U., 2008, The GEOROC database as part of a growing geoinformatics network, *in* Brady, S.R., Sinha, A.K., and Gundersen, L.C., *eds*., Geoinformatics 2008—Data to Knowledge: U.S. Geological Survey Scientific Investigations Report 2008-5172, p. 42–43.

Schaefer, B.F., Turner, S., Parkinson, I., Rogers, N., and Hawkesworth, C., 2002, Evidence for recycled Archean oceanic mantle lithosphere in the Azores plume: Nature, v. 420, p. 304–307, http://dx.doi.org/10.1038/nature01172.

Scherstén, A., Elliott, T., Hawkesworth, C., and Norman, M., 2004, Tungsten isotope evidence that mantle plumes contain no contribution from the Earth's core: Nature, v. 427, p. 234–237, http://dx.doi.org/10.1038/nature02221.

Sobolev, A.V., Hofmann, A.W., Sobolev, S.V., and Nikogosian, I.K., 2005, An olivine-free mantle source of Hawaiian shield basalts: Nature, v. 434, p. 590–597, http://dx.doi.org/10.1038/nature03411.

Sobolev, A.V., Hofmann, A.W., Kuzmin, D.V., Yaxley, G.M., Arndt, N.T., Chung, S.-L., Danyushevsky, L.V., Elliott, T., Frey, F.A., Garcia, M.O., Gurenko, A.A., Kamenetsky, V.S., Kerr, A.C., Krivolutskaya, N.A., Matvienkov, V.V., Nikogosian, I.K., Rocholl, A., Sigurdsson, I.A., Sushchevskaya, N.M., and Teklay, M., 2007, The amount of recycled crust in sources of mantle-derived melts: Science, v. 316, p. 412–417, http://dx.doi.org/10.1126/Science. 1138113.

Sun, S.-S., and McDonough, W.F., 1989, Chemical and isotopic systematics of oceanic basalts: implications for mantle composition and processes, *in* Saunders, A.D., and Norry, M.J., *eds.,* Magmatism in the Ocean Basins: Geological Society, London, Special Publications, v. 42, p. 313–345, http://dx.doi.org/10.1144/GSL.SP.1989.042.01.19.

Tatsumi, Y., 2000, Continental crust formation by crustal delamination in subduction zones and complementary accumulation of the enriched mantle I component in the mantle: Geochemistry, Geophysics, Geosystems, v. 1, 1053, http://dx/doi.org/10.1029/2000GC000094.

Toplis, M.J., 2005, The thermodynamics of iron and magnesium partitioning between olivine and liquid: criteria for assessing and predicting equilibrium in natural and experimental systems: Contributions to Mineralogy and Petrology, v. 149, p. 22–39, http://dx.doi.org/10.1007/s00410-004-0629-4.

Wang, Z.R., and Gaetani, G.A., 2008, Partitioning of Ni between olivine and siliceous eclogite partial melt: experimental constraints on the mantle source of Hawaiian basalts: Contributions to Mineralogy and Petrology, v. 156, p. 661–678, http://dx.doi.org/10.1007/s00410-008-0308-y.

Weaver, B.L., 1991, The origin of ocean island basalt end-member compositions: trace element and isotopic constraints: Earth and Planetary Science Letters, v.

104, p. 381–397, http://dx.doi.org/10.1016/0012-821X(91)90217-6.
Wilkinson, L., Hill, M., Welna, J.P., and Birkenbeuel, G.K., 1992, SYSTAT for Windows: Statistics, Version 5, SYSTAT Inc., Evanston, IL.
Willbold, M., Elliott, T., and Archer, C., 2009, ε^{182}W in ocean island basalts and the role of core-mantle interaction (Abstract): Goldschmidt Conference, Geochimica et Cosmochimica Acta, Supplementary, 73, Davos, Switzerland, A1444.
Zhang, M., O'Reilly, S.Y., Wang, K.-L., Hronsky, J., and Griffin, W.L., 2008, Flood basalts and metallogeny: The lithospheric mantle connection: Earth-Science Reviews, v. 86, p. 145–174, http://dx.doi.org/10.1016/j.earscirev.2007.08.007.
Zindler, A., and Hart, S., 1986, Chemical geodynamics: Annual Review of Earth and Planetary Sciences, v. 14, p. 493–571, http://dx.doi.org/10.1146/annurev.ea.14.050186.002425.

Received March 2015
Accepted March 2015
First published on the web June 2015

For access to Greenough and MacKenzie (2015) electronic supplementary materials (ESM Tables 1 through 4), please visit GAC's open source GC Data Repository, Igneous Rock Associations link at: http://www.gac.ca/wp/?page_id=306.

REVIEW

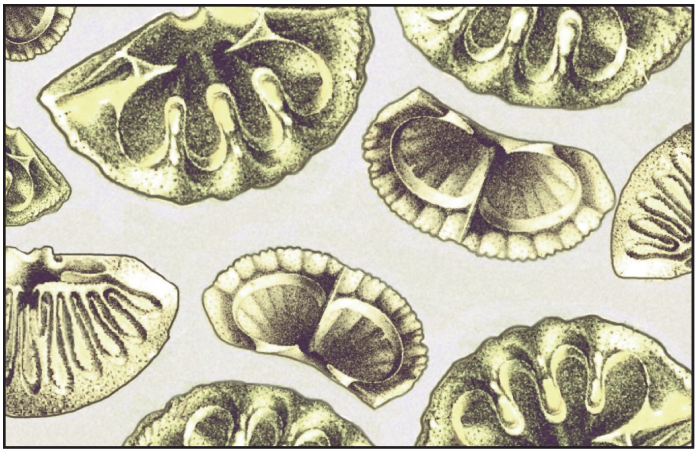

EDUARD SUESS GEOLOGIST: Catalogue of the Exhibition

Professor Dr. Dr. *h. c. mult.* A.M. Celâl Şengör

İstanbul Technical University (2015)
İstanbul, Turkey, 76 p.
5 Turkish Liras (plus shipping); Softcover
For purchase, e-mail: Dr. Celâl Şengör (sengor@itu.edu.tr)
after 30th September 2015
Electronic version available free

Reviewed by Bruce Ryan
Geological Survey of Newfoundland & Labrador
Department of Natural Resources
Box 8700, St. John's
Newfoundland–Labrador, A1B 4J6, Canada
E-mail: bruceryan@gov.nl.ca

This neat little book, containing less than eighty pages and profusely illustrated, is a compilation of selected material about the great Austrian geologist Eduard Suess (1831–1914), celebrating his lifetime of contributions to geoscience and his country. The book is a catalogue and explanatory commentary to accompany a recent (April 17 to May 11, 2015) exhibition saluting Suess' exemplary life, displayed at the Cultural Office of the Austrian Consulate-General in Istanbul, Turkey. The author, Dr. Celâl Şengör, contributed the exhibit material from his own library. Şengör clearly admires Suess and cherishes the manuscripts and other items he has in his collection. I wish I had seen the actual exhibit and been further enlightened by Dr. Şengör!

Dr. Celâl Şengör is a world-renowned geologist whose writings include many articles that show his passion for those who founded the tenets upon which current geological thinking rests. One of his heroes is clearly Eduard Suess. The respect and admiration Şengör has for Suess shine in this book and in two more substantial papers published in *Geoscience Canada* (Vol. 42, no. 2, p. 181–246) and the *Austrian Journal of Earth Sciences* (Vol. 107, p. 6–82). Şengör expresses great regret that so few geologists appreciate the influence that the fertile mind of Suess had upon our science, and he is determined to correct this educational deficiency. He sheds light on the life of this remarkable man, and leads us through the perceptive observations that steered Suess to contemplate how the patterns of land and sea came to be. Suess was a scientist who, in the modern vernacular, was 'thinking outside the box.'

Let me tell you how I first came to know the name of Eduard Suess. One of my undergraduate textbooks, A.O. Woodford's *Historical Geology,* recounted how Suess had used the *Glossopteris* flora to add South America to the other land masses (Africa, Madagascar, India, Australia) he had already amalgamated into his recently christened supercontinent of Gondwanaland. I came upon his name again in *Elements of Structural Geology*, where E. Sherbon Hills credited Suess' monumental tome *Das Antlitz der Erde* (*The Face of the Earth*) as *the* pioneering study of the large scale tectonics of continents and oceans. I gained a sense that this man was a thinker on a grand scale, yet he seemed to be relegated to 'asides' in our courses and many other texts. He was re-introduced to me in grad school by the late Bob Stevens, and my interest was rekindled when I later collected geologically-themed postage stamps, because Suess' image appeared on an Austrian stamp. With the publication of Şengör's book and the companion pieces noted above, Eduard Suess should now be elevated to his rightful position among the giants of geology, and recognized for many other contributions.

Reviewing a publication dedicated to an exhibit of antiquarian objects is daunting, because descriptions cannot be directly associated with tangible artifacts. The reader, and the reviewer, have to imagine 'being there and seeing that' on the basis of illustrated guides such as this one. This illuminating and informative volume of archival research meets this objective ... and far more than this. The body of the text is divided into chapters that address specific facets of Suess' professional, personal, and political life. I must admit that I am a biased reader, because a love of history was instilled in me in grade school and a love of geology was nurtured at university. So, when the two are combined, my eyes light up and my mind drifts back in time in more ways than one!

In the 'Introduction' Şengör awards Suess the distinction of being "probably the greatest geologist who ever lived" and

then proceeds to summarize the great man's geological accomplishments and his humanitarian contributions. We are first introduced to Suess' masterpiece *Das Antlitz der Erde* (*The Face of the Earth*), a synthesis of world tectonics described as "the greatest book in the history of geology". In the 'Life and Family' chapter, Sengor focuses on Suess' personal side, giving us a glimpse into his forebears, along with pivotal events in his upbringing and education. A chapter entitled 'First Studies' documents some of Suess' early work, and tells us how geology became Suess' passion when he lived in Prague in the mid-1800s. Şengör marvels, as should the reader, at Suess' capacity to comprehend and synthesize, as a teenager, the voluminous geological literature needed for his first scientific publication – a few pages in an 1851 tourist guidebook to the spa town of Karlsbad. The chapter also recounts how Suess developed an interest in graptolites, sent his findings to Joachim Barrande, but was seemingly 'scooped' by Barrande! In spite of this scientific impropriety, Suess eventually brought his findings to the palaeontological community, even applying Barrande's taxonomy to the graptolites. The chapter entitled 'Palaeontological Studies' deals with Suess' dedication to studying fossils, especially brachiopods. Immaculate line drawings reproduced here from some of these publications show not only his observational depth but also his artistic talent. In this age of pixels and polygons it is all too easy to overlook the painstaking pen work that went into such superb illustrations. His palaeontological contributions, which continued for nearly another fifty years, made him a 'household name' among his contemporaries in France and England. A chapter entitled 'Studies on Urban Geology: Foundation of Urban Geology' gives the reader a look at the 'practical geology' side of Eduard Suess and shows how his grasp of engineering served the city of Vienna. His insights went far beyond geology, as demonstrated by his suggested cure for a typhoid outbreak – bring in fresh drinking water! His 1862 book about the geological aspects of Vienna led to his election to the city council, heralding 30 years of political activism. The references to him as a "mad" driver behind the city's late 1860s decision to construct a system of mammoth aqueducts to bring fresh water from the Alps are a teaser for more reading about this largely unknown side of his career.

The book next returns to Suess as a 'traditional' hard-rock geologist, giving a record of his influential work in 'Stratigraphic Studies.' This chapter reveals how his insights into sea-level fluctuations led him to propose the former existence of a major water body across central Europe and part of Asia, now referred to as the Para-Tethys Sea. These studies also led him to contemplate the mechanism of global sea-level changes. Suess' documentation of abrupt changes in the fossils associated with differing depositional environments steered him to the conclusion that Charles Darwin's theories did not give enough weight to variations precipitated by environmental fluctuations. He also came to an astute conclusion about Alpine structure: the igneous rocks of the southern Alps were deformed along with their sedimentary envelope. Clearly, the prevailing idea that the igneous rocks were responsible for Alpine mountain building could not be correct. His interest in tectonic studies was born, and is explored further in the next chapter, 'The Beginning of Suess' Tectonic Studies,' which provides a fascinating glimpse into his rapid evolution from a local expert to a global thinker. His studies of a simple anticlinal structure in salt mines near Krakow in 1868 soon led to the recognition that this same structure extended along the entire Alpine front. He went on to propose that such folds were a consequence of large-scale horizontal movements of the Earth's crust and that this motion was likely the dominant force in mountain building. His 1873 ruminations on "slow and heterogeneous motion" of the entire surface of the Earth as being the instigator of worldwide mountain ranges, made evident in Şengör's English translation of the obscure original German summary of the paper, underscores how Suess' prescient analysis set the stage for what would eventually present itself as plate tectonics, although he viewed thermal contraction of the surface as the driving mechanism. Şengör highlights *Die Entstehung der Alpen* (*The Origin of the Alps*) as expounding hypotheses that "inaugurated the modern era" of global tectonic studies; it is, indeed, a window into the mind of a geologist who viewed the whole Earth as a dynamic and intertwined physical and biological system. A chapter entitled 'Tectonic Studies' further explores these ideas, especially as developed in his colossal, five-volume treatise *Das Antlitz der Erde* (*The Face of the Earth*) published between 1883 and 1909. It specifically highlights Suess' rejection of many of the outdated notions of the times. He embraced the uniformitarian views of Charles Lyell and James Hutton, and his views of the Earth spanned the scale from hand specimen to mountain range to continent. Here, we first encounter Suess' proposal that the closure of the Tethys Ocean was responsible for the formation of the imposing mountains of the Alpine-Himalayan chain. We are also reminded of Suess' belief that fluctuations in the volumes of water in the world's oceans caused worldwide regressions and transgressions seen in the geological record. Şengör comments on some notions that have stood the test of time, as well as others that have collapsed under the weight of more recent geological interpretations. Although appropriate for an exhibit guide, this synthesis is a far-too-brief overview of Suess' tome, considering the treatment afforded other aspects of Suess' professional and personal life. Fortunately, those who want more can easily find it in Şengör's complementary treatment of Suess in the recent *Geoscience Canada* and *Austrian Journal of Earth Sciences* articles.

Suess, it seems, also had a very pragmatic side. A short discussion of his role in economic geology and of the importance of his views on gold and silver to finance is presented in a chapter entitled 'Monetary Politics and the Valuable Metals.' He penned two books on the topic of metals in relation to monetary systems, one dedicated to gold and the other to silver, and served as a consultant to the governments of several countries. A chapter entitled 'The Last Scientific Writings of Suess' is dedicated to four papers postdating the completion of *Das Antlitz der Erde*. The earliest of these was a 1909 summary dealing with the evolution of life relative to the environmental effects of the biosphere. Contributions on the history and philosophy of science and the physical and historical aspects of the Danube River demonstrate that his breadth of study did not diminish with age. Suess' very last paper, on the forces responsible for mountain building, receives a series of interesting queries from Şengör, who wonders why this 1913 publication makes no mention of Alfred Wegener's newly minted concept of continental drift and laments the fact that

we will never know the reasons for its omission! The final chapter returns to Suess as 'The Politician,' recounting his enormously important civic contributions. He was not, in some cases, averse to tackling the oftentimes sensitive issue of the relation between church and state. The final paragraph expresses his desire to remain a 'man of the people,' avoiding political accolades and titles, and the 'Epilogue' further emphasizes his indifference to glorifying monikers and worldly goods. He preferred to live a life that at its close was marked by "a tranquil conscience and an innerly cheerful spirit." Here, Celâl Şengör challenges us to emulate this man of modest means who came to the end of his geological and political journey at his residence in Vienna on April 26, 1914.

The layout of this little book is quite pleasing, especially in its abundance of colour illustrations of items from the exhibit, and I detected very few printing glitches. Given the wealth of illustrative material, the many publications cited, and the need to cross-reference from place to place and time to time, a few misconnections are almost inevitable. For example, a couple of figure captions are misplaced, and scattered typographical errors are apparent. There are a couple of references to items that could have been appreciated only by attending the exhibition, and their inclusion seems extraneous without illustration. The rendering of some material – such as large maps – for the printed page is in places plagued by very fine and/or fuzzy and/or indecipherable print, but these challenges are also to be expected. Even if all detail cannot be resolved, the reader can grasp the significance of such material when cross-referenced to the text. The minor blemishes can be overlooked, and they do not seriously overpower or detract from the narrative and the overall appearance of the book. Unlike the multilingual Celâl Şengör, most of us cannot read the illustrated papers in their original script, and Dr. Şengör has provided yeoman service for us all, with his careful translations and allied commentary.

Overall, this book is delightfully enlightening and readable. At 5 Turkish Liras, it is a bargain for geological history buffs, and it will give you unforgettable insight into a very perceptive late 19th and early 20th century scholar of the Earth sciences. The text and illustrations constitute history, geology and politics all rolled into one, but the reader must remember that the book's contents and layout reflect its original purpose – a guide to an exhibit. Despite such limitations, it is a concise story of a champion of our science and an incredible man. Celâl Şengör is to be congratulated and praised for his initiative in organizing and curating the exhibit and for bringing the profound thinking of this remarkable geologist to an audience that would otherwise not be aware of Suess' contributions to the foundations of tectonics and his beloved Austria. Şengör characterizes him as an 'admirable idol,' and deservedly so. Having past and contemporary idols was par for the course when I was immersed in university geology studies decades ago, but nowadays I get strange looks when I inquire of such among students and neophyte geologists because they are largely oblivious to the science's great 'movers and shakers.' This book is a reminder that as we look up in awe at the world's great mountain ranges and contemplate their origin, we should also look down because we are 'standing on the shoulders of giants,' like Eduard Suess who decades ago pondered the same questions.

I will end this review with one last personal note, harking back to my own time at Memorial University in St. John's during the heady days when global plate tectonics became a new paradigm for Earth dynamics. We keenly absorbed the ideas of our own great Appalachian geologist and continental drift advocate, Harold ('Hank') Williams, and briefly rubbed shoulders with John Dewey, Jack Bird, Maarten de Wit and a host of other enthusiastic proponents. After reading this book, I cannot help but see Suess in the same light as the lately departed Hank – both were mega-thinkers who moved continents (albeit in different ways!) to make mountains. I can imagine them now excitedly debating their principles and tectonic mechanisms 'on the Other Side.' So, I unreservedly encourage you to make room for this little book in your bookcase, even if you have to move mountains of other ones to do it!

Corporate Members

Platinum

Memorial University

Gold

Anglo American Exploration (Canada) Ltd.
Newfoundland and Labrador Department of Natural Resources
Northwest Territories Geological Survey

Silver

British Columbia Geological Survey
IBK Capital Corp.
Royal Tyrrell Museum of Palaeontology
Yukon Geological Survey

Nickel

Acadia University

GEOLOGICAL ASSOCIATION OF CANADA (2015-2016)

OFFICERS

President
Victoria Yehl
Vice-President
Graham Young
Past President
Brian Pratt
Secretary-Treasurer
James Conliffe

COUNCILLORS

Alwynne Beaudoin
Oliver Bonham
James Conliffe
David Corrigan
Lori Kennedy
Andy Kerr
Brad McKinley
David Pattison
Sally Pehrsson
Brian Pratt
Dène Tarkyth
Chris White
Victoria Yehl
Graham Young

STANDING COMMITTEES

Communications: TBA
Finance: Dène Tarkyth
Publications: Chris White
Science Program: David Corrigan

GEOSCIENCE CANADA

JOURNAL OF THE GEOLOGICAL ASSOCIATION OF CANADA
JOURNAL DE L'ASSOCIATION GÉOLOGIQUE DU CANADA

2015 VOLUME 42 GSCNA7 42 271-372
PRINT EDITION ISSN 0315-0941
ONLINE EDITION ISSN 1911-4850